WSRC-TR-2003-00232, Rev. 0
SRT-RPP-2003-00105, Rev. 0

Key Words:
RPP-WTP
Envelope C
Precipitation
Ion-Exchange

Retention:
Permanent

Key WTP R&T References:
Test Specification 24590-WTP-TSP-RT-01-006, Rev. 0
Task Plan WSRC-TR-2001-00425, Rev. 1
Test Exceptions 24590-WTP-TEF-RT-02-063
R&T Focus Area Pretreatment-Precipitation
Test Scoping Statement(s) S-126

PARAMETERS INFLUENCING THE FORMATION OF POST-FILTRATION SOLIDS IN THE 241-AN-107 AND 241-AN-102 HANFORD HIGH-LEVEL WASTE SIMULANT

J. T. Coates, J. M. Brown, J. D. Navratil, D. Denard, and K. Cole, Clemson University

September 24, 2003

Westinghouse Savannah River Company
Savannah River Site
Aiken, SC 29808

Prepared for the U.S. Department of Energy Under Contract Number DE-AC09-96SR18500

SRS savannah river site ™

WSRC-TR-2003-00232, Rev. 0
SRT-RPP-2003-00105, Rev. 0

FINAL REPORT

PARAMETERS INFLUENCING THE FORMATION OF POST-FILTRATION SOLIDS IN THE 241-AN-107 AND 241-AN-102 HANFORD HIGH-LEVEL WASTE SIMULANTS

J. T. Coates, J. M. Brown, J. D. Navratil, D. Denard, and K. Cole

Issue Date: September 24, 2003

Environmental Engineering and Science
Clemson University
Anderson, SC 29625

TABLE OF CONTENTS

LIST OF FIGURES

LIST OF TABLES

LIST OF ACRONYMS AND ABBREVIATIONS

BNFL – British Nuclear Fuel Limited
Dk – Dark
DOE – Department of Energy
EDTA – Ethylenediaminetetraacetic acid
HLW – High Level Waste
ICP-AES – Inductively Coupled Plasma–Atomic Emission Spectroscopy
LAW – Low Activity Waste
Lt – Light
Mp – Mass precipitate
Mt – Mass total
NOC – Newly Optimized Condition
ORP – Oxidation Reduction Potential
RPP – River Protection Project
Rxn -- Reaction
SCUREF – South Carolina Research Education Foundation
Sim 7 – Simulant 7
Sim 8 – Simulant 8
Sim A – Simulant A
Sim B – Simulant B
$t_{1/2}$ – Half life
TRU – Transuranic
U/F – Ultra filtration
UV/VIS – Ultra-violet/Visible
WSRC – Westinghouse Savannah River Company
WTP – Waste Treatment Plant

ABSTRACT

Envelope 'C' high-level waste simulants were prepared to represent the chemical composition of the supernates of two tanks, 241-AN-107 and –102 located at the Hanford Site in Washington State. Experiments were conducted with these simulants to determine the impact of several chemical and physical parameters on the phenomena of post-filtration precipitation. Baseline experiments were conducted for flow sheet conditions, which involved a reaction of each simulant with 0.075 M strontium nitrate, 0.05 M sodium permanganate, and 1.0 M added sodium hydroxide at 50 ^{o}C for four hours. Simulants were filtered at 0.1 μm and stored in the dark under a nitrogen blanket. Chemical and physical parameters investigated were categorized as either reaction or filtrate variables. Reaction variables examined the effect of reaction temperature, free sodium hydroxide concentration, reagent concentrations, and shear level during the precipitation reaction on post-filtration solids formation. Filtrate variables examined the effects of light intensity, temperature of the filtrate, filtration at 50 ^{o}C (omitted for AN-102), filter pore size (omitted for AN-102), and oxidation-reduction potential (ORP) on post-filtration solids formation. Experiments were designed to study both primary effects and secondary effects of the parameters.

Data presented for the 241-AN-107 primary effects study indicated that post-filtration solids formed with all treatments examined given sufficient time. However, in the short term (within 48 hours), reacting the simulant at flow sheet conditions but eliminating the addition of sodium hydroxide from the reaction mixture and minimizing exposure to oxygen in the filtrates minimized the formation of precipitates. In addition, the formation of post-filtration solids could also be minimized by reducing the concentration of sodium permanganate to approximately 0.01 M.

With exception of two experimental conditions, the 8-hr hold of the filtrate at 100 °C and the oxygen sparge, solids that formed during the 48-hr period were very light in color. The filtrates sparged with oxygen contained brown solids within six hours, and significant black solids formed in the filtrates held at 100 °C for eight hours. The formation of brown solids in the filtrates sparged with oxygen is commensurate with permanganate reduction in alkaline media to manganese hydroxide, which is a white precipitate, and subsequent oxidation in the presence of air to the brown manganese (III) oxy-hydroxide and oxide and ultimately to the black manganese dioxide. Formation of black solids in the 8-hr hold filtrates supports the hypothesis that the precipitation reaction kinetics are too slow for the reaction to be complete after a four hour reaction time.

Very near the end of the analytical effort for the AN-241-107 primary effects study, discussions were initiated concerning reconsideration of the reaction conditions. A 'newly optimized condition' (NOC) was proposed in which the concentration of reactants was reduced to 0.03 M strontium nitrate and sodium permanganate. In addition, the sodium hydroxide concentration was set at 0.3 M (0.0 M added to the AN-102 simulant), and a reaction temperature at 25 $^{\circ}$C. A 2^3 factorial experiment using the NOC reaction and varying the sodium permanganate concentration, the light level and the influence of oxygen was designed.

During the 16-day observation period, dark solids appeared in all treatment pairs in contact with the atmosphere. Dark solids also formed for the light/nitrogen pairs reacted at 0.01 and 0.03 M sodium permanganate. Dark solids did not form for reaction at the NOC and at the NOC with 0.01 M sodium permanganate. Therefore, it would appear that reacting at the NOC or at lower permanganate concentration could mitigate the formation of dark solids within 16 days of an oxidation reaction with a 241-AN-107 waste.

Cation concentration for manganese and iron measured in the 16-day filtrates did not show a measurable decrease with time, even though solids collected at the end of the 16 days did indicate the presence of manganese and iron. Therefore, rate constants describing the formation of those solids could not be determined. Rate constants describing the formation of strontium solids during the 16-day period were calculated. Half-lives calculated for filtrates maintained in the light ranged from 15.3 to 21.2 $days^{-1}$ while those maintained in the dark ranged from 22.4 to 60.3 $days^{-1}$ suggesting that light may play an important role in the precipitation of strontium.

The primary effects study for the 241-AN-102 simulant resulted in the formation of brown to black solids in all treatments except the zero molar added sodium hydroxide and the 25 ^{o}C reaction under otherwise baseline conditions, the NOC, and the 0.01 M sodium permanganate reaction under otherwise NOC. Estimated rate constants and half-lives describing the loss of manganese from filtrates during the 16-day observation period were calculated. Half-lives ranged between 7 and 495 days. Treatment conditions exhibiting small half-lives could potentially result in an accumulation of post-filtration solids that may be problematic in the ion exchange process. Conditions involving light and oxygen exposure had the shortest half-lives.

Secondary effects studied for the 241-AN-102 simulant involved examining the effect of 0.0 M added sodium hydroxide and a 25 ^{o}C reaction condition with 0.03 M strontium, 0.03 M permanganate, light, and the presence of oxygen. Results indicated that a 25 ^{o}C reaction temperature is not effective in inhibiting the formation post-filtration solids when crossed with primary effects variables that did promote solids formation. Lowering the reaction temperature from 50 to 25 °C should have resulted in less of a reaction precipitate leaving more iron in solution as noted above. However, the behavior of iron in response to the lowered reaction temperature follows that of manganese suggesting that co-precipitation or adsorption may be an important removal mechanism for iron.

The 0.0 M added NaOH reaction condition does not promote solid formation and may inhibit the formation of solids when crossed with other primary effects variables that promote solid formation. Exposure to light is also seen to be very effective in promoting the formation of dark brown to black post-filtration solids.

For all treatment conditions, white or clear solids on the bottom of the flasks were the first to appear. In some filtrates, these solids were then covered by a thin layer of light brown solids. Light solids that appeared on the surface generally became darker with time, presumably as they were oxidized.

In summary, the data suggests that for the base case conditions, lowered reaction temperature and the absence of added NaOH do not result in the formation of dark solids within 16-days. Similarly, the variable evaluated for the newly optimized conditions that did not result in the formation of dark solids was the 0.01 M permanganate treatment. The newly optimized conditions also did not result in the formation of dark solids.

Post-filtration solids that formed in both the AN-107 and –102 filtrates were completely soluble in 0.5 molar nitric acid. Additionally, the mass of predominantly manganese containing solids that formed in the filtrates was small, generally in the mg/L range.

1.0 SUMMARY OF TESTING

1.1 OBJECTIVES

- The purpose of this task was to determine the first order effects for selected physical and chemical parameters that lead to post-filtration precipitation of manganese- and iron-containing solids in Sr/TRU 241-AN-107 and –102 simulant filtrates. Additionally, second order effects were explored after some of the first order effects were eliminated.

- First order effects were studied using a completely random experimental design where replicated experiments for each of the physical and chemical parameters noted in WSRC-TR-2001-00425/SRT-RPP-2001-00147, Revision 1 and the R&T Test Exception 24590-WTP-TEF-RT-02-063 were compared to baseline experiments.

- Second order effects were studied using a factorial experimental design for first order parameters that resulted in a negative main effect response.

1.2 CONDUCT OF TESTING

Testing was performed on a 100 to 150 mL scale using 241-AN-107 and -102 nonradioactive simulants in 250 mL Erlenmeyer flasks. The simulants were diluted to a sodium concentration of 6 M and heated to 50 ^{o}C in a circulating water bath. Simulants were then adjusted to 1 M free hydroxide by the addition of 17 M sodium hydroxide (NaOH). One molar strontium nitrate ($SrNO_3$) was added to the reaction mixture to achieve a final concentration of 0.075 M strontium (Sr). After reacting for a period of 15 minutes, 1 M sodium permanganate ($NaMnO_4$) was added to achieve a final concentration of 0.05 M permanganate (MnO_4^-), and the suspension was allowed to react for a period of 4 hours. Following the reaction period, the mixture was cooled to room temperature (23-25 ^{o}C) in a re-circulating water bath, centrifuged to remove bulk solids and filtered with 0.1 micron nylon filters. Filtrates were collected and stored in the dark under a nitrogen blanket during the observation period. Details of the above procedure are provided in Bannochie, 2002.

Treatment variables examined the effects of reaction temperature, free sodium hydroxide concentration, reagent concentrations, filtration at 50 ^{o}C (omitted for AN-102), shear level of the precipitate, and filter pore size (omitted for AN-102) on post-filtration solids formation. Filtrate variables examined the effects of light intensity, temperature of the filtrate, and oxidation-reduction potential (ORP) on post-filtration solids formation. Light intensity was adjusted by storing the filtrate directly under a fluorescent light as opposed to the base case conditions of being stored in the dark. The light intensity at the surface of the filtrate was measured to be 1600 Lux. To examine the effect of temperature, the filtrate was heated to 100 ºC for eight hours. Filtrates were also sparged with oxygen and nitrogen gases (omitted in AN-102) in an attempt to raise or lower the bulk redox potential of the filtrate.

In addition to studying the above reaction and treatment variables, experiments were conducted to study the formation of post-filtration solids for a set of experimental conditions termed the newly optimized conditions (NOC). The concentration of reactants for the NOC

was 0.03 M $SrNO_3$ and $NaMnO_4$ and 0.3 M added NaOH. The reaction temperature was maintained at 25 °C for 4 hours. The NOC were examined during the secondary effects study for 241-AN-107 and the primary effects study for 241-AN-102.

Testing was performed in accordance with technical task plan (Bannochie and Nash, 2001) and the test exception (Abodishish, 2002).

1.3 RESULTS AND PERFORMACE AGAINST OBJECTIVES

The first objective of this testing was to evaluate the influence of several chemical and physical parameters individually (primary effect) on post-filtration solids formation for two Hanford waste tank simulants, 241-AN-107 and -102. In this work with the 241-AN-107 simulant, the research suggests that eliminating the addition of sodium hydroxide from the reaction mixture and minimizing exposure to oxygen in the filtrates may minimize the formation of solids. Studies with the 241-AN-102 simulant resulted in the formation of brown to black solids in all treatments except four: the zero molar added sodium hydroxide, the 25 °C reaction temperature at the baseline condition, the NOC, and the 0.01 M sodium permanganate reaction for the NOC.

The second objective was to determine synergistic effects of the negative primary effects variables crossed with (among and between) select positive primary effects variables. During the 16-day observational period for the 241-AN-107 simulants, dark solids appeared in all treatment pairs in contact with the atmosphere. Dark solids also formed for the light/nitrogen pairs reacted at 0.01 and 0.03 M sodium permanganate. Dark solids did not form during the 16-day period for reaction at the NOC and at the NOC with 0.01 M sodium permanganate. Studies with the 241-AN-102 simulant indicated that the 0.0 M added NaOH reaction condition did not promote solids formation within the 16-day period and may inhibit the formation of solids when crossed with other primary effects variables that promote solids formation. Exposure to light was also seen to be very effective in promoting the formation of dark brown to black post-filtration solids.

1.4 QUALITY REQUIREMENTS

This task was performed in accordance with Quality Assurance Project Plan EES-01-001, Rev. 2. September 24, 2002 and the technical task plan WSRC-TR-2001-00425/SRT-RPP-2001-00147, “Evaluation of Post-Filtration Precipitation Mechanisms”. The technical work associated with this task was performed by a sub-tier supplier (Clemson University) under a South Carolina Research Education Foundation (SCUREF) contract. Appendix A in the above technical task plan contains a graded application of the NQA-1-1989 and NQA-2a-1990 QA Programmatic elements applicable to this task. Since the tests do not affect the quality of a high level waste (HLW) form, the requirements of DOE/RW-0333P Revision 10 do not apply to this task.

1.5 ISSUES

No issues were identified.

2.0 INTRODUCTION

The Department of Energy (DOE) has established the River Protection Project (RPP) to oversee nuclear waste treatment at the Hanford Site in Washington State. High-level waste (HLW) stored in tanks has been segregated into envelopes based on general tank chemistry and processing requirements. At Hanford, at least two tanks are classified as Envelope C waste. An Envelope C waste is defined as an alkaline supernate containing organic complexants [e.g., ethylenediaminetetraacetic acid (EDTA), gluconate, citrate, etc.], high strontium (Sr)-90 activity, and transuranic (TRU) elements (e.g., plutonium (Pu) and americium (Am)). The goal of the RPP Waste Treatment Plant (WTP) is to process the different waste envelopes into high level waste (HLW) and low activity waste (LAW) streams and to vitrify each stream separately.

The treatment process for Envelope C waste is a batch process consisting of evaporation, precipitation, cross-flow ultrafiltration (U/F), ion exchange, and ultimately vitrification (McCabe and Nash, 2000). Envelope C waste treatment required removal of strontium to below 1.1×10^{-3} Ci/mole waste sodium and the TRU elements to below 1.5×10^{-5} Ci/mole sodium (Townson, 1999). New requirements are 20 Ci Sr/m^3-glass and 100 nCi Tru/m^3-glass. Strontium nitrate is added for isotopic dilution, and sodium permanganate is used as an organic oxidant and to promote the formation of adsorptive species in the waste. Precipitate formation effectively reduces the concentration of TRU elements to acceptable levels.

The treatment process is being designed using both simulant and actual Envelope C waste. Nonradioactive simulant recipes for tanks 241-AN-107 and 241-AN-102 wastes were developed by Westinghouse Savannah River Company (WSRC) to mimic, both physically and chemically, actual tank waste.

In the course of developing the treatment scheme for the Envelope C waste, it was discovered that solids formed in the filtrate of treated waste. After the treated waste was filtered at 0.1 micrometers (μm), solids appeared in the filtrate within days. These solids have been observed in both treated Envelope C tank waste and in the simulant waste (Nash and Rosencrance, 2000). Different hypotheses were proposed to explain the appearance of post-filtration solids. If reaction kinetics are slow, a four-hour reaction time may be insufficient for the reaction to be completed. Complexation and hydrolysis may also kinetically limit the precipitation reaction. The chelating agents present in the waste could affect precipitation by keeping the metal cations complexed during the reaction. The rate of hydrolysis of the free metal cations may also affect post-filtration solids formation. Sub-micron (less than 0.1 μm) particles not captured by the filter could agglomerate over time and form visible solids. It was also hypothesized that visible light may photochemically promote solids growth in the filtrate. Similarly, photochemical reactions due to the decay of nuclides in the waste could play a role in post-filtration solids formation.

Post-filtration solids entering the ion exchange column could potentially reduce the removal of target nuclides by blocking exchange sites. In addition, solids could build up in the resin

and increase the pressure drop across the resin bed and thus alter process efficiency. The formation of post-filtration solids must therefore be addressed before final design is completed. (Bannochie and Nash, 2001).

Variables that affected the permanganate oxidation reaction and the filtrate were studied. Variables included in this investigation are listed in the experimental detail section and literature findings in support of their use are discussed below.

Under alkaline conditions, sodium permanganate is reduced to manganese hydroxide ($Mn(OH)_2$), which is easily oxidized by ambient air to manganese (III) oxyhydroxide ($MnO(OH)$) and oxide (Mn_2O_3) and can ultimately be oxidized to manganese dioxide (MnO_2) (Cotton and Wilkinson, 1988). These reactions depend on the redox state of the solution. E_H values of less than -0.2 V at high pH favor the formation of Mn (II) hydroxides. E_H values of greater than -0.1 favor the reduction to Mn (IV) oxides.

As temperature affects reaction kinetics, it may therefore affect the formation of post-filtration solids. In a British Nuclear Fuel Limited (BNFL) study published by Hildred, et al. (2000), effects of temperature on particle formation were briefly examined. The study indicated that as temperature increased, particles became more crystalline in structure. Cho et al. (2000) investigated the formation of lepidocrocite fine particles by oxidation of ferrous hydroxide between the temperatures of 20 ºC and 30 ºC and reported that an increase in temperature resulted in increased reaction rates and smaller lepidocrocite particle sizes.

Filter pore size was examined to investigate the hypothesis that submicron particles agglomerated into visible solids. A larger filter pore size (0.45 μm vs. 0.1 μm) should allow a larger number of smaller particles to pass into the filtrate. Therefore, a larger mass of small particles may be present in filtrate that is treated with larger filter pore sizes. Agglomeration of the smaller particles could result in the formation of visible solids. Likewise, fewer post-filtration solids are expected in filtrates that are filtered at 0.1 μm.

Several researchers have reported the effects of light and ionizing radiation on the formation of submicron sized particles. Mallick, et al. (2001) reported that ultraviolet (UV) irradiation of seeded gold particles produced nanoparticles with size and shape control. Kuga, et al. (1996) showed that UF_5 nano-particles were photoproduced by InfraRed MultiPhoton Dissociation, and that the formation of particles was enhanced by ionizing radiation from an alpha (α)-emitting Am-241 source. These observations indicate that particle growth can be affected by light energy and radiation energy.

Both reducing and oxidizing environments could also impact the formation of post-filtration solids. Kamei and Ohmoto (2000), reported that the rate of oxidation in an aqueous solution was approximately equal to the rate of dissolved oxygen consumption. In a study on the formation of particles by oxidation of an aqueous suspension of ferrous hydroxide, Cho, et al. (2000) observed that increasing the oxygen concentration in a system decreased the formation of particles from 0.60 μm to 0.35 μm.

3.0 EXPERIMENTAL DETAIL

The experimental methods used to accomplish the research objectives consisted of preparing a simulant, treating the simulant to oxidize and precipitate metal cations, filtering it at 0.1 μm to collect filtrates, exposing filtrates to several physical and chemical conditions for either 48 hours or 16 days depending on the experimental requirements, and analyzing the filtrates to determine the quantity and composition of post-filtration solids. Each of these aspects will be discussed in detail in the following sections.

Initially, post-filtration solids formation was monitored visually for a 48-hr period. During this period, particle size measurements were taken in an attempt to obtain kinetic data. These efforts were abandoned due to the formation of visible solids in the filtrates before the measurement of sub-micron and micron sized particles. The initial 48-hr period was selected because the process flow sheet called for processing through the ion exchange resin within 48 hours. Subsequent discussions at Hanford during a review indicated that filtrates might require one week to process through the ion exchange media. Therefore the author made a decision to visually monitor the filtrates for approximately 16 days.

3.1 SIMULANT PREPARATION

Experiments were performed with simulant wastes representing the contents of Hanford tanks 241-AN-107 and 241-AN-102. Simulant recipes shown in Appendix A (Eibling and Nash, 2001; Eibling, 2003) were prepared using ACS-grade chemicals. Replicate simulants were prepared using the WSRC-recipes shown in Table A.1 and A.2. Simulants were prepared in sufficient quantities to replicate all proposed experiments. The 241-AN-107 simulant pair was aged under atmospheric conditions, in a closed Nalgene® container for a period of one month prior to conducting experiments. Replicate 241-AN-102 simulants were aged under a nitrogen blanket for a period of one week prior to experimentation and stored under nitrogen for the duration of the investigation. After preparation and aging, simulants were diluted to 6 M sodium immediately prior to conducting each experiment.

During the investigation, visual observations regarding changes in color of the simulants and spectrophotometer measurements were used to indicate chemical or physical changes in the simulants with time. Slight color changes were apparent during the first week of aging. Generally simulants became slightly darker in color. Changes in the ultraviolet and visible wavelength spectra (190-1100 nm) were monitored using a Beckman DU Series 600 Spectrophotometer.

3.2 BASELINE EXPERIMENTS

Baseline experiments were conducted for each of the waste simulants (241-AN-107 and 241-AN-102). Replicate aliquots of the simulants were diluted to a sodium concentration of 6 M and heated to 50 ^{o}C in a circulating water bath. Simulants were then adjusted to 1 M free hydroxide by the addition of 17 M sodium hydroxide (NaOH). One molar strontium nitrate

($SrNO_3$) was added to the reaction mixture to achieve a final concentration of 0.075 M strontium (Sr). After reacting for a period of 15 minutes, 1 M sodium permanganate ($NaMnO_4$) was added to achieve a final concentration of 0.05 M permanganate (MnO_4^-), and the suspension was allowed to react for a period of 4 hours. Following the reaction period, the mixture was cooled to room temperature (23-25 ^oC) in a re-circulating water bath, centrifuged to remove bulk solids and filtered at 0.1 micrometers. Filtrates were collected and stored in the dark under a nitrogen blanket during the observation period. Details of the above procedure are provided in Bannochie, 2002.

3.3 PRIMARY EFFECTS STUDY

Variations from the base case treatment and filtrate conditions are summarized in Table 3.3.1 for the AN-107 and AN-102 studies. Treatment variables (hereafter referred to as reaction variables) examined the effects of reaction temperature, free sodium hydroxide concentration, reagent concentrations, and shear level of the precipitate on post-filtration solids formation. Filtrate variables examined the effects of light intensity, temperature of the filtrate, filtration at 50 ^oC (omitted for AN-102), filter pore size (omitted for AN-102), and oxidation-reduction potential (ORP) on post-filtration solids formation. Light intensity was adjusted by storing the filtrate directly under a fluorescent light as opposed to the base case conditions of being stored in the dark. The light intensity at the surface of the filtrate was measured to be 1600 Lux. To examine the effect of filtrate temperature, the filtrate was heated to 100 ºC for eight hours. Filtrates were also sparged with oxygen and nitrogen (omitted in AN-102) gases in an attempt to lower or raise the bulk redox potential of the filtrate.

Table 3.3.1 Variations From the Base Case Included in the Primary Effects Study for 241-AN-107 and 241-AN-102

AN-241-107	AN-241-102
Reaction Variables	**Reaction Variables**
15 °C Rxn	
25 °C Rxn	25° C Rxn
0.01 M Sodium Permanganate	0.01 M Sodium Permanganate
0.25 M Sodium Permanganate	0.03 M Sodium Permanganate
0.01 M Strontium Nitrate	
0.02 M Strontium Nitrate	0.03 M Strontium Nitrate
0.0 M added NaOH	0.0 M added NaOH
0.2 M added NaOH	
Shear @ 10,000 RPM	Shear @ 10,000 RPM
Filtrate Variables	**Filtrate Variables**
Light	Light
Filter Pore Size	
8 Hr Hold @ 100 °C	8 Hr Hold @ 100 °C
Oxygen Sparge	Oxygen Sparge
Nitrogen Sparge	
Filter @ 50 °C	
	NOC Variables
	NOC Base Case
	NOC 0.01 M Sodium Permanganate
	NOC Light
	NOC Oxygen

3.4 SECONDARY EFFECTS STUDY

Synergistic or cross effects for selected primary effects variables were investigated for both 241-AN-107 and -102 simulants. Variables investigated for the AN-107 simulant were variations from the Newly Optimized Conditions (NOC) and included the variables that provided a negative main effect response during the primary effects study. Experimental conditions for the NOC included dilution to 6 M Na, reaction at 25 °C for 4 hours, addition of 0.3 M sodium hydroxide, and 0.03 M strontium nitrate and sodium permanganate, filtration at 0.1 μm, and storage in the dark under nitrogen. Variables investigated included the cross of a reaction with 0.01 M, or the base case value of 0.03 M, sodium permanganate with the storage conditions noted in Figure 3.4.1. In addition to investigating the second order effects, a factorial design was used to obtain both primary effects and tertiary effects for a 2^3 design. This design was used to obtain primary effects data for the NOC because the primary effects study for AN-107 did not include the NOC. Each experiment was replicated.

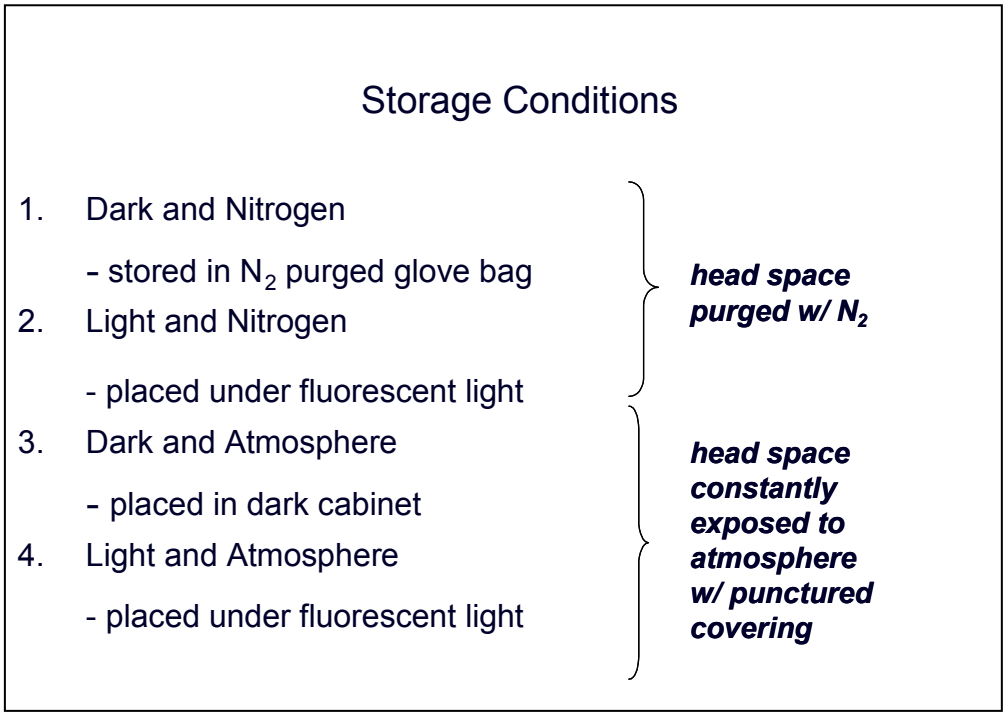

Figure 3.4.1 Storage Conditions for the 241-AN-107 Factorial Design Experiments

Experimental conditions for the 241-AN-102 secondary effects study are summarized in Figure 3.4.2 and focus on the zero effect variables from the primary effects study crossed with selected reaction and filtrate variables. This study examined the secondary effects for the baseline experiments only. The secondary effects of 0.0 M added sodium hydroxide and 25 °C reaction temperature crossed separately with 0.03 M strontium nitrate, 0.03 M sodium permanganate, light and oxygen sparge were investigated. These experiments were also replicated.

3.5 ANALYSIS OF FILTRATES AND POST-FILTRATION SOLIDS

During the observation period, 10-mL aliquots of the filtrates were collected periodically and filtered at 0.1 μm. The aliquots were then acidified to pH 1 or below and analyzed by ICP-AES to determine the concentration of the important cations in the filtrates. These data were used to evidence the formation of post-precipitation solids over time. The filtrates were also monitored visually throughout the observation period. Additionally, the E_H was measured periodically throughout the observation period for baseline filtrates as well as those sparged with oxygen and nitrogen in order to determine the ability of these variables to affect the bulk redox potential of the filtrate.

At the end of the observation period, the filtrates were re-filtered at 0.1 μm. Filter solids were then analyzed gravimetrically to determine the quantity of solids produced. Visual observations were made to give a general indication of the solids composition. In addition,

filter solids were dissolved in 0.5 M nitric acid and analyzed by ICP-AES to determine the major cations present in the particulate mass.

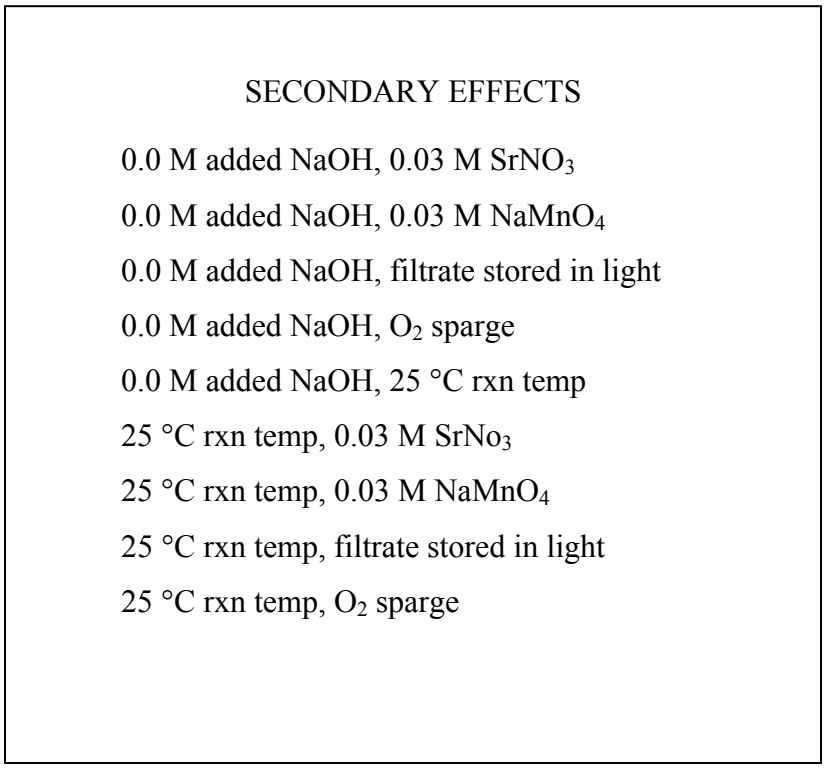

Figure 3.4.2 Secondary Effects Experiments Conducted for the 241-AN-102 Simulant

4.0 DISCUSSION

4.1 CHARACTERIZATION OF SIMULANTS 241-AN-107 AND 241-AN-102

Simulants 241-AN-107 and 241-AN-102 were prepared in replicate bulk quantities sufficient to conduct all of the first and second order experiments. Replicate 241-AN-107 simulants were designated as simulant 7 and 8, and replicate 241-AN-102 simulants were designated as simulant A and B. The simulants were aged at least one week before conducting the experiments. During the first week after preparation, ultraviolet/visible (UV/VIS) analysis was obtained to compare to similar scans collected during the experimental phase of this work. In addition, an aliquot of each simulant was analyzed by ICP-AES to determine the actual cation concentration in the simulant.

4.1.1 UV/Vis Analysis

UV/VIS scans are shown in Figures 4.1.1.1 through 4.1.1.8 for the 241-AN-107 and 241-AN-102 simulants. Scans were obtained using a 1 cm fused silica cell over a wavelength range of 200 to 1100 nm and a 0.1 cm fused silica cell over the ultraviolet range of 200 to

400 nm. An examination of the scans using the 1 cm cell did not reveal significant absorption in the visible range for any of the simulants. Ultraviolet scans using the 0.1 cm cell revealed significant absorption, but little difference over the 51 to 58 days monitored for the simulants. These data indicate that changes in the composition of the simulants with time as measured by UV/VIS did not appear to be significant.

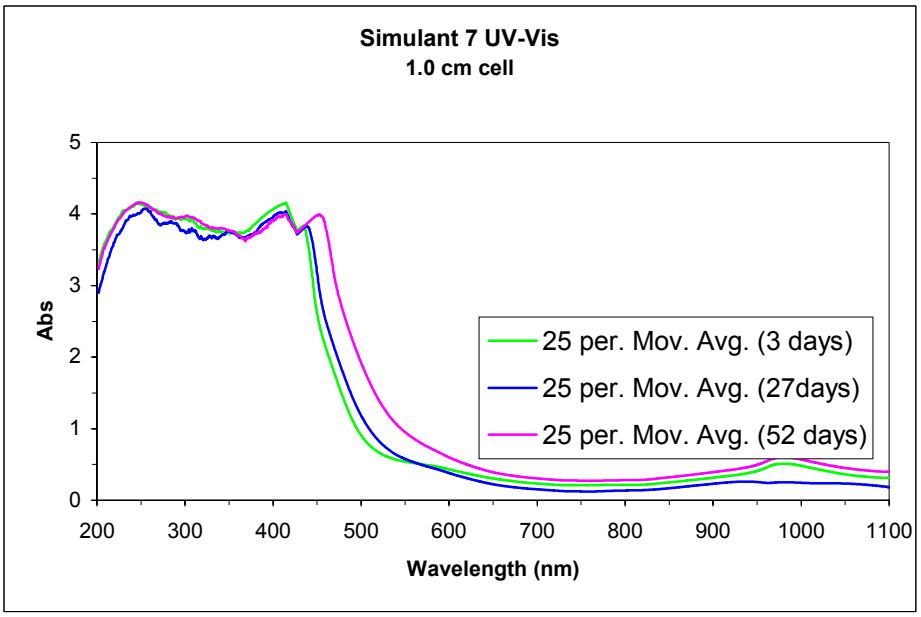

Figure 4.1.1.1 UV/VIS Spectra of Simulant 7 Used in the 241-AN-107 Experiments

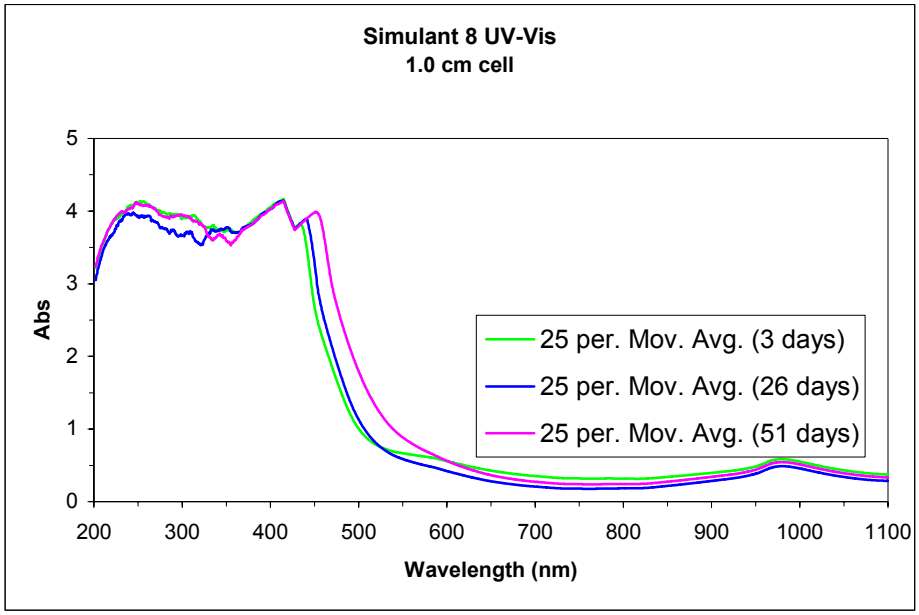

Figure 4.1.1.2 UV/VIS Spectra of Simulant 8 Used in the 241-AN-107 Experiments

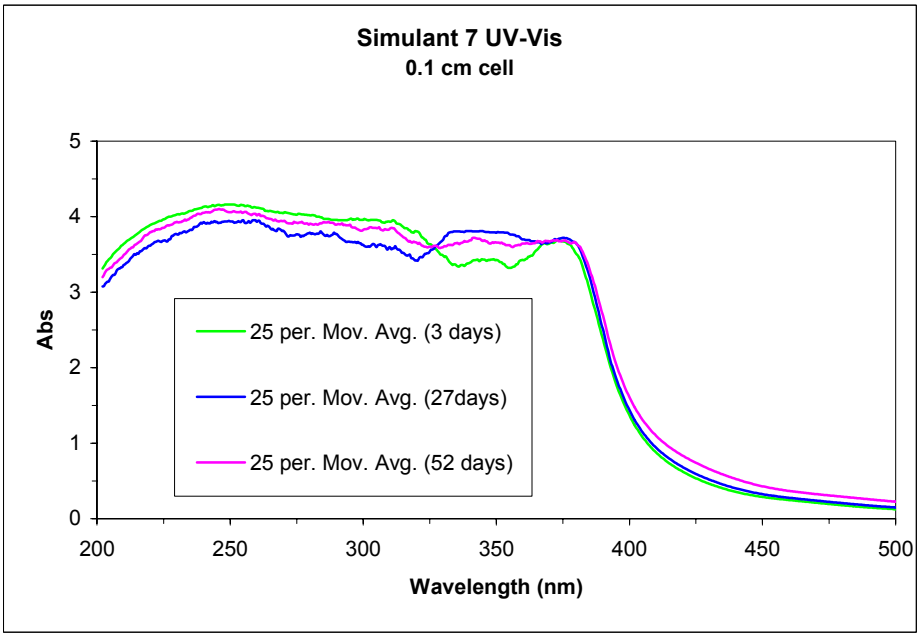

Figure 4.1.1.3 UV Spectra of Simulant 7 Used in the 241-AN-107 Experiments

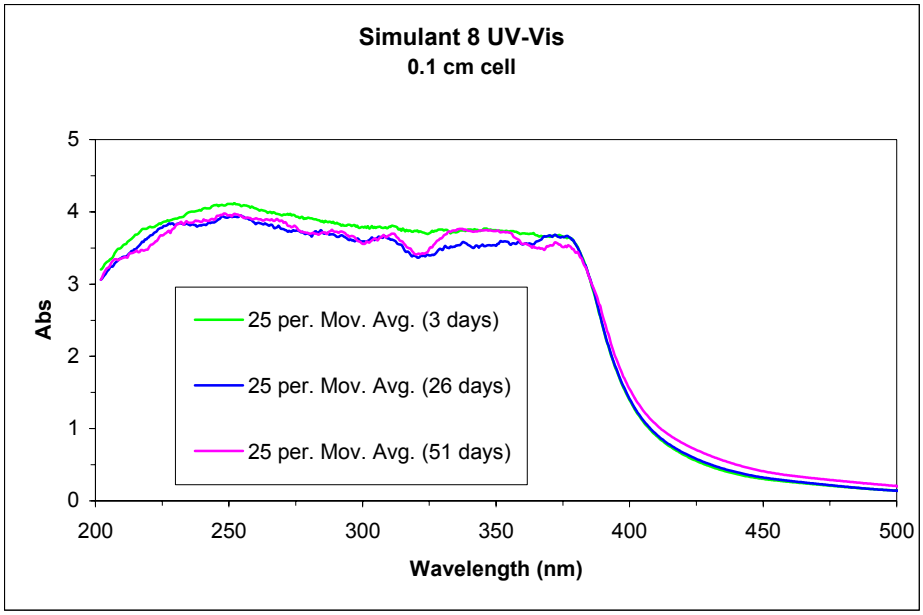

Figure 4.1.1.4 UV Spectra of Simulant 8 Used in the 241-AN-107 Experiments

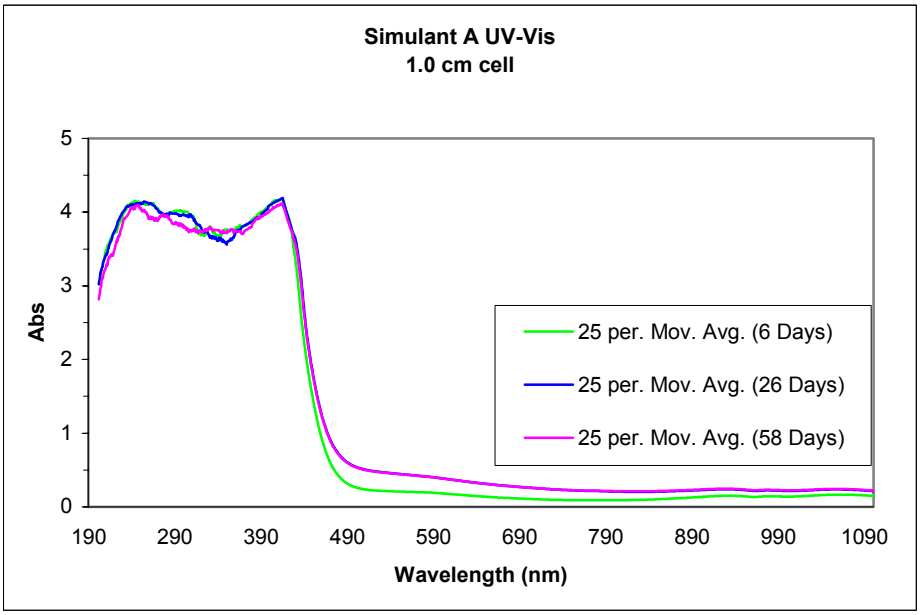

Figure 4.1.1.5 UV/VIS Spectra of Simulant A Used in the 241-AN-102 Experiments

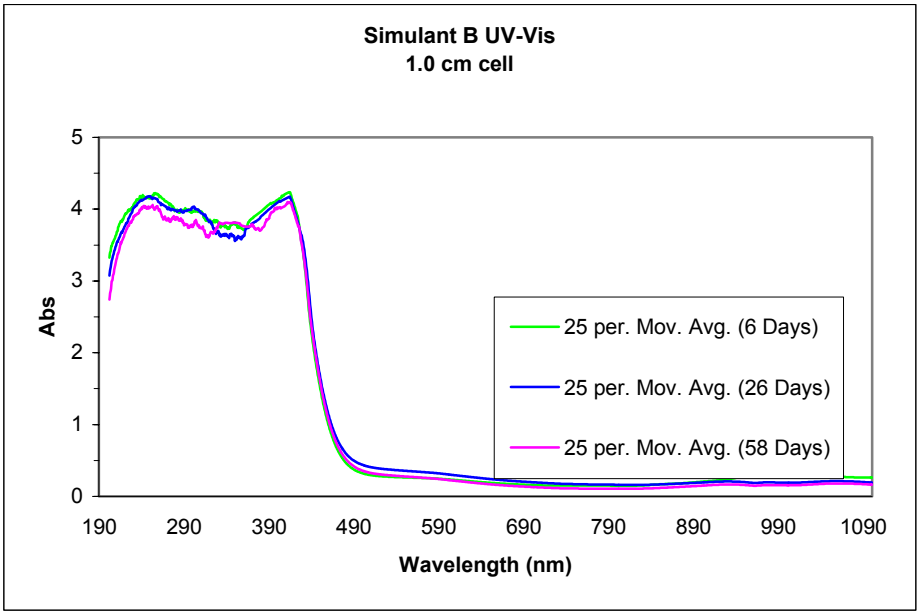

Figure 4.1.1.6 UV/VIS Spectra of Simulant B Used in the 241-AN-102 Experiments

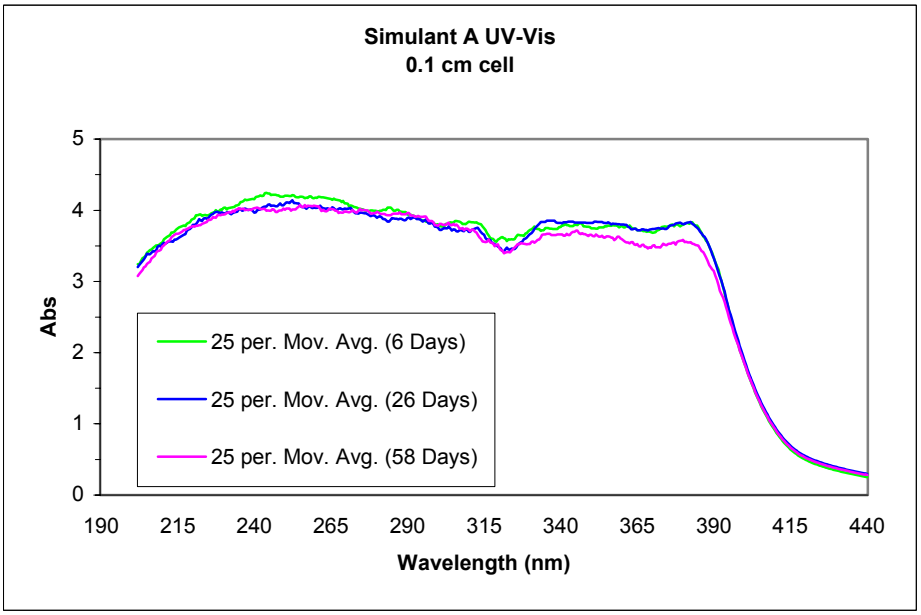

Figure 4.1.1.7 UV Spectra of Simulant A Used in the 241-AN-102 Experiments

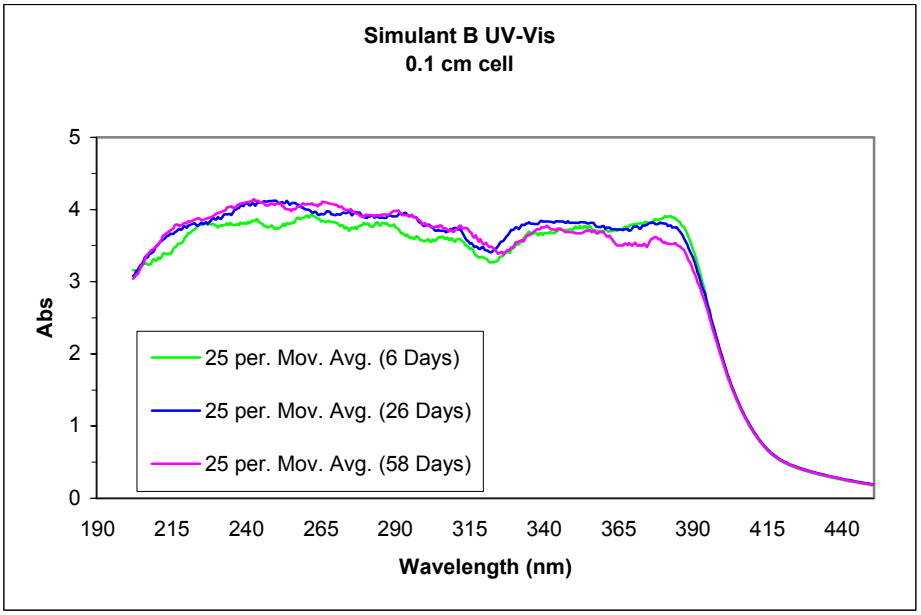

Figure 4.1.1.8 UV Spectra of Simulant B Used in the 241-AN-102 Experiments

4.1.2 ICP Analysis

Cation concentrations in simulants used during the AN-107 and AN-102 post filtration studies are shown in Table 4.1.2.1. Target values are shown to provide comparison with measured concentration. For most of the cations, measured values agree reasonably well with target values with the exception of phosphorus and potassium. Sodium levels were not measured by ICP-AES.

Table 4.1.2.1 Concentration of Selected Cations in the AN-107 and AN-102 Simulants at 6M Na.

	AN-107 Sim 7	AN-107 Sim 8	AN-107 Avg	AN-107 Target	AN-102 Sim A	AN-102 Sim B	AN-102 Avg	AN-102 Target
Elem	mg/L	mg/L	mg/L	mg/L	mg/L	mg/L	mg/L	mg/L
Al3082	514	430	472	386	9899	9846	9872	9231
B_2497	33	33	33	35	25	25	25	27
Ca3179	871	625	748	591	364	372	368	369
Ce4186	55	53	54	52	ND	ND	ND	32
Cr3578	140	134	137	177	201	199	200	190
Cu3247	33	33	33	30	19	19	19	19
Fe2599	1656	1662	1659	1691	30	30	30	31
K_7664	2207	2145	2176	1808	1668	1688	1678	1467
La3949	53	49	51	45	13	14	14	12
Mg2790	13	10	12	25	ND	ND	ND	0
Mn2576	551	557	554	564	21	21	21	23
Mo2020	39	38	39	36	36	36	36	23
Nd4061	109	103	106	95	26	26	26	25
Ni2316	537	540	538	531	310	314	312	313
P_1774	484	481	482	362	1931	1280	1606	1355
Pb2203	397	397	397	388	134	136	135	138
Si2516	6	7	7	0	20	18	19	0
Sr3464	9	6	7	7	2	2	2	2
Zn2062	47	48	48	46	4	4	4	4
Zr3391	65	62	64	70	9	10	10	9

4.2 PERMANGANATE OXIDATION REACTION

4.2.1 Visual Observations During The Reaction

Replicate 241-AN-107 simulants (simulant 7 and 8) were observed to be shades of dark coffee before initiation of the permanganate reaction. Simulant 8 was slightly darker than simulant 7. The addition of strontium nitrate to the reaction mixture resulted in the immediate formation of a white crystalline solid. Immediately following the addition of sodium permanganate, a large mass of brown precipitate formed, thereby masking the actual color of the reaction mixture.

Filtrate colors ranged from a light olive color to a dark coffee color with simulant 7 filtrates being lighter than simulant 8 filtrates. Base case reactions were replicated throughout the study, and noticeably lighter filtrates were observed as the simulant aged even though visible absorbance did not change noticeably during the study period. Filtrates for the base case condition were generally medium coffee color. Those exposed to light were light olive. Simulants treated with 1.0, 0.2 and 0.0 M added NaOH were successively lighter in color beginning with a dark coffee color. Simulants treated with 0.025 and 0.01 M sodium permanganate had an increasingly darker coffee color than the base case condition of 0.05 M. Digital photographs of the filtrates were taken and are included in Appendix B.

241-AN-102 simulants were observed to be greenish brown before reaction. During the reaction, the dark mass of precipitate formed masked the simulant color. However, after filtering, distinct colors were apparent in the filtrates. Most of the reaction conditions produced filtrates that exhibited a greenish yellow color. Filtrates that differed in color were those exposed to light, which appeared to take on a distinctly lime green color; those exposed

to oxygen, which became darker and took on an orange tint; those reacted with 0.03 M strontium nitrate, which were green in appearance; and those reacted with lower concentrations of sodium permanganate, which took on an orangish brown color that was correspondingly darker with lower concentrations of sodium permanganate. The latter filtrates lost much of their brown tint and became more yellow upon aging. Digital photographs are included in Appendix F.

4.3 PRELIMINARY STUDIES

During the early stages of this investigation, two preliminary studies were conducted before final reaction conditions were established for both the 241-AN-107 and -102 simulants. These experiments were conducted using the 241-AN-107 simulant to gain familiarity with the reaction and to evaluate the formation of post-filtration solids for 0.0 M added and 1.3 M added sodium hydroxide (conditions were to have been at 1.0 M added sodium hydroxide). Also included in these preliminary studies were many of the variables ultimately promulgated for the design of the primary and secondary effects studies.

Listed in Table 4.3.1 is a summary of the results for the 0.0 M sodium hydroxide experiments. Included are replicates of the base case scenario and several experiments conducted at reaction temperatures of 50 °C and 25 °C. Also included in the table are days noting the presence or absence of solids in each of the filtrates. The importance of these results is not found in the details, but in the overall summary of the observations. First, for the base case experiments, post-filtration solids were not observed during the observation period (28 to 37 days). Secondly, for experiments conducted at 50 °C post-filtration solids were observed before the 28-day period only when air was sparged into the filtrates. Thirdly, with exception of one replicate, post-filtration solids were observed during the 28-day period for all experiments conducted at 25 °C. In summary, this initial study strongly suggests that reaction temperature and the presence of entrained air in the filtrates may play a role in the formation of post-filtration solids.

A summary of results for the second preliminary study, in which 1.3 M sodium hydroxide was added to the base case reaction, is provided in Table 4.3.2. The formation of post-filtration solids was examined for reaction variables (temperature and concentration of reactants), and several filtrate variables (light, filter pore size, oxygen sparge, nitrogen sparge, carbon dioxide sparge, and an elevated temperature of the filtrate). Unlike Table 4.3.1, the time that solids appeared in the filtrates is presented in hours. The overall observation is that solids formed within hours for all experiments. By comparison to results presented in Table 4.3.1, it appears that concentrations of 1.3 to 2.0 molar added sodium hydroxide significantly impact the formation of post-filtration solids within hours of the permanganate reaction and subsequent filtration at 0.1 μm.

Table 4.3.1 Presence of Solids in AN-107 Filtrates for the 0.0 M Sodium Hydroxide Preliminary Experiments

Condition	Time Solid Appeared (days)
Base Case	ND@37
Base Case Replicate	ND@28
50 °C Reaction	
▪ Light, 0.1 μm, Air Sparge	28
▪ Light, 0.45 μm, Air Sparge	28
▪ Dark, 0.1 μm, Air Sparge	28
▪ Dark, 0.45 μm, Air Sparge	28
▪ Light, 0.1 μm, N_2 Sparge	ND @ 28
▪ Light, 0.1 μm, N_2 Sparge	ND @ 28
▪ Light, 0.45 μm, N_2 Sparge	ND @ 28
▪ Light, 0.45 μm, N_2 Sparge	ND @ 28
▪ Dark, 0.1 μm, N_2 Sparge	ND @ 28
▪ Dark, 0.45 μm, N_2 Sparge	ND @ 28
▪ Dark, 0.45 μm, N_2 Sparge	ND @ 28
25 °C Reaction	
▪ Light, 0.1 μm, N_2 Sparge	11
▪ Light, 0.1 μm, Air Sparge	3
▪ Light, 0.1 μm, N_2 No Sparge	25
▪ Light, 0.45 μm, N_2 Sparge	8
▪ Light, 0.45 μm, Air Sparge	8
▪ Light, 0.45 μm, N_2 No Sparge	ND @ 25
▪ Dark, 0.1 μm, N_2 Sparge	11
▪ Dark, 0.1 μm, Air Sparge	1
▪ Dark, 0.1 μm, N_2 No Sparge	19
▪ Dark, 0.45 μm, N_2 Sparge	20
▪ Dark, 0.45 μm, Air Sparge	11
▪ Dark, 0.45 μm, N_2 No Sparge	20

Table 4.3.2 Presence of Solids in AN-107 Filtrates for the 1.3 M Sodium Hydroxide Preliminary Experiments

Condition	Time Solid Appeared (hours)
Base Case	15
Base Case Replicate	3
Light	10
Light Replicate	3
Filter Size 0.45 μm	15
Filter Size 0.45 μm Replicate	3
25 °C reaction	10
25 °C reaction Replicate	10
60 °C reaction	4
60 °C reaction Replicate	4
0.07 M Sodium Permanganate	15
0.07 M Sodium Permanganate Replicate	7
0.01 M Sodium Permanganate	6
0.01 M Sodium Permanganate Replicate	18
0.01 M Calcium Nitrate	<16
0.01 M Calcium Nitrate Replicate	<16
0.03 M Calcium Nitrate	<16
0.03 M Calcium Nitrate Replicate	<16
2 M added NaOH	9
2 M added NaOH Replicate	9
Filtrate Held for 8 Hours @ 100 °C	1
Filtrate Held for 8 Hours @ 100 °C Replicate	2
Oxygen Bubbled in Filtrate	2 (turbid)
Oxygen Bubbled in Filtrate Replicate	3 (turbid)
Nitrogen Bubbled in Filtrate	50
Nitrogen Bubbled in Filtrate Replicate	8.5
Carbon Dioxide Bubbled in Filtrate	2
Carbon Dioxide Bubbled in Filtrate Replicate	4

4.4 RESULTS OF THE 241-AN-107 EXPERIMENTS

The formal conduct of the 241-AN-107 experiments included an investigation to determine the effect of single variables on the formation of post-filtration solids (primary effects). Similarly, a second set of experiments was completed to determine second order synergistic effects on the formation of post-filtration solids (secondary effects). Data obtained for these experiments included visual observations to indicate the color of filtrates and to document the appearance of visible solids, ICP-AES analysis of the filtrates to document changes in cation concentrations with time, gravimetric analysis to document solids formation at the end

of the visual observation period, solubility of the precipitate in 0.5 M nitric acid, ICP-AES analysis to determine the cationic composition of the precipitate, and photographic record of both the filtrates and post-filtration solids formation. ICP-AES analyses were conducted using filtrates in which the waste sodium molarity was less than 6 molar due to the addition of reactants. These data have been normalized to 6 molar waste sodium for comparative purposes and should not be considered as measured quantities at 6 molar waste sodium.

4.4.1 Primary Effects Study

Visual Observations

Variables investigated for the 241-AN-107 primary effects study are listed in Table 4.4.1.1. The appearance of post-filtration solids during the 48-hr observation period is also included in the table. With exception of two experimental conditions, the 8-hr hold of the filtrate at 100 °C and the oxygen sparge, solids that formed during the 48-hr period were very light in color. The filtrates sparged with oxygen contained brown solids within six hours, and significant black solids formed in the filtrates held at 100 °C for 8 hours. The formation of brown solids in the filtrates sparged with oxygen is commensurate with permanganate reduction in alkaline media to manganese hydroxide, which is a white precipitate, and subsequent oxidation in the presence of air to the brown manganese (III) oxy-hydroxide and oxide and ultimately to the black manganese dioxide. Formation of black solids in the 8-hr hold filtrates supports the hypothesis that the precipitation reaction kinetics are too slow for the reaction to be complete after a 4 hour reaction time.

It is also important to note that a reduction of added sodium hydroxide from the base case condition of 1.0 M to 0.2 and 0.0 M resulted in no solids being formed during the 48-hr period. Recall also, for preliminary experiments conducted at 0.0 M added sodium hydroxide, at 50 °C, and in the absence of sparged air (Table 4.3.1), solids did not form in the filtrates during the 28-day observation period.

Both preliminary and primary effects studies strongly suggest that a low reaction temperature (25 °C), the presence of dissolved oxygen, and concentrations of added sodium hydroxide at 1.0 M favor the formation of post-filtration solids in the filtrate within the first 48 hours after ultra filtration. In addition, light may also promote the formation of solids. This observation was supported by experiments in which filtrates were exposed to laser light. During the preliminary experiments, base case filtrates were continuously exposed to a laser source. Visible solids formed within 48 hours of exposure.

Table 4.4.1.1 Presence of Solids in AN-107 Filtrates for the Primary Effects Study

PRIMARY EFFECTS STUDY	**Time Visible (hours)**	COLOR OF SOLIDS
Base Case	7	White, Some Brown @ 12-24 Hr
Base Case Replicate	7	White, Some Brown @ 12-24 Hr
Light	7	White, Some Brown @ 12-24 Hr
Light Replicate	7	White, Some Brown @ 12-24 Hr
Filter Size 0.45 M	7	White, Some Brown @ 12-24 Hr
Filter Size 0.45 M Replicate	7	White, Some Brown @ 12-24 Hr
25 °C reaction	6	White
25 °C reaction Replicate	6	White
0.01 M Sodium Permanganate	24-48	Turbid, Yellow
0.01 M Sodium Permanganate Replicate	24-48	Turbid, Yellow
Filtrate Held for 8 Hours at 100 °C	0	Significant Black Solids During Heating
Filtrate Held for 8 Hours at 100 °C Replicate	0	Significant Black Solids During Heating
Oxygen Bubbled in Filtrate	6	Brown colloids
Oxygen Bubbled in Filtrate Replicate	6	Brown colloids
Nitrogen Bubbled in Filtrate	48	White
Nitrogen Bubbled in Filtrate Replicate	48	White
0.025 M Sodium Permanganate	0	Possibly Some White Solids at 48 Hr
0.025 M Sodium Permanganate Replicate	0	Possibly Some White Solids at 48 Hr
Filter at 50 °C	3	White, Some Brown @ 12-24 Hr
Filter at 50 °C Replicate	48	White
0 M NaOH Added	0	None at 48 Hr
0 M NaOH Added Replicate	0	None at 48 Hr
0.2 M NaOH Added	0	None at 48 Hr
0.2 M NaOH Added Replicate	0	None at 48 Hr
0.01 M Strontium Added	24	White
0.01 M Strontium Added Replicate	24	White
0.02 M Strontium Added	24	White
0.02 M Strontium Added Replicate	24	White
15 °C reaction	48	White
15 °C reaction Replicate	48	White
10 Minute Shear	18	White
10 Minute Shear Replicate	18	White

Additional evidence supporting the theory that dissolved oxygen and possibly light promoted the formation of post-filtration solids was investigated by creating replicate filtrates for the base case condition where filtrates were stored under a nitrogen blanket in the dark and creating replicate filtrates stored under nitrogen in the light (1600 lux). Filtrates were stored under these conditions for 48 hours then purged with oxygen for 15 minutes and stored under an oxygen blanket for 48 hours. During the 48-hour periods, samples of the filtrates were filtered at 0.1 μm and the final filtrates analyzed by ICP-AES for manganese, iron and strontium. These data are summarized in Table 4.4.1.2 and include the average concentration in the filtrate and the standard deviation in parenthesis. By comparing the base case-N_2 data with the Light-N_2 data for each of the cations, there is no evidence to suggest the formation of Mn, Fe, or Sr solids in the filtrates. However, after a 15-min sparge of each of the test filtrates with oxygen, visible solids were observed at the end of the 48-hr period. ICP-AES analyses of these filtrates support the visual observation. The concentrations of both Mn and

Fe in the filtrates sparged with oxygen are significantly lower than concentrations measured in filtrates processed under a nitrogen blanket, suggesting the loss of Mn and possibly Fe solids from solution. Digital photographs of the particulate masses were taken to document the presence of solids in the filtrates purged with oxygen and are included in Figures 4.4.1.1 and 4.4.1 2.

Table 4.4.1.2 The Effect of Oxygen on the Concentration of Manganese, Iron, and Strontium in Filtrates

Sample	**Condition**	**AverageConcentration in Filtrate**		
		Fe mg/L (sd)	**Mn mg/L (sd)**	**Sr mg/L (sd)**
0528-211A	Base Case, N_2	44.3 (2.1)	33.1 (1.5)	76.6 (3.2)
0528-211B	Base Case, N_2	45.2 (1.4)	34.0 (1.0)	80.1 (2.2)
0528-211A	Base Case, O_2	42.1 (1.6)	22.5 (1.8)	77.1 (3.2)
0528-211B	Base Case, O_2	40.8 (1.1)	21.7 (0.9)	78.1 (1.9)
0528-111A	Light, N_2	45.1 (0.5)	34.0 (0.2)	81.6 (0.5)
0528-111B	Light, N_2	43.1 (1.5)	35.3 (1.1)	74.8 (2.3)
0528-111A	Light, O_2	40.7 (2.0)	25.0 (5.2)	79.5 (1.2)
0528-111B	Light, O_2	37.9 (2.9)	22.7 (4.7)	73.5 (2.5)

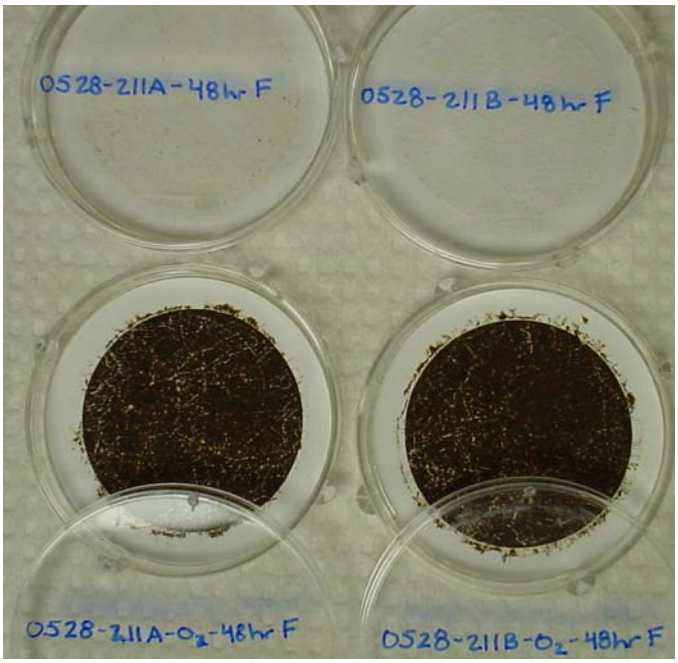

Figure 4.4.1.1 Particulates Collected After 48 hours Exposure to Oxygen for the Base Case Condition.

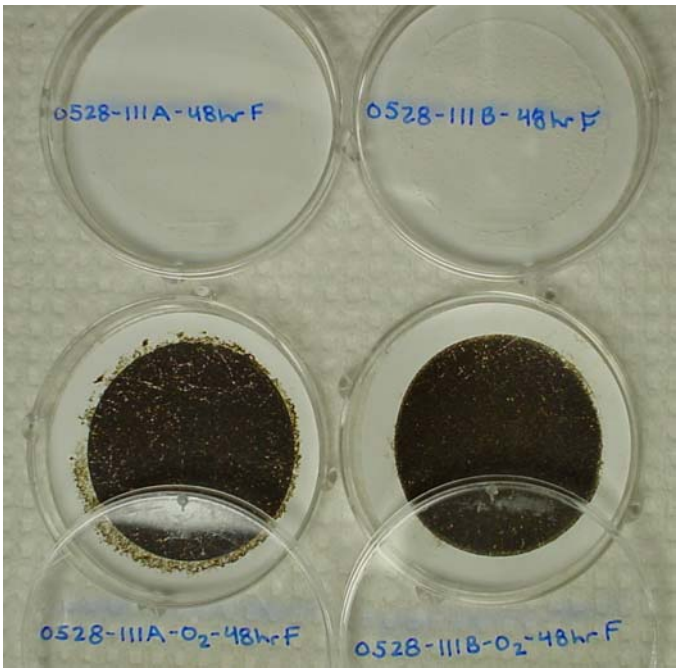

Figure 4.4.1.2 Particulates Collected After 48 hours Exposure to Oxygen for the Light Condition.

Change in Metals Concentration During the 48-Hour Observation Period for AN-107

During the 48-hr observation period, filtrate samples were collected and filtered at 0.1 µm at time zero and at 6, 12, 24, and 48 hours. Each of the filtrates was analyzed by ICP-AES to determine the concentration of the important cations in the simulant. A decrease in concentration of a cation would suggest the formation of post-filtration solids containing that cation in the filtrates. Included in Figures 4.4.1.3 through 4.4.1.7 are Mn, Fe, and Sr data for a base case condition, exposure to light, an 8-hr hold at 100 °C, and 0.0 M added sodium hydroxide, respectively. Similar plots of the ICP-AES data for the remainder of the variables investigated during the primary effects study are included in Appendix C. Tabulated data for all cations measured in the filtrates is also included in Appendix C.

Figure 4.4.1.3 Manganese, Iron and Strontium Concentration in the 0 – 48 hr. Base Case

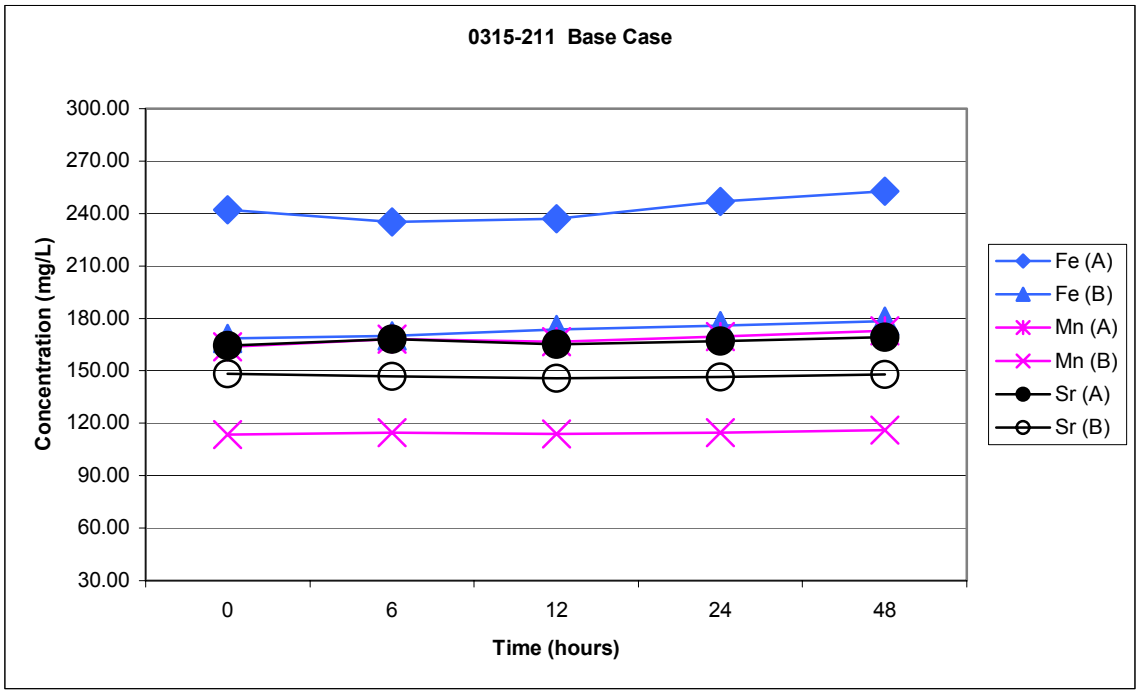

Filtrates

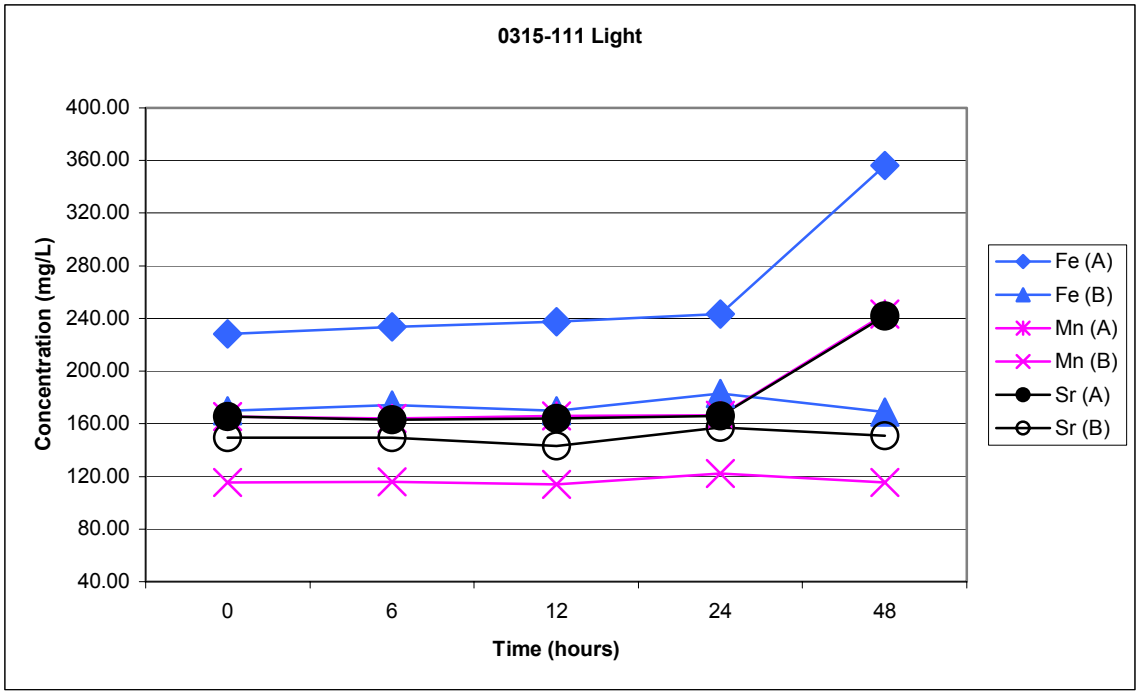

Figure 4.4.1.4 Manganese, Iron and Strontium Concentration in the 0 – 48 hr. Filtrate Exposed to Light

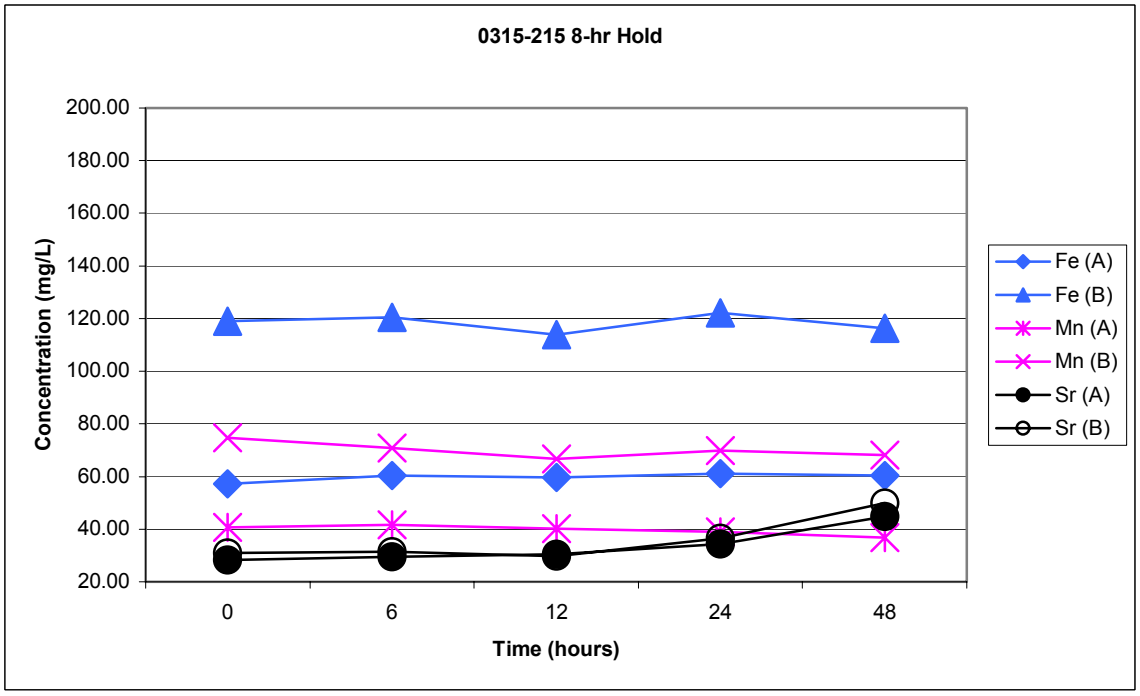

Figure 4.4.1.5 Manganese, Iron and Strontium Concentration in the 0 – 48 hr. Filtrate, 8-hr Hold at 100 °C Filtrates

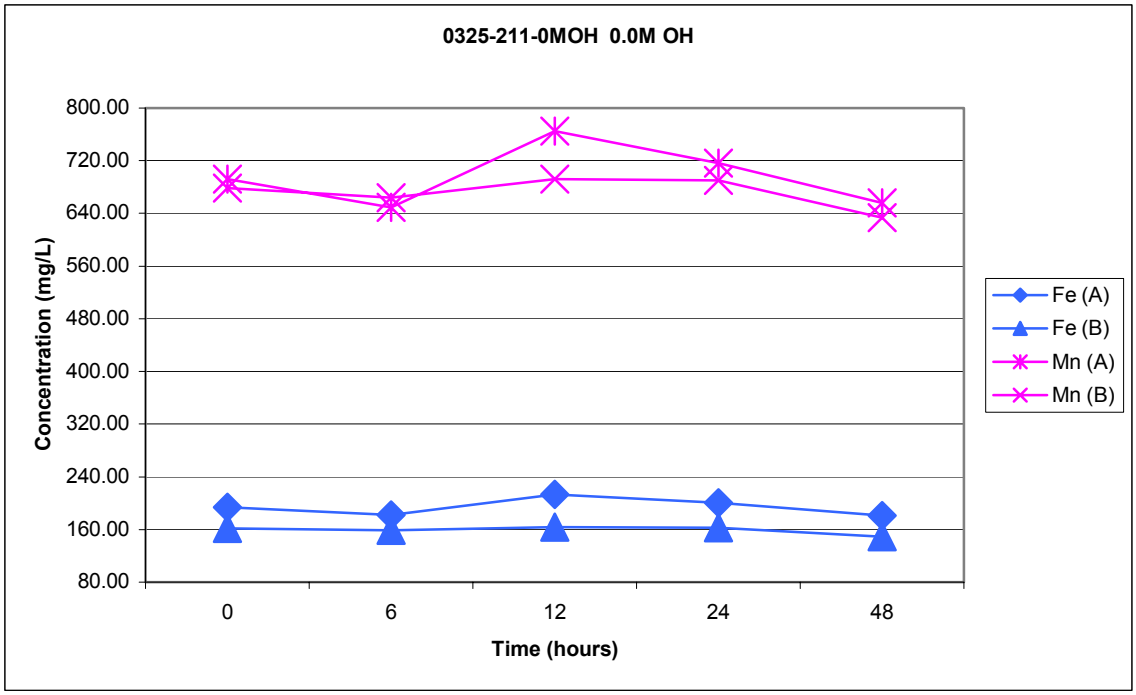

Figure 4.4.1.6 Manganese and Iron Concentration in the 0 – 48 hr. Filtrates With No Added NaOH

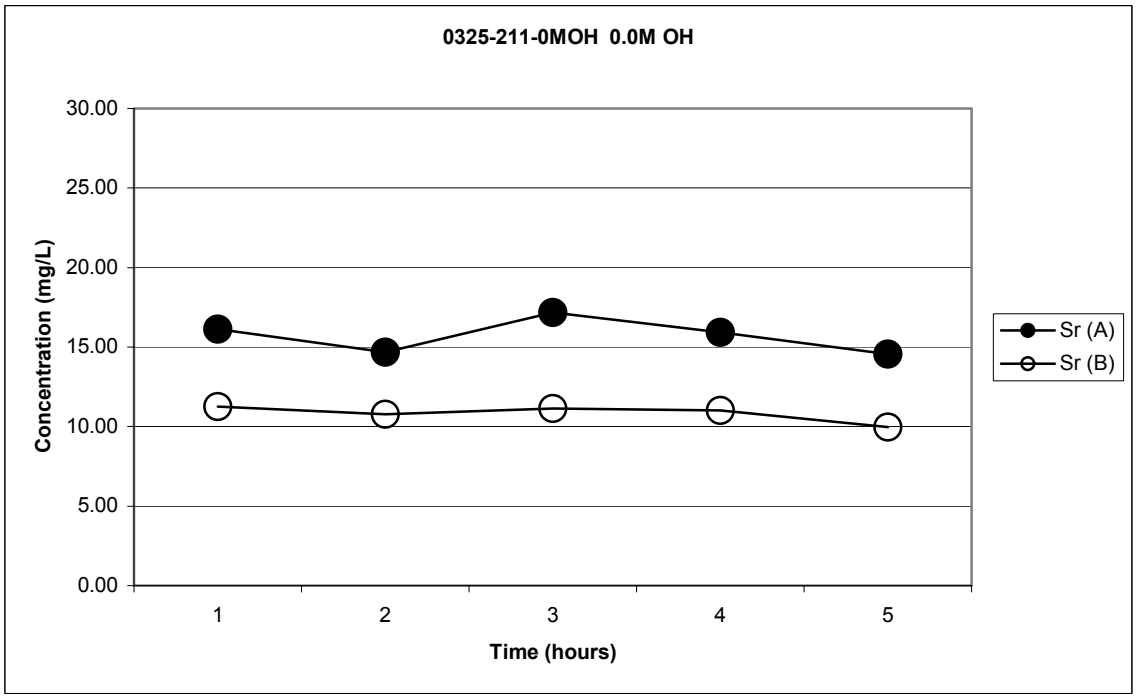

Figure 4.4.1.7 Strontium Concentration in the 0 – 48 hr. Filtrates With No Added NaOH

Two important observations can be made from examining the data presented in Appendix C. First, with exception of filtrates exposed to oxygen and filtrates held at 100 °C for 8 hours after the precipitation reaction, the concentration of the cations included in the data sets is relatively constant over the 48-hr period, providing no evidence that post-filtration solids formed during the period. To support the observed precipitation, digital photographs were taken of the particulate mass collected at the end of the 48-hr period and these are shown in Appendix D. The 0-48 hr plot for the filtrates exposed to oxygen (Figure C.13b) does not appear to be as invariant as the others, suggesting the loss of Mn solids and possibly Fe and Sr from solution. Second, there is a difference in the magnitude of the concentration for each of the cations as a function of treatment condition.

From the tabulated data in Appendix C, bar graphs representing the mean concentration for each cation measured for the base case condition, and two treatment variables (reaction temperature and added sodium hydroxide) are shown in Figures 4.4.1.8 through 4.4.1.11. Similar bar graphs for the remainder of the variables are included in Appendix C. Plotted in the bar graphs are mean data for all replicated base case conditions for each AN-107 simulant (simulant 7 or simulant 8) averaged over the 48-hr period and mean data for each treatment averaged over the 48-hr period for the appropriate simulant. Also included on the bar graphs are the appropriate error estimates. A careful review of the data presented here and in Appendix C indicates that the only cations that differed significantly between treatments and the base case condition were manganese, iron, strontium, neodymium, lanthanum, cerium and zirconium.

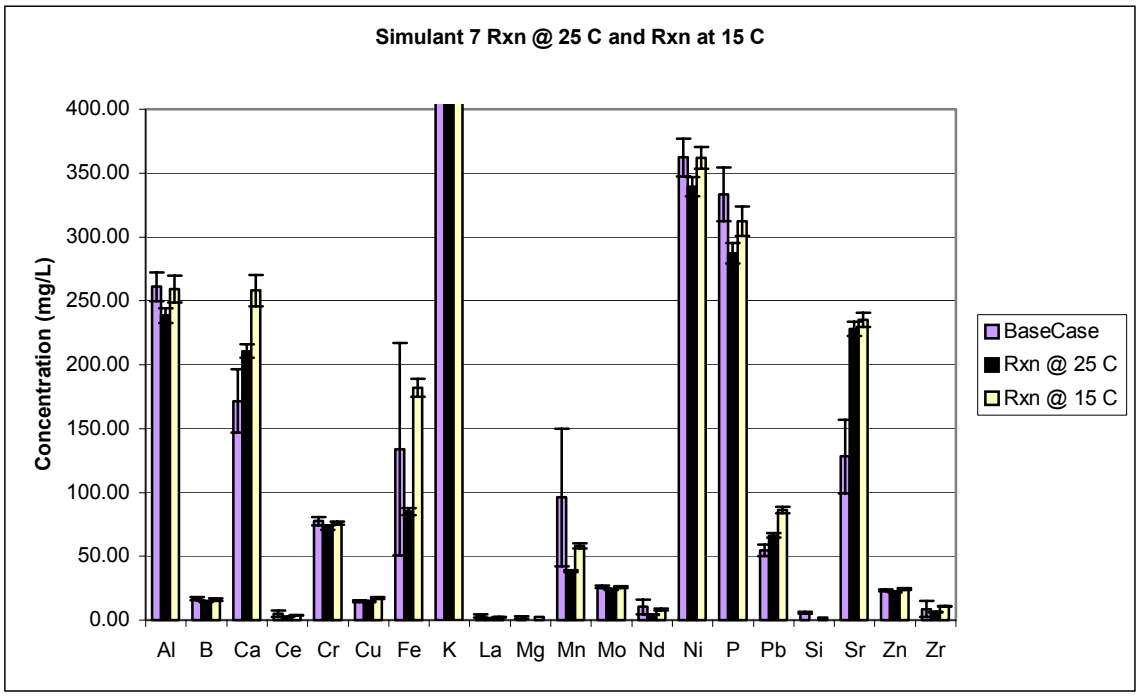

Figure 4.4.1.8a Mean Cation Concentration for the 0 – 48 hr. Reaction Temperature Filtrate for Simulant 7 (AN-107)

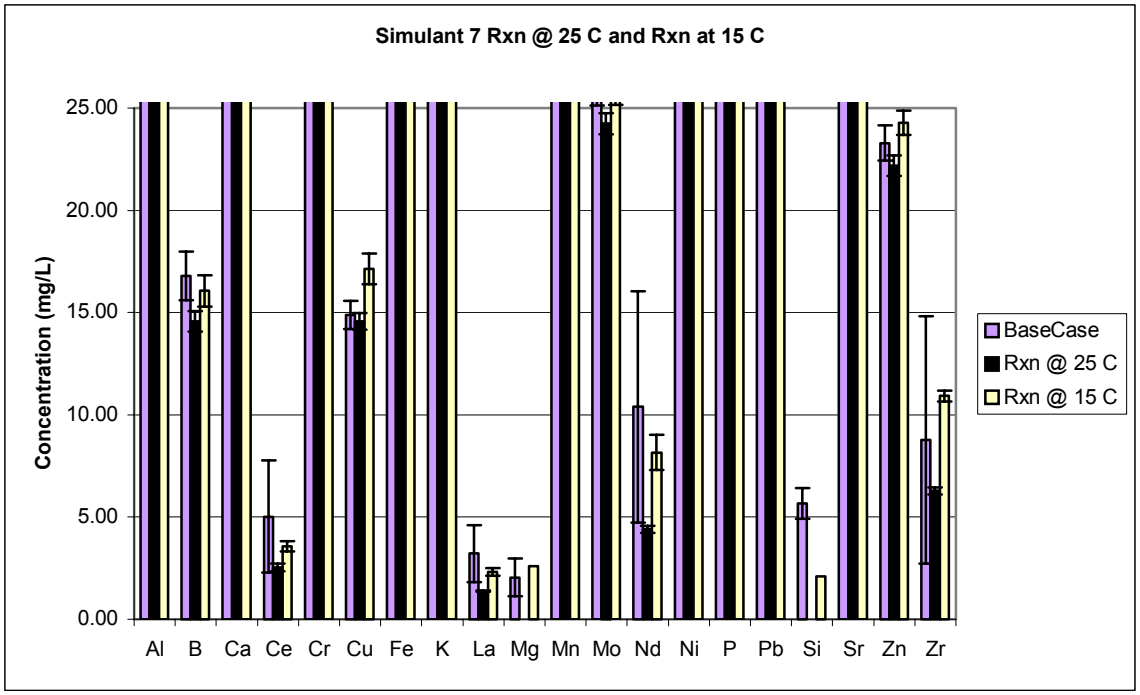

Figure 4.4.1.8b Figure 4.4.1.8a Scaled to see Minor Cations

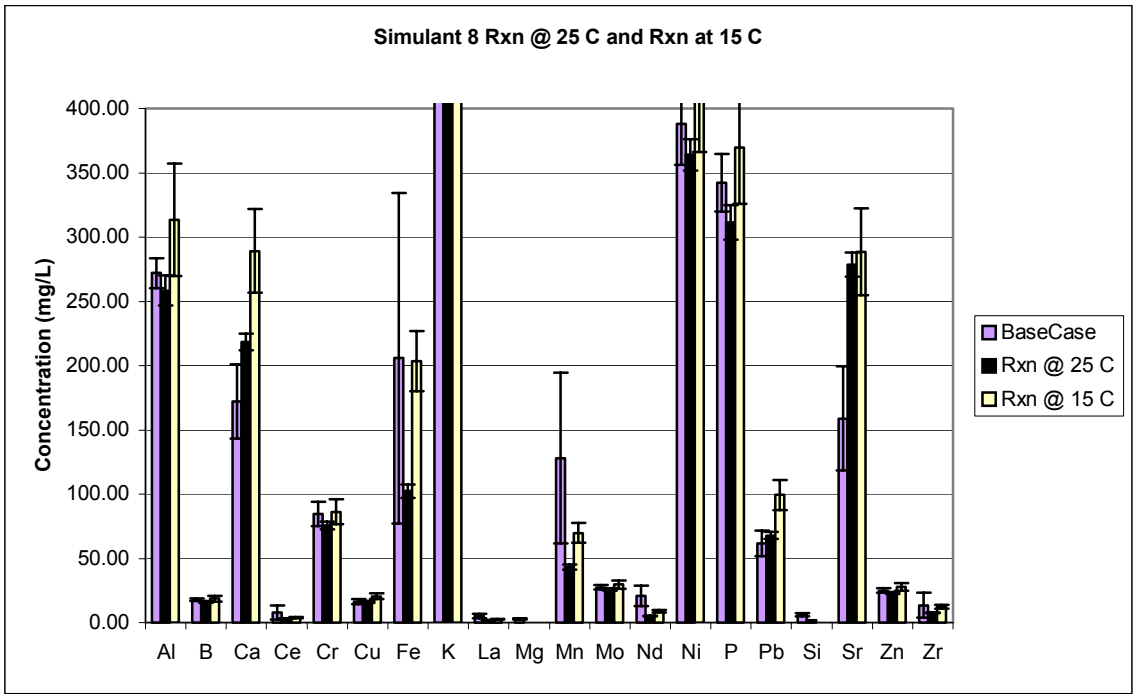

Figure 4.4.1.9a Mean Cation Concentration for the 0 – 48 hr. Reaction Temperature Filtrate for Simulant 8 (AN-107)

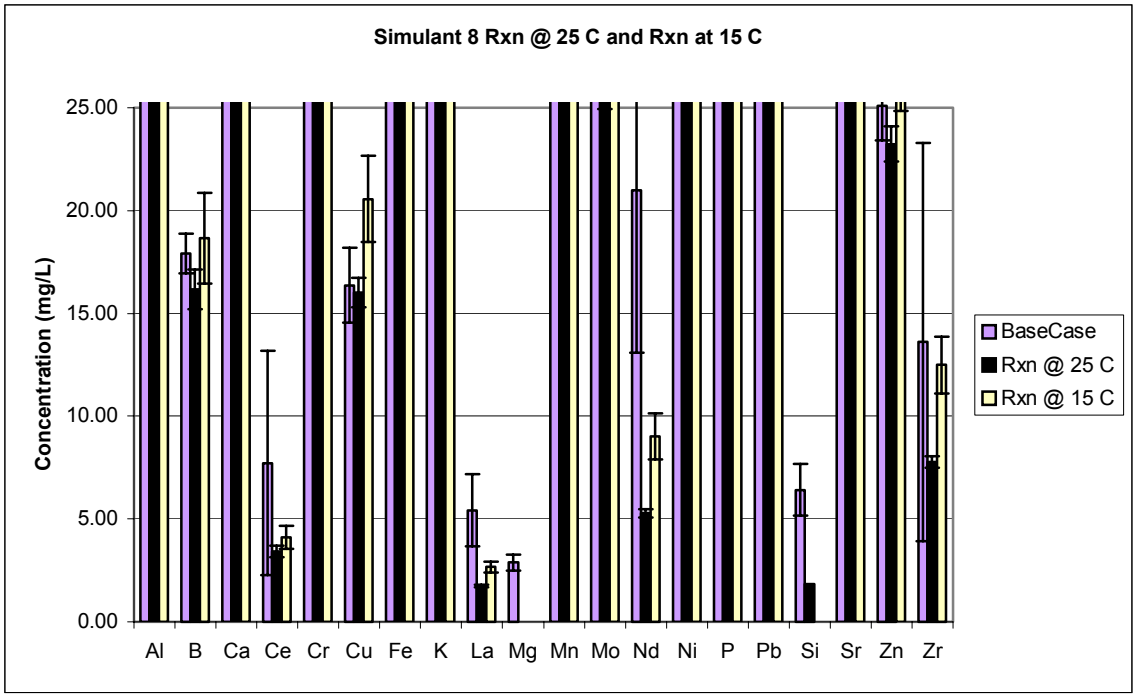

Figure 4.4.1.9b Figure 4.4.1.9a Scaled to see Minor Cations

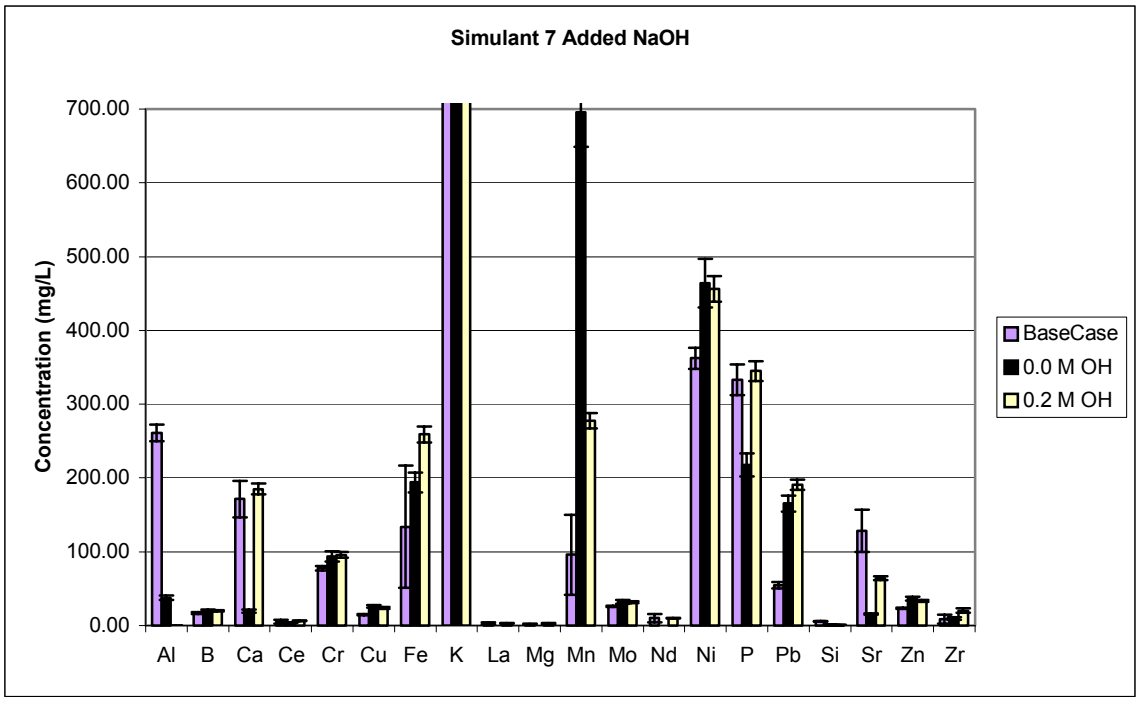

Figure 4.4.1.10a Mean Cation Concentration for the 0 –48 hr. Filtrates with Added NaOH for Simulant 7 (AN-107)

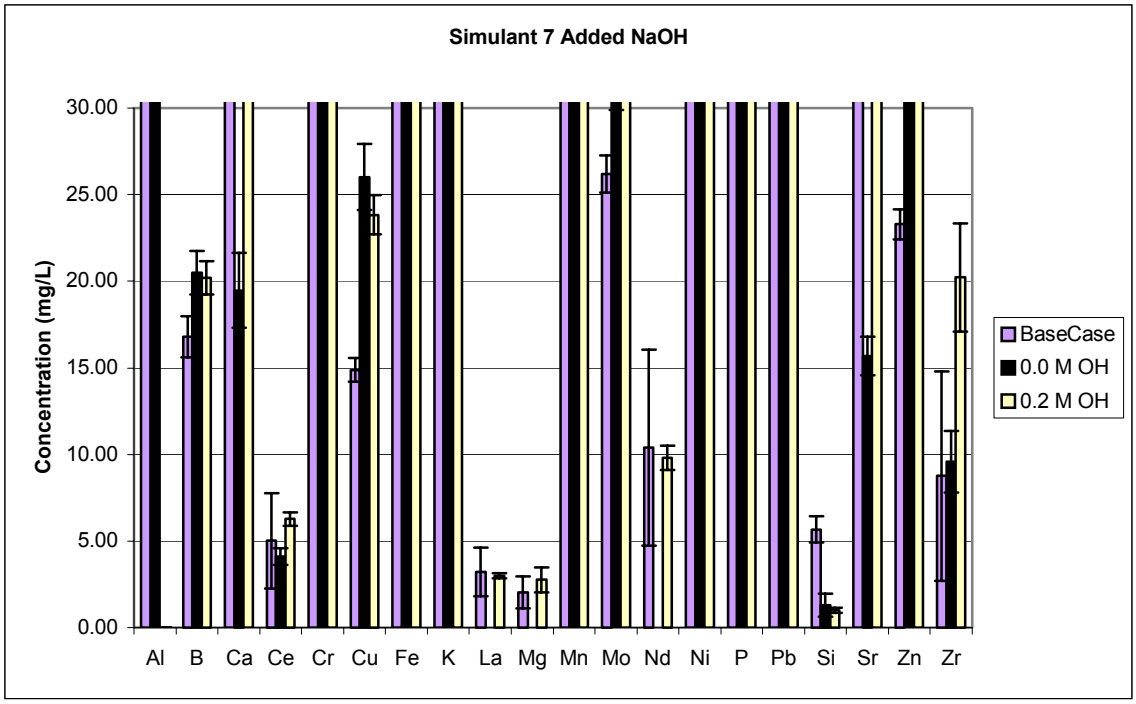

Figure 4.4.1.10b Figure 4.4.1.10a Scaled to see Minor Cations

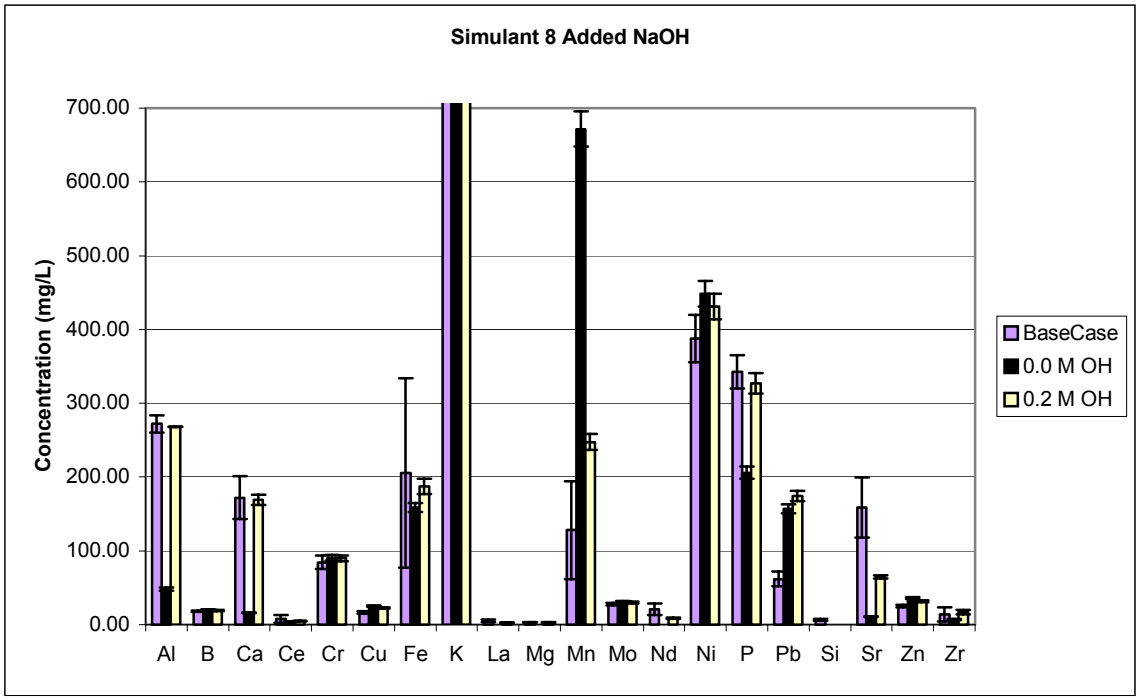

Figure 4.4.1.11a Mean Cation Concentration for the 0 – 48 hr. Filtrates with Added NaOH for Simulant 8 (AN-107)

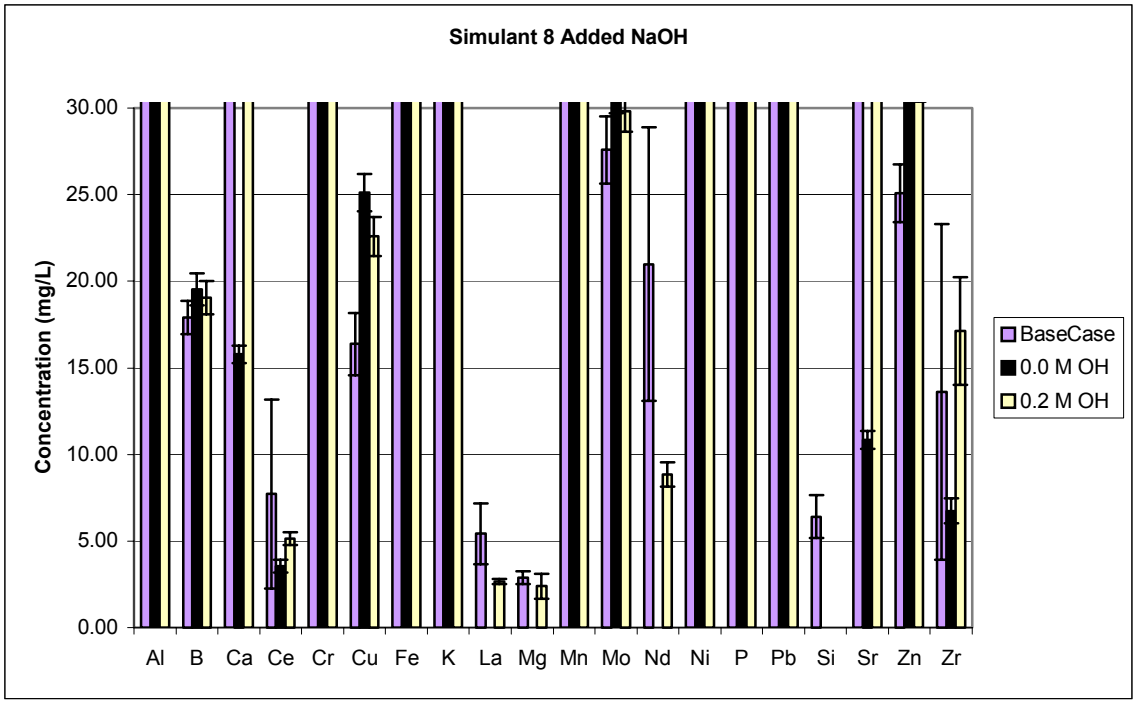

Figure 4.4.1.11b Figure 4.4.1.11a Scaled to see Minor Cations

Comparisons to the base case condition can also be made for all filtrate variables and reaction variables from these plots. Considering the filtrate variables, namely, sparged oxygen and nitrogen, light and filtration at 0.45 μm, and shear (Appended Figures C.14 through C.18), several observations can be made. Sparging the filtrates with nitrogen did not significantly affect the 0 to 48-hr average filtrate concentration of Mn, Fe, Sr, Ce, La, Nd, and Zr. This observation is plausible since purging the filtrates with nitrogen had little effect on the E_H of the bulk filtrate, (Figure 4.4.1.12). Exposing the filtrate to visible light also did not appear to be significant compared to the base case condition. However, filtering at 0.45 μm did seem to lower the concentration of the above cations with exception of strontium in the filtrates relative to the base case. This observation was unexpected since filtering at 0.45 μm would allow smaller colloids to pass the filter and thus represent a surface for particle agglomeration. It is plausible that filtering at 0.45 μm and acidifying the filtrate before ICP-AES analysis would result in a higher concentration of the cations compared to the base case, which was filtered at 0.1 μm. This observation remains unexplained.

Similar comparisons can also be made for the reaction variables, namely, reaction temperature, added sodium hydroxide, sodium permanganate addition and strontium nitrate addition. Each of these reaction variables were investigated for three levels; reaction temperature at 15, 25 and 50 °C, added sodium hydroxide at 0.0, 0.2, and 1.0 M, sodium permanganate addition at 0.01, 0.025, and 0.05 M, and strontium nitrate addition at 0.01, 0.02, and 0.075 M. These data are summarized on three-dimensional plots in Figures 4.4.1.13 through 4.4.1.16 respectively.

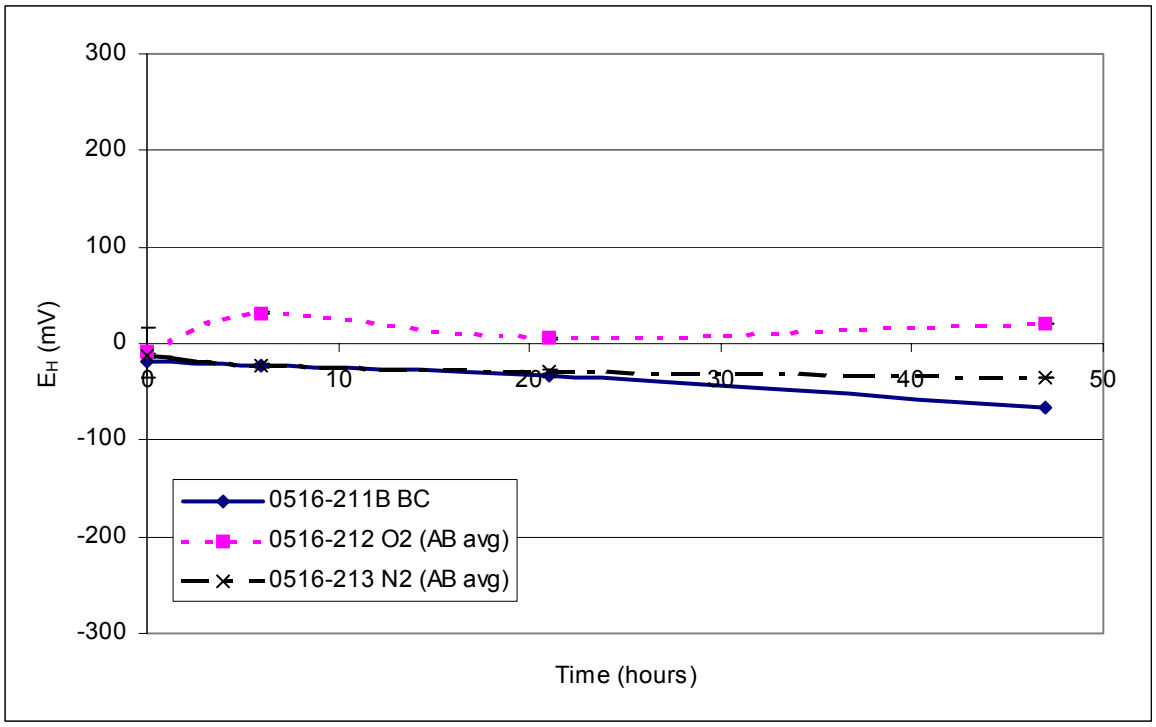

Figure 4.4.1.12 E_H Measurements for the AN-107 Base Case, Oxygen Purge, and Nitrogen Purge Filtrates

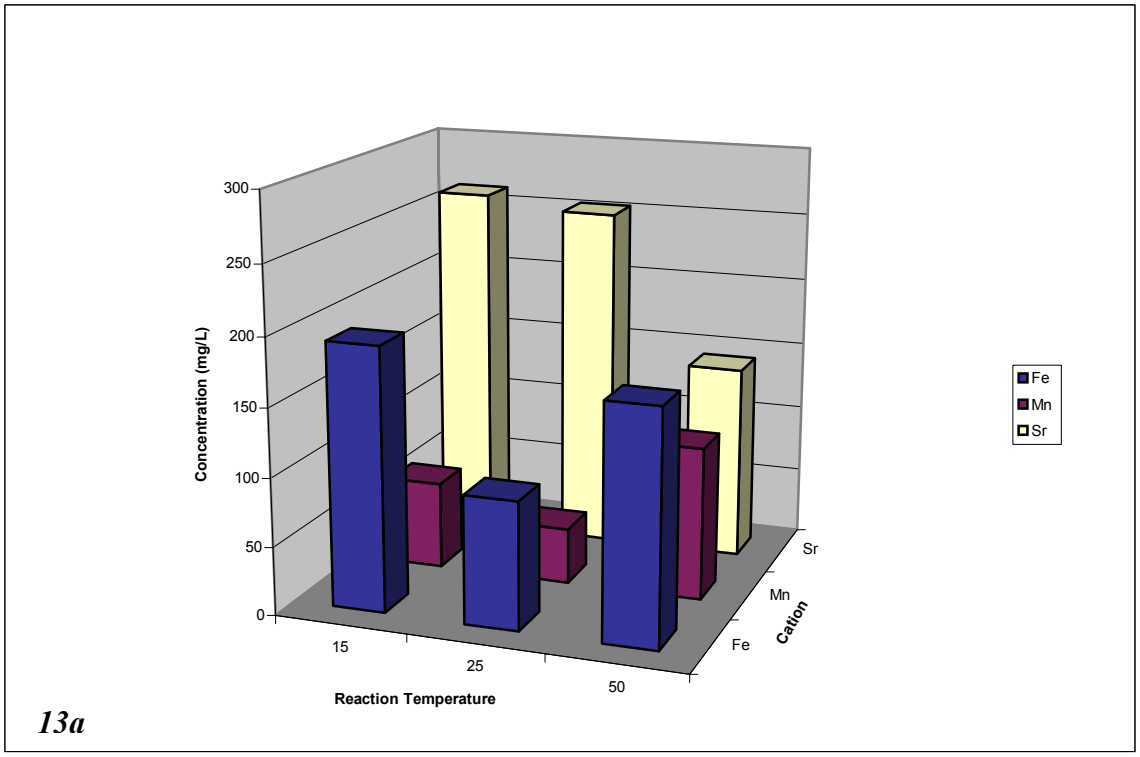

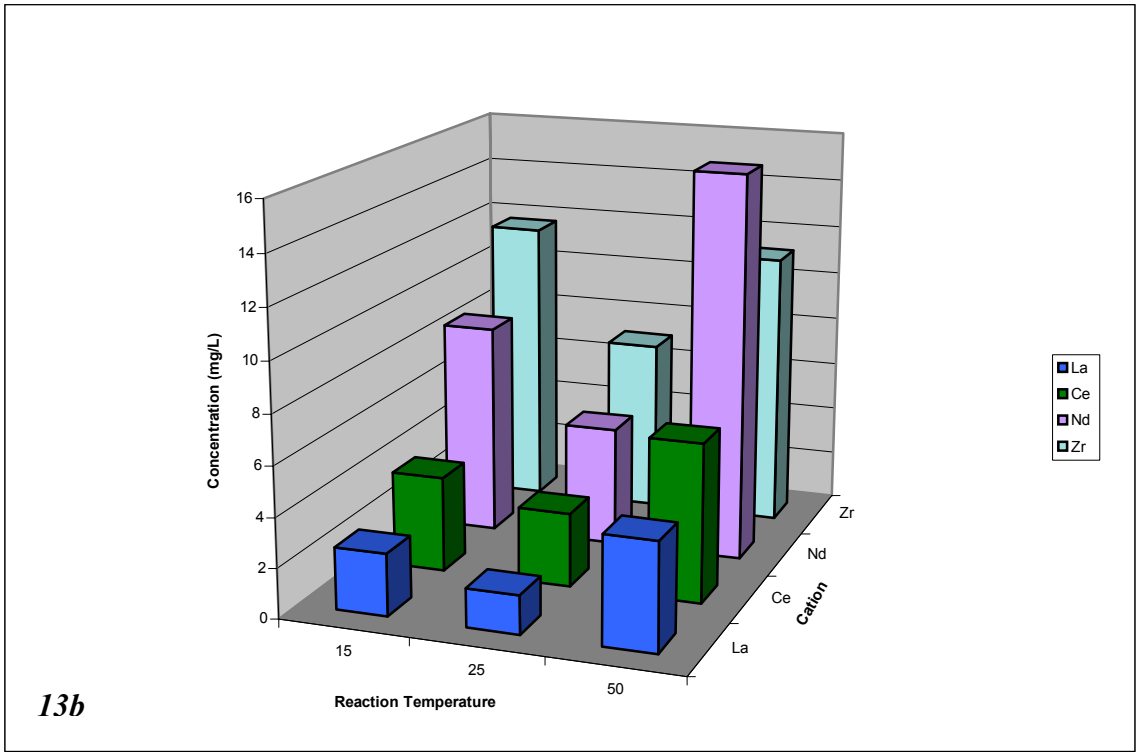

Figure 4.4.1.13 a & b Mean 0 – 48 hr. Concentration of Selected Cations Plotted as a Function of Temperature

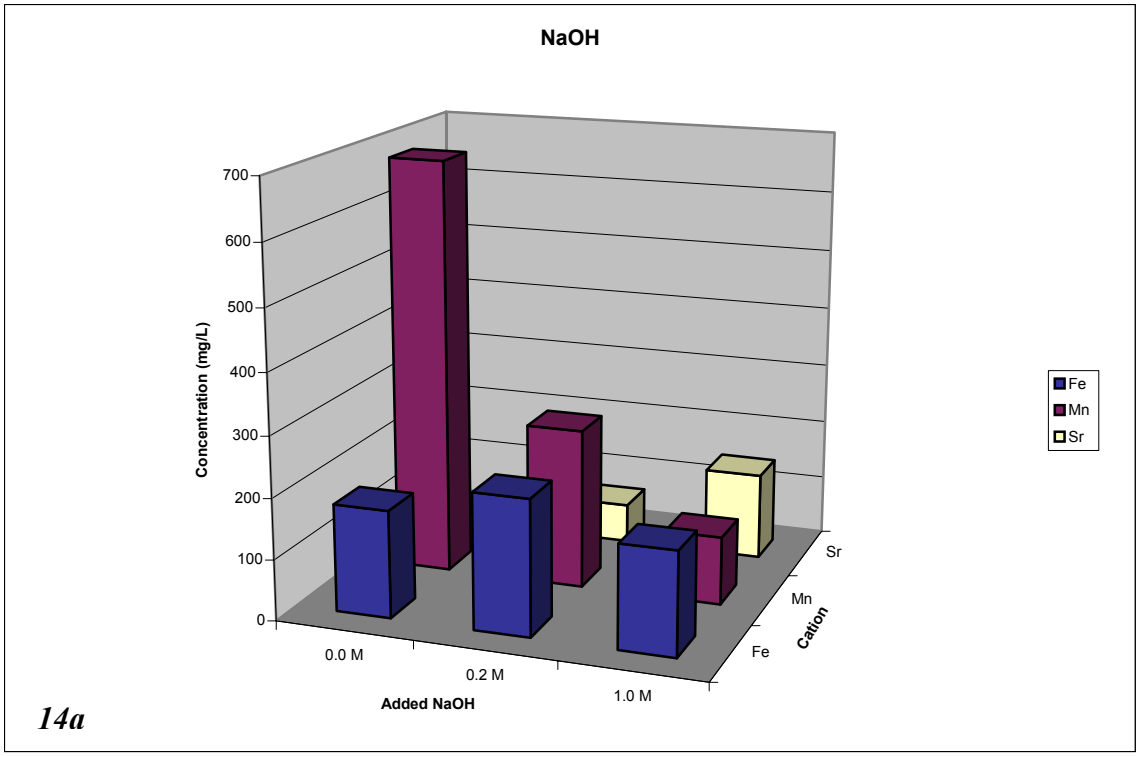

14a

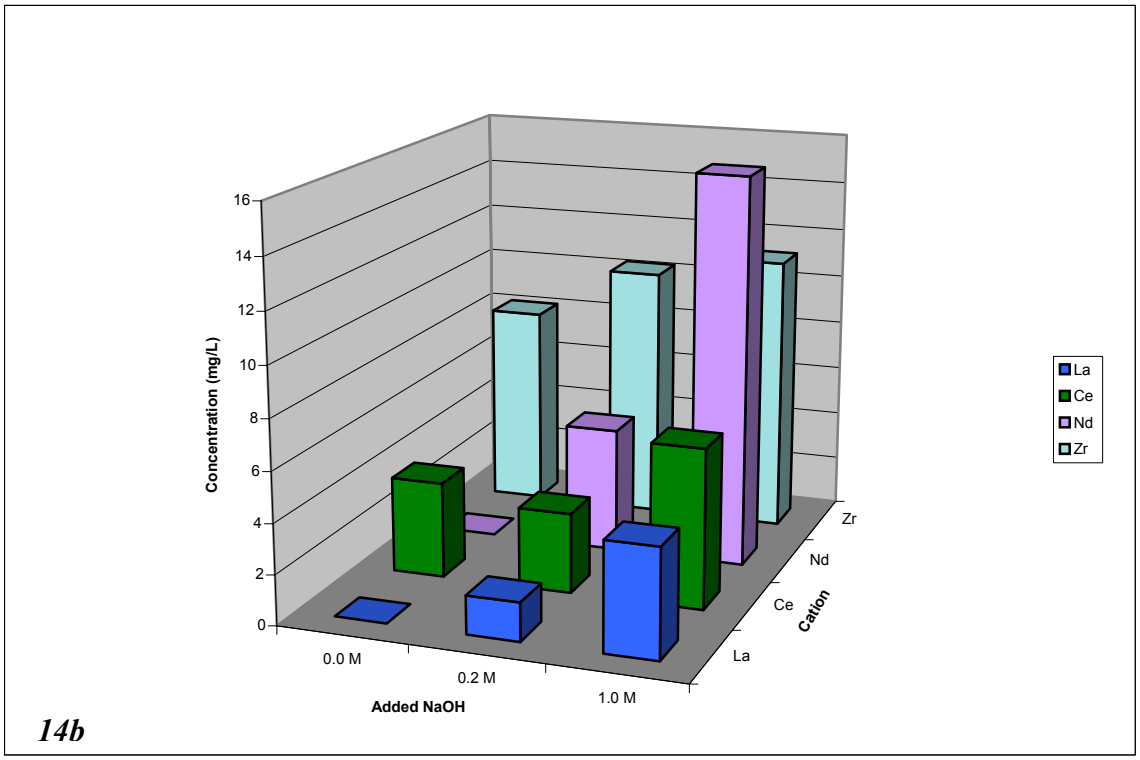

14b

Figure 4.4.1.14 a & b Mean 0 – 48 hr. Concentration of Selected Cations Plotted as a Function of Added NaOH

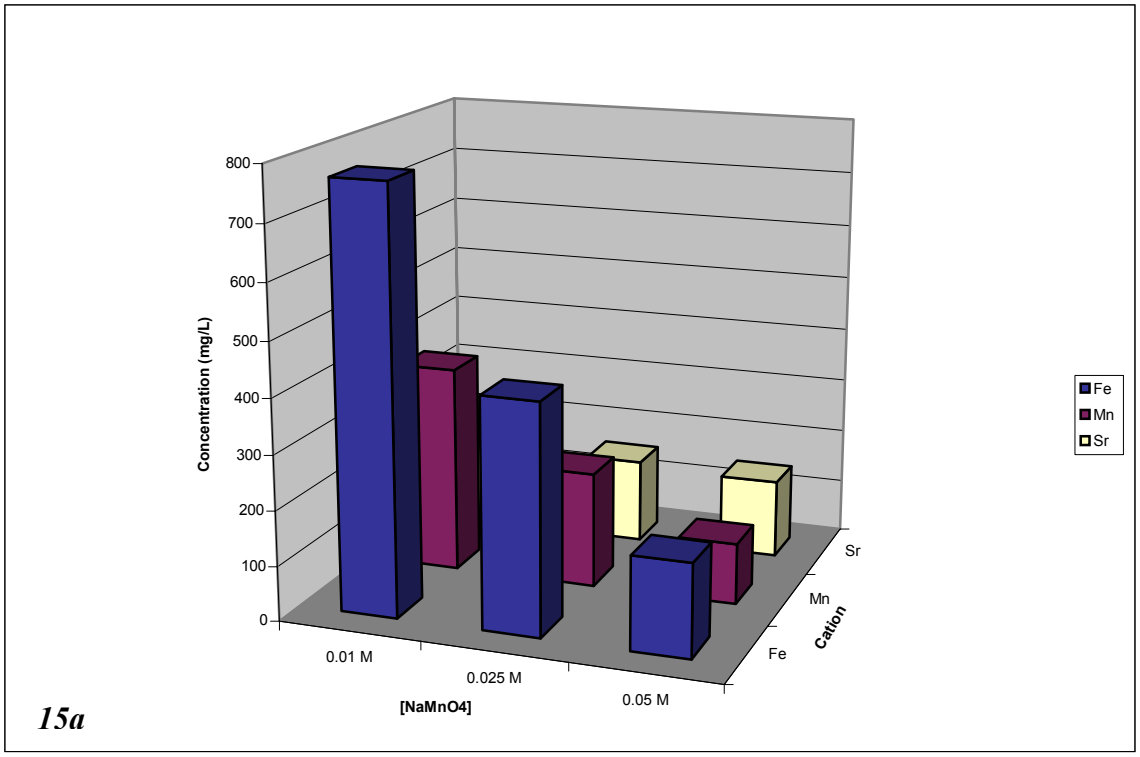

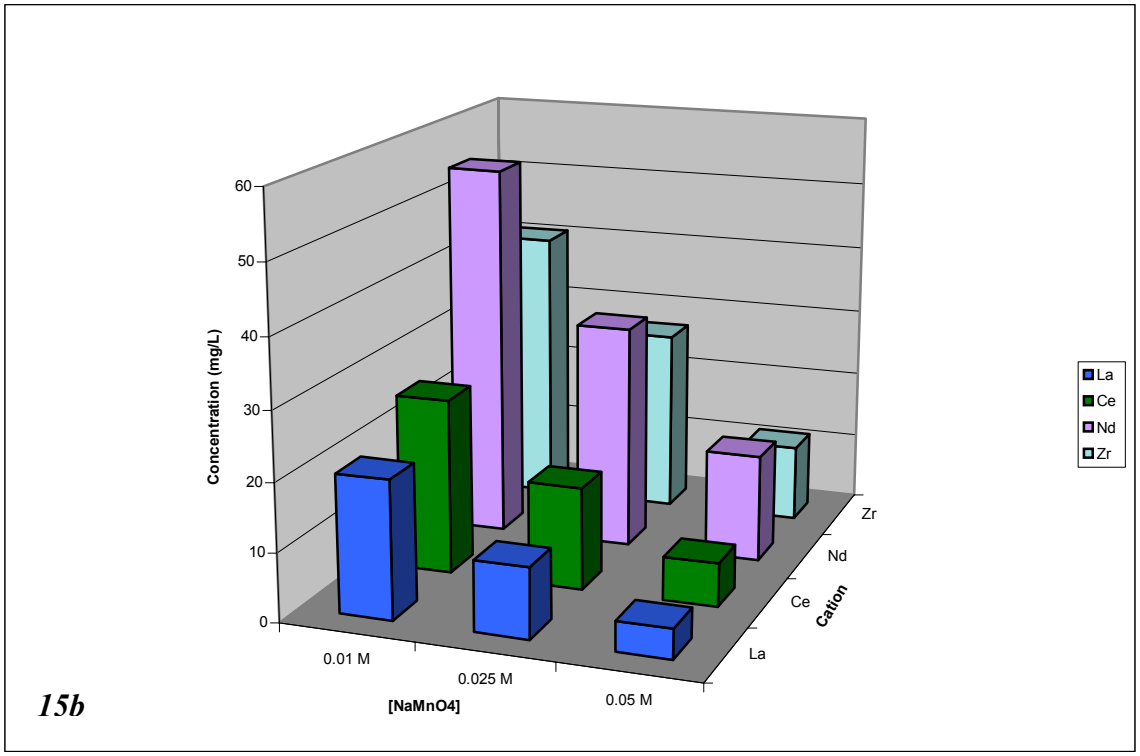

Figure 4.4.1.15 a & b Mean 0 – 48 hr. Concentration of Selected Cations Plotted as a Function of Permanganate Concentration

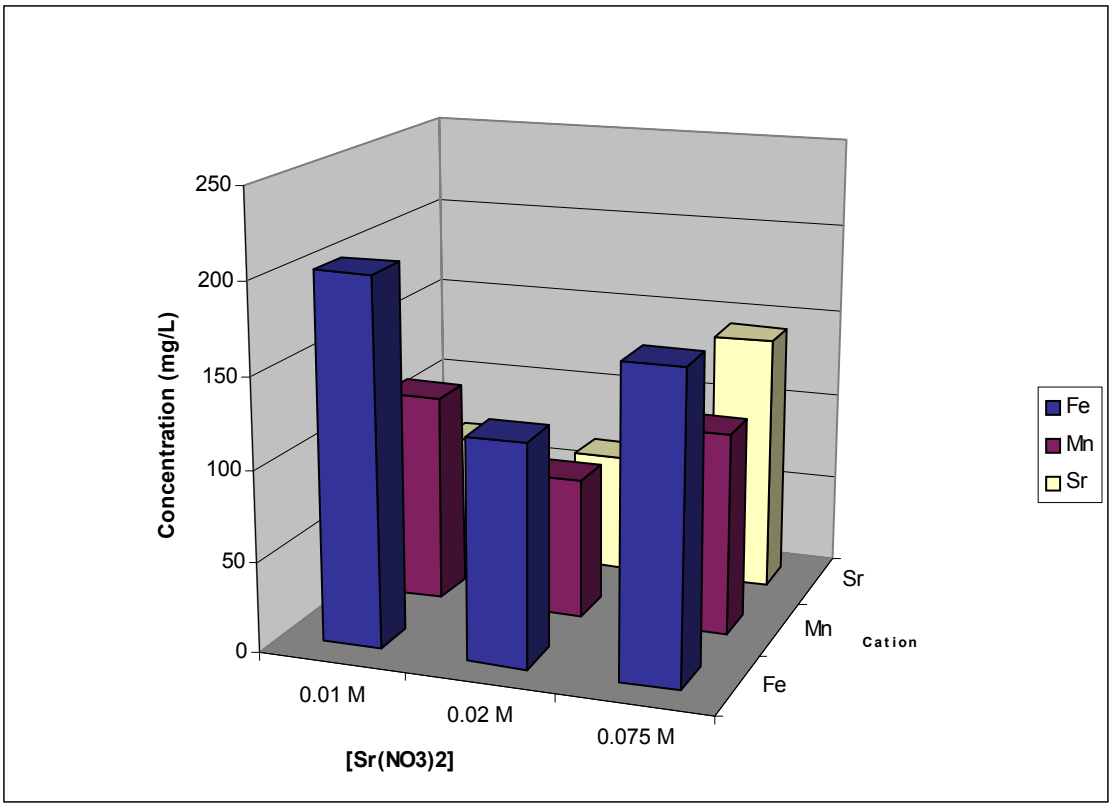

16a

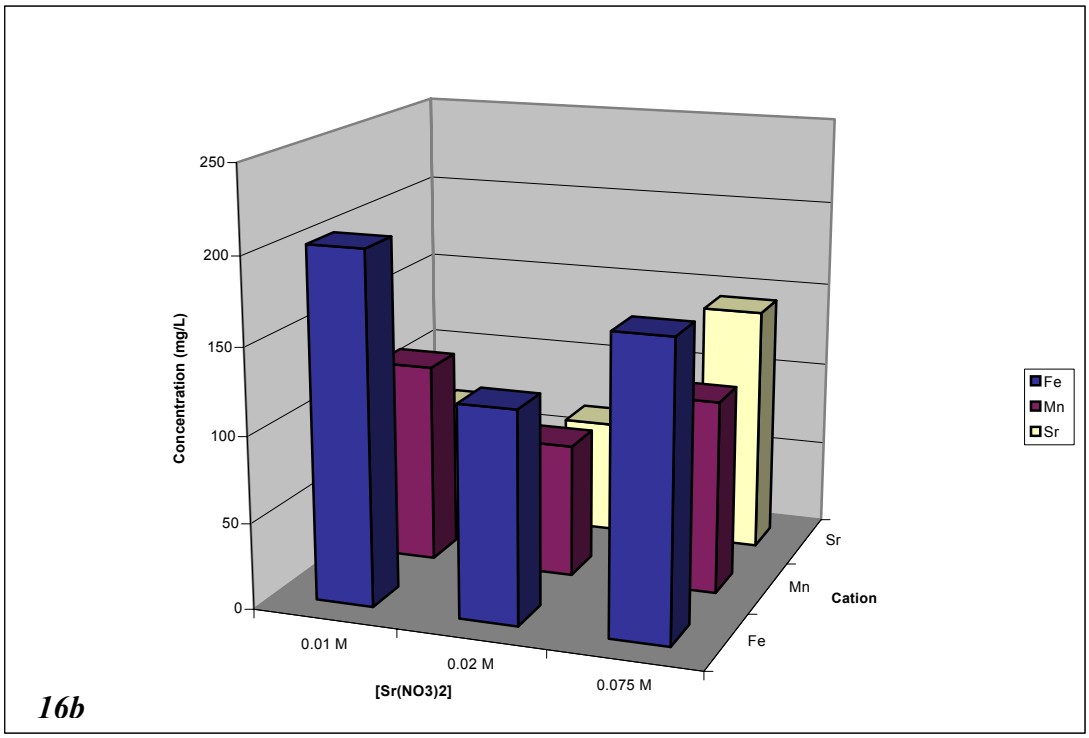

16b

Figures 4.4.1.16 a & b Mean 0 – 48 hr. Concentration of Selected Cations Plotted as a Function of Strontium Concentration

Metal ion concentration data at time zero (0 to 48 hr data since concentration as a function of time, did not vary) after reaction and filtration is plotted as a function of reaction temperature in Figure 4.4.1.13a and b. Concentration data for strontium was inversely proportional to reaction temperature, reflecting a decrease in solubility of strontium carbonate with increasing temperature. Concentration data for the other metals generally increased with increasing temperature with the notable exception for reaction at 25 ^{0}C. These results are unexpected since increasing reaction temperature should increase reaction rates thus increasing the mass of initial precipitate formed during the reaction and decrease the concentration of metal ion remaining in solution.

Cation data plotted as a function of added NaOH, Figures 4.4.1.14a & b, suggests that as free hydroxide increases, manganese precipitation increases (during the initial reaction) thus decreasing the concentration of manganese in the filtrate. Iron and strontium concentration in the filtrates either remain relatively constant or increase slightly, suggesting that increasing free hydroxide does not affect the formation of initial iron or strontium precipitates as drastic as manganese. The concentration of La, Ce, Nd, and Zr in the filtrate increases with increasing free hydroxide, suggesting that adsorption onto the manganese solid may not play a significant role in the removal of these cations.

Cation data plotted as a function of concentration of manganese in the reaction mixture, Figures 4.4.1.15a & b, shows that as the reactant concentration (manganese) increases, the concentration of manganese and other metals decrease, suggesting that adsorption may be an important removal mechanism, when the free hydroxide ion concentration is constant at 1.0 molar.

Strontium data presented in Figures 4.4.1.16a & b, does not appear to trend with increasing reactant concentration. However, the concentration of metal cations plotted may be slightly higher at the higher reactant concentration. The obvious dip in the data presented at a Sr reactant concentration of 0.02 M remains unexplained.

Change in Metals Concentration in Filtrates Between 48 Hours and Final Filtration

Results from the preliminary study indicated the filtrates from reactions carried out at 1.3 and 2.0 added sodium hydroxide resulted in the formation of dark post-filtration solids within hours of the reaction. During the initial 48-hr period after the permanganate oxidation reaction for the primary effects study, dark solids only appeared in filtrates exposed to a 15-minute oxygen sparge and in filtrates that were maintained at 100 °C for 8 hours following the reaction. To observe the formation of additional solids beyond the 48-hr observation period, the primary effects study filtrates were stored for an additional 17 to 74 days. After the additional period, filtrates were again filtered at 0.1 μm and analyzed by ICP-AES. A summary of these data is presented in Table 4.4.1.3. Since the data presented are ratios of the cationic concentration of the 0 to 48 hr and the final filtrate concentration, actual measured data are tabulated. Data for manganese, iron, and strontium are listed for the base case replicates and replicates for reaction and filtrate variables. Presented is data representing the ratio of the mean 0 to 48-hr filtrate concentration to the concentration of Mn,

Fe, and Sr in the filtrates after final filtration. A ratio of 1.0 would therefore indicate no loss of the cation from solution during the extended storage period.

The average ratio presented for Mn suggests that in almost all treatments, additional manganese solids formed during the extended storage period. Two of the treatments, namely, the 0.0 M added sodium hydroxide and the 0.01 M sodium permanganate addition had average ratios of 1.19 and 1.11 respectively suggesting very little formation of manganese solids. The remainder of treatment conditions are represented with ratios of 1.42 to 13.60. Digital photographs shown in Appendix D of particulates collected during final filtration confirm the presence of dark brown to black solids. A photo of the filter for the 0.0 M added sodium hydroxide was not taken because visible solids were not present in the filtrate. Although no visible solids were evident for this sample, it is possible that an inspection of a filtered sample may have revealed a small amount of solids present. This supposition is based on the appearance of the particulate mass for the 0.01 M sodium permanganate. Recall that the average Mn ratios for the 0.0 M NaOH and the 0.01 M Mn were 1.19 and 1.11, respectively, and there was a small accumulation of brown solids on the filter for the 0.01 M Mn treatment. (see photo D.5)

During the preliminary study and the primary effects study usig the 241-AN-107 simulant, several samples were submitted for X-Ray Diffraction analysis (XRD). These spectra are included in Appendix G. With the exception of one sample, namely a filtrate filtered at 0.45 μm and maintained in the dark under a nitrogen blanket, crystalline manganese solids were not detected. Manganese solids that formed during observation periods were likely amorphous and transparent to XRD. Crystalline solids detected included sodium nitrate and nitrite,sodium oxalate, Trona ($Na_3H(CO_3)_2$-$2H_2O$), sodium carbonate, sodalite, and strontium carbonate. Crystalline strontium carbonate was present only in the sample reacted at 25 ^oC.

Table 4.4.1.3 Ratio of Concentration for Fe, Mn, Sr (0-48 Hr avg/final filtrate concentration)

Filtrate Sample	Days from rxn to final filtration	Fe (mg/L)				Mn (mg/L)				Sr (mg/L)			
		48 hr	Final	Ratio	Avg Ratio	48 hr	Final	Ratio	Avg Ratio	48 hr	Final	Ratio	Avg Ratio
Light	76	176.7	ND			123.2	ND			122.5	ND		
	76	117.9	ND			79.4	ND			102.1	ND		
0.45 µm	76	48.7	33.5	1.45	1.39	39.9	5.8	6.88	13.60	92.0	87.9	1.05	1.06
	76	89.5	65.8	1.36		67.0	2.1	32.52		93.7	88.0	1.06	
Filter @ 50 °C	76	159.3	136.3	1.17	1.28	119.0	46.5	2.56	2.14	79.8	73.6	1.08	1.15
	66	257.4	188.8	1.36		154.6	81.5	1.920		94.4	77.8	1.21	
8 hour hold	76	40.1	23.8	1.68	1.48	26.6	2.5	10.64	5.24	22.5	28.6	0.79	0.78
	76	80.0	57.6	1.39		47.3	11.6	4.08		24.1	31.3	0.77	
0 M OH	66	141.6	115.7	1.22	1.23	507.9	427.8	1.19	1.19	11.5	4.1	2.80	2.59
	66	116.2	94.5	1.23		490.3	413.4	1.19		7.9	3.4	2.32	
0.2 M OH	66	186.3	99.7	1.87	1.35	199.6	115.4	1.73	1.48	46.3	37.5	1.23	1.25
	66	134.7	138.7	0.97		178.1	139.3	1.28		46.5	36.8	1.26	
0.01 M Mn	48	534.6	586.4	0.91	1.03	269.7	274.2	0.98	1.11	123.6	128.8	0.96	1.09
	48	553.5	470.4	1.18		265.2	208.0	1.28		132.5	105.8	1.25	
0.025 M Mn	52	215.6	198.8	1.08	1.08	130.9	89.7	1.46	1.42	96.2	88.7	1.08	1.11
	52	369.1	341.4	1.08		164.0	118.0	1.39		118.2	105.1	1.12	
0.01 M Sr	52	165.4	92.1	1.80	1.58	62.0	30.4	2.04	2.21	41.7	36.9	1.13	1.25
	52	185.0	129.4	1.43		104.0	44.6	2.33		56.0	41.3	1.36	
0.02 M Sr	52	86.1	65.7	1.31	1.31	53.9	21.3	2.53	2.49	44.9	40.2	1.12	1.11
	52	88.4	68.0	1.30		55.5	23.1	2.45		49.8	44.9	1.11	
Rxn @ 25 °C	47	57.9	51.1	1.13	1.17	26.1	8.9	2.93	2.93	155.1	132.8	1.17	1.45
	47	69.6	58.2	1.20		29.5	10.1	2.92		189.6	105.1	1.80	
Rxn @ 15 °C	40	122.1	109.5	1.12	1.21	39.0	20.2	1.93	2.14	157.9	147.0	1.07	1.16
	40	136.5	103.7	1.32		46.9	19.9	2.36		193.7	155.9	1.24	
O_2	19	48.5	39.6	1.22	1.19	31.9	16.4	1.95	1.93	86.0	79.3	1.08	1.03
	19	45.2	39.0	1.16		32.4	17.0	1.91		77.4	79.5	0.97	
N_2	19	49.9	44.0	1.13	1.19	38.2	23.1	1.65	1.78	84.1	83.9	1.00	1.09
	19	49.9	40.2	1.24		38.7	20.0	1.94		87.5	74.1	1.18	
Shear	59	40.8	36.3	1.12	1.21	33.4	9.5	3.52	3.30	83.5	86.6	0.96	0.99
	59	36.1	27.1	1.33		32.0	10.3	3.11		73.1	71.4	1.02	
Base Case	78	165.1	128.8	1.282	1.26	114.4	49.9	2.2926	2.42	113.5	110.9	1.0234	1.07
	50	72.7	59.3	1.226		49.8	18	2.7667		74.4	65.4	1.1376	
Base Case	78	117.8	92.2	1.278	1.36	77.9	30.4	2.5625	2.23	100	98.4	1.0163	1.14
	68	255.8	182.8	1.399		146.4	70.4	2.0795		145.5	116.1	1.2532	

In summary, data presented for the primary effects study suggests that post-filtration solids form in all treatments considered given sufficient time. However, in the short term, within 48 hours, reacting the simulant at process conditions, but eliminating the addition of sodium hydroxide from the reaction mixture and minimizing exposure to oxygen in the filtrates may minimize the formation. In addition, the formation of post-filtration solids could also be minimized by reducing the concentration of sodium permanganate to approximately 0.01 M from the process design of 0.05 M. This change however may seriously impact the formation of reaction precipitates and reduce decontamination of the nuclides in the actual waste (discussions in the project review meeting, 2002).

4.4.2 Secondary Effects Study

Very near the end of the analytical effort for the AN-241-107 primary effects study, discussions were initiated concerning reconsideration of the reaction conditions. A 'newly optimized conditions' (NOC) was proposed in which the concentration of reactants was reduced from 0.075 M strontium nitrate and 0.05 M sodium permanganate to 0.03 and 0.03 M respectively. In addition, the sodium hydroxide concentration would be at 0.3 M added and the reaction temperature was proposed to be 25 $^{\circ}$C. Since these conditions were not included in the original task plan, we proposed to investigate these conditions and include variables that resulted in minimal post-filtration solids formation from the primary effects study. A 2^3 factorial experiment using the NOC reaction and varying the sodium permanganate concentration from 0.03 M to 0.01 M (A treatment, two levels), light and dark (B treatment, two levels) and the presence or absence of oxygen (C treatment, two levels) was designed. The factorial design is presented in Table 4.4.2.1.

Table 4.4.2.1 Factorial Design for the Newly Optimized Conditions

2^3 Factorial Design			
Effect	**A**	**B**	**C**
	$[MnO_4^-]$	Lt/Dk	ATM/N_2
(1)	0.03 M	Dark	N_2
a	0.01 M	Dark	N_2
b	0.03 M	Light	N_2
ab	0.01 M	Light	N_2
c	0.03 M	Dark	Atm
ac	0.01 M	Dark	Atm
bc	0.03 M	Light	Atm
abc	0.01 M	Light	Atm

Visual Observations

The visual observation period was extended to 16 days for two reasons. First, with exception of the treatment conditions, 8-hr hold at 100 °C and the oxygen sparge, all remaining treatments included in the primary effects study did not result in the formation of post-filtration solids. Secondly, some concern was expressed that ion exchange at the treatment facility may not be accomplished within 24 to 48 hours; therefore, determining the potential for the formation of post-filtration solids in filtrates for several days should be investigated. Included in Table 4.4.2.2 are visual observations noting the time solids formed in the filtrates. The cross effect of light and atmosphere at the newly optimized condition resulted in the formation of dark post-filtration solids between days 4 and 5. The cross effect of 0.01 M sodium permanganate and light also resulted in the formation of solids within 6 to 7 days. The cross effect of 0.01 M sodium permanganate and atmosphere did not result in the formation of solids within the 16-day observation period.

Table 4.4.2.2 Appearance of Solids in Filtrates During the 16-Day Period (AN-107)

VISUAL OBSERVATIONS FOR THE AN-107 NOC FACTORIAL EXPERIMENTS					
			White Solids	**Ring on Flask**	**Dark Solids**
0.03 M	Light	ATM	1 – 2 d	4 d	4 – 5 d
0.03 M	Dark	ATM	3 – 6 d	X	X
0.03 M	Light	N_2	2 – 3 d	5 d	5 – 6 d
0.03 M	Dark	N_2	5 – 9 d	X	X
0.01 M	Light	ATM	2 d	5 d	5 – 6 d
0.01 M	Dark	ATM	2 d	X	X
0.01 M	Light	N_2	3 d	6 d	6 – 7 d
0.01 M	Dark	N_2	3 d	X	X

In addition to examining secondary effects, the primary effects of a reduced level of sodium permanganate, the presence of air, and light on the NOC; and the tertiary effect of 0.01 M sodium permanganate, atmosphere and light can be measured from the factorial design. The primary effect of light resulted in the formation of solids within 5 to 6 days. The primary effect of atmosphere or 0.01 M sodium permanganate did not result in the formation of solids within 16 days. The tertiary effect resulted in the formation of solids within 5 to 6 days. From visual observations, it appears that with respect to the NOC, the presence of light may result in the formation of post-filtration solids.

At the end of the 16-day observation period, all filtrate samples were filtered at 0.1 μm and digital photographs of the filters were taken to further document the formation of solids. These photographs are shown in Figure 4.4.2.1. As can be seen, dark solids formed in all filtrates maintained in contact with air. The presence of dark solids on the filters correlate well with the visual observation for the cross effects of light and atmosphere for the NOC,

the primary effect of light for the NOC, and the cross effect of 0.01 M permanganate and light for the NOC. However, visual observations for the neither the cross effect of 0.01 sodium permanganate and atmosphere for the NOC, nor the primary effect of atmosphere correlate with the presence of solids on the respective filter. White solids formed early, but dark solids were not observed at day 16.

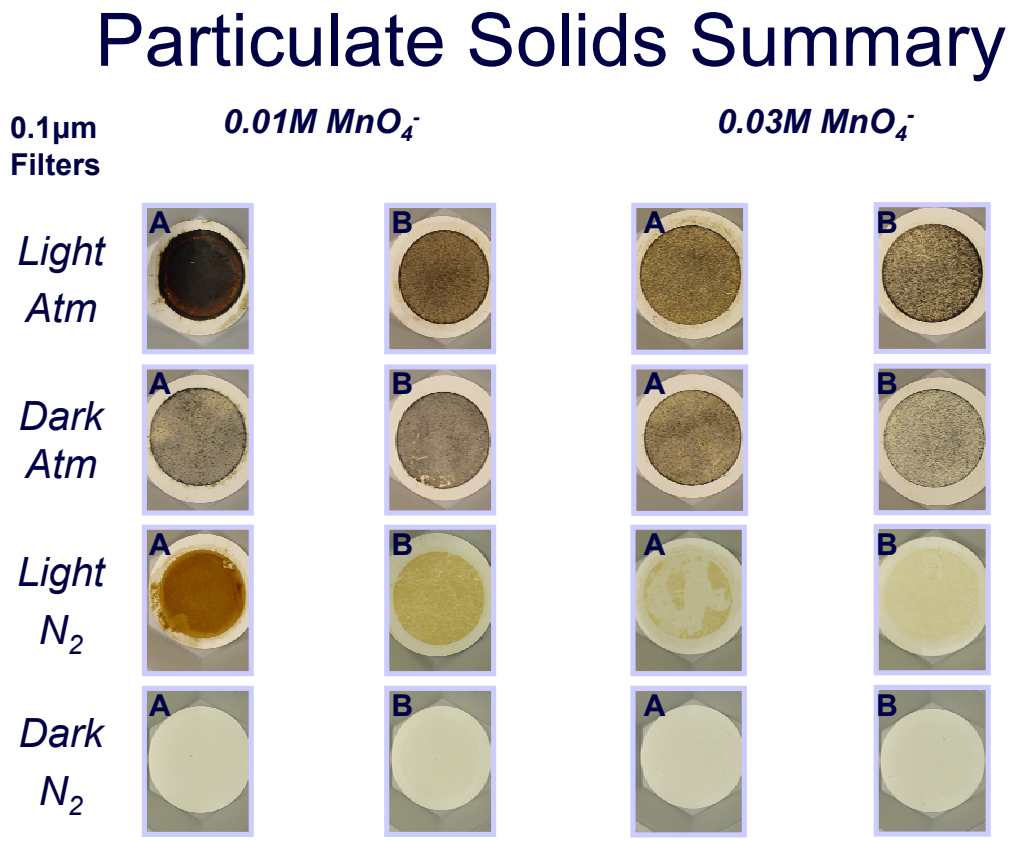

Figure 4.4.2.1 Particulate Solids Summary for the AN-107 Secondary Effects Study

The tertiary effect of 0.01 M permanganate, light and atmosphere, resulted in the formation of solids within 5 to 6 days and is confirmed by the presence of dark solids on the respective filter. For the NOC, dark solids were not observed on the filter or in the filtrate at day 16. In addition dark solids were not expressed for the primary effect of 0.01 M permanganate. Therefore, it would appear that reacting at the NOC or at a lower permanganate concentration could mitigate the formation of dark solids within 16 days of an oxidation reaction with a 241-AN-107 waste.

Discrepancies between the photographic record of the particulate filters and the visual observations noted in the above paragraph for two conditions (0.03 M Mn, dark, atmosphere and the 0.01 M Mn, dark, atmosphere) are not understood. However, it is plausible that the light colored solids noted in Table 4.4.2.2 were oxidized by oxygen in the atmosphere during filtration and drying to Mn (III) and Mn (IV) oxy-hydroxides and oxides respectively (Cotton and Wilkinson, 1988).

Change in Metal Ion Concentrations During the 16-Day Observation Period for the Secondary Effects Study for 241-AN-107

During the sixteen-day period of observation, aliquots of the filtrates were collected, filtered at 0.1µm, and analyzed by ICP-AES to determine metal ion concentrations. A summary of these data is presented in Appendix E in tabular form. Data for Mn, Fe and Sr are plotted in Figures 4.4.2.2 through 4.4.2.13 respectively. The 0.03 M Mn data cover an observation period of 16 days and the 0.01 M Mn data span an 18-day observation period. Interestingly, data for manganese does not indicate that manganese was lost from solution during the sixteen days. This observation does not correlate with several of the photographic records of particulate filters (Figure 4.4.2.1), specifically, the secondary effect of 0.01 M sodium permanganate with (1) atmosphere and (2) light, the secondary effect of 0.03 M sodium permanganate with light, and the tertiary effect of 0.01 M Mn, light, and atmosphere. Although dark solids are seen on the filters for these conditions, the concentration of soluble manganese measured in the filtrates at specific times during the 16-day period does not decrease with time.

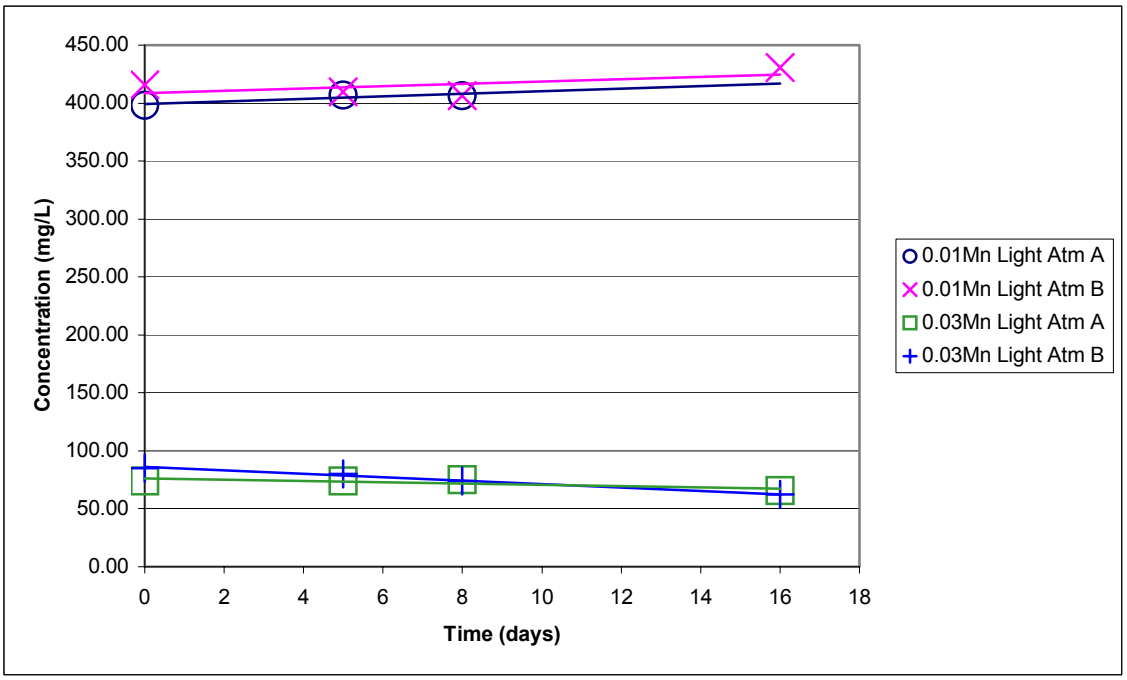

Figure 4.4.2.2 Manganese Concentration in 0-16 Day Filtrates for Manganese, Light, and Atmosphere

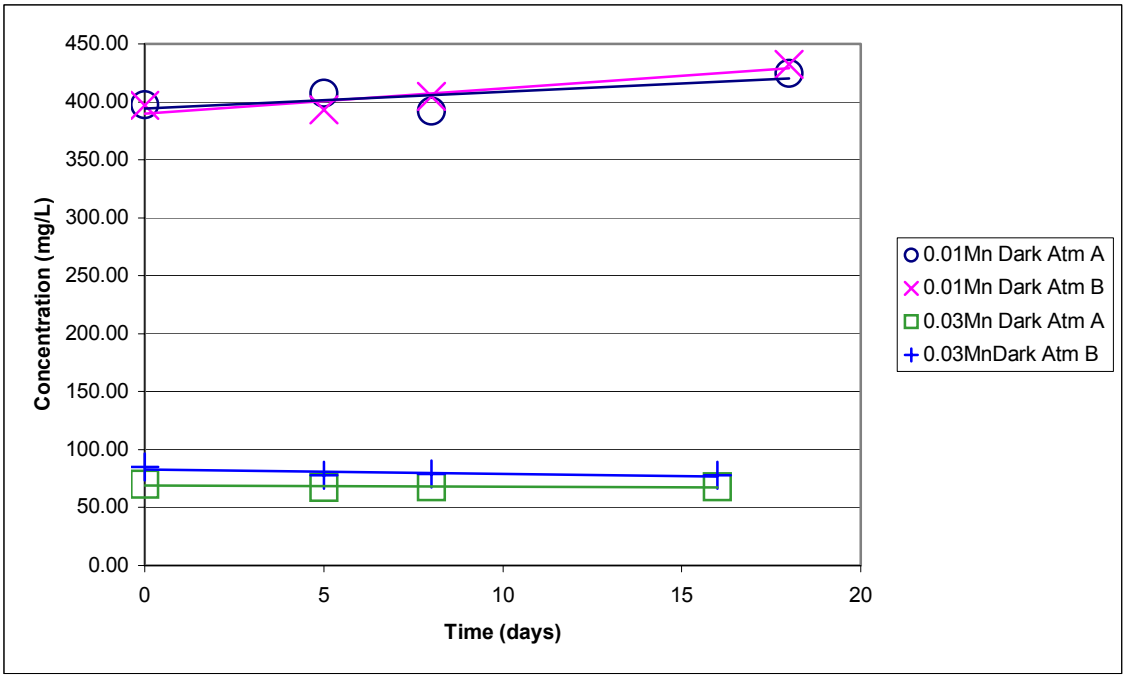

Figure 4.4.2.3 Manganese Concentration in 0-16 Day Filtrates for Manganese, Dark, and Atmosphere

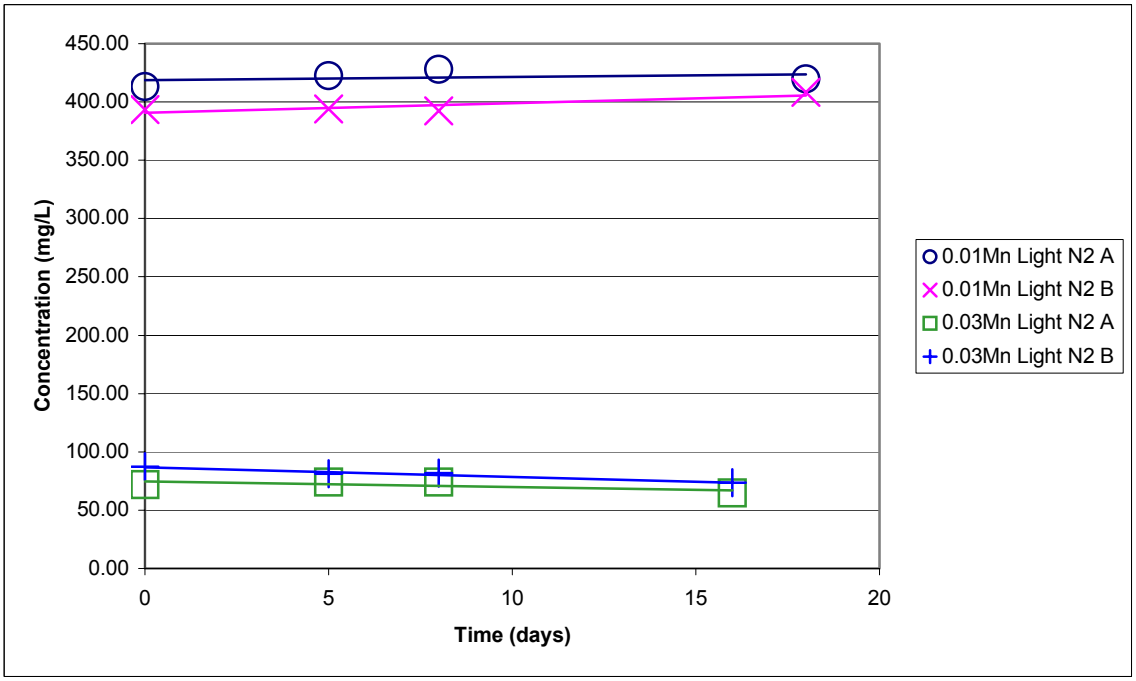

Figure 4.4.2.4 Manganese Concentration in 0-16 Day Filtrates for Manganese, Light, and Nitrogen

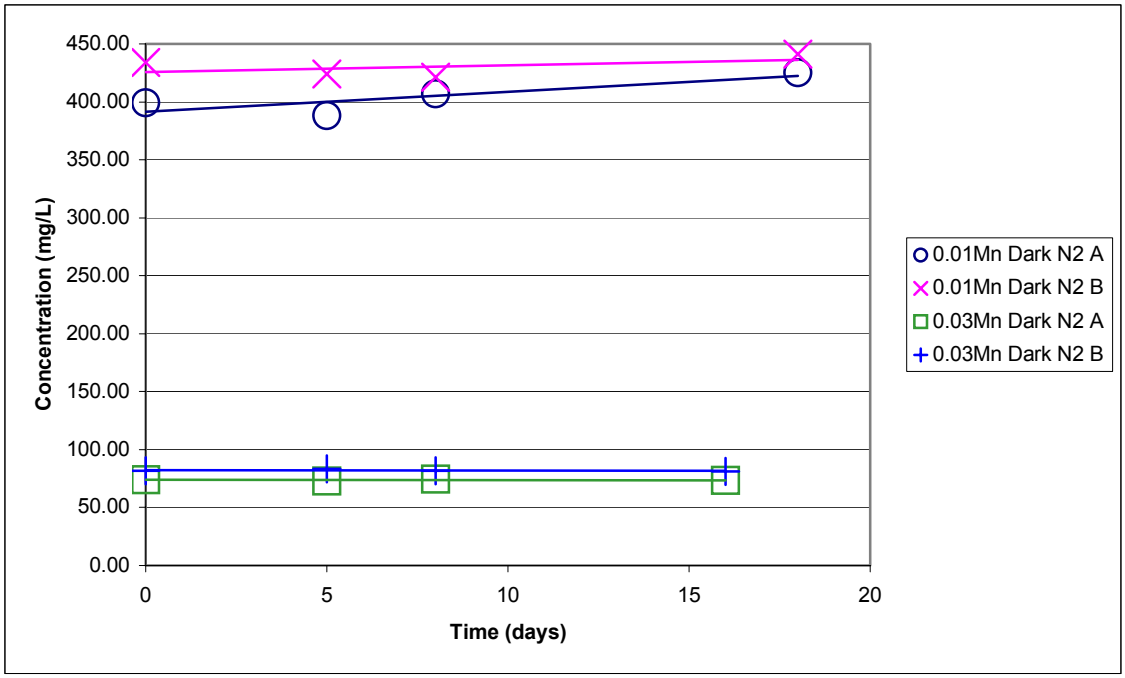

Figure 4.4.2.5 Manganese Concentration in 0-16 Day Filtrates for Manganese, Dark, and Nitrogen

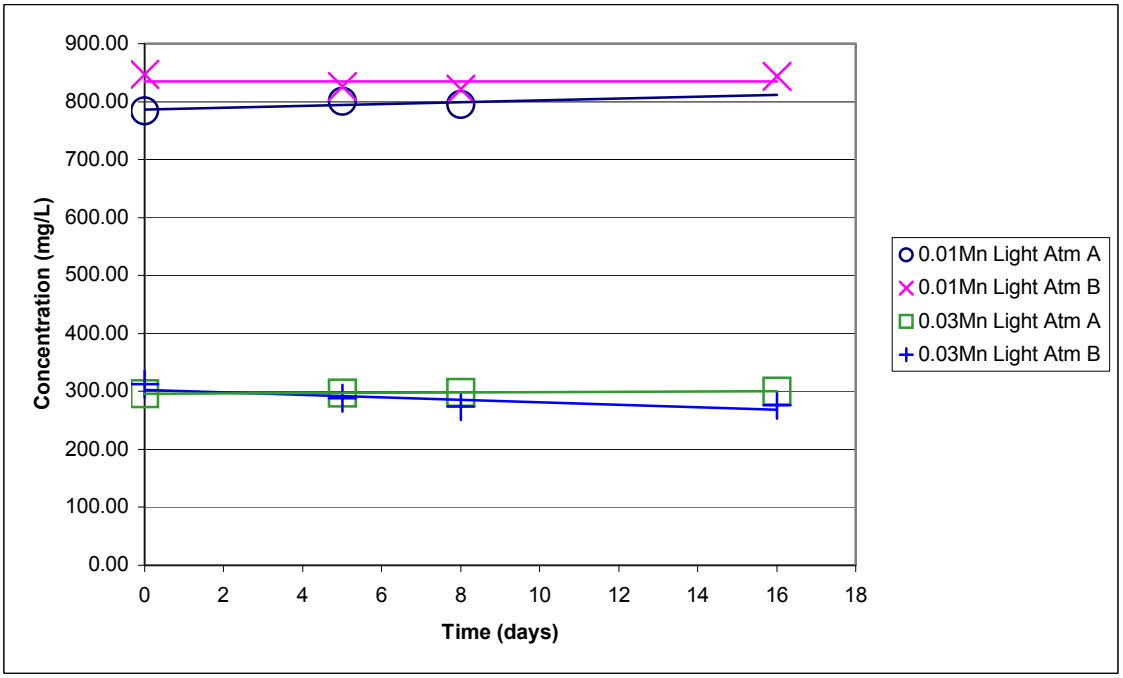

Figure 4.4.2.6 Iron Concentration in 0-16 Day Filtrates for Manganese, Light, and Atmosphere

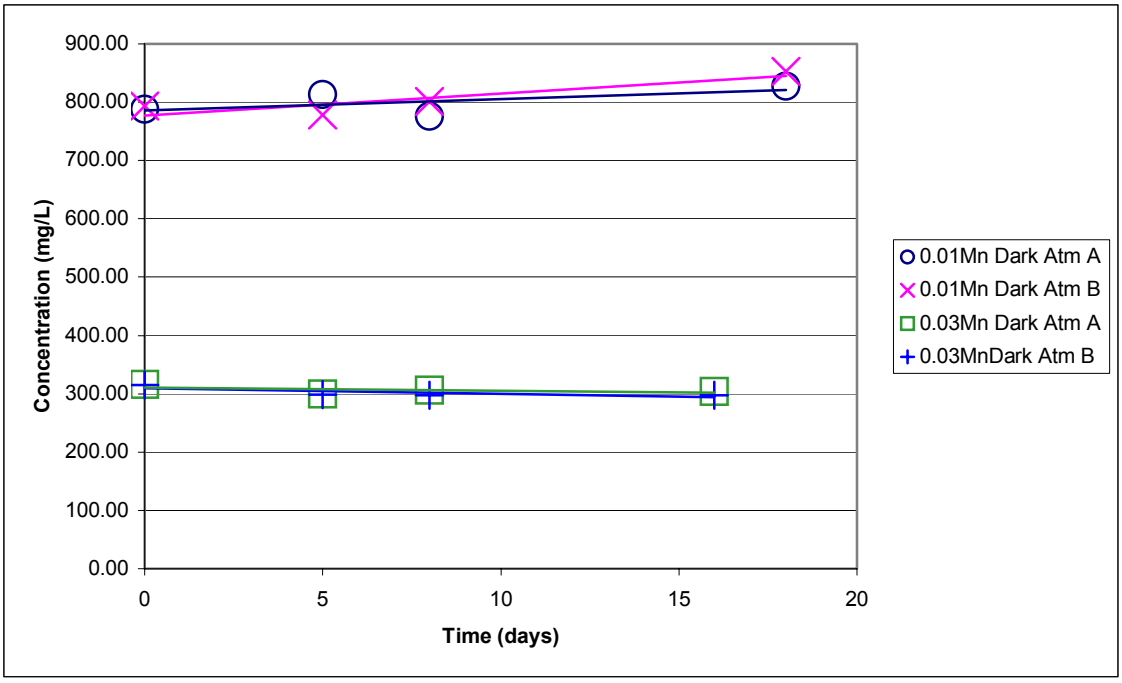

Figure 4.4.2.7 Iron Concentration in 0-16 Day Filtrates for Manganese, Dark, and Atmosphere

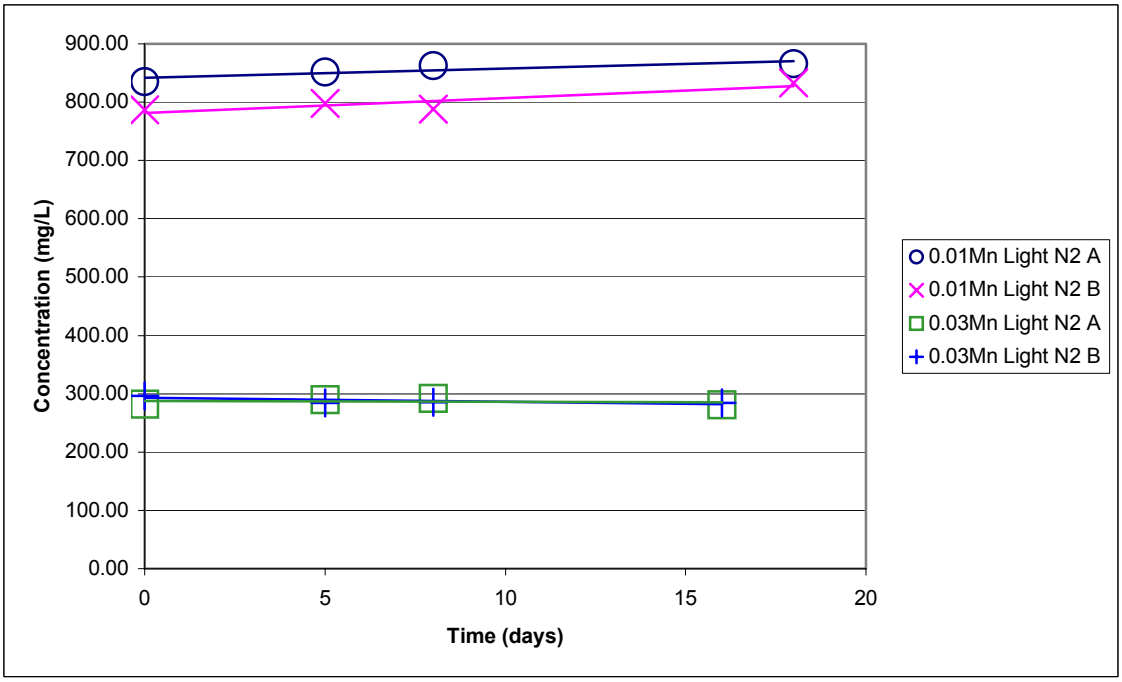

Figure 4.4.2.8 Iron Concentration in 0-16 Day Filtrates for Manganese, Light, and Nitrogen

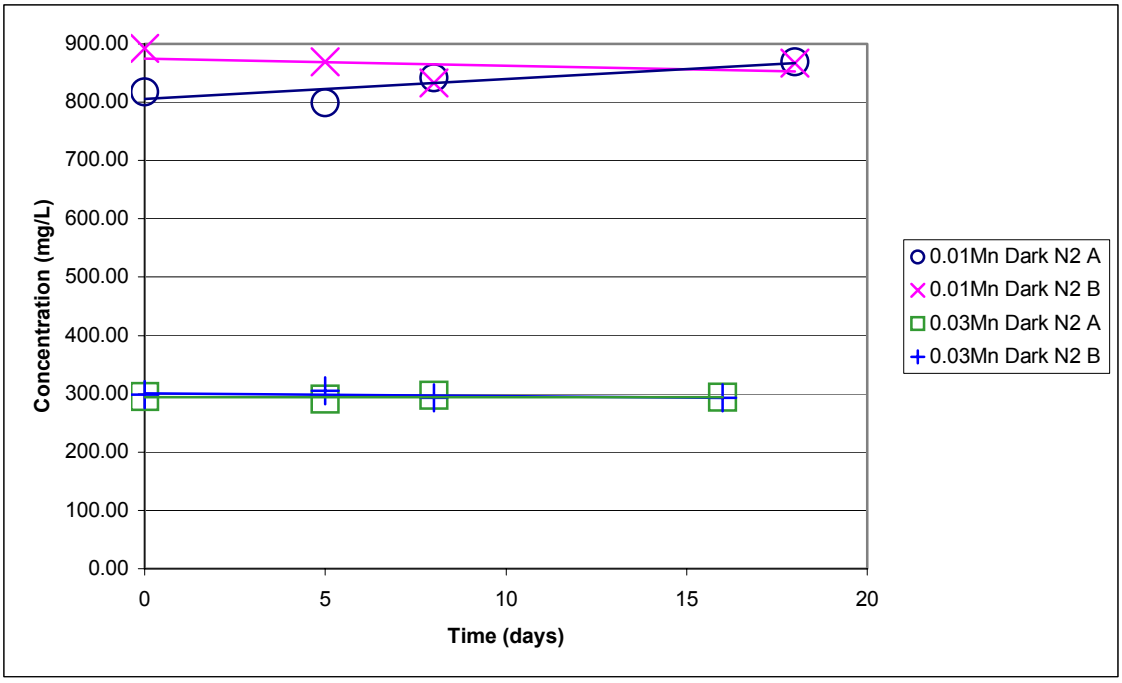

Figure 4.4.2.9 Iron Concentration in 0-16 Day Filtrates for Manganese, Dark, and Nitrogen

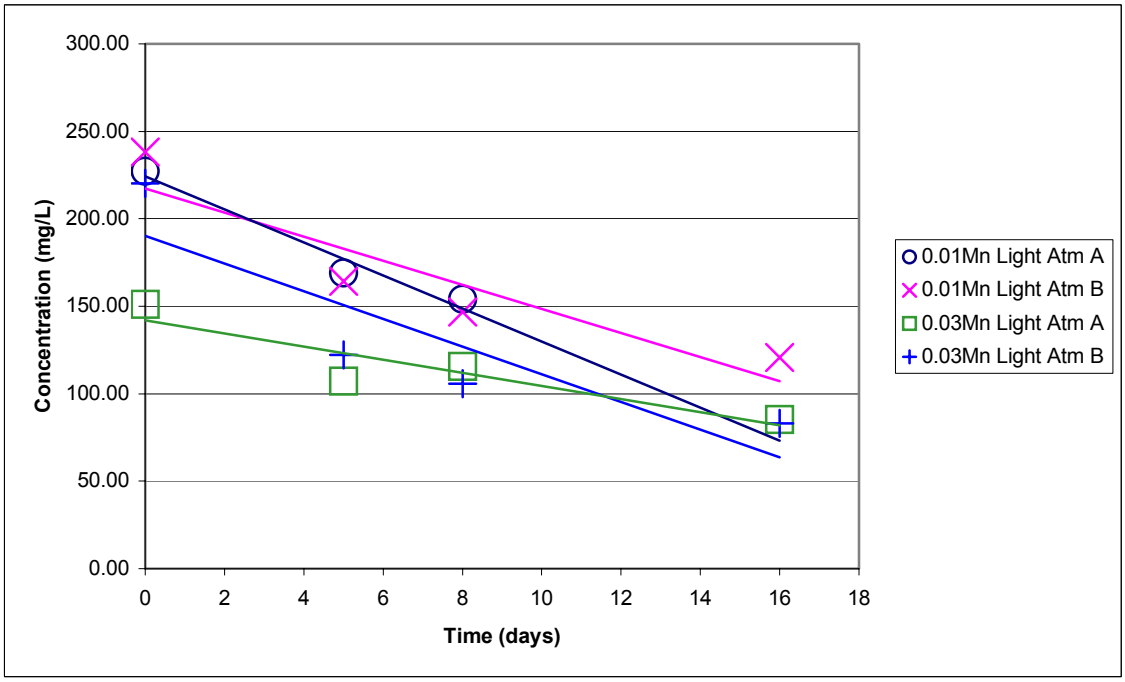

Figure 4.4.2.10 Strontium Concentration in 0-16 Day Filtrates for Manganese, Light, and Atmosphere

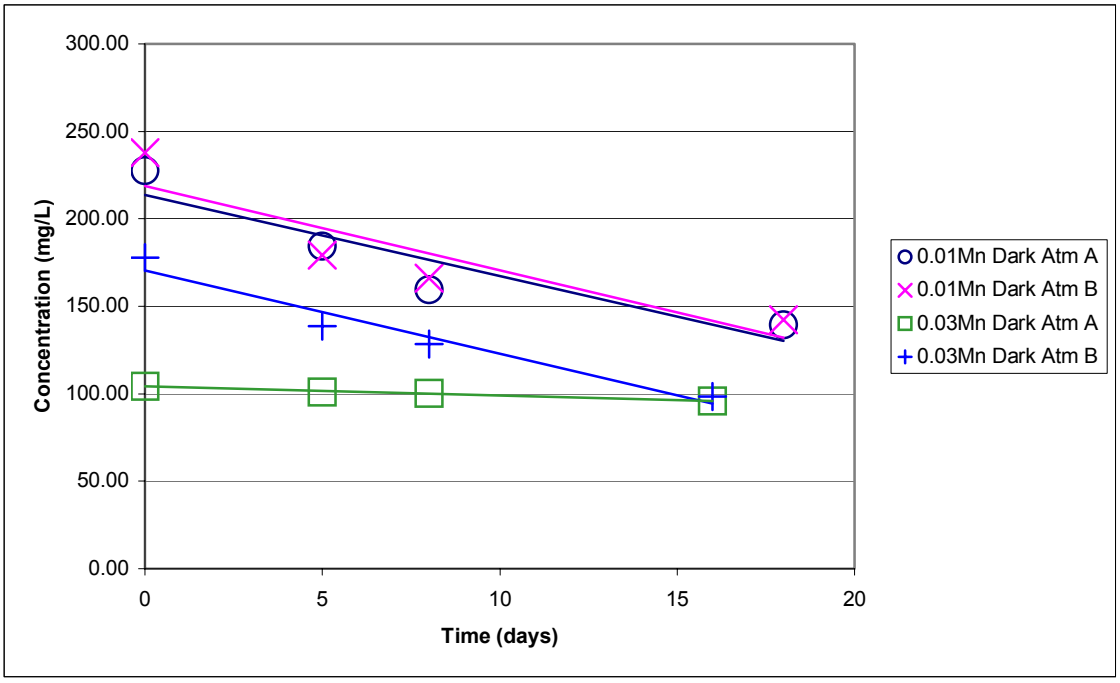

Figure 4.4.2.11 Strontium Concentration in 0-16 Day Filtrates for Manganese, Dark, and Atmosphere

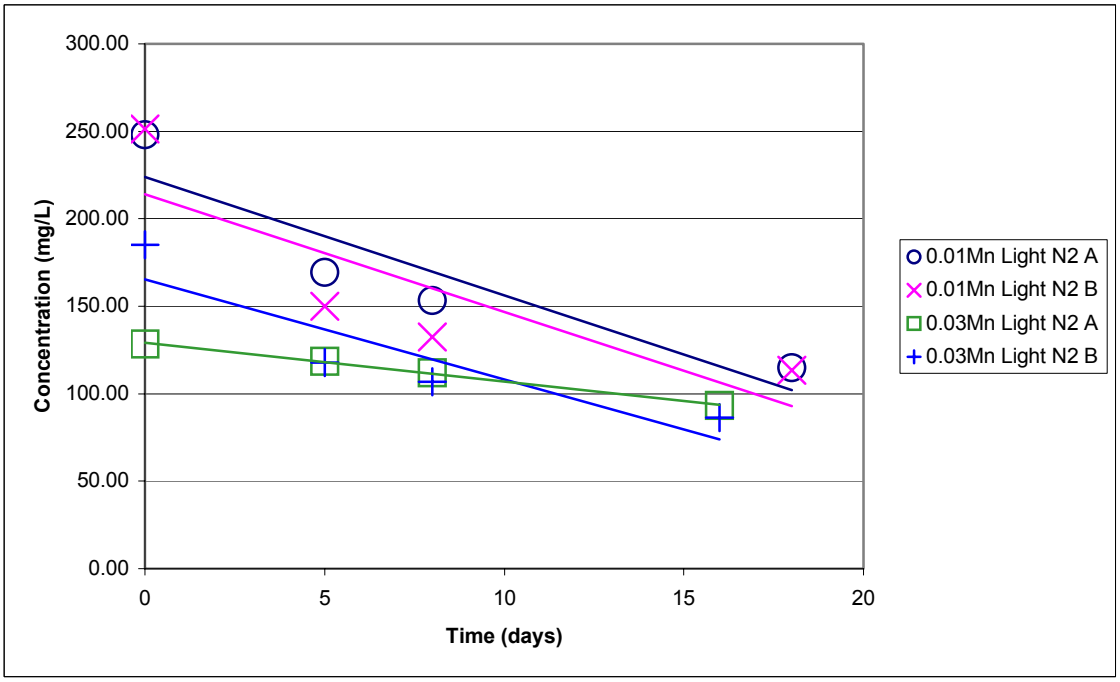

Figure 4.4.2.12 Strontium Concentration in 0-16 Day Filtrates for Manganese, Light, and Nitrogen

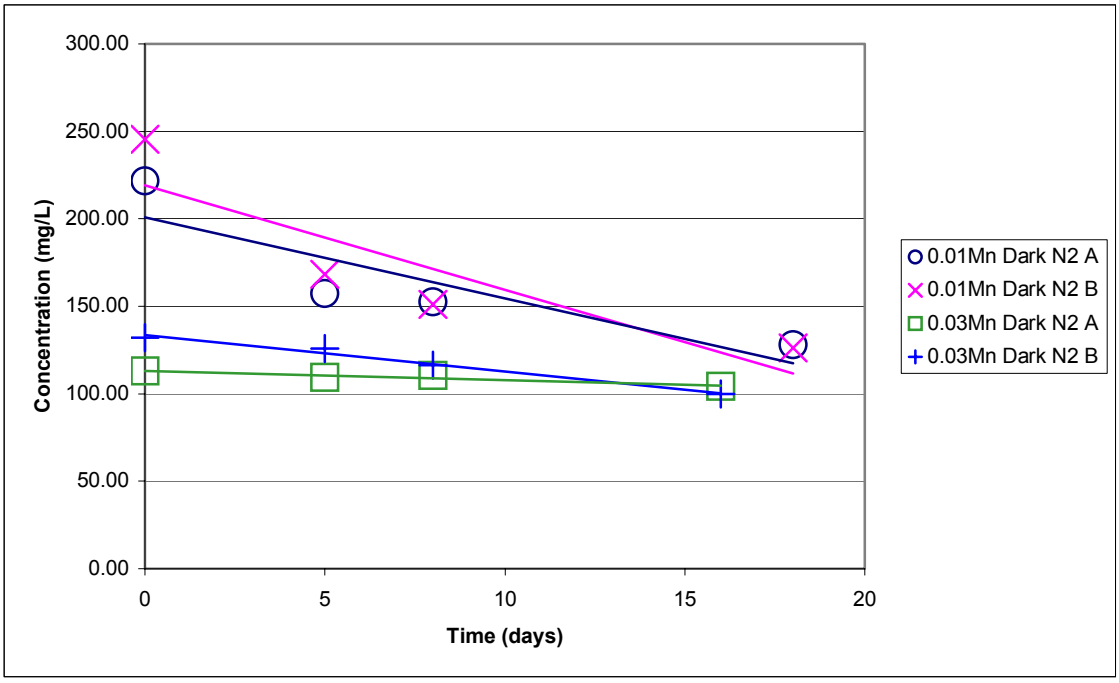

Figure 4.4.2.13 Strontium Concentration in 0-16 Day Filtrates for Manganese, Dark, and Nitrogen

This discrepancy may be explained by an examination of the error structure for the ICP-AES analysis presented in Table E.1 through E.7. Tables 4.4.2.3 and 4.4.2.4 include a summary of standard deviation and the range for filtrate analyses conducted during the 16-day period and predicted mass of manganese on filters. As can be seen, the standard deviation of the manganese ICP-AES analyses for the 0.03 M sodium permanganate experiments ranged from 0.46 to 7.44 mg/L, and for the 0.01 M experiments the standard deviation ranged from 4.31 to 14.65 mg/L. Standard errors of this magnitude translate into a range for the mass of manganese collected on filters of 0.046 to 1.47 mg. A similar analysis of the data presented in Table 4.4.2.4 representing the range or spread of the manganese concentration measured in the filtrates translates into a mass of manganese collected on filters of 0.1 to 3.6 mg. From these data it is conceivable that within the bound of error for the ICP-AES measurements, solids could be collected on filters without being indicated by the change in concentration of manganese with time in the filtrates. To determine if this mass of manganese solids collected on the 47 mm filters used in the study appeared visibly similar to the masses of dark solids noted in Figures 4.4.2.1, suspensions of manganese (III) oxy-hydroxide were prepared such that upon filtering, 0.4, 1.0 and 3.0 mg of manganese would be deposited on the filters. This would result in a mass of manganese (III) oxy-hydroxide of 0.64, 1.6, and 4.8 mg respectively. A digital photograph of these filters is shown in Figure 4.4.2.14, which also includes a precipitate mass of manganese (IV) dioxide. As can be seen, the visual appearance of solids is similar to solids collected from the filtrates for the secondary effects study and shown in Figure 4.4.2.1.

Table 4.4.2.3 Error Estimate of ICP-AES Analysis for Manganese Measured in the Secondary Effects Filtrate

	0.03 M Mn SD (mg/L)	**Mass on Filter (mg)**	**0.01 M Mn SD (mg/L)**	**Mass on Filter (mg)**
DK N_2	0.46 (NS)	0.046	6.31 (NS)	0.63
	0.70 (NS)	0.070	14.65 (NS)	1.47
LT N_2	3.28 (NS)	0.33	6.0 (DS)	0.60
	4.36 (NS)	0.44	7.17 (DS)	0.72
DK ATM	0.91 (DS)	0.09	9.82 (DS)	0.98
	2.52 (DS)	0.25	13.97 (DS)	1.40
LT ATM	3.29 (DS)	0.34	4.31 (DS)	0.43
	7.44 (DS)	0.74	7.47 (DS)	0.75

NS = No Dark Solids Present
DS = Dark Solids Present

Table 4.4.2.4 Range of ICP-AES Analysis for Manganese Measured in the Secondary Effects Filtrate

	0.03 M Mn Range (mg/L)	**Mass on Filter (mg)**	**0.01 M Mn Range (mg/L)**	**Mass on Filter (mg)**
DK N_2	1.0 (NS)	0.10	36.0 (NS)	3.60
	1.5 (NS)	1.15	15.8 (NS)	1.58
LT N_2	6.9 (NS)	0.69	19.0 (DS)	1.90
	10.6 (NS)	1.06	12.4 (DS)	1.24
DK ATM	2.1 (DS)	0.21	25.2 (DS)	2.52
	5.3 (DS)	0.53	30.6 (DS)	3.06
LT ATM	7.0 (DS)	0.70	8.20 (DS)	0.82
	17.2 (DS)	1.72	18.8 (DS)	1.88

NS = No Dark Solids Present
DS = Dark Solids Present

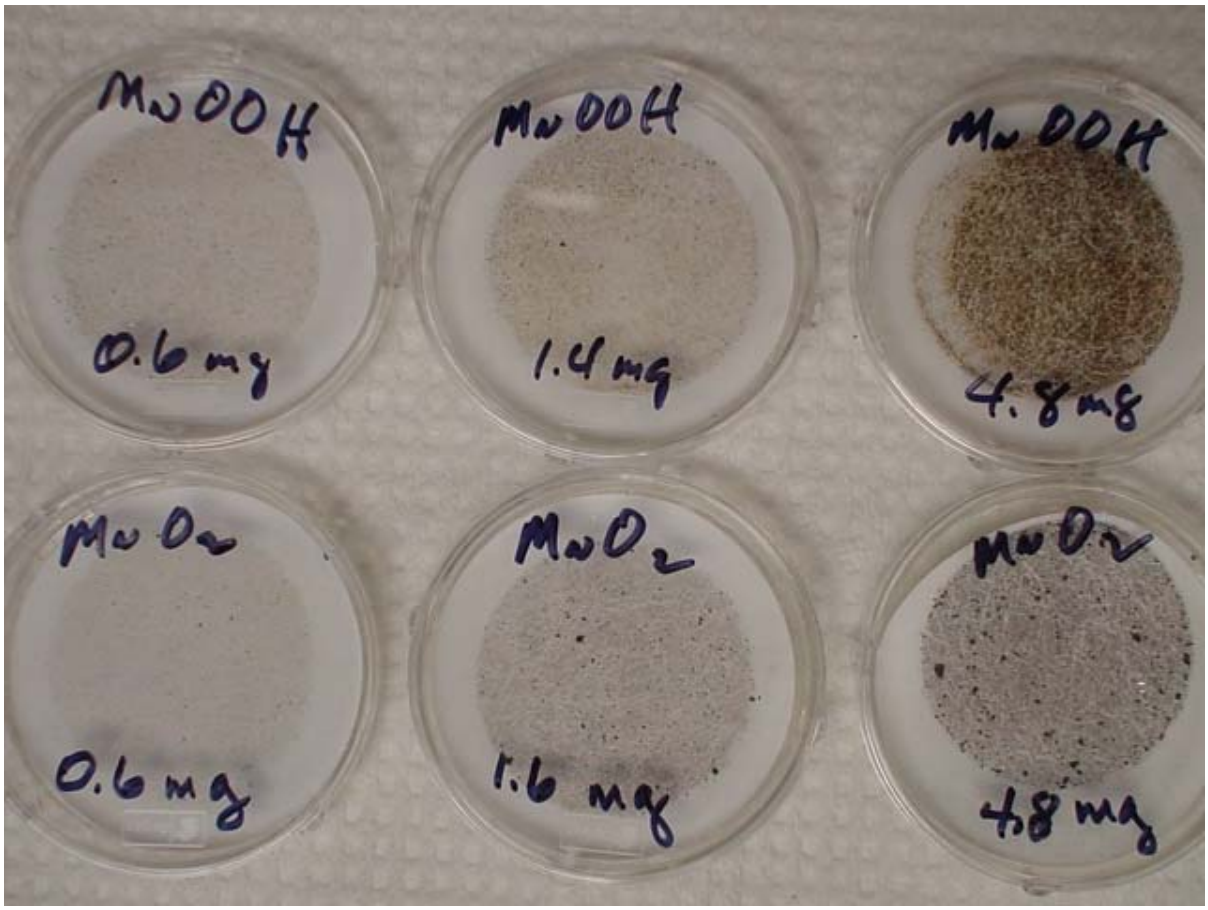

Figure 4.4.2.14 Manganese (III) Oxy-hydroxide and Manganese (IV) Dioxide on Filters

Data presented for iron plotted in Figures 4.4.2.6 through 4.4.2.9 also did not indicate the loss of iron from solution during the 16-day period. Since iron did not appear to be a major constituent in the precipitate mass collected and analyzed during the primary effects experiments (Table 4.4.1.3), the mass of iron possibly adsorbed onto the manganese solids would not be indicated from analysis of the 0-16 day filtrates.

Strontium data presented in Figures 4.4.2.10 through 4.4.2.13 indicate that strontium was lost from solution during the 16-day period for all treatment combinations. The initial strontium concentration at time zero for the 0.03 M permanganate treatment appears to be lower than the concentration in the 0.01 M permanganate reaction. Rate constants and half-lives describing the loss of strontium from the filtrates during the 16-day period are listed in Table 4.4.2.5. These constants were calculated from four data points and therefore should be considered as estimates. Although not significantly different, the half-lives calculated for filtrates maintained in the light ranged from 15.3 to 21.2 $days^{-1}$ while those maintained in the dark ranged from 22.4 to 60.3 $days^{-1}$. Post-filtration solids formation in the NOC (0.03 M Mn, Dark, N_2) is predicted to be much slower than the cross effect conditions reported. It should be noted that the total mass of solids formed during the 16-day period depends on the initial concentration of strontium in the filtrates. In general, the initial strontium concentrations in the filtrates were higher for the 0.01 M permanganate reaction condition.

Table 4.4.2.5 Calculated First Order Rate Constants for Loss of Strontium from AN-107 Secondary Effects Filtrates

	Sim 7	R^2	Sim 8	R^2	Combined	R^2	$t_{1/2}$ (Days)
.01Mn Light Atm	0.0498	0.9775	0.0350	0.8677	0.0369	0.8825	18.78
.03Mn Light Atm	0.0330	0.8759	0.0576	0.8649	0.0453	0.7864	15.30
.01Mn Dark Atm	0.0263	0.9003	0.0264	0.8706	0.0263	0.8827	26.36
.03Mn Dark Atm	0.0052	0.9845	0.0359	0.9847	0.0206	0.3372	33.65
.01Mn Light N2	0.0402	0.9230	0.0398	0.7697	0.0400	0.8290	17.33
.03Mn Light N2	0.0203	0.9917	0.0451	0.8815	0.0327	0.7716	21.20
.01Mn Dark N2	0.0276	0.8349	0.0341	0.8503	0.0309	0.8293	22.43
.03Mn Dark N2	0.0049	0.9012	0.0180	0.9803	0.0115	0.5932	60.27

Characterization of Solids that Formed During the 16 Days

Solids collected from the filtrate samples at the end of the observation period were completely soluble in 20 mL of 0.5 M nitric acid. ICP-AES analysis of the solutions is presented in Table 4.4.2.6 for Mn, Fe, Sr, Ce, La, Nd, and Zr and represents the percent of the initial cation concentration present in the precipitates collected from the 241-AN-107 secondary effects filtrates. A tabulation of the remaining metals is also presented in Appendix E, Table E.8.

Data presented in the table indicate that the compositions of solids precipitated from the filtrates were composed primarily of manganese and strontium with lesser amounts of iron included in the composition. Interestingly, though the samples reacted with 0.01 M permanganate had higher time zero concentrations of manganese in the filtrate, larger percentages of manganese precipitated from the 0.03 M permanganate reactions (light/N_2 and light/atm) compared to the 0.01 M permanganate reaction condition. With exception of the 0.01 M permanganate reaction maintained in the dark under an atmospheric blanket, the remaining filtrates maintained in the dark indicated that low percentages of the initial manganese were present in the post-filtration solids. The percent of iron in the initial filtrates found in the precipitated solids generally tracked the manganese results, suggesting co-precipitation of iron with the manganese precipitate.

With exception of the 0.03 M permanganate reaction maintained in the dark, the percent of initial filtrate mass of strontium converted to a precipitate within the 16-day period ranged from 19 to 51% (Table 4.4.2.6). The highest conversion was reported for the 0.01 M permanganate reaction exposed to light, 44% for filtrates maintained in the atmosphere and 51% for filtrates maintained under a nitrogen blanket. It appears that light may play a more important role in the precipitation of strontium than exposure to the atmosphere.

Table 4.4.2.6 Percent of the Initial Cation Concentration Present in the Precipitates Collected from the 241-AN-107 Secondary Effects Filtrates

	0.03 M Mn	0.03 M Mn	0.03 M Mn	0.03 M Mn	0.01 M Mn	0.01 M Mn	0.01 M Mn	0.01 M Mn
Element	SIM7-DkN2	SIM7-LtN2	SIM7-DkAtm	SIM7-LtAtm	SIM7-LtN2	SIM7-DkAtm	SIM7-LtAtm	SIM7-Dk2N2
Mn	0.04	7.58	0.01	10.01	1.61	1.84	5.57	0.13
Fe	0.02	0.52	0.02	0.75	0.22	0.79	2.67	0.04
Sr	2.46	19.28	0.67	32.51	50.87	33.71	43.63	22.89
La	0.36	3.86	ND	7.12	6.34	5.43	8.49	2.79
Ce	0.06	2.50	ND	3.78	2.53	1.81	4.52	0.65
Nd	0.03	0.94	ND	1.71	1.06	1.61	2.85	0.50
Zr	0.11	0.19	0.08	0.21	0.15	0.46	1.12	0.11

4.5 RESULTS OF THE 241-AN-102 EXPERIMENTS

4.5.1 Primary Effects Study

Visual Observations

Variables investigated for the 241-AN-102 primary effects study are listed in Table 4.5.1.1 with notation indicating the time at which visible solids appeared in the respective filtrates during the 16-day observation period. At the end of the 16-day period, filtrates were filtered under a nitrogen blanket to gravimetrically determine the mass of solids formed and the color and texture of the solids. The presence of brown to black solids on the filters is also indicated in the table.

Several observations warrant discussion. First, white or very light brown solids appeared in all filtrates during the 16-day period. These solids appeared within 1 day in all treatment conditions except the 0.0 M added NaOH, and light solids appeared in this filtrate at day 4. Light colored solids appeared in the filtrates from the newly optimized conditions and the associated treatment variables at later times. Namely, they appeared in the NOC at 6 to 8 days, and in the NOC-0.01 M permanganate, NOC-light and NOC-O_2 at day 6, 10 and 13, respectively. Secondly, dark solids were visible in many of the filtrates, namely the base case 'B' replicate, 0.01 and 0.03 M permanganate treatments, the 0.03 M Sr treatment, the base case treatment stored in the light, the 8-hr hold at 100 ^{o}C and the NOC treatment stored in the light. Observations for the 8-hour hold at 100 ^{o}C samples indicating the presence of solids were made during the 8-hr period. The presence of brown to black solids on the filters correlates with the visual observations noted for all filtrates. Digital photographs of the filtrates and particular filters are included in Appendix F.

For all treatment conditions, white or clear solids on the bottom of the flasks were the first to appear. In some filtrates, these solids were then covered by a thin layer of light brown solids. Light solids that appeared on the surface generally became darker with time, presumably as they were oxidized. The presence of brown to black solids is indicated from visual observations of the filtrates, but should be evaluated from particulate data for better clarity.

Table 4.5.1.1 Visual Observations for 241-AN-102 Post Filtration Precipitation Study

Sample Condition	Filtrate Color	Light solids on bottom	Light solids on surface	Dark solids on surface	Dark solids on bottom
Base Case	Yellow/olive oil	Day 1	Day 8	X	X
Light	Yellow/lime green	Day 1	X	Day 1	X
O_2 Sparge	Yellow/orange	Day 1	Day 8	X	X
0.0 M (added) OH^-	Yellow	Day 4	X	X	X
0.03 M Sr	Olive/lime green	Day 1	Day 4	~Day 14	X
Shear @ 10,000 rpm	Yellow	Day 1	Day 4	X	X
8 hr @ 100 °C	Yellow	Hour 6	X	Hour 3	Hour 6
0.01 M Mn	Tea	Day 1	Day 1	~Day 8	X
0.03 M Mn	Lighter Tea	Day 1	Day 1	~Day 12	X
Base Case	Yellow/olive oil	Day 1	Day 2	~Day 12	X
25 °Rxn	Yellow/olive	Day 1	Day 1	X	X
NOC-BC (1)	Yellow/olive	Day 8		X	X
NOC-.01M Mn	Brownish yellow	Day 6	X	X	X
NOC-BC (1)	Yellow	Day 6	X	X	X
NOC-O_2	Orangish yellow	Day 3 (B) 13 (A)	X	X	X
NOC-Light	Greenish yellow	Day 10	Day 2	Day 10	Day 10

X denotes no solids present at Day 16

Light solids are white to light brown
Dark solids are dark brown to black

From the particulate data collected at the end of the 16-day period, all treatments indicated the presence of brown to black solids except the 0.0 M added NaOH and the 25 °C reaction conditions compared to the base case scenario; and the NOC and NOC 0.01 M Mn. It should also be noted that for both the AN-107 base case and NOC experiments that were reacted at 25 °C no brown to black solids formed during the 16-day period.

In summary, the data suggests that for the base case conditions, lowered reaction temperature and the absence of added NaOH do not result in the formation of dark solids within 16-days. Similarly, the variable evaluated for the newly optimized conditions that did not result in the formation of dark solids was the 0.01 M permanganate treatment. The newly optimized conditions also did not result in the formation of dark solids.

Bulk E_H was monitored during the 16 day period for the baseline and newly optimized conditions in addition to the respective oxygen purge treatments. These data are presented in Figures 4.5.1.1 and 4.5.1.2. Oxygen purge samples were sparged with oxygen for 15 minutes on day 0, and the headspace was purged with oxygen for 15 minutes on days 1, 2, 4, 8, and 16, afterwards, samples were taken for ICP-AES analysis. As can be seen, the bulk E_H of the

solutions was not significantly altered by the oxygen purge. This is supported by the lack of dark solids formed in the NOC oxygen sample and by the presence of dark solids on the bottom of the baseline oxygen sample only after appearance of dark solids on the surface.

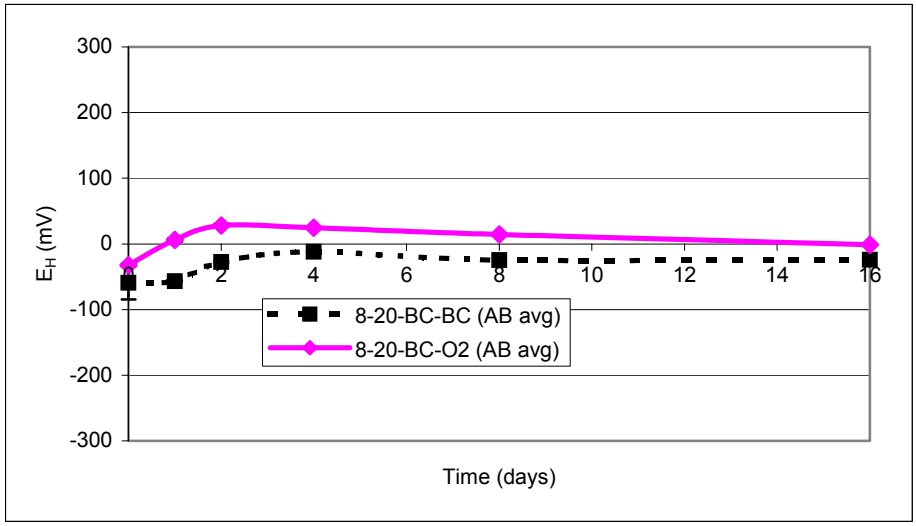

Figure 4.5.1.1 E_H Measurements for the AN-102 Base Case and Oxygen Purge Filtrates

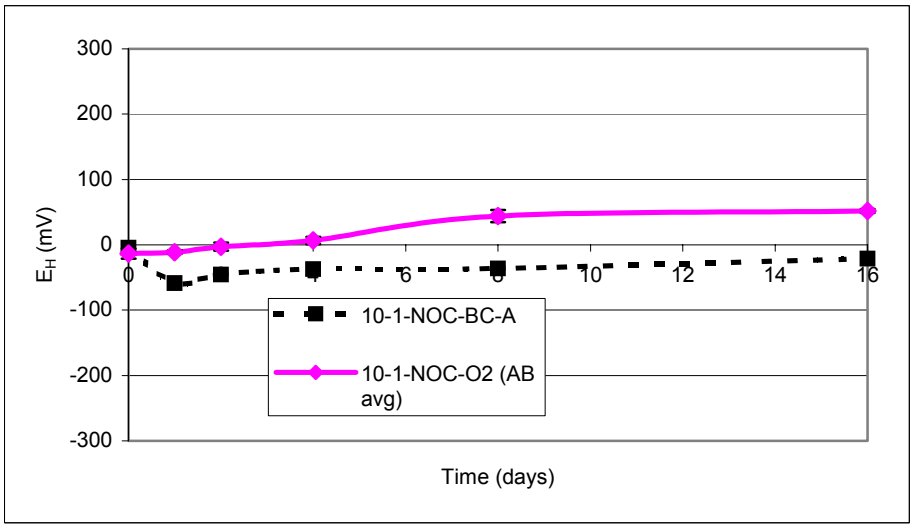

Figure 4.5.1.2 E_H Measurements for the AN-102 NOC Base Case and Oxygen Purge Filtrates

Change in Metal Ion Concentration During the 16-Day Observation Period for AN-102

During the 16-day period, 10-mL aliquots of the filtrates were collected and filtered at 0.1 µm at time zero; days 1, 2, 4, 8, and 16. Aliquots collected at time zero, day 8 and day 16 were acidified to pH 1 or below and analyzed by ICP-AES. A decrease in the concentration of cations present in the filtrates with time would suggest precipitation of solids containing

the respective cation. These data are shown in Figures 4.5.1.3 through 4.5.1.8 for Mn, Fe, and Sr for each treatment condition included in the baseline primary effects study. Data plots for the treatments included in the primary effects study for the NOC are shown in Figures 4.5.1.9 through 4.5.1.14. The notation 'A' and 'B' indicates replicates of the treatment with simulant A and simulant B. The notation used for the AN-107 study was '7' and '8' indicating treatments with simulant 7 and 8. ICP-AES data for cerium, lanthanum, neodymium, and zirconium for each of the primary effects considered for the base case condition and the newly optimized condition are summarized in Table 4.5.1.2, which is discussed later.

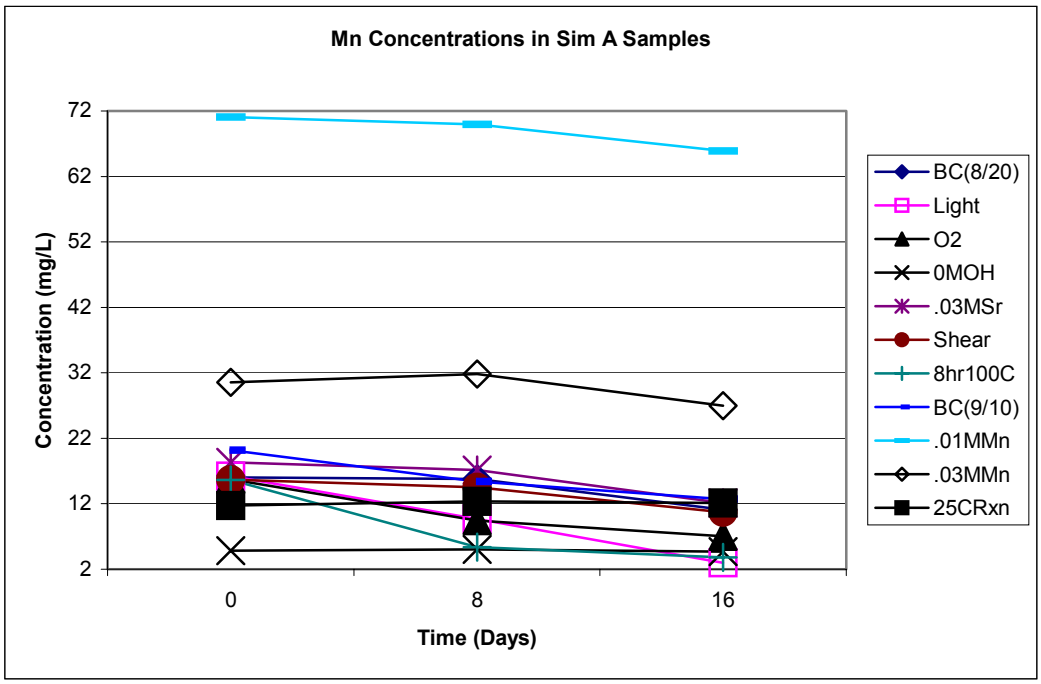

Figure 4.5.1.3a Manganese Concentration in Replicate A Filtrates for the AN-102 Baseline Primary Effects Study

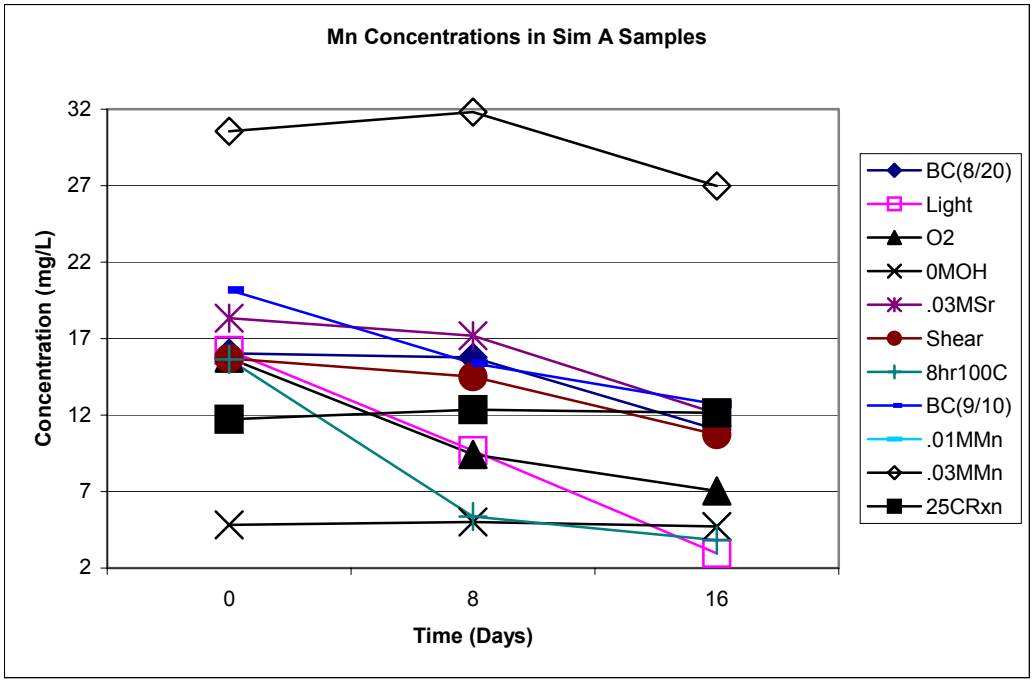

Figure 4.5.1.3b Manganese Concentration in Replicate A Filtrates for the AN-102 Baseline Primary Effects Study (Data Scaled for Clarity. 0.01 M Mn Condition not shown)

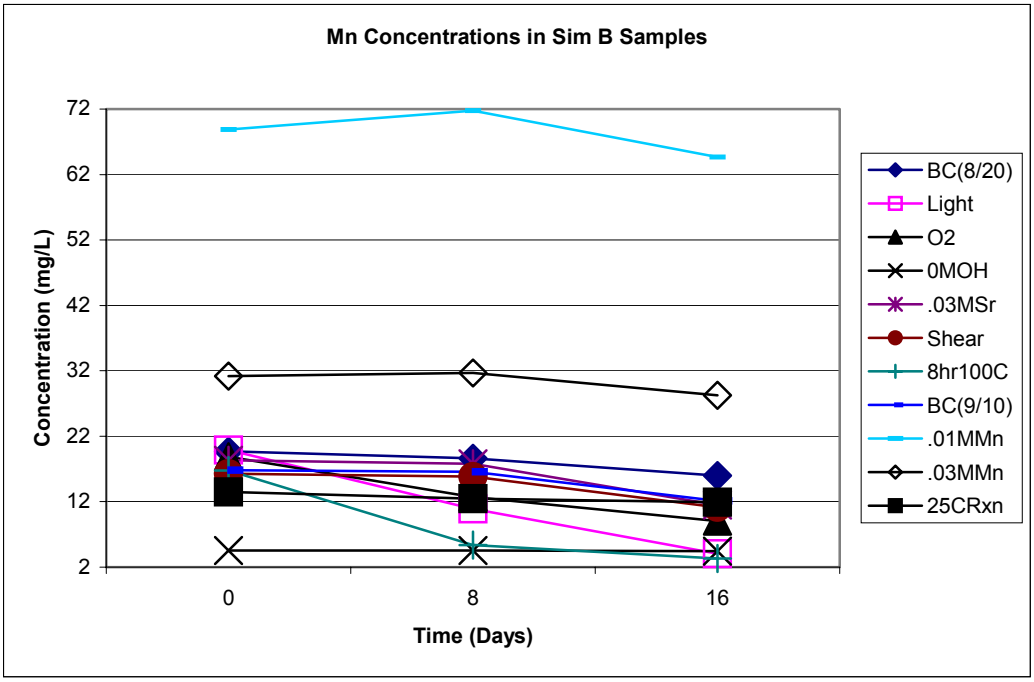

Figure 4.5.1.4a Manganese Concentration in Replicate B Filtrates for the AN-102 Baseline Primary Effects Study

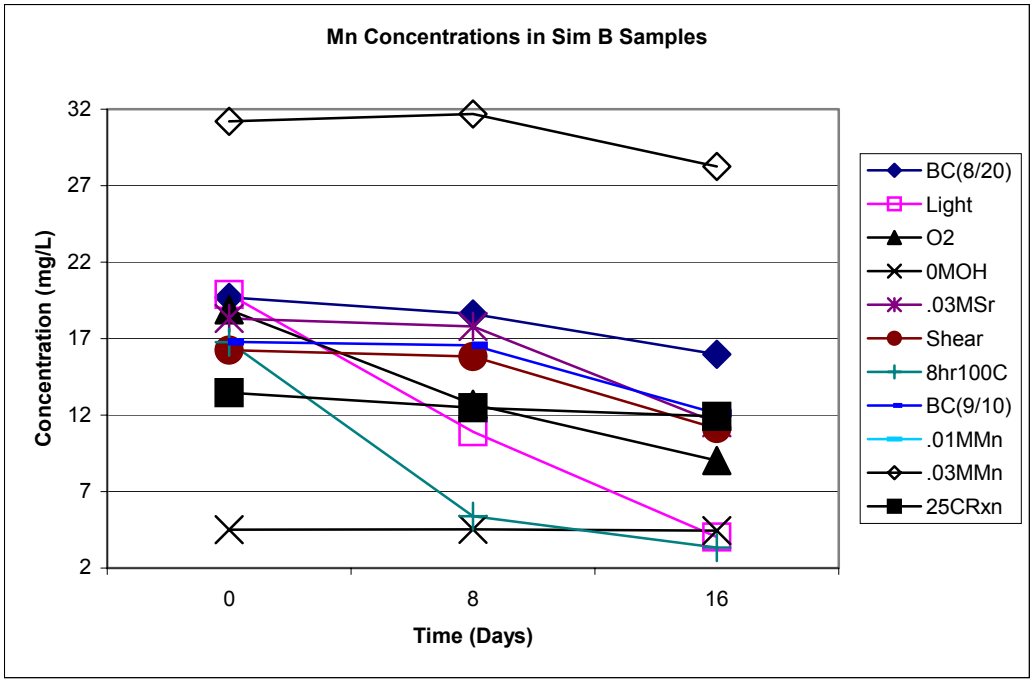

Figure 4.5.1.4b Manganese Concentration in Replicate B Filtrates for the AN-102 Baseline Primary Effects Study (Data Scaled for Clarity. 0.01 M Mn not shown)

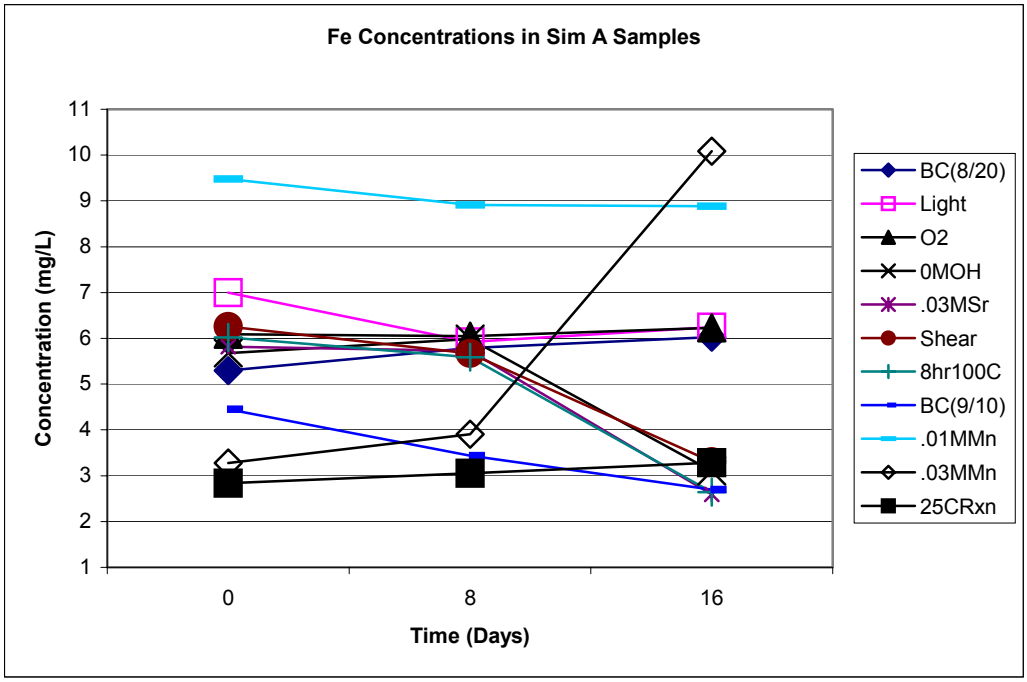

Figure 4.5.1.5 Iron Concentration in Replicate A Filtrates for the AN-102 Baseline Primary Effects Study

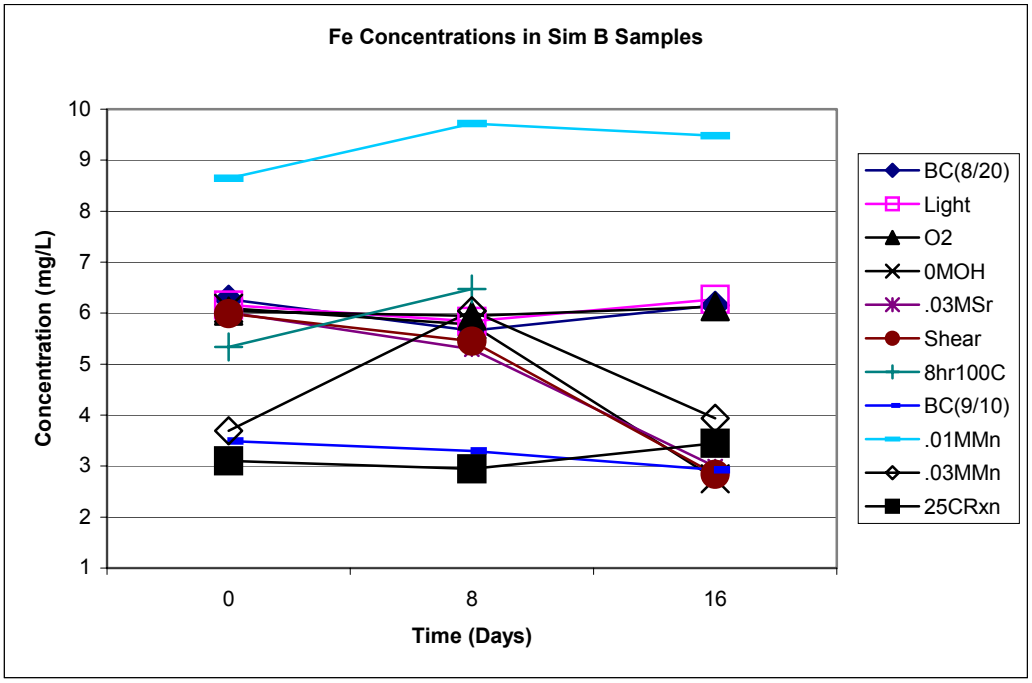

Figure 4.5.1.6 Iron Concentration in Replicate B Filtrates for the AN-102 Baseline Primary Effects Study

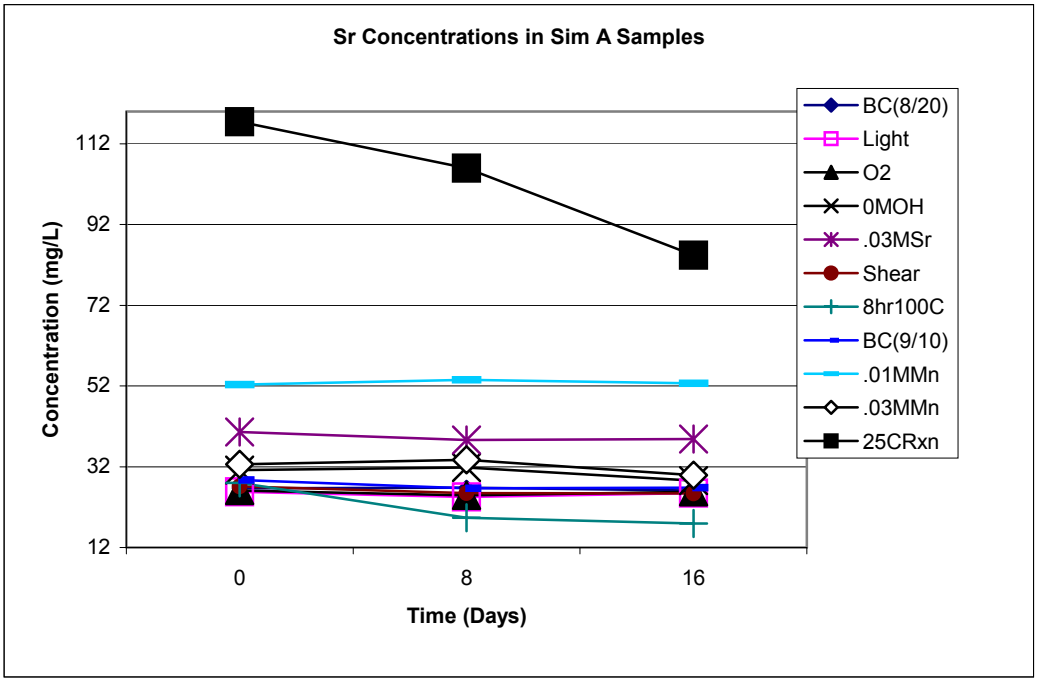

Figure 4.5.1.7a Strontium Concentration in Replicate A Filtrates for the AN-102 Baseline Primary Effects Study

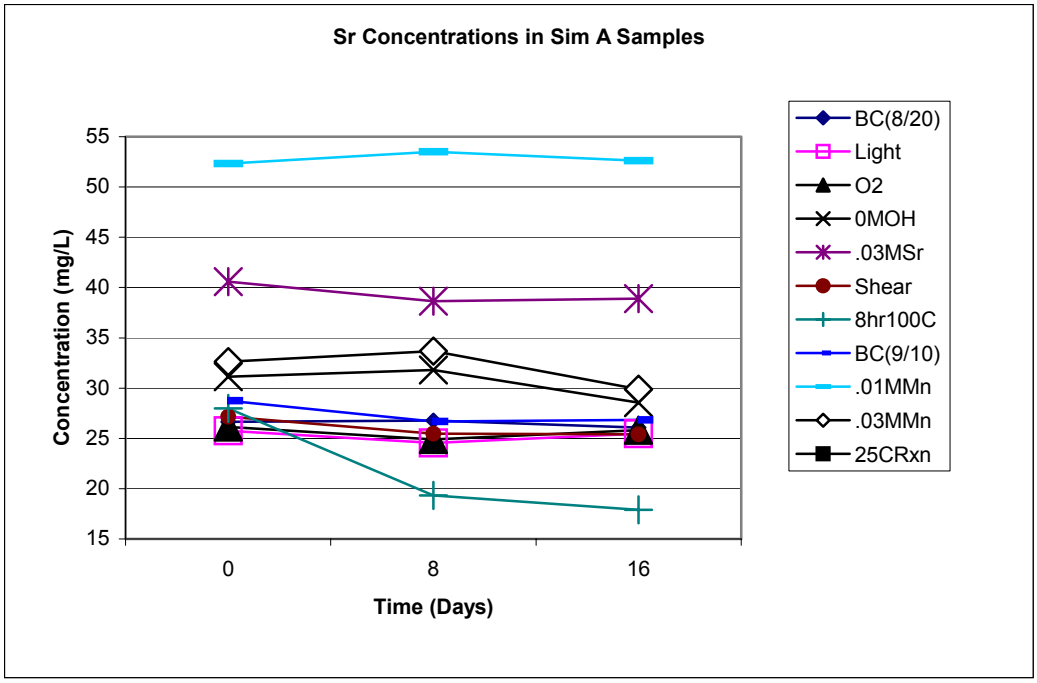

Figure 4.5.1.7b Strontium Concentration in Replicate A Filtrates for the AN-102 Baseline Primary Effects Study (Data Scaled for Clarity, 25 °C Rxn Condition not shown)

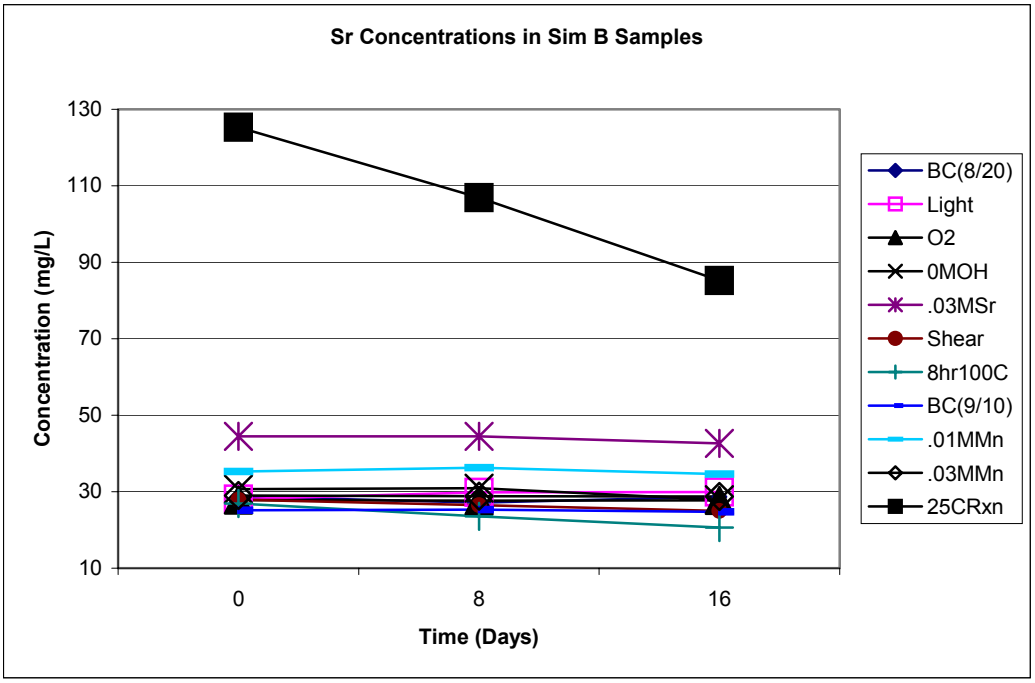

Figure 4.5.1.8a Strontium Concentration in Replicate B Filtrates for the AN-102 Baseline Primary Effects Study

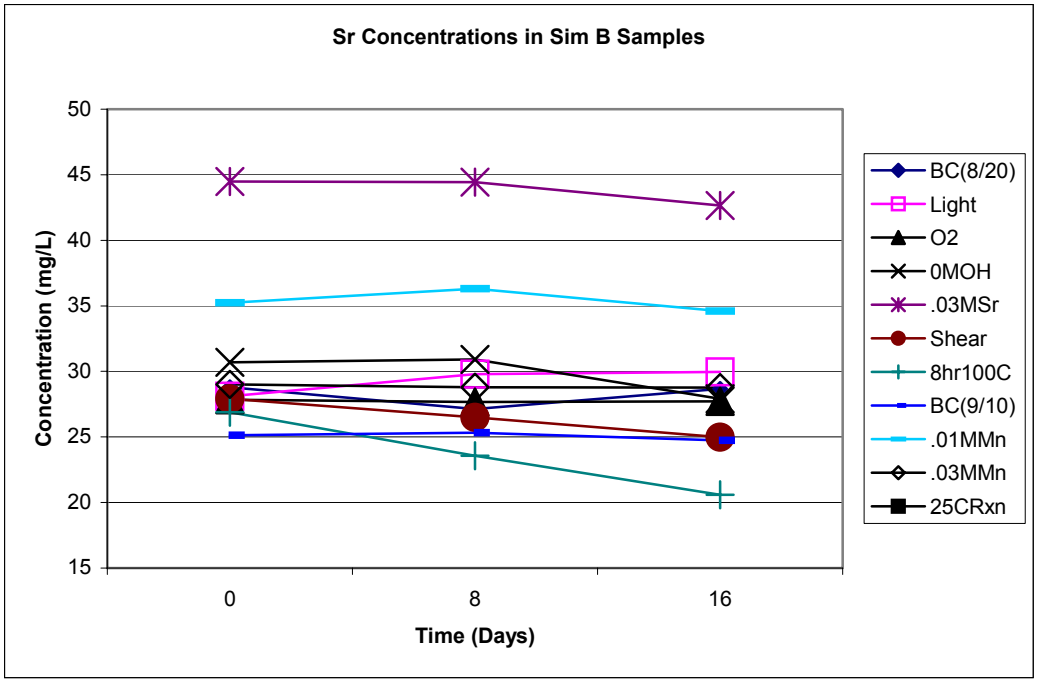

Figure 4.5.1.8b Strontium Concentration in Replicate B Filtrates for the AN-102 Baseline Primary Effects Study (Data Scaled for Clarity, 25 °C Rxn Condition not shown)

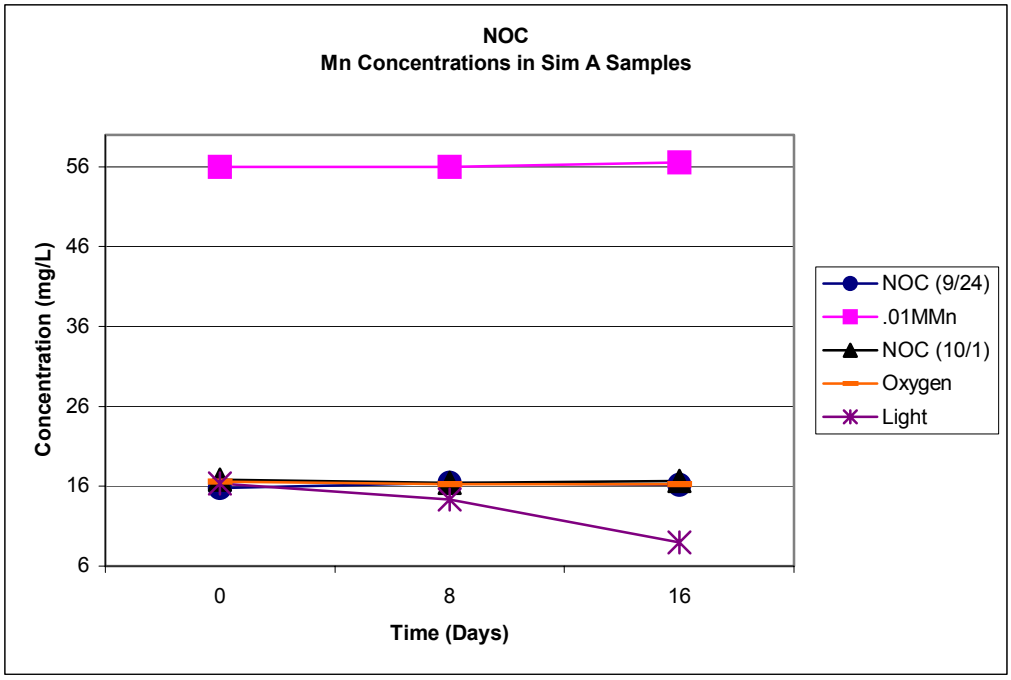

Figure 4.5.1.9 Manganese Concentration in Replicate A Filtrates for the AN-102 NOC Primary Effects Study

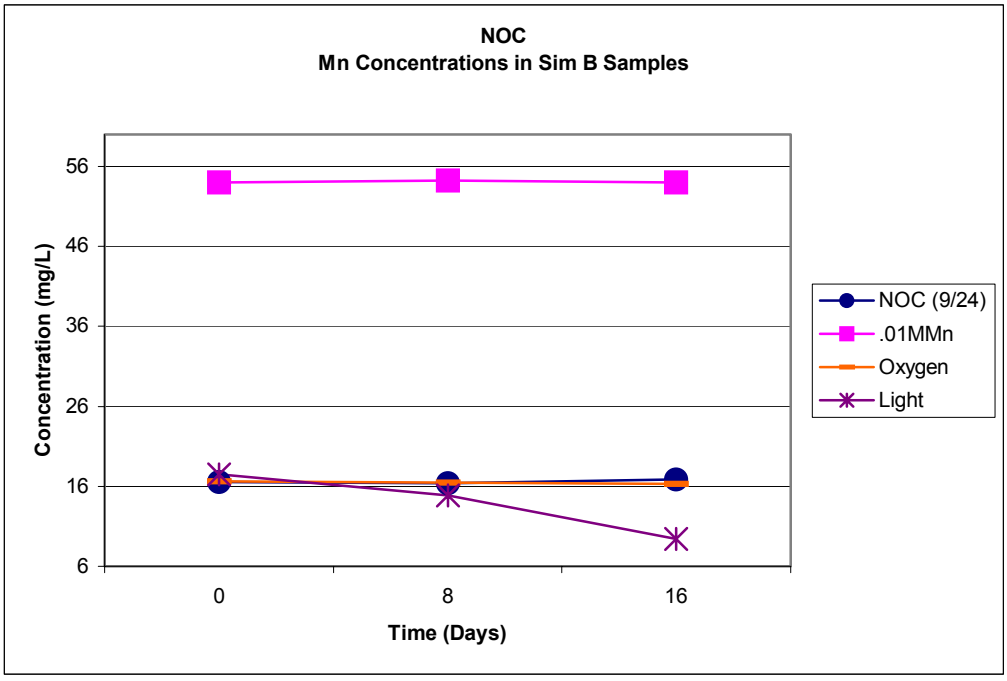

Figure 4.5.1.10 Manganese Concentration in Replicate B Filtrates for the AN-102 NOC Primary Effects Study

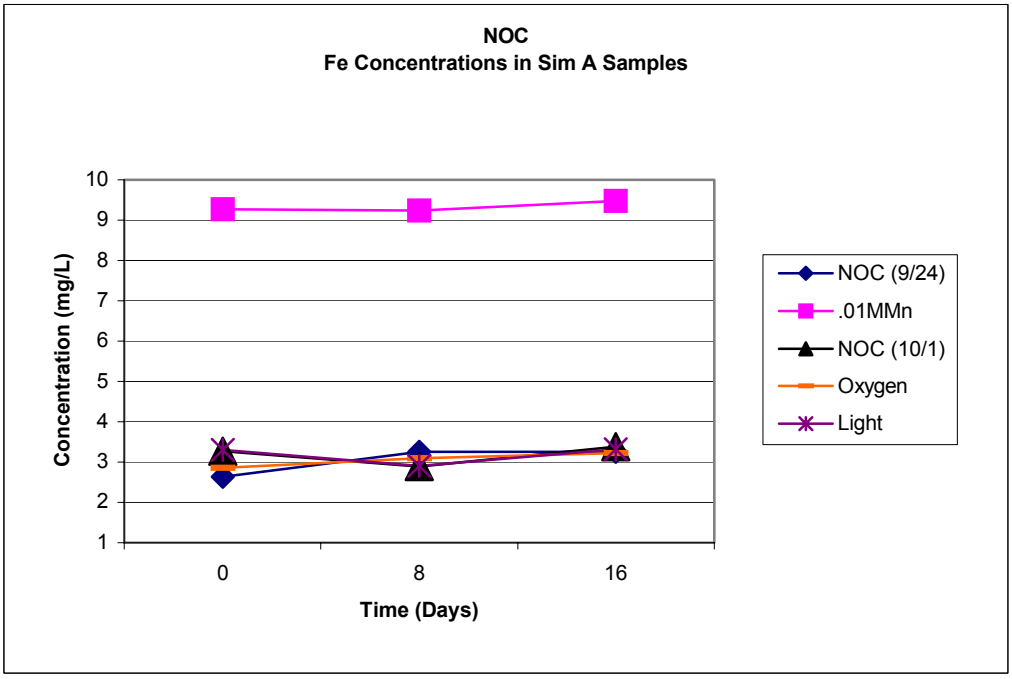

Figure 4.5.1.11 Iron Concentration in Replicate A Filtrates for the AN-102 NOC Primary Effects Study

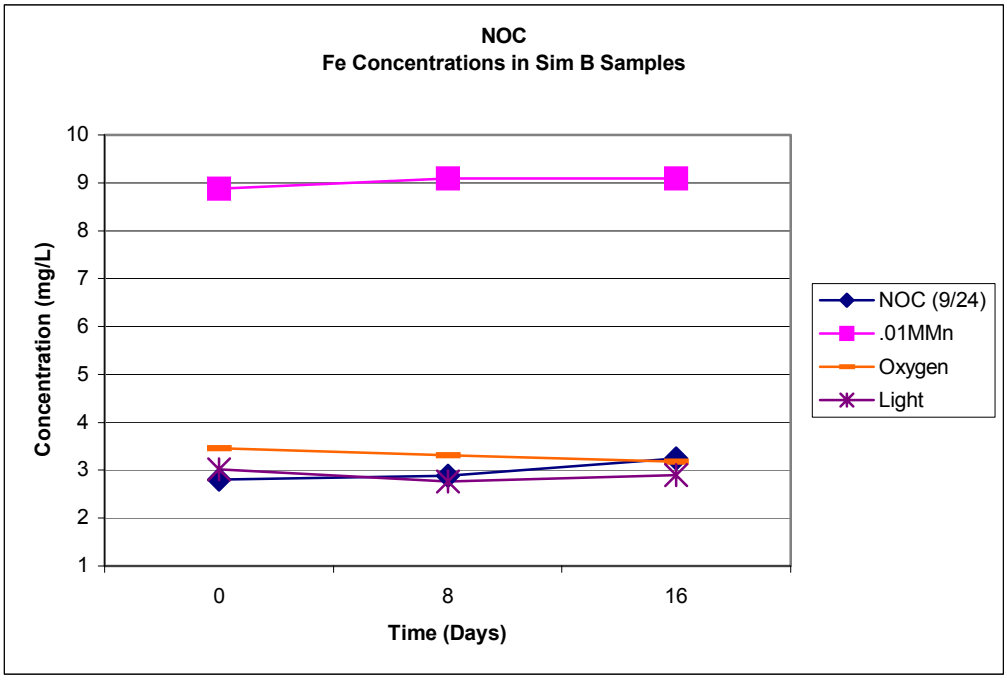

Figure 4.5.1.12 Iron Concentration in Replicate B Filtrates for the AN-102 NOC Primary Effects Study

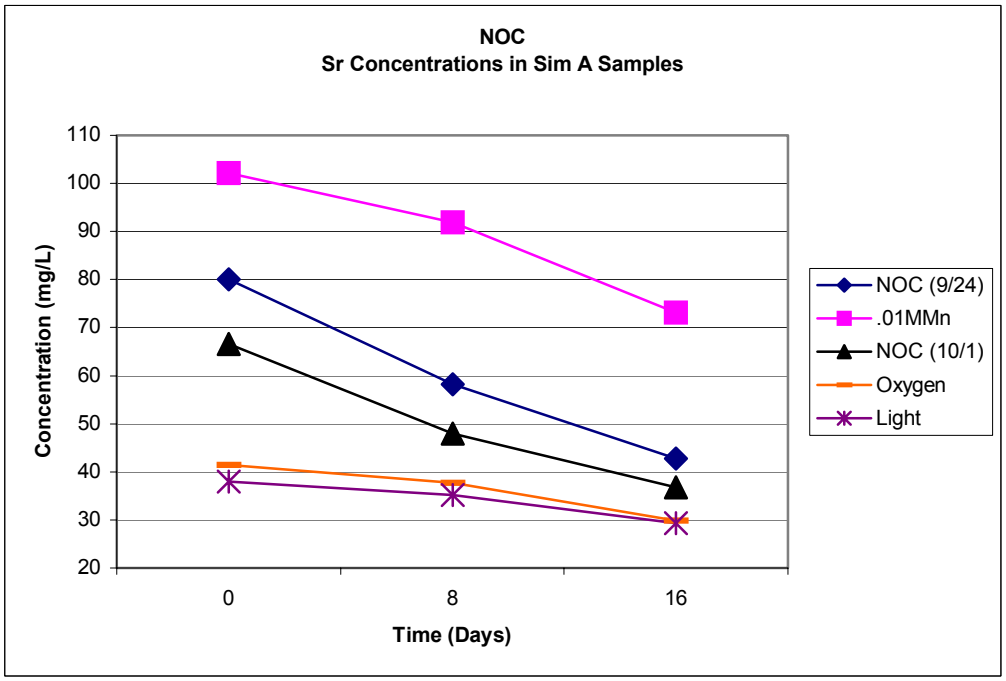

Figure 4.5.1.13 Strontium Concentration in Replicate A Filtrates for the AN-102 NOC Primary Effects Study

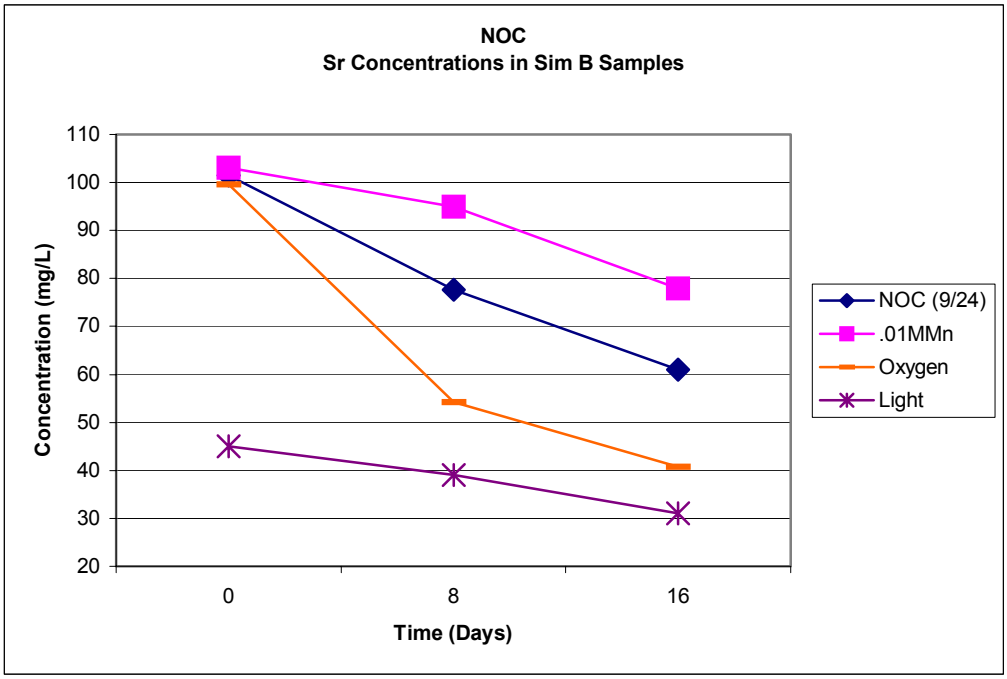

Figure 4.5.1.14 Strontium Concentration in Replicate B Filtrates for the AN-102 NOC Primary Effects Study

Data presented for Mn in Figures 4.5.1.3 and 4.5.1.4 indicate that the Mn concentration in the 0.0 M added NaOH and 25 °C reaction conditions did not decrease during the 16-day period. Recall from the above discussion, the only treatment conditions that did not result in the appearance of dark solids on the filter cakes were the 0.0 M added NaOH and 25 °C reaction conditions. Similarly, comparisons of the manganese data presented for the variables studied for the NOC indicate that the concentration of soluble manganese decreased only for the light condition, Figures 4.5.1.9 and 4.5.1.10. These results also agree with the photographic evidence noting the presence of dark solids on the respective filters.

Some of the data presented for strontium in Figures 4.5.1.7a & b and 4.5.1.8a & b for the base case variables and in Figures 4.5.1.13 and 4.5.1.14 for the NOC variables also show a decrease in soluble strontium during the 16-day period. Five of the variables, namely, 0.0 M added NaOH, 0.03 M Sr, 8-hr hold at 100 °C, shear at 10,000 rpm, and the 25 °C reaction investigated during the base case study and all of the variables investigated during the NOC study suggest the formation of strontium post-filtration solids. Interestingly, all of the NOC variables and the 25 °C reaction experiment conducted during the base case study were reacted at 25 °C. The time zero strontium concentration in these filtrates was significantly higher than the commensurate strontium concentration for the reactions conducted at 50 °C during the base case study. These higher values likely reflect the increased solubility of strontium carbonate at lower temperatures which would lower the isotopic dilution effect. Supersaturated conditions at the lower temperature could result in the slow formation of additional strontium carbonate during the 16-day period. Alternatively, the lower

permanganate levels with the NOC could result in less oxidation of EDTA and therefore more chelate available to solubilize strontium. Absorption of carbon dioxide could also account for additional precipitation of strontium. Even though filtrates were maintained under a nitrogen blanket during the 16-day period, they were exposed to the atmosphere while sampling at time zero, and at days 1, 2, 4, 8, and 16.

The decrease in the soluble strontium concentration for the remaining four of the five variables noted in the above paragraph, namely, 0.0 M OH, 0.03 M Sr, 8-hr hold, and shear correlate with a similar decrease in the soluble iron concentration, Figures 4.5.1.5 and 4.5.1.6. Two possible scenarios may explain the simultaneous decrease in concentration of these two cations. First both iron and strontium solids could have formed during the 16-day period, or only one was formed, and the reduction in concentration of the other cation was a result of co-precipitation or adsorption. Since strontium carbonate forms during the initial precipitation reaction, it is plausible that strontium carbonate forms during the 16-day period and that iron may adsorb onto the solids.

One could also argue that iron co-precipitated with the formation of manganese solids since there is a commensurate decrease in the iron and manganese concentrations for three of the four variables currently being discussed. However, for the remainder of the variables investigated during the base case study, there is no indication that iron co-precipitated with or was adsorbed onto the manganese solids. These observations may be more easily understood by examination of Table 4.5.1.2, which summarizes the change in concentration of several cations during the 16-day period for the primary effects study.

Table 4.5.1.2. Concentration of Selected Cations for the 0-16 Day Observation Period for the 241-AN-102 Primary Effects Study

Cation Concentrations Over 16 Days (mg/L)							
Sample	**Mn**	**Fe**	**Sr**	**Ce**	**La**	**Nd**	**Zr**
BC 8/20	**21.4 - 16.2**	C 5.87 ± .361	C 27.3 ± 1.12	ND <.2125	ND <.175	C 2.51 ± .456	C 0.811 ± .225
BC 9/10	**18.5 - 12.4**	C 3.38 ±.606	C 26.2 ± 1.50	ND <.221	C 0.349 ± .0495	C 3.08 ± .396	C 0.719 ± .0680
0MOH	C 4.68 ± .217	**5.89 - 2.93**	**30.9 - 28.2**	ND <.213	ND <.175	**1.35 - ND<.513**	**.575 - ND<.150**
.03M Sr	**18.3 - 11.8**	**5.92 - 2.79**	**42.5 - 40.8**	ND <.213	ND <.175	**3.54 - 1.86**	**0.846 - 0.163**
.01M Mn	**70.0 - 65.3**	C 9.18 ± .427	C 44.1 ± 9.57	C 0.362 ± .0558	C 1.72 ± .0891	C 9.95 ± .285	C 5.20 ± .119
.03M Mn	**30.9 - 27.6**	C 5.16 ± 2.60	C 30.5 ± 2.15	ND <.221	C 0.822 ± .0435	C 5.07 ± .708	C 1.92 ± .122
25C Rxn	C 12.4 ± .608	C 3.11 ± .222	**121 - 84.8**	ND <.213	C 1.17 ± .0674	C 5.03 ± .336	C .910 ± .0321
Light	**18.1 - 3.64**	C 6.24 ± .411	C 27.3 ± 2.34	ND <.2125	ND <.175	C 2.37 ± .546	C 0.827 ± .134
O2	**17.3 - 8.04**	C 6.06 ± .0955	C 26.7 ± 1.20	ND <.2125	ND <.175	C 2.38 ± .544	C 0.807 ± .113
8hr100C	**16.2 - 3.59**	**5.68 - 2.64**	**27.4 - 19.2**	ND <.213	ND <.175	**3.26 - 1.62**	**0.760 - ND<.15**
shear	**16.0 - 10.9**	**6.12 - 3.07**	**27.5 - 25.2**	ND <.213	ND <.175	**3.82 - 2.22**	**0.757 - ND<.15**
NOC 9/24	C 16.3 ± .347	C 3.01 ± .274	**90.8 - 51.9**	ND <.2125	C 1.55 ± .101	C 6.22 ± .233	C 2.69 ± .0612
NOC 10/1	C 16.6 ± .230	C 3.18 ± .251	**66.7 - 36.7**	ND <.2125	C 1.02 ± .0471	C 5.98 ± .104	C 2.30 ± .0288
NOC .01Mn	C 55.1 ± 1.16	C 9.18 ± .200	**103 - 75.5**	ND <.2125	C 2.03 ± .0474	C 9.48 ± .287	C 6.35 ± .123
NOC O2	**16.6 - 16.2**	C 3.19 ± .207	**70.5 - 35.3**	ND <.2125	C 0.878 ± .208	C 5.57 ± .617	C 2.22 ± .0694
NOC Light	**17.0 - 9.20**	C 3.04 ± .230	**41.5 - 30.1**	ND <.2125	C 1.08 ± .0651	C 6.18 ± .318	C 2.42 ± .0978

The data presented in this table also suggests that the soluble concentration of the cations measured immediately after reaction and filtration varied depending on the treatment

condition. In the table these values are noted as constant values designated with a 'C' and represent average values for the 16-day period for those element concentrations that were invariant, and as the first value noted for cations that did decrease during the 16-day period. For example, in the data range presented for Mn, 21.4 – 16.2, (for the BC 8/20 sample) the value of 21.4 represents the initial concentration of Mn in the filtrate.

Time zero concentration data for each treatment condition are shown in Figures 4.5.1.15 through 4.5.1.20 for Mn, Fe, Sr, La, Nd, and Zr respectively. Cerium concentrations were below detection limits in all filtrates. Clearly, the concentration of these cations in the filtrates immediately after reaction and filtration is dependent on the treatment condition. Data presented in the figures includes error estimates, either a difference in two values or a standard deviation when the averages were calculated from more than two measurements. Statistics were not applied to determine significant differences due to the large number of comparisons to be made with so few degrees of freedom. Instead, significance is implied based on a comparison of concentration values for treatment conditions and considering overlapping error estimates.

The Mn concentration at time zero (Figure 4.5.1.15) for the base case does not differ significantly from the 0.03 M Sr, light, O_2, and shear conditions. With exception of the 0.03 M Sr condition, all were reacted at base case conditions and therefore should be similar. The 25 °C reaction condition, 0.0 M added NaOH, and the 8-hr hold at 100 °C result in a lower initial concentration compared to the base case condition. Conversely, the 0.01 and 0.03 M Mn treatments resulted in higher initial concentrations compared to the base case condition of 0.05 M permanganate. These observations are reasonable given that the conditions that are similar to the base case did not involve a change in reaction conditions, with exception of 0.03 M Sr condition and the shear condition, which only affected the quality of the precipitate. Conditions that differed did involve a change in reagent parameters.

Lowering the reaction concentration of manganese likely resulted in a lower mass of precipitate, which would decrease the removal of soluble manganese if soluble manganese is scavaged by the manganese precipitate (McKenzie, 1980). Increasing the reaction time and temperature would increase the rate and extent of the precipitation reaction, thus lowering the manganese concentration relative to the base case. Decreasing the reaction temperature should have decreased the rate and extent of the precipitation reaction, thus increasing the manganese concentration relative to the base case. However, as evidenced in Figure 4.5.1.15, the manganese concentration was lower than the base case, which cannot be explained.

Lowering the concentration of permanganate in the reaction mixture could also affect the manganese concentration in the filtrate by increasing the degree of solution metal ion complexation. A lower concentration of oxidant (sodium permanganate) may result in a higher concentration of organic ligand, thus increasing complexation and solubility of the metal.

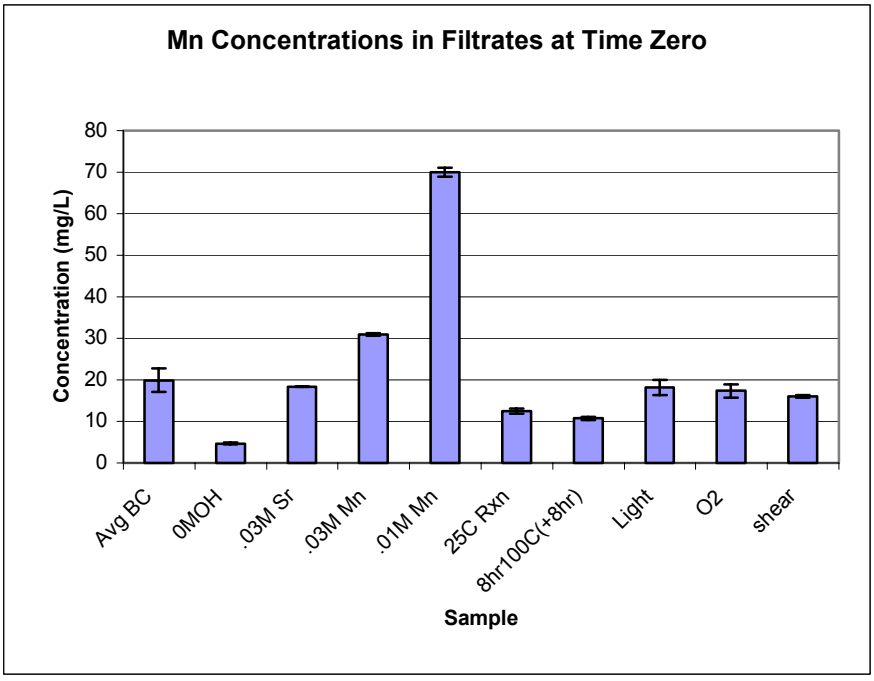

Figure 4.5.1.15 Manganese Concentration in Time Zero Filtrates for the Variables Included in the AN-102 Baseline Primary Effects Study

The time zero concentrations of iron (Figure 4.5.1.16) for the 0.01 M permanganate treatment and the 25 °C reaction condition appear to be significantly different from the base case condition. The iron concentration in the 0.01 M permanganate treatment is higher than the base case. This is reasonable given that a permanganate reaction concentration of 0.01 M compared to a treatment at 0.05 M (base case) would result in less of a reaction precipitate and consequently less iron removed by co-precipitation or adsorption. The apparent lower concentration of iron for the 25 °C reaction condition is as of yet unexplained. Lowering the reaction temperature from 50 to 25 °C should have resulted in less of a reaction precipitate leaving more iron in solution as noted above. However, the behavior of iron in response to the lowered reaction temperature follows that of manganese.

Data presented for strontium (Figure 4.5.1.17) is more difficult to rationalize. First, error estimates for many of the treatment conditions are very small, and the means are similar in magnitude. Four reaction treatments may be significantly different than the base case condition, namely, the 0.03 M strontium treatment, 0.01 M permanganate treatment, 25 °C reaction condition and the 8-hr hold at 100 °C. With exception of the 8-hr hold condition, all appear to be have higher concentration of strontium than the base case. Adding less strontium and permanganate to the reaction mixture may result in less of a reaction precipitate and less removal of strontium by co-precipitation or adsorption. Additionally, as previously stated a lower reaction concentration of oxidant could result in less oxidation of the organic complexants thus increasing complexation and solubility.

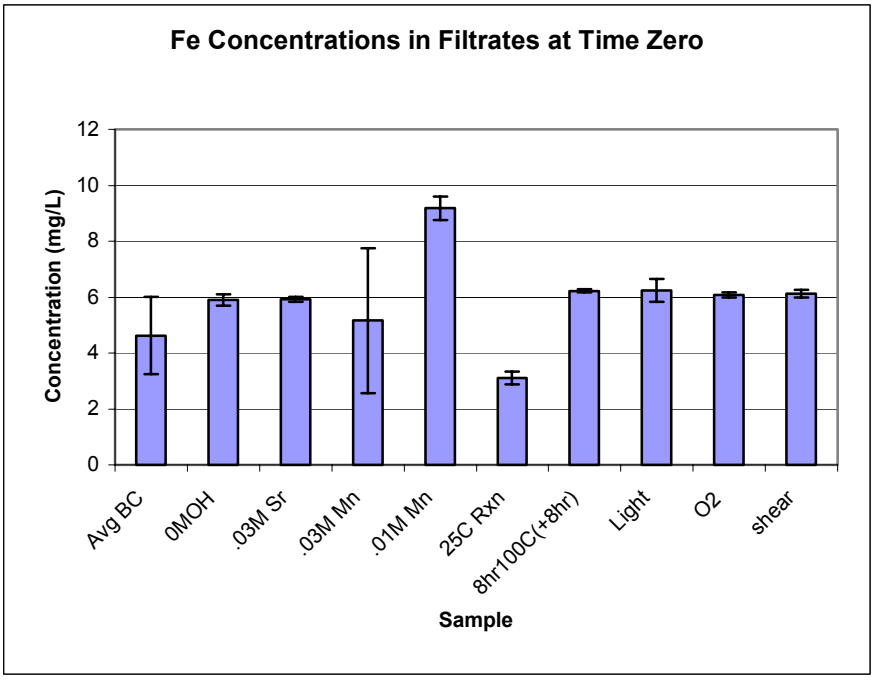

Figure 4.5.1.16 Iron Concentration in Time Zero Filtrates for the Variables Included in the AN-102 Baseline Primary Effects Study

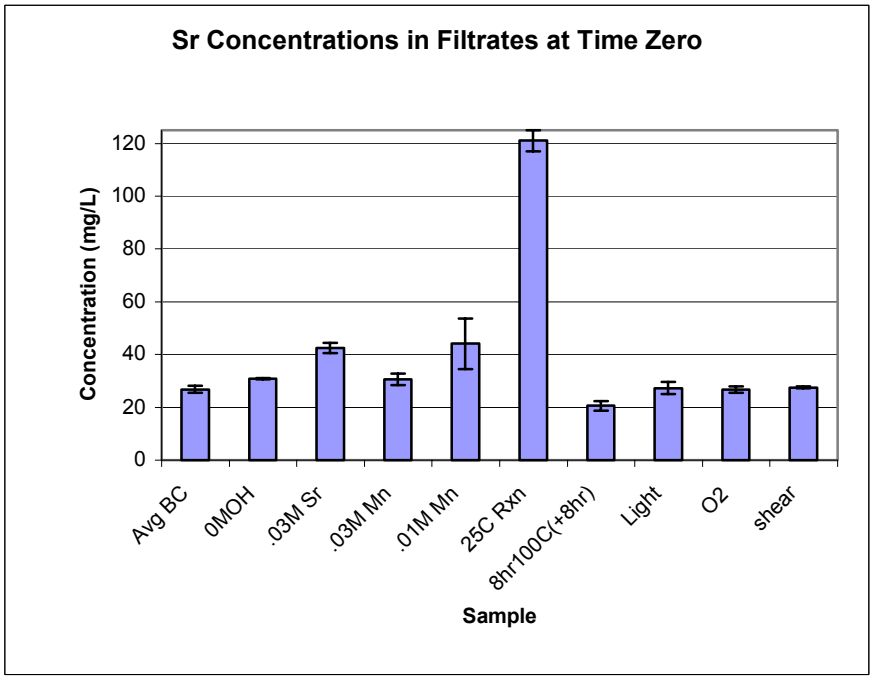

Figure 4.5.1.17 Strontium Concentration in Time Zero Filtrates for the Variables, Included in the AN-102 Baseline Primary Effects Study

The most noticeable effect on time zero strontium concentrations is that of a lowered reaction temperature, which resulted in less strontium removal and thus higher strontium concentrations in the time zero filtrate. This effect is most likely a result of the increased solubility of strontium at lower temperatures. This rationale may be counterintuitive since all reaction mixtures were cooled to 25 ^{o}C before filtering, which would contradict the above explanation. However, kinetic limitations regarding attainment of equilibrium solubility may result in the observed solubility of strontium.

Data presented for lanthanum, neodymium, and zirconium in Figures 4.5.1.18, 19, and 20 appear also to differ for many of the reaction variables. Lanthanum concentration at time zero for the reaction at 0.0 M added NaOH was below detection. In addition, the lanthanum concentration for two of the treatment variables, namely, exposure to light and oxygen was also below detection. Presumably the removal mechanism for these surrogates is by adsorption, and as a result, the time zero concentration of each should be higher than the base case condition when the change in reaction variable resulted in less of a precipitate mass of manganese oxy-hydroxide or oxide during the initial permanganate oxidation reaction. Likewise, the time zero concentrations of the surrogates with exception of lanthanum, should be elevated or reduced in correspondence with time zero manganese concentrations. However, the 25 ^{o}C reaction condition and the filtrate held at 100 ^{o}C for 8 hours does not follow this pattern. No data exist to explain the difference; however, it is possible that the nature of particles formed in the initial reaction precipitate may differ between 25 and 50 ^{o}C, resulting in less adsorption and a higher concentration in the filtrate. For the 8 hr hold sample, sorption may be more complete, that is less kinetically hindered, thus resulting in a lower concentration in the filtrate.

This relationship can be seen through a comparison of Figures 4.5.1.15 and 4.5.1.18 through 4.5.1.20.

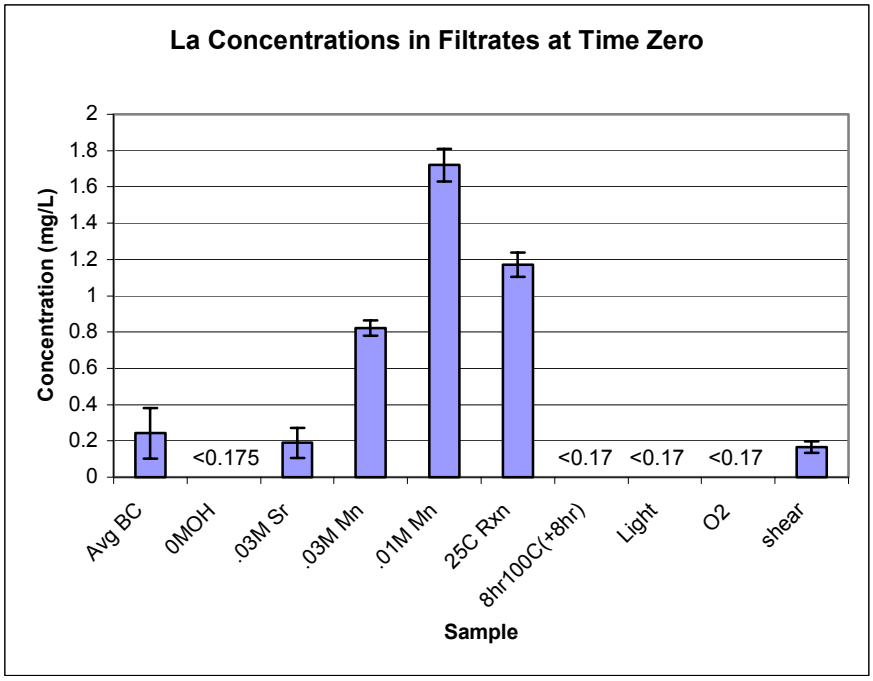

Figure 4.5.1.18 Lanthanum Concentration in Time Zero Filtrates for the Variables Included in the AN-102 Baseline Primary Effects Study

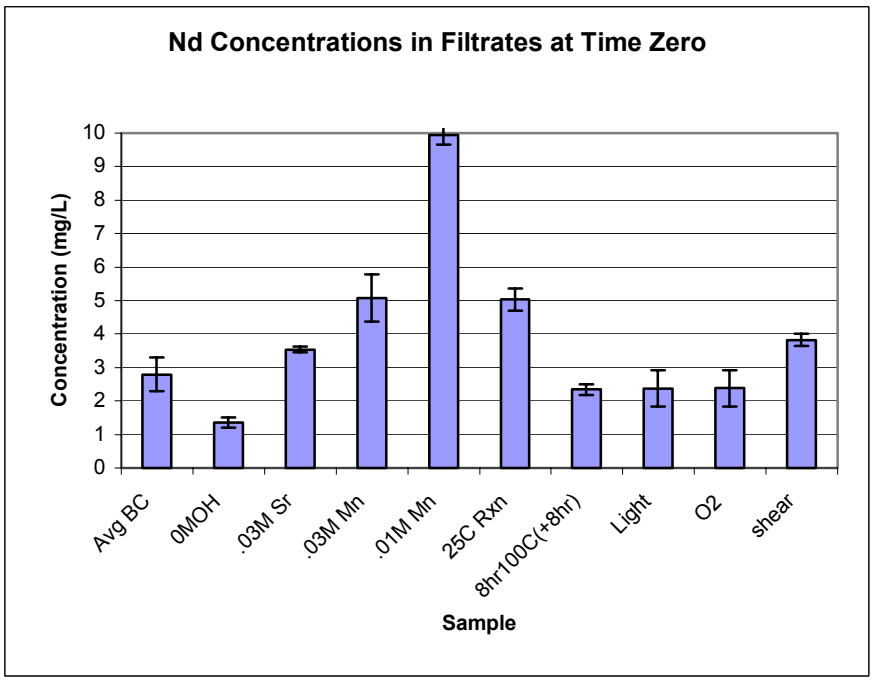

Figure 4.5.1.19 Neodymium Concentration in Time Zero Filtrates for the Variables Included in the AN-102 Baseline Primary Effects Study

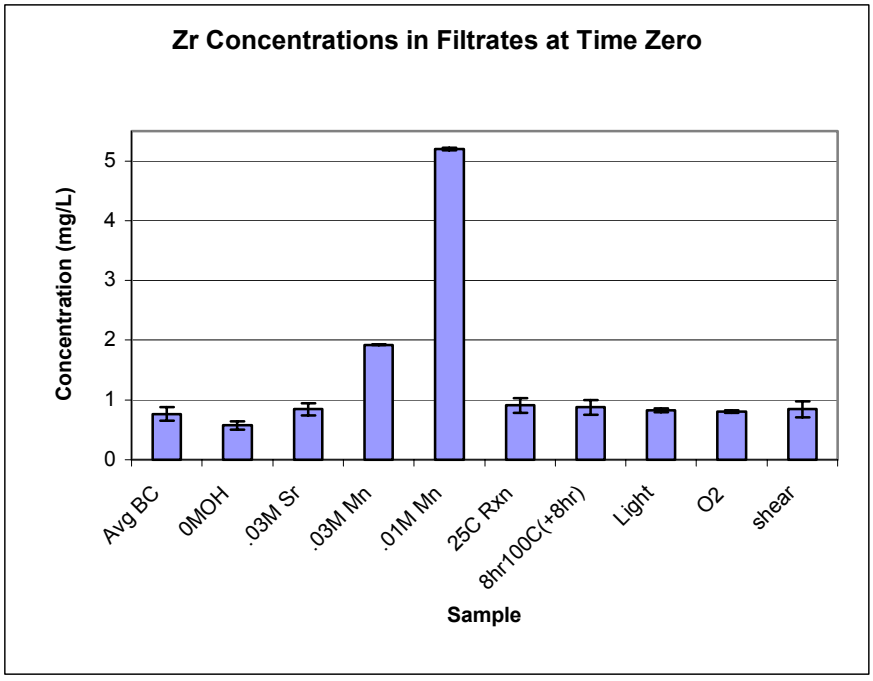

Figure 4.5.1.20 Zirconium Concentration in Time Zero Filtrates for the Variables Included in the AN-102 Baseline Primary Effects Study

Similar data plots are also presented for experiments conducted for the newly optimized condition. Shown in Figures 4.5.1.21 through 4.5.1.26 are data for Mn, Fe, Sr, La, Nd, and Zr. The Mn and Fe data suggest that the only variable tested that differed from the baseline condition was the NOC where the Mn concentration in the reaction mixture was lowered to 0.01 M. Recall that in the baseline primary effects study, Figure 4.5.1.15 and 4.5.1.16, the time zero concentration for both Mn and Fe were higher than the baseline values for the 0.01 M Mn reaction condition, but not for the 0.03 M Mn reaction condition.

The time zero strontium concentration for all of the variables tested differed from the baseline condition. All were higher than the base case condition, (0.075 Mn, 0.05 Sr, and 50 °C reaction temperature). This is most likely due to the fact that all of the NOC experiments were conducted at room temperature. Recall the base case reaction temperature was at 50 °C while the NOC reaction temperature was 25 °C. A lowering of the reaction temperature would decrease the rate of reaction, and for a four reaction time, the extent reaction. Less of an initial precipitate could result in less adsorption of co-metals. An increase in the concentration of organic ligands due to the addition of less oxidant (permanganate) could also account for the increase in filtrate concentration of strontium.

Time zero concentration data for the surrogate cations shown in Figures 4.5.1.24 through 4.5.1.26 are higher than the baseline condition for all variables tested. Three reaction conditions of the NOC, namely the 25 °C reaction temperature and the lower concentrations of Sr and Mn in the reaction mixture, (compared to the baseline conditions), likely affect the formation of the manganese precipitate during the reaction. A smaller mass of precipitate

would translate into a higher concentration of cations in the time zero filtrates if the primary removal mechanism for the cations were adsorption onto the manganese precipitate.

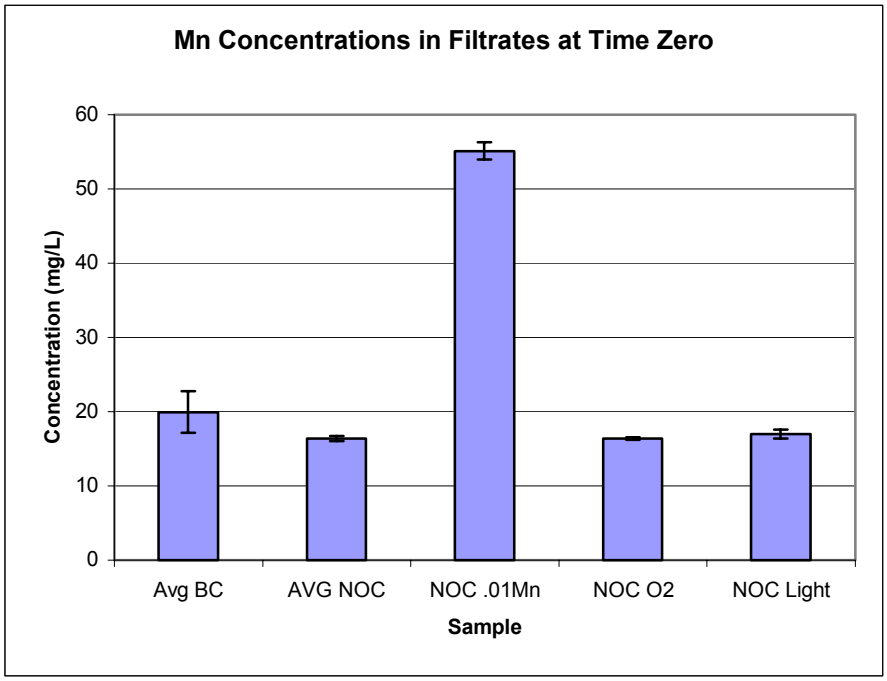

Figure 4.5.1.21 Manganese Concentration in Time Zero Filtrates for the Variables Included in the AN-102 NOC Study

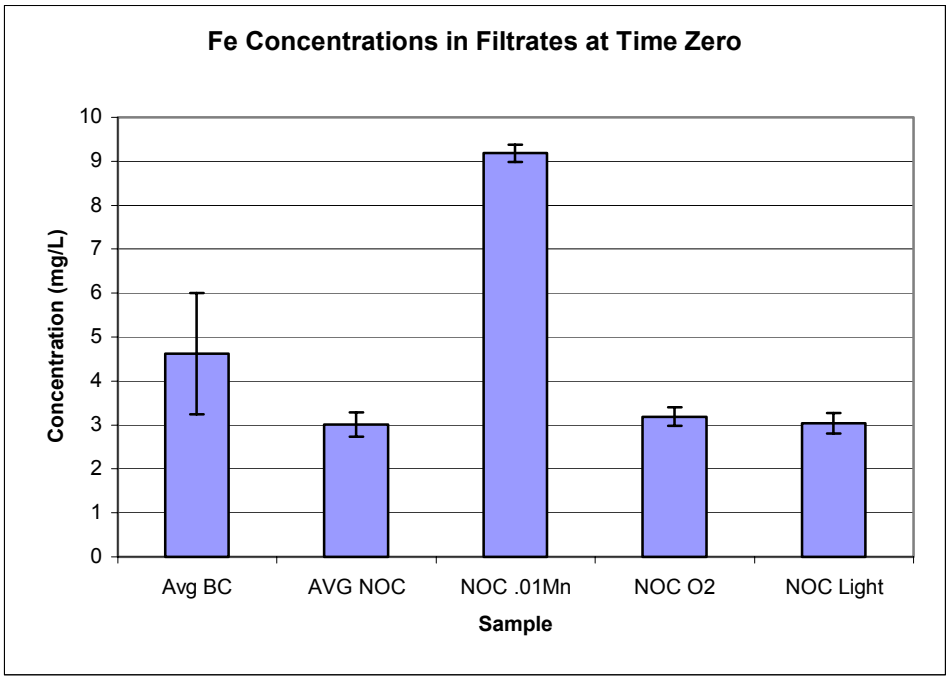

Figure 4.5.1.22 Iron Concentration in Time Zero Filtrates for the Variables Included in the AN-102 NOC Study

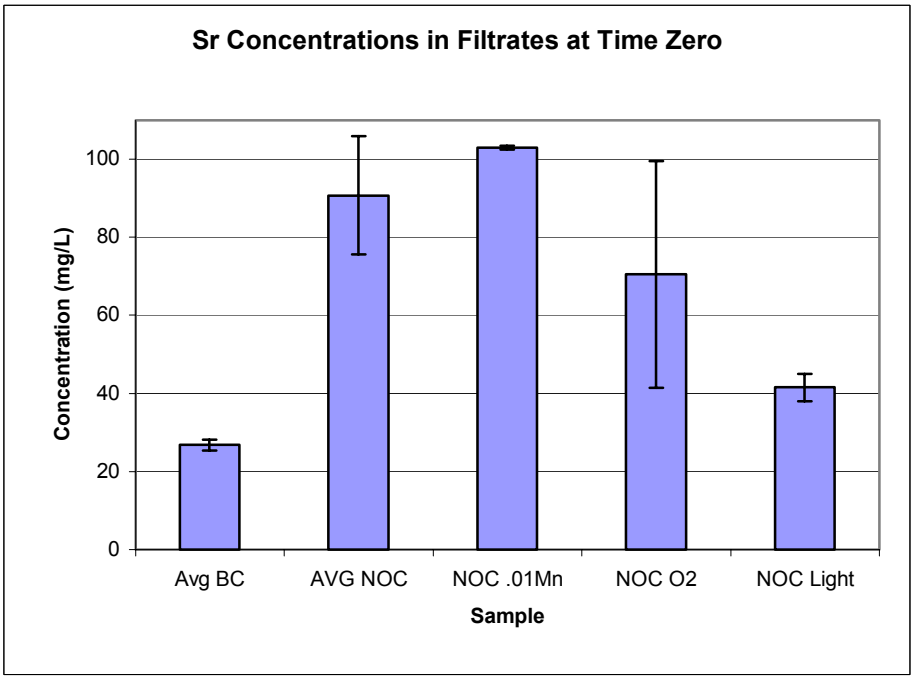

Figure 4.5.1.23 Strontium Concentration in Time Zero Filtrates for the Variables Included in the AN-102 NOC Study

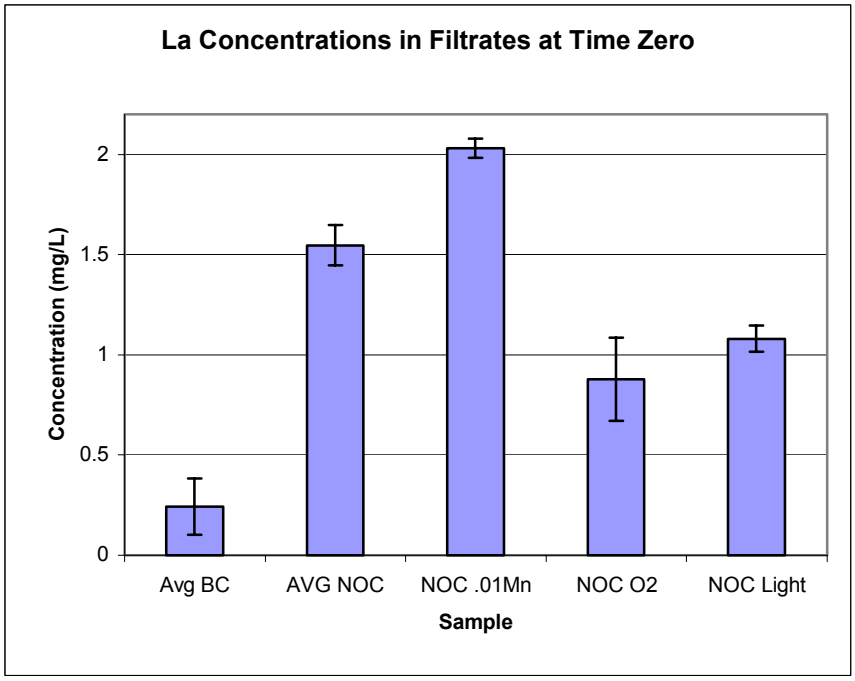

Figure 4.5.1.24 Lanthanium Concentration in Time Zero Filtrates for the Variables Included in the AN-102 NOC Study

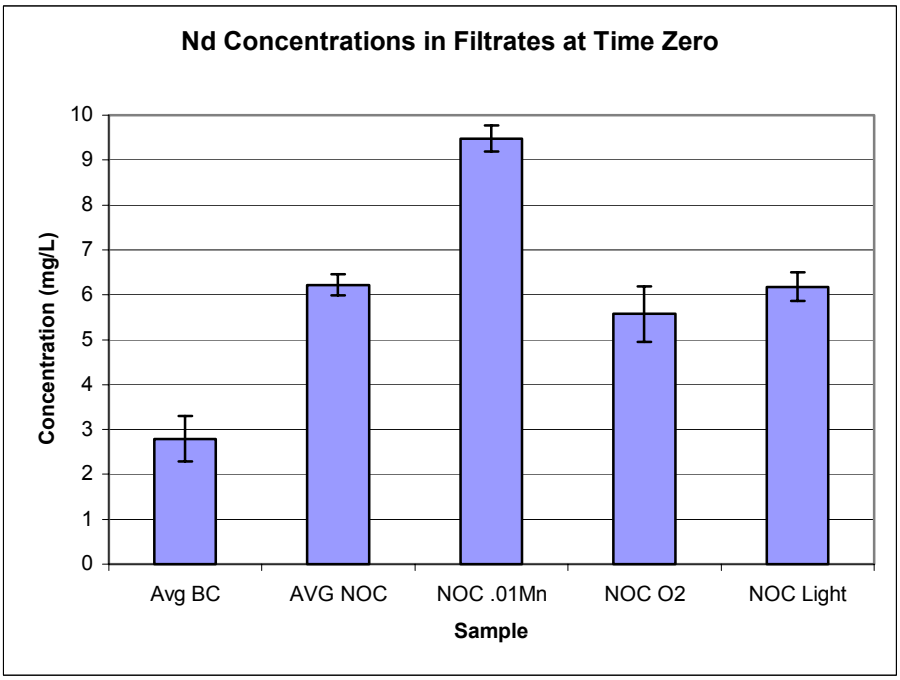

Figure 4.5.1.25 Neodymium Concentration in Time Zero Filtrates for the Variables Included in the AN-102 NOC Study

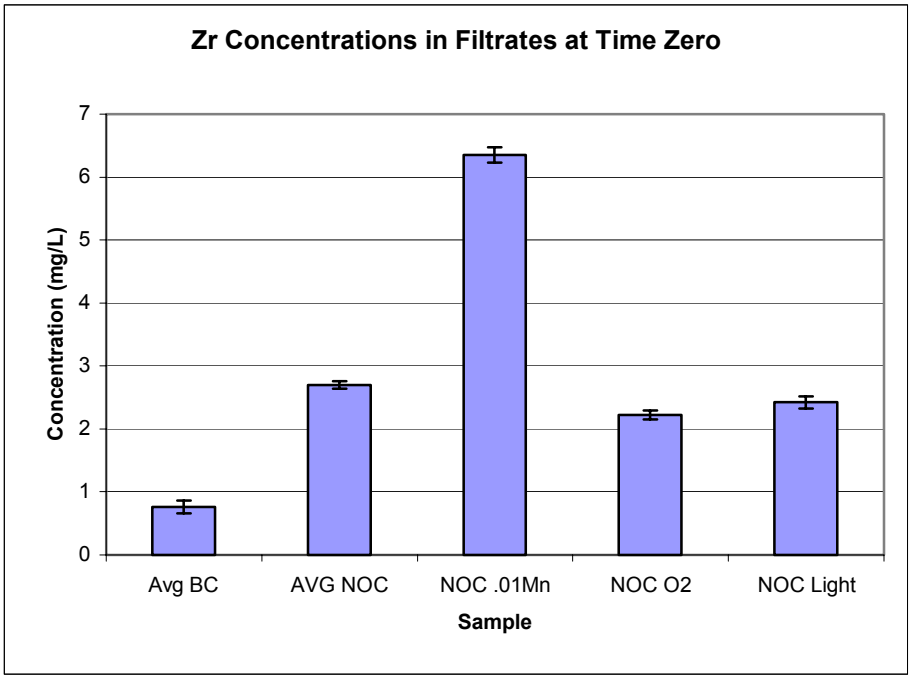

Figure 4.5.1.26 Zirconium Concentration in Time Zero Filtrates for the Variables Included in the AN-102 NOC Study

During the conduct of the 241-AN-102 primary effects study, the manganese concentration in the reaction mixture was 0.01, 0.03, and 0.05 M. A plot of the time zero filtrate data for Mn, Fe, and Sr is shown in Figure 4.5.1.27 as a function of the manganese reaction concentration. For each of the cations, the time zero concentration is inversely proportional to the Mn reaction concentration. A similar effect was seen for Ce, La, Nd, and Zr (Figure 4.5.1.28). A lower concentration of Mn in the reaction mixture would result in a lower mass of precipitate, which would decrease the removal of soluble manganese and all other co-precipitating or co-adsorbing cations (McKenzie, 1980). Again, it is also possible that a lower reaction concentration of permanganate resulted in less destruction of organic ligands, thus increasing complexation and solubility of the metals.

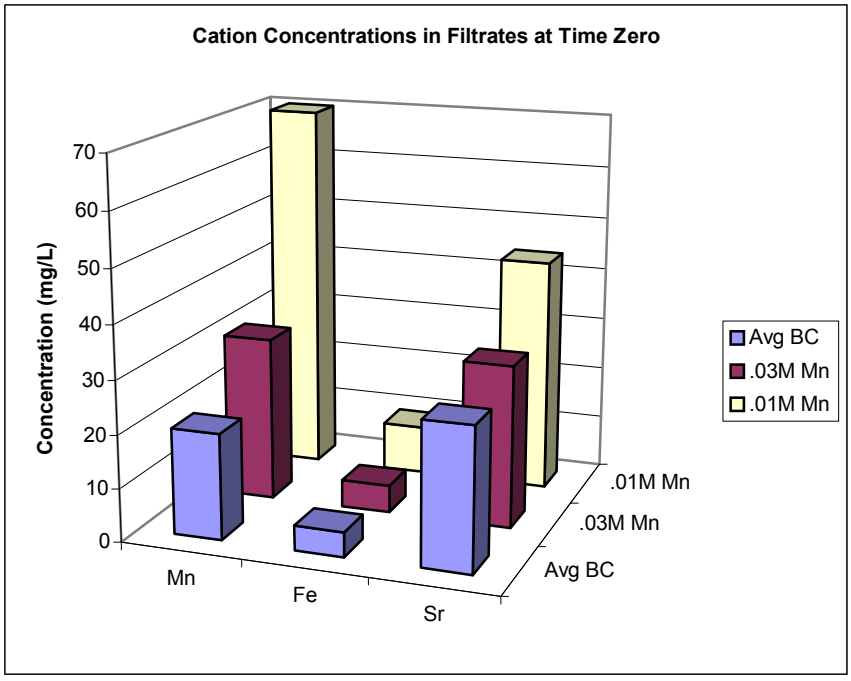

Figure 4.5.1.27 Time Zero Filtrate Concentration of Mn, Fe, and Sr as a Function of Mn Reaction Concentration

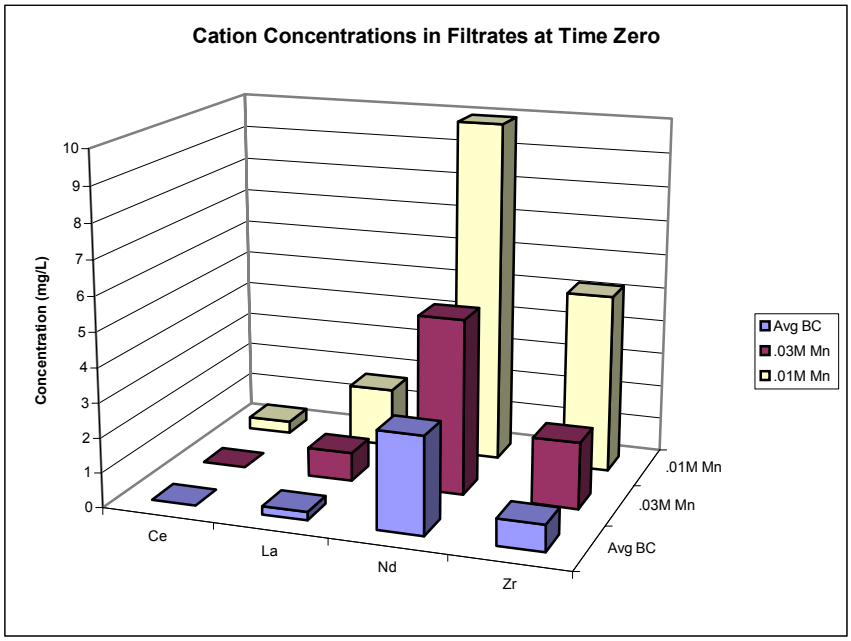

Figure 4.5.1.28 Time Zero Filtrate Concentration of Ce, La, Nd, and Zr as a Function of Mn Reaction Concentration

Characterization of Solids Formed During the 16 Days

At the end of the 16-day observation period, samples were filtered to determine the mass of post-filtration solids that formed in the filtrates. Samples were filtered under nitrogen to reduce the formation of sodium bicarbonate on the filters by reaction of the base media with carbon dioxide in the atmosphere. Mass data was normalized to the final filtrate volume of 100 mls and corrected for soluble solids retained on the filters. The initial volume of filtrate stored was 150 mls, and five 10-mL aliquots were removed during the 16-day period for ICP-AES analysis. Post-filtration solids concentration data for all of the primary effects variables is shown in Figure 4.5.1.29 and is presented to show the magnitude of solids formed for the baseline primary effects study compared to the NOC primary effects study. The amount of post-filtration solids formed for the NOC samples was significantly lower, by an order of magnitude, than for many of the variables tested during the baseline study with exception of the 0.0 M added NaOH.

Post-filtration solids that formed during the 16-day period not only included manganese solids, but a significant accumulation of white solids. Precipitates were dissolved in 0.5 M nitric acid and analyzed by ICP-AES to determine the major cations present in the particulate mass. These data are presented in Tables 4.5.1.3 and 4.5.1.4 for the baseline and NOC experiments respectively. Represented in the tables are the percents of each cation present in the precipitate mass relative to the time zero mass of the cation in the filtrate. The predominant cations found in the precipitate mass are manganese and phosphorus, with sporadic notations of silica and strontium. Sodium concentrations in the samples were not measured.

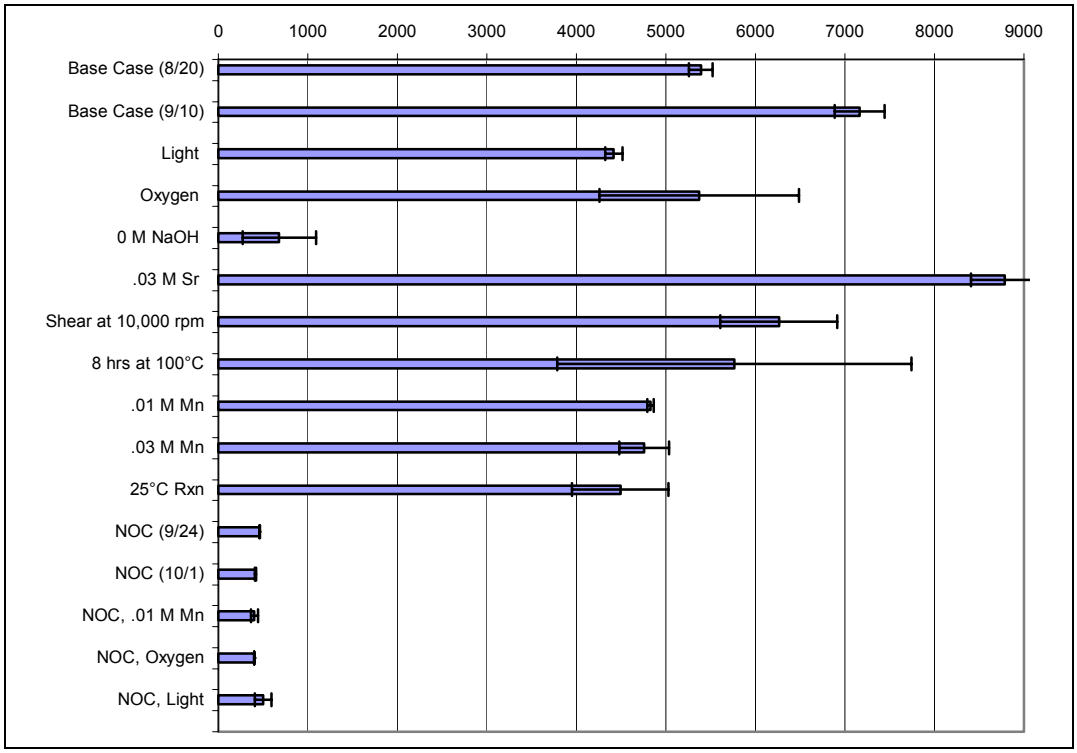

Figure 4.5.1.29 Solids Concentration (mg/L) in Filtrates after 16 Days for the AN-102 Baseline and NOC Experiments

Table 4.5.1.3 Percent of Cation Mass Present in the Solids Relative to Time Zero Cation Mass in the AN-102 Baseline Primary Effects Study

Percent of Cation Present at Time 0 Found in Dissolved Solids (=mass in solid/mass in time 0 filtrate*100)										
Elem	Average BC	Oxygen	Light	Shear	8 hr 100C	25C Rxn	.03M Mn	.01M Mn	.03M Sr	0MOH
Al	0.37	0.33	0.40	0.43	0.24	0.35	0.10	0.09	0.34	0.06
B	ND	ND	ND	ND	ND	ND	ND	ND	ND	ND
Ca	ND	ND	ND	0.39	ND	1.07	ND	ND	0.25	ND
Ce	ND	ND	ND	ND	ND	ND	ND	ND	ND	ND
Cr	0.36	0.30	0.47	0.43	0.20	0.31	0.11	0.12	0.39	0.05
Cu	ND	ND	ND	ND	ND	ND	ND	ND	ND	ND
Fe	ND	ND	ND	ND	ND	ND	ND	ND	ND	ND
K	0.37	0.33	0.40	0.42	0.17	0.34	0.10	0.09	0.35	0.07
La	ND	ND	ND	ND	ND	5.04	ND	ND	ND	ND
Mg	ND	ND	ND	ND	ND	ND	ND	ND	ND	ND
Mn	**11.61**	**35.53**	**49.73**	**16.92**	**33.68**	**2.13**	**5.75**	**3.79**	**18.83**	**ND**
Mo	ND	ND	ND	ND	ND	ND	ND	ND	ND	ND
Nd	ND	ND	ND	ND	ND	1.48	ND	ND	ND	ND
Ni	0.39	0.34	0.41	0.46	0.18	0.35	0.10	0.10	0.38	0.07
P	**16.37**	**7.68**	**1.23**	**11.30**	**23.52**	**0.29**	**32.57**	**34.58**	**31.15**	**2.32**
Pb	0.37	0.54	0.83	0.46	0.34	0.23	0.16	0.24	0.38	ND
Si	ND	ND	ND	**8.84**	**114.23**	ND	**12.56**	**4.51**	**30.92**	ND
Sr	0.38	0.40	0.68	0.51	0.46	**19.36**	ND	0.16	0.46	ND
Zn	ND	ND	ND	ND	ND	ND	ND	ND	ND	ND
Zr	ND	ND	ND	ND	ND	ND	ND	ND	ND	ND

The manganese level in the 0.0 M added NaOH baseline experiments were below detection. The percent noted for the 25 °C reaction temperatures, 0.01 and 0.03 M Mn conditions were significantly lower than those due to filtrate variables, suggesting again that a reduced mass of manganese solids was present in the filtrate after 16 days. The mass percent found in these filtrates was 2.13 to 5.75 percent of the time zero mass to 10 to 50 percent noted for the base case reaction condition. The highest percent of manganese was found in the light condition, oxygen condition, and the 8 hr hold experiments.

Strontium and manganese were the predominant cations present in post-filtration solids collected for the NOC primary effects study. The mass percent of strontium in the precipitates relative to the time zero masses ranged from 10.4 to 25.3 for reaction and treatment conditions included in the study. These relatively high values reflect the increased solubility of strontium at the 25 ^{o}C reaction condition and subsequent precipitation, likely as carbonates. Again this explanation is only plausible if solubility was impacted due to kinetic limitations. Reaction mixtures conducted at 50 ^{o}C were quickly cooled to 25 degrees, centrifuged, and filtered immediately.

Recall that dark solids were not present on the 16-day particulate filters (Appendix F) for the NOC base case experiments. Similar filters for the 0.01 M manganese and oxygen treatments were devoid of a significant particulate mass and were light brown and gray in color. Percent manganese measured on these filters was non-detect to 0.04 percent. However, solids collected on the particulate filters for the light treatment were dark

crystalline solids (observed by light microscope) and were composed primarily of manganese (Table 4.5.1.4).

Table 4.5.1.4 Percent of Cation Mass Present in Solids Relative to Time Zero Cation Mass in AN-102 NOC Primary Effects Study

Percent of Cation Present at Time 0 Found in Dissolved Solids (=mass in solid/mass in time 0 filtrate*100)				
Elem	Avg NOC	NOC-.01Mn	NOC-Light	NOC-O2
Al	0.07	0.07	0.08	0.06
B	ND	ND	ND	ND
Ca	ND	0.48	ND	ND
Ce	ND	ND	ND	ND
Cr	0.05	0.04	0.07	0.06
Cu	ND	ND	ND	ND
Fe	ND	ND	ND	ND
K	0.07	0.06	0.08	0.07
La	ND	ND	ND	ND
Mg	ND	ND	ND	ND
Mn	ND	0.04	**27.53**	ND
Mo	ND	ND	ND	ND
Nd	ND	ND	ND	ND
Ni	0.07	0.07	0.08	0.08
P	0.54	0.06	0.17	0.23
Pb	ND	0.05	0.51	ND
Si	ND	ND	1.47	ND
Sr	**25.28**	**10.43**	**12.24**	**15.11**
Zn	ND	ND	ND	ND
Zr	ND	ND	ND	ND

Estimated rate constants and half-lives describing the loss of manganese from filtrates during the 16-day observation period are listed in Table 4.5.1.5 for the 241-AN-102 primary effects study. Also listed in the table is the percent of manganese lost from solution compared with the initial filtrates. These data indicate a good correlation to the estimated half-lives for the treatment conditions. For example, the half-lives calculated for the 0.01 M and 0.03 M permanganate reaction condition are 161 and 99 days respectively, and the mass of manganese lost from the filtrates was 3.8 and 5.8% respectively. Similarly, the estimated half-lives calculated for the light and oxygen treatment were 6.9 and 14.4 days, and the mass of manganese lost from the filtrates was 49.7 and 33.7% respectively. Treatment conditions exhibiting small half-lives could potentially result in an accumulation of post-filtration solids that may be problematic in the ion exchange process.

Table 4.5.1.5 Estimated First Order Rate Constants and Half-lives for Loss of Manganese From the Primary Effects Filtrates During the 16-Day Observational Period

	Simulant A		Simulant B		Combined			
	$k\ (d^{-1})$	R^2	$k\ (d^{-1})$	R^2	$k\ (d^{-1})$	R^2	$t_{1/2}$ (Days)	(Mp/Mt)*100
BC 8/20	0.0231	0.7828	0.0131	0.9359	0.0181	0.4166	38	11.6
BC 9/10	0.0289	0.9897	0.0205	0.7827	0.0247	0.8627	28	
0.03M Sr	0.0259	0.8641	0.0291	0.7963	0.0275	0.8219	25	18.8
0.01M Mn	0.0047	0.8997	0.0039	0.3598	0.0043	0.5468	161	3.8
0.03M Mn	0.0078	0.5268	0.0062	0.6355	0.0070	0.5413	99	5.8
Light	0.2007	0.9589	0.0997	0.9799	0.1002	0.9516	7	49.7
O_2	0.0502	0.9750	0.0461	0.9981	0.0481	0.8577	14	35.5
8hr@100C	0.0879	0.9180	0.1009	0.9479	0.0944	0.9301	7	33.7
Shear	0.0239	0.8972	0.0237	0.8033	0.0238	0.8280	29	16.9
NOC O_2	0.0014	0.8249	0.0013	0.9939	0.0014	0.8371	495	ND
NOC Light	0.0378	0.9042	0.0386	0.9333	0.0382	0.9088	18	27.5

4.5.2 Secondary Effects Study

Visual Observations

Variables investigated for the AN-102 secondary effects study are listed in Table 4.5.2.1 with notation indicating the time at which visible light and dark solids appeared in the respective filtrates during the 16-day observation period. At the end of the 16-day period, filtrates were filtered under a nitrogen blanket to gravimetrically determine the mass of solids formed and the color and texture of the solids.

All filtrates were yellow or greenish-yellow in color, with the 25 ^{o}C Rxn, light sample having more of a green tint. Light-colored or clear solids appeared on the bottom of all sample flasks by day 1, with the exception of the 0 M OH/25 ^{o}C Rxn, and the 25 ^{o}C Rxn/0.03 M Mn samples in which they appeared on days 8 and 10, respectively. Light-colored solids also appeared on the surface of all filtrates between days 1 and 4. It was observed that the light-colored surface solids in most samples became darker with time, presumably due to oxidation. Samples were maintained under a nitrogen blanket except for the short intervals when ICP-AES samples were collected. Such solids were noted recorded as dark solids when they became medium brown in color. All samples reacted at the 25 ^{o}C reaction condition had dark solids present on the surface of the filtrate and/or the bottom of the flask by day 16 with the exception of the sample reacted with 0.0 M added NaOH. Correspondingly, none of the samples reacted with 0.0 M added NaOH had visible dark solids in the filtrates by day 16 except for the sample that was exposed to the light. Digital photographs of all filtrates can be found in Appendix F.

Table 4.5.2.1 Visual Observations for 241-AN-102 Post-Filtration Precipitation Study (Secondary Effects Experiments)

Sample Condition	Filtrate Color	Light solids on bottom	Light solids on surface	Dark solids on surface	Dark solids on bottom
0M OH, 0.03 M Sr	Yellow/lime green	Day 1 Clear crystal	Day 4	X	X
0M OH, 0.03 M Mn	Yellow/lime green	Day 1 Clear crystals	Day 4	X	X
0M OH, Light	Yellow/lime green	Day 1 Clear crystals	Day 2	Day 7	Day 16
0M OH, O_2	Yellow/lime green	Day 1 Clear crystals	Day 4	X	X
0M OH, 25°C Rxn	Yellow/lime green	Day 8	Day 4	X	X
25°C Rxn, 0.03 Sr	Yellow/green	Day 1	Day 1	Day 16	X
25°C Rxn, light	Green/yellow	Day 1	Day 1	Day 4	Day 10
25°C Rxn, O_2	Yellow	Day 1	Day 1	X	Day 10
25°C Rxn, 0.03 M Mn	Yellow	Day 10	Day 4	Day 16	Day 10

X denotes no solids present at Day 16

Light solids are white to light brown
Dark solids are dark brown to black

All filtrate observations regarding the presence of dark solids correlate with observations of the respective particulate filters, with the exception of the 0 M OH, O_2 and 25 ^{o}C sample, in which light brown solids noted on the filter could not be seen in the filtrate. This discrepancy could be due to a masking of the solids by the color of the filtrate or to the solids simply being too small to be seen in the filtrate. Light brown to black solids were present on all particulate filters except for those produced by the 0 M OH reaction condition crossed with 0.03 M added Sr, 0.03 M added Mn, or the 25 ^{o}C reaction condition.

In summary, these observations indicate that a 25 ^{o}C reaction temperature is not effective in inhibiting the formation of post-filtration solids when crossed with other variables that may promote solid formation. The 0.0 M added NaOH reaction condition does not promote solid formation and may inhibit the formation of solids when crossed with other variables that promote solid formation. Exposure to light is also seen to be very effective in promoting the formation of dark brown to black post-filtration solids.

Change in Metals Concentration During the 16 Day Observation Period for AN-102

ICP-AES data are shown for Mn, Fe, and Sr in Figures 4.5.2.1 through 4.5.2.6 for all samples included in the secondary effect study. Data for these cations as well as for cerium, lanthanum, neodymium, and zirconium are summarized in Table 4.5.2.2. Recall that a decrease in the concentration of cations present in the filtrates over the 16-day observation period indicates the formation of solids composed of the respective cations.

Data presented in Figures 4.5.2.1 and 4.5.2.2 indicate that manganese concentrations did not decrease significantly in any of the samples reacted with 0.0 M added NaOH, with the exception of those exposed to light. Conversely, manganese concentrations did decrease significantly in all samples reacted at 25 ^{o}C except for those reacted with 0.0 M added NaOH. Decreases in soluble manganese concentrations corresponded to the formation of dark post-filtration solids in filtrates, as is evidenced by photographs of the respective filters from final filtration of the samples (Appendix F). These findings indicate the importance of 0.0M added NaOH in inhibiting the formation of post-filtration solids, the importance of light exposure in promoting solids formation, and the failure of a low reaction temperature to prevent the formation of solids when crossed with other variables that promote their formation. Interestingly, as can be seen in Figure 4.5.2.7, secondary samples reacted with 0.0 M NaOH with exception of the 0.03 M Mn, which is essentially constant, all had lower manganese concentrations in filtrates at time zero, which is in line with a similar observation made for the 0.0 M added NaOH sample in the primary effects study. Manganese concentrations in samples reacted at 25 ^{o}C, with exception of the 0.03 M Mn, were also slightly lower than those observed for the respective primary effects samples. Although the mechanisms producing these effects are unclear, it is important to note that reaction conditions that result in decreased manganese concentrations in the filtrate thereby reduce the amount of manganese solids that can potentially form.

The data for iron, presented in Figures 4.5.2.3 and 4.5.2.4, indicate that iron concentrations did not decrease significantly in any of the secondary effects samples. However, as can be seen in Figure 4.5.2.8, samples reacted with 0.0 M added NaOH did have slightly lower time zero iron concentrations in their filtrates, which cannot be supported by data from the primary effects sample with 0.0 M added NaOH, (Figure 4.5.1.16). Time zero iron concentrations in samples reacted at 25 ^{o}C did not differ significantly from the base case.

Concentrations of all other cations (Ce, La, Nd, Zr) remained relatively constant over the 16-day period (Table 4.5.2.2). Time zero concentrations of La and Nd, however, are elevated in samples reacted at 25 ^{o}C and lowered in samples reacted with 0.0 M added NaOH (Figures 4.5.2.10 and 4.5.2.11). Additionally, a lower level of added sodium permanganate seems to have had the effect of increasing the time zero concentrations of not only Mn, but also La, Nd, and Zr, offsetting the effects of 0.0 M added NaOH (Figures 4.5.2.7 through 4.5.2.12).

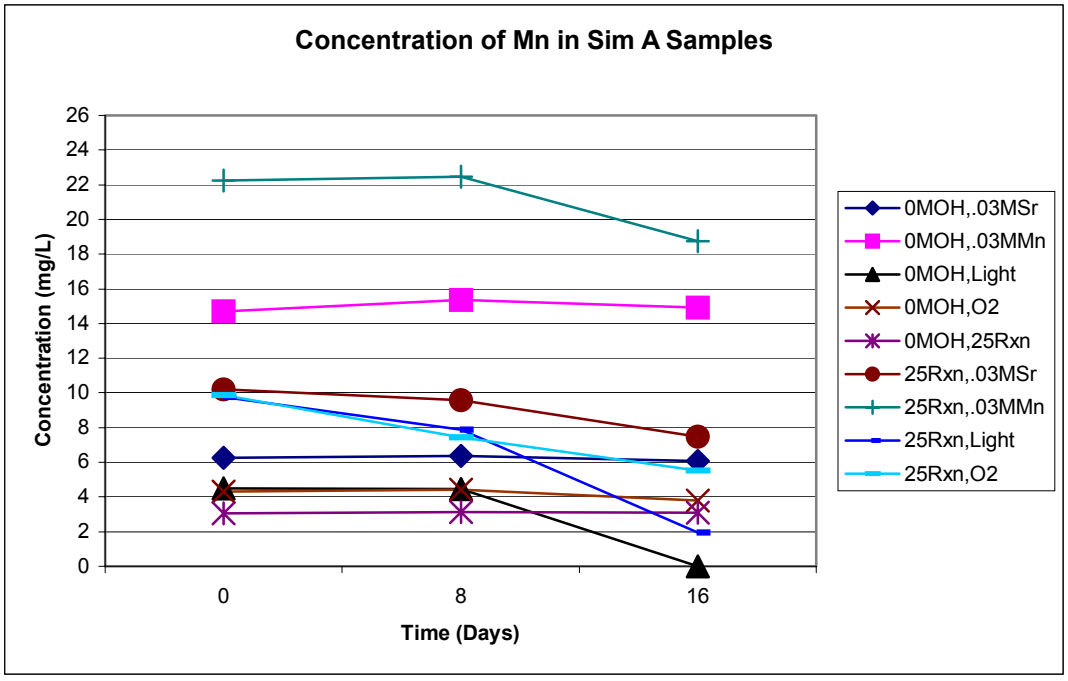

Figure 4.5.2.1 Concentration of Manganese in the 0-16 Day Simulant A Filtrates for the Baseline Secondary Effects Study (AN-102)

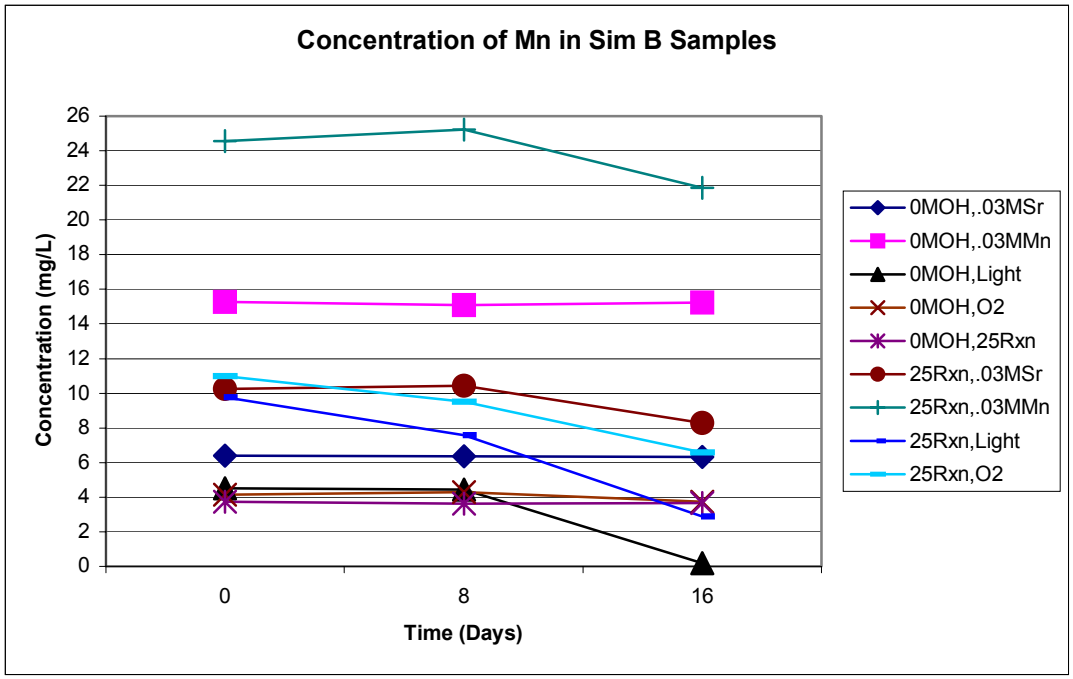

Figure 4.5.2.2 Concentration of Manganese in the 0-16 Day Simulant B Filtrates for the Baseline Secondary Effects Study (AN-102)

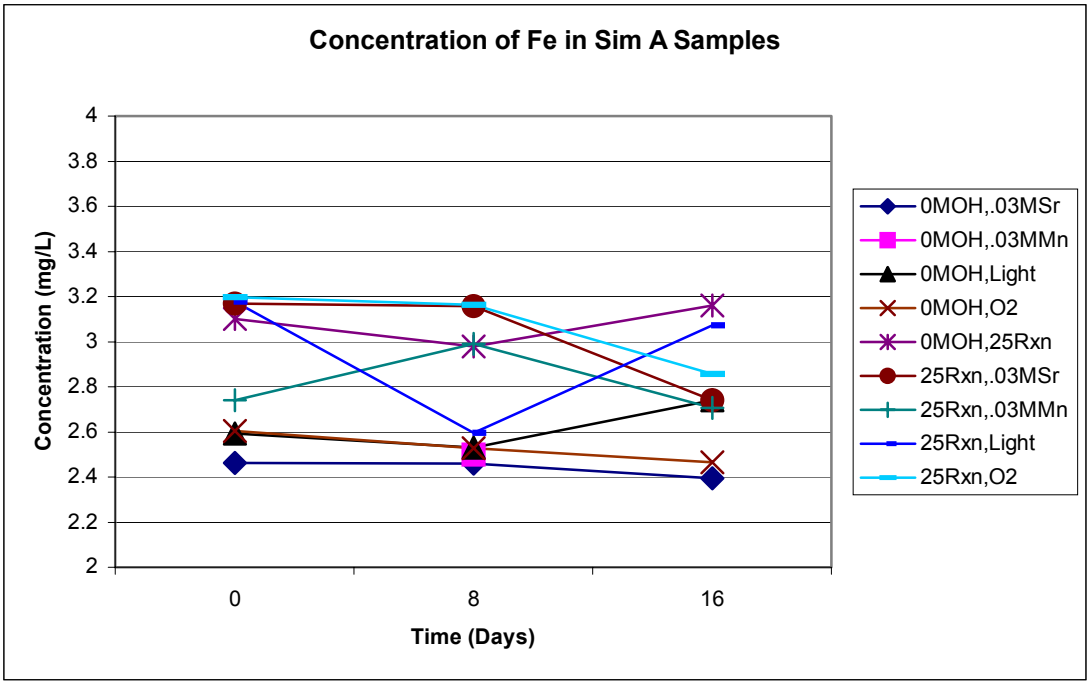

Figure 4.5.2.3 Concentration of Iron with 0-16 Day Simulant A Filtrates for the Baseline Secondary Effects Study (AN-102)

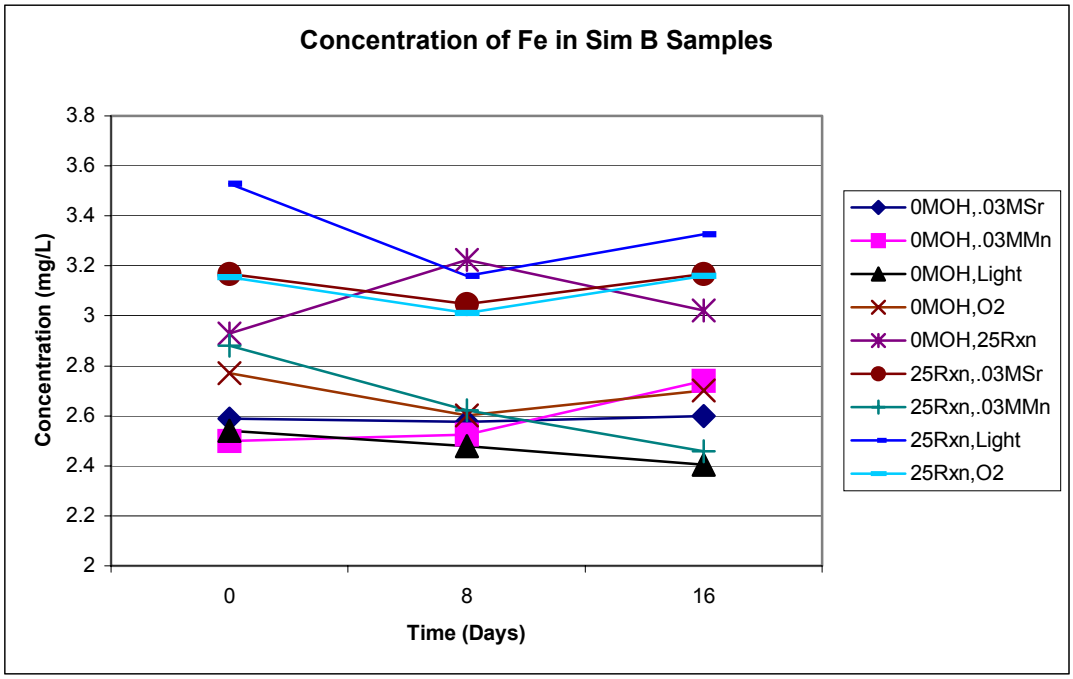

Figure 4.5.2.4 Concentration of Iron in the 0-16 Day Simulant B Filtrates for the Baseline Secondary Effects Study (AN-102)

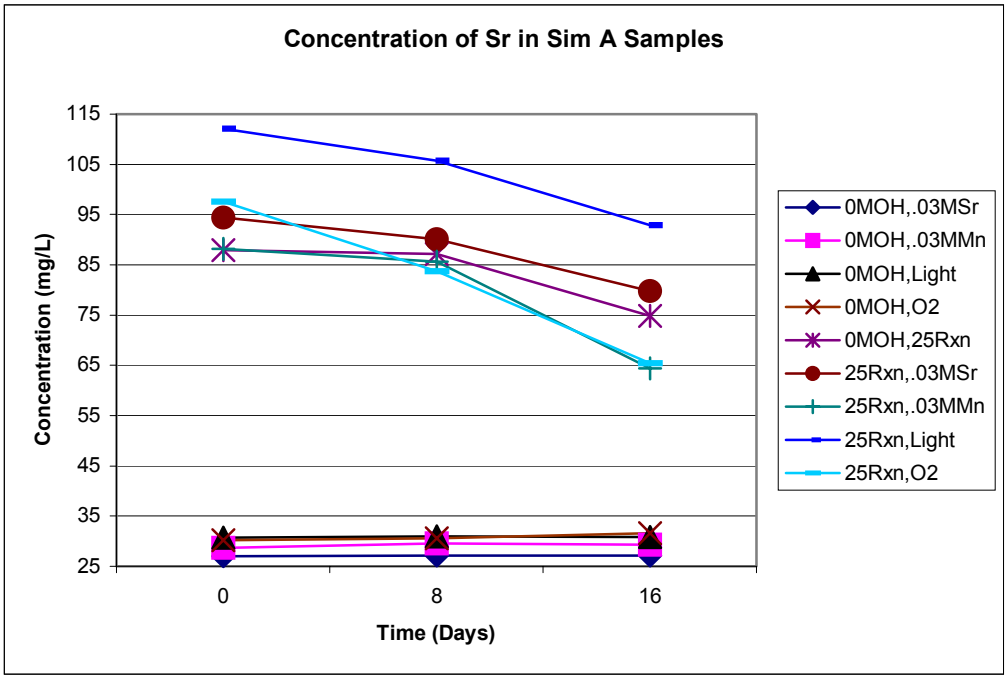

Figure 4.5.2.5 Concentration of Strontium in the 0-16 Day Simulant A Filtrates for the Baseline Secondary Effect Study (AN-102)

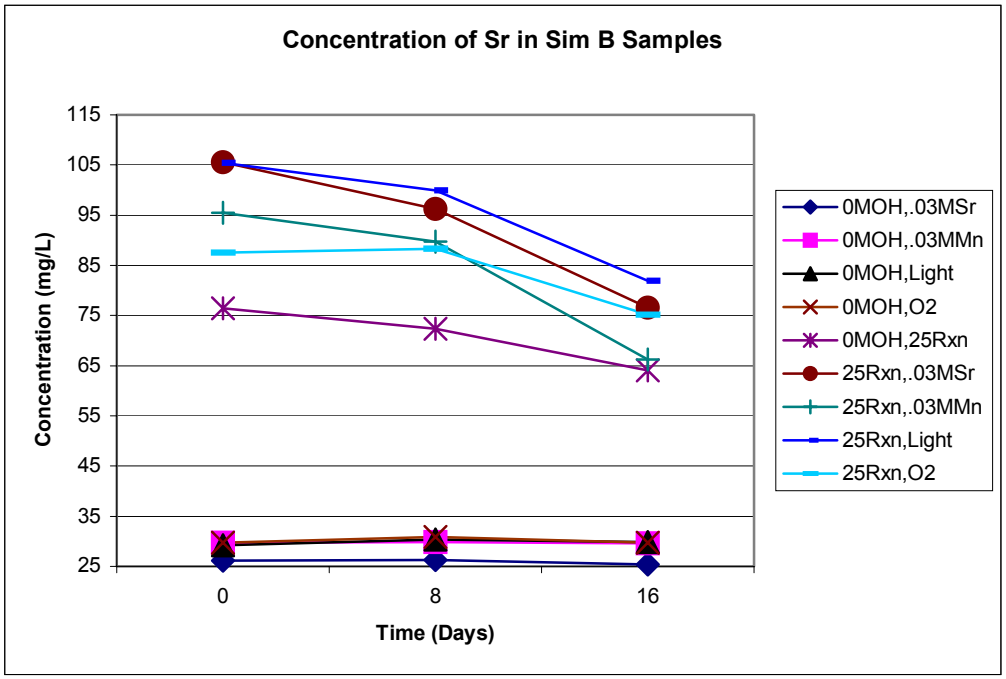

Figure 4.5.2.6 Concentration of Strontium in the 0-16 Day Simulant B Filtrates for the Baseline Secondary Effects Study (AN-102)

Table 4.5.2.2 Concentration of Selected Cations for the 0-16 Day Observation Period for the Baseline Secondary Effects Study (AN-102)

Cation Concentrations Over 16 Days (mg/L)							
	Mn	**Fe**	**Sr**	**Ce**	**La**	**Nd**	**Zr**
0MOH,.03MSr	C 6.30 ± .127	C 2.51 ± .0856	C 26.5 ± .708	ND<0.213	ND<0.175	C 1.33 ± .121	C 0.594 ± .0174
0MOH,.03MMn	C 15.1 ± .250	C ~2.40	C 29.4 ± .400	ND<0.213	C 0.482 ± .0545	C 3.069 ± .185	C 1.54 ± .0679
0MOH,Light	**4.49 - 0.093**	C 2.55 ± .115	C 30.3 ± .68	ND<0.213	ND<0.175	C 0.956 ± .0732	C 0.537 ± .0322
0MOH,02	C 4.12 ± .282	C 2.61 ± .111	C 30.4 ± .726	ND<0.213	ND<0.175	C 0.959 ± .168	C 0.565 ± .0286
0MOH,25Rxn	C 3.39 ± .321	C 3.07 ± .113	**82.2 - 69.4**	ND<0.213	C 0.262 ± .0183	C 1.97 ± .163	C 0.462 ± .0150
25Rxn,.03MSr	**10.2 - 7.89**	C 3.08 ± .170	**100 - 88.0**	**0.415 - ND<.2125**	C 1.13 ± .122	C 5.54 ± .431	C 0.812 ± .0645
25Rxn,.03MMn	**23.4 - 20.3**	C 3.70 ± .206	**109 - 94.9**	C 0.320 ± .0482	C 1.46 ± .0333	C 5.61 ± .135	C 1.84 ± .196
25Rxn,Light	**9.77 - 3.40**	C 3.14 ± .312	**109 - 87.4**	C ~ 0.32	C 1.09 ± .152	C 4.77 ± .296	C .780 ± .0834
25Rxn,O2	**10.4 - 6.06**	C 3.09 ± .131	**92.5 - 70.3**	ND <.213	C 1.23 ± .155	C 4.97 ± .441	C 0.836 ± .103

Table 4.5.2.2 summarizes the ICP-AES data for all secondary effect samples. Concentration ranges appearing in bold differed significantly over the 16-day observation period. Those values preceded by the letter "C" remained relatively constant throughout the 16-day period.

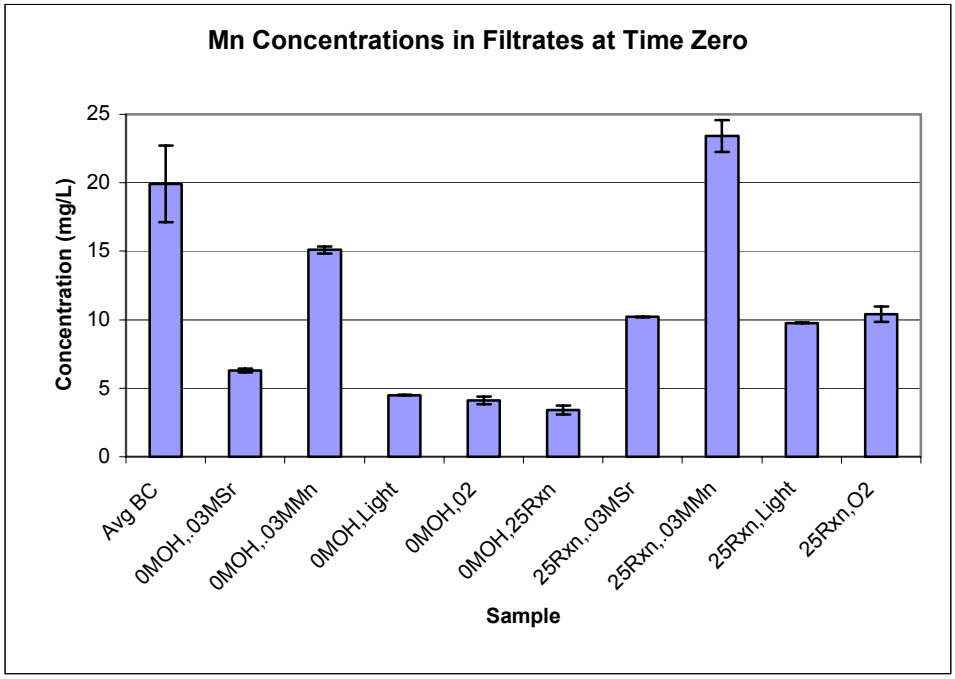

Figure 4.5.2.7 Manganese Concentration in Time Zero Filtrate for the Variables Included in the AN-102 Secondary Effects Study

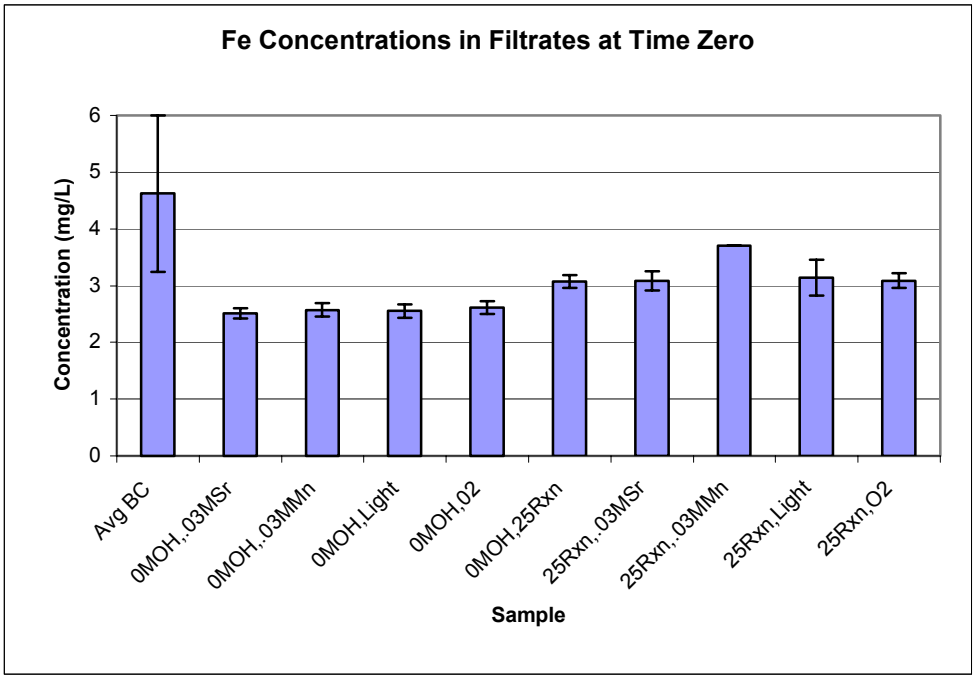

Figure 4.5.2.8 Iron Concentration in Time Zero Filtrate for the Variables Included in the AN-102 Secondary Effects Study

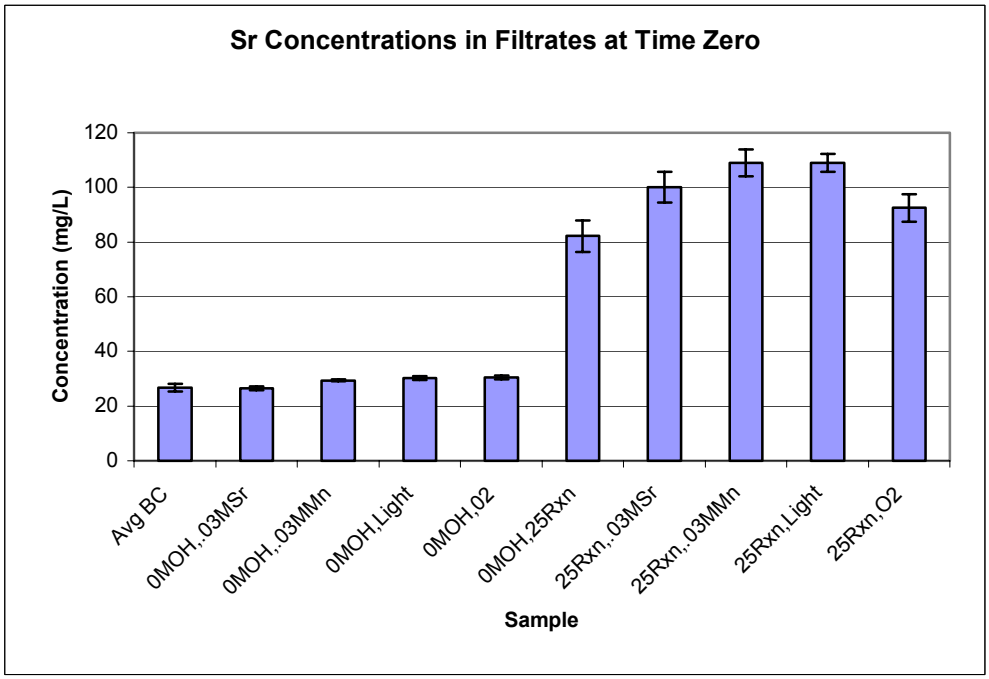

Figure 4.5.2.9 Strontium Concentration in Time Zero Filtrate for the Variables Included in theAN-102 Secondary Effects Study

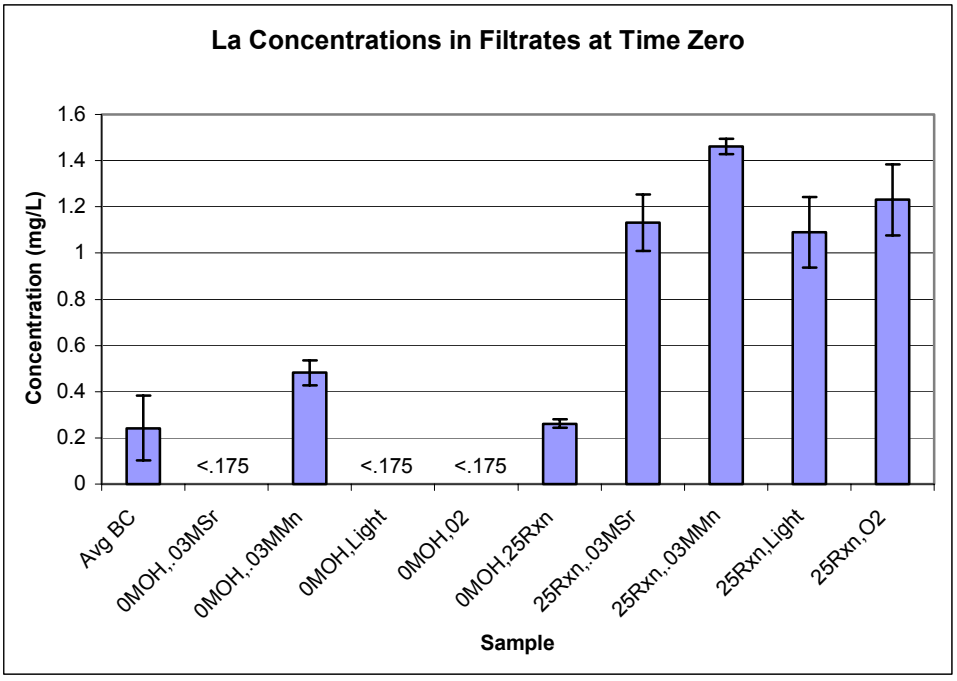

Figure 4.5.2.10 Lanthanum Concentration in Time Zero Filtrate for the Variables Included in the AN-102 Secondary Effects Study

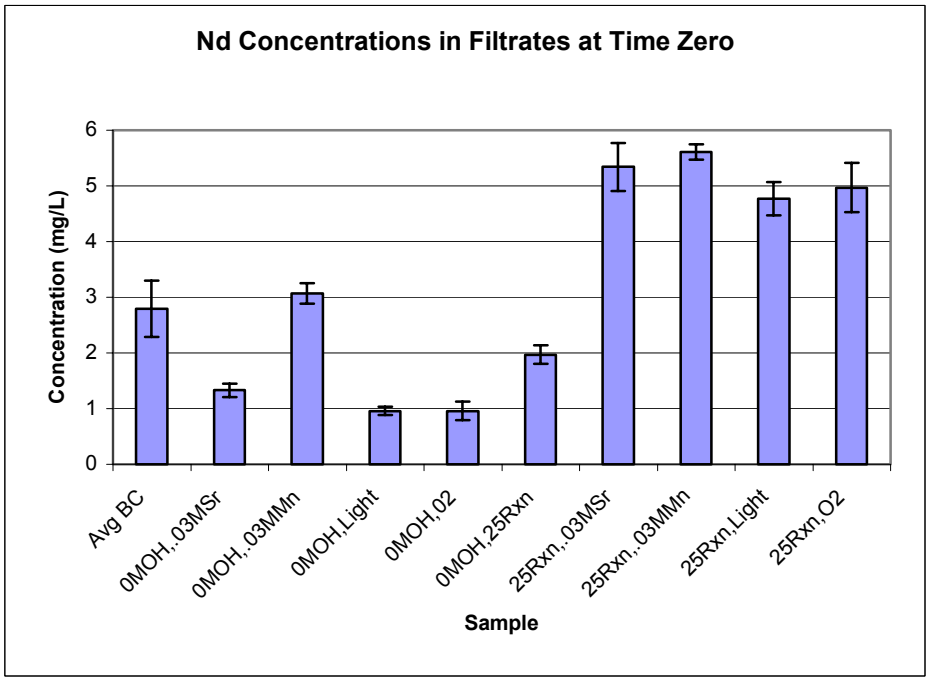

Figure 4.5.2.11 Neodymium Concentration in Time Zero Filtrate for the Variables Included in the AN-102 Secondary Effects Study

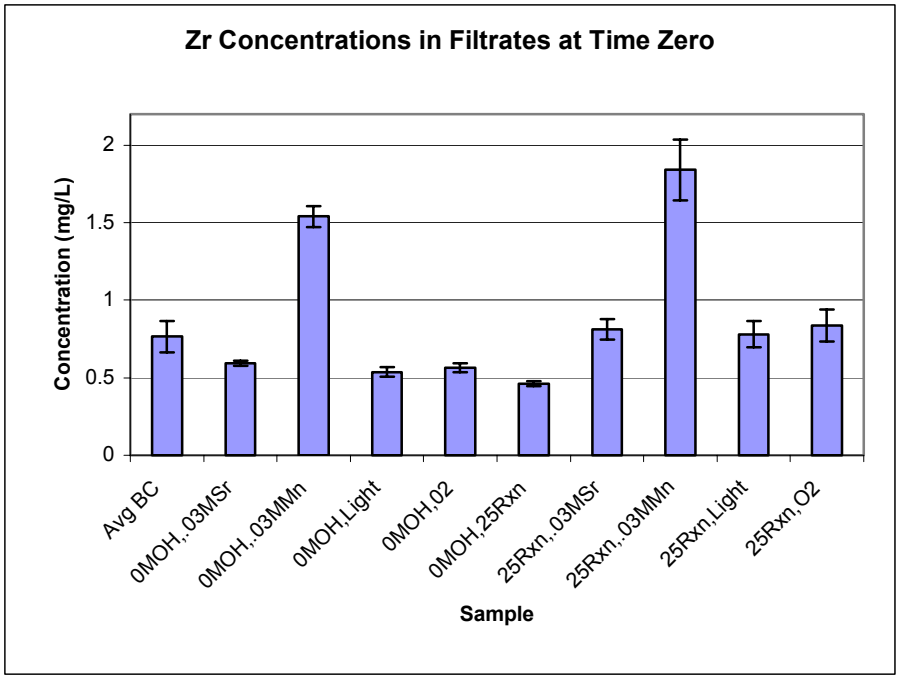

Figure 4.5.2.12 Zirconium Concentration in Time Zero Filtrate for the Variables Included in the AN-102 Secondary Effects Study

Characterization Of Solids Formed During The 16 Days

At the end of the 16-day observational period, samples were filtered to determine the mass of post-filtration solids that formed in the filtrates. Samples were filtered under nitrogen to reduce the formation of sodium bicarbonate on the filters by reaction of the base media with carbon dioxide in the atmosphere. Mass data was normalized to a filtrate volume of 100 mls. The initial volume of filtrate stored was 150 mls. Five 10-mL aliquots were removed during the 16-day period for ICP-AES analysis. Solids concentration data for all of the primary effects variables is shown in Figure 4.5.2.13 and is presented to show the magnitude of solids formed for the baseline secondary effects study. The amount of post-filtration solids formed for all samples reacted with 0.0 M added NaOH was significantly larger than that for the primary effect of 0.0 M NaOH, with the exception of the sample reacted at 25 ^{o}C. Of the four samples that produced more solids than during the primary effects study, all produced masses of solids that were not significantly different from those produced by the primary effect baseline experiments, with the exception of the sample exposed to the light, which produced less solids (Figure 4.5.1.28). None of the samples reacted at 25 ^{o}C produced masses of solids that were significantly different from the 25 ^{o}C primary effect samples except for the replicate 0.03 M Mn samples and replicate 0.0 M OH samples, which both produced significantly less solids. All 25 ^{o}C experiments produced less solids than the primary effects baseline samples except for those sparged with oxygen.

Solids that formed during the 16-day period not only included dark manganese solids, but a significant accumulation of white solids. Precipitates were dissolved in 0.5 M nitric acid and

analyzed by ICP-AES to determine the major cations present in the particulate mass. These data are presented in Table 4.5.2.3. Represented in the table is the percent of cation present in the precipitate mass relative to the time zero mass of cation in the filtrate. The predominant cations found in precipitate masses were manganese and phosphorus in samples reacted with 0.0 M NaOH and manganese and strontium in samples reacted at 25 ^{o}C. There was also a predominance of cerium in the 25 ^{o}C samples that were exposed to oxygen and in those that were reacted with 0.03 M Mn. Sodium concentrations in the samples were not measured.

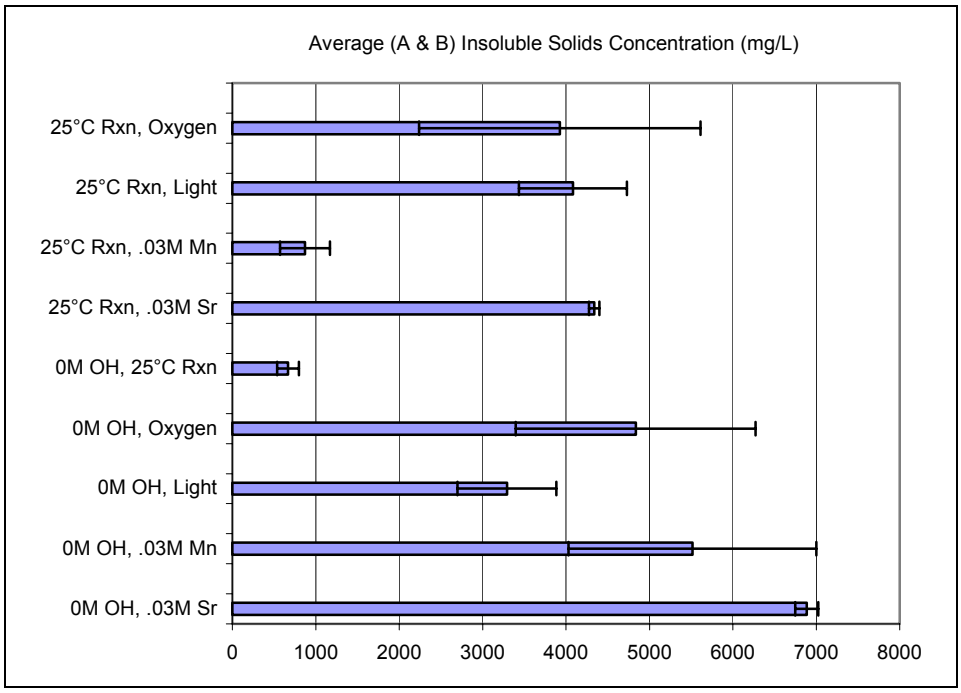

Figure 4.5.2.13 Concentration of Solids as a Function of Treatment Condition in the Baseline Secondary Effects Samples (AN-102)

Recall from Table 4.5.1.3 that manganese was below detection in the precipitates of the 0.0 M added NaOH primary effect samples. In the secondary effects samples, however, 55.6 percent of the time-zero-mass of manganese precipitated from filtrates exposed to light during the 16 day period, and 7.21 percent from filtrates sparged with oxygen (Table 4.5.2.3). The percentages of manganese that precipitated from secondary 25 ^{o}C reaction samples were all higher than that of the primary effect 25 ^{o}C reaction sample, with the exception of the sample reacted with 0.0 M NaOH. Similar to the primary effect 25 ^{o}C reaction sample, relatively large percentages of the time-zero-mass of strontium were found in all secondary effect samples reacted at 25 ^{o}C.

Table 4.5.2.3 Percent of Cation Mass Present in the Solids Relative to Time Zero Cation Mass in Filtrates for the AN-102 Secondary Effects Study

	Percent of Cation Present at Time 0 Found in Dissolved Solids (=mass in solid/mass in time 0 filtrate*100)								
Elem	0MOH,O2	0MOH,Light	0MOH,.03Sr	0MOH,.03Mn	25C Rxn,0MOH	25C Rxn,.03Mn	25C Rxn,O2	25C Rxn,.03Sr	25C Rxn,Light
Al	0.0998	0.0716	0.0983	0.0851	0.0731	0.0972	0.530	0.332	0.354
B	ND	ND	ND	ND	ND	ND	ND	ND	ND
Ca	ND	ND	ND	ND	ND	0.457	0.817	0.649	0.820
Ce	ND	ND	ND	ND	ND	**10.1**	**25.2**	ND	ND
Cr	0.0813	0.0768	0.130	0.0996	0.0688	0.0884	0.463	0.352	0.363
Cu	ND	ND	ND	ND	ND	ND	ND	ND	ND
Fe	ND	ND	ND	ND	ND	ND	ND	ND	ND
K	0.0901	0.0772	0.0982	0.0893	0.0812	0.103	0.539	0.359	0.357
La	ND	ND	ND	ND	ND	ND	ND	ND	ND
Mg	ND	ND	ND	ND	ND	ND	ND	ND	ND
Mn	**7.21**	**55.6**	0.783	ND	ND	**9.94**	**31.2**	**14.0**	**43.9**
Mo	ND	ND	ND	ND	ND	ND	0.385	0.374	0.346
Nd	ND	ND	ND	ND	ND	ND	ND	ND	1.80
Ni	0.0984	0.0818	0.114	0.0947	0.0842	0.120	0.568	0.399	0.410
P	**19.8**	**12.9**	**23.0**	**21.9**	0.142	0.295	1.31	0.479	0.333
Pb	0.184	0.207	0.114	0.0982	ND	0.220	1.02	0.376	0.936
Si	ND	ND	ND	1.63	ND	ND	ND	ND	ND
Sr	0.161	0.253	ND	ND	**5.21**	**5.40**	**24.6**	**11.6**	**12.0**
Zn	ND	ND	ND	ND	ND	ND	ND	ND	ND
Zr	ND	ND	ND	ND	ND	ND	ND	ND	ND

Estimated rate constants and half-lives describing the loss of manganese from filtrates during the 16-day observation period are listed in Table 4.5.2.4 for the 241-AN-102 secondary effects study. Also listed in the table are the percentages of manganese lost from solution in the initial filtrates. These data indicate a good correlation to the estimated half-lives for the treatment conditions. For example, the half-lives calculated for the 0.0 M NaOH/light pair and the 25 ^{o}C reaction/light pair are small (3.5 and 7.9 days), and the mass of manganese lost from the filtrates was 56 and 44% respectively. Similarly, the estimated half-lives calculated for the 25 ^{o}C reaction/0.03 M Sr pair and the 25 ^{o}C reaction/0.03 M Mn pair were 43 and 77 days, and the mass of manganese lost from the filtrates was 10 and 14% respectively. Treatment conditions exhibiting small half-lives could potentially result in an accumulation of post-filtration solids that may be problematic in the ion exchange process.

Table 4.5.2.4 Estimated First Order Rate Constants and Half-lives for Loss of Manganese From the Secondary Effects Filtrates During the 16-Day Observational Period

	Simulant A		Simulant B		Combined			
	$k\ (d^{-1})$	R^2	$k\ (d^{-1})$	R^2	$k\ (d^{-1})$	R^2	$t_{1/2}$ (Days)	$(M_p/M_t)*100$
0MOH, Light	0.2037	0.7514	0.1988	0.7541	0.2012	0.7525	3	55.6
25Rxn,.03MSr	0.0193	0.8904	0.0131	0.6813	0.0162	0.7309	43	9.9
25Rxn,.03MMn	0.0106	0.7027	0.0073	0.5907	0.0090	0.3757	77	0.14
25Rxn,Light	0.1003	0.8484	0.0762	0.8984	0.0882	0.8427	8	43.9
25Rxn,O2	0.0364	0.9999	0.0318	0.9411	0.0341	0.8395	20	31.2

5.0 CONCLUSIONS

Data presented for the 241-AN-107 primary effects study indicated that post-filtration solids formed with all treatments examined given sufficient time. However, in the short term (within 48 hours), reacting the simulant at flow sheet conditions but eliminating the addition of sodium hydroxide from the reaction mixture and minimizing exposure to oxygen in the filtrates minimized the formation of precipitates. In addition, reducing the concentration of sodium permanganate to approximately 0.01 M could also minimize the formation of post-filtration solids.

With exception of two experimental conditions, the 8-hr hold of the filtrate at 100 °C and the oxygen sparge, solids that formed during the 48-hr period were very light in color. The filtrates sparged with oxygen contained brown solids within six hours, and significant black solids formed in the filtrates held at 100 °C for 8 hours. The formation of brown solids in the filtrates sparged with oxygen is commensurate with the oxidation (in the presence of air) to brown manganese (III) oxy-hydroxide and oxide and ultimately to the black manganese dioxide. Formation of black solids in the 8-hr hold filtrates supports the hypothesis that the precipitation reaction kinetics are too slow for the reaction to be complete after a 4 hour reaction time.

Very near the end of the analytical effort for the AN-241-107 primary effects study, discussions were initiated concerning reconsideration of the reaction conditions. A 'newly optimized condition' (NOC) was proposed in which the concentration of reactants was reduced to 0.03 M strontium nitrate and sodium permanganate. In addition, the sodium hydroxide concentration was set at 0.3 M (0.0 M added to the AN-102 simulant), and a reaction temperature at 25 °C. Dark solids appeared in all treatment pairs in contact with the atmosphere. Dark solids also formed for the light/nitrogen pairs reacted at 0.01 and 0.03 M sodium permanganate. Dark solids did not form for reaction at the NOC and at the NOC with 0.01 M sodium permanganate. Therefore, it would appear that reacting at the NOC or at lower permanganate concentration could mitigate the formation of dark solids within 16 days of an oxidation reaction with a 241-AN-107 waste.

Rate constants describing the formation of manganese or iron containing solids could not be calculated for the 16-day observation period. However, rate constants describing the formation of strontium solids during the 16-day period were calculated. Half-lives calculated for filtrates maintained in the light ranged from 15.3 to 21.2 $days^{-1}$ while those maintained in the dark ranged from 22.4 to 60.3 $days^{-1}$ suggesting that light may play an important role in the precipitation of strontium.

The primary effects study for the 241-AN-102 simulant resulted in the formation of brown to black solids in all treatments except the zero molar added sodium hydroxide and the 25 ^{o}C reaction under otherwise baseline conditions, the NOC, and the 0.01 M sodium permanganate reaction under otherwise NOC.

Secondary effects studied for the 241-AN-102 simulant involved examining the effect of 0.0 M added sodium hydroxide and a 25 ^{o}C reaction condition with 0.03 M strontium, 0.03 M permanganate, light, and the presence of oxygen. Results indicated that a 25 ^{o}C reaction

temperature is not effective in inhibiting the formation post-filtration solids when crossed with primary effects variables that did promote solids formation. Lowering the reaction temperature from 50 to 25 °C should have resulted in less of a reaction precipitate leaving more iron in solution as noted above. However, the behavior of iron in response to the lowered reaction temperature follows that of manganese suggesting that co-precipitation or adsorption may be an important removal mechanism for iron.

The 0.0 M added NaOH reaction condition does not promote solid formation and may inhibit the formation of solids when crossed with other primary effects variables that promote solid formation. Exposure to light is also seen to be very effective in promoting the formation of dark brown to black post-filtration solids.

In summary, the AN-102 and –107 data suggest that for the base case condition, a lower reaction temperature and the absence of added NaOH inhibit the formation of dark solids within 16-days. Similarly, the variable evaluated for the newly optimized conditions that did not result in the formation of dark solids was the 0.01 M permanganate treatment. The newly optimized conditions also did not result in the formation of dark solids.

Post-filtration solids that formed in both the AN-107 and –102 filtrates were completely soluble in 0.5 molar nitric acid. Additionally, the mass of predominantly manganese containing solids that formed in the filtrates is small, generally in the mg/L range and may not pose a significant problem in contact with the ion-exchange resin. In any event solids collected in the resin bed would likely be solubilized during regeneration of the resin.

REFERENCES

Abodishish, H.A. R&T Test Exception, 24590-WTP-TEF-RT-02-063. September, 2002.

Bannochie, C.J. and Nash, C.A. Task Technical and Quality Assurance Plan: Evaluation of Post-Filtration Precipitation Mechanisms. WSRC-TR-2001_00425, Revision 1, November, 2001.

Bannochie, C.J. Standardized Baseline Precipitation Procedure for Hanford RPP Studies. WSRC-TR-2002-00138, Rev.0, March, 2002.

Cho, H., Kawasaki, H., and Kumazawa, H. Formation of Needle-like Lepidocrocite Fine Particles by Oxidation of an Aqueous Suspension of Ferrous Hydroxide in a Bubble Column. The Canadian Journal of Chemical Engineering. 78:842-846. 2000.

Cotton, F.A. and Wilkinson, G. Advanced Inorganic Chemistry. 5th edition. Wiley, John, and Sons Incorporated. Pp. 699, 706, 1988.

Ebling, R.E. Development of a Supernate Simulant for Hanford Tank 241-AN-102 Waste (U). WSRC-TR-2002-00040, Rev. 0. SRT-RPP-2002-00012, Rev. 0. February, 2003.

Eibling, R.E. and Nash, C.A. Hanford Waste Simulants Created to Support the Research and Development on the River Protection Project – Waste Treatment Plant. Savannah River Technology Center. WSRC-TR-2000-00338. SRT-RPP-2000-00017. February, 2001.

Hildred, K.L, Townson, P.S., Hutson, G.V., and Williams, R.A. Characterization of Particulates in the BNFL Enhanced Actinide Removal Plant. Powder Technology. 108:164-172. 2000.

Kamei, G. and Ohmoto, H. The Kinetics of Reactions Between Pyrite and O_2-bearing Water Revealed from In-situ Monitoring of DO, E_H and pH in a Closed System. Geochimica et Cosmochimica Acta. 64(15):2585-2601. 2000.

Kuga, Y.; Isomura, S.; Takeuchi, K.; and Okuyama, K. Growth Enhancement of UF_5 Nano-particles Assisted by α-ray Ionization. Applied Physics A. Materials Science and Processing. 62:373-379. 1996.

Mallick, K.; Wang, Z.L.; and Pal, T. Seed-mediated Successive Growth of Gold Particles Accomplished by UV Irradiation: A Photochemical Approach for Size-controlled Synthesis. Journal of Photochemistry and Photobiology A: Chemistry. 140:75-80. 2001.

McCabe; D. J.; and Nash, C. A. BNFL River Protection Project Flowsheet Technical Support at SRTC Update. Savannah River Technology Center. April , 2000.

McKenzie, R.M. The Adsorption of Lead and Other Heavy Metals on Oxides of Manganese and Iron. Aust. J. Soil Res. 18:61-73. 1980.

Nash, C.A. and Rosencrance, S.W. Initial Project Scoping Meeting. Rich Laboratory. Clemson University. October 19, 2000.

Townson, P. S. Pilot Scale Inactive LAW Entrained Solids Removal and Sr/TRU Precipitant Filtration Test Specification. TSP-W375-99-00007, Revision 0. River Protection Project, Waste Treatment Plant. August, 1999.

APPENDIX A

Simulant Recipes

Table A.1 Recipe for AN-107 Simulant

Experiment C-7 Recent

Volume of Feed		1000	mL

In a tared 1000 mL Volumetric Flask add

	grams	Actual Wt, grams
Water	200	

Transition Metals and Complexing agents

Compounds	Formula	Mass Needed	Actual Wt, grams
Calcium Nitrate	Ca(NO3)2.4H2O	3.48	
Cerium Nitrate	Ce(NO3)3.6H2O	0.164	
Cesium Nitrate	CsNO3	0.027	
Copper Nitrate	Cu(NO3)2.2.5H2O	0.110	
Ferric Nitrate	Fe(NO3)3.9H2O	12.23	
Lanthanum Nitrate	La(NO3)3.6H2O	0.142	
Lead nitrate	Pb(NO3)2	0.620	
Magnesium Nitrate	Mg(NO3)2.6H2O	0.264	
Manganous Chloride	MnCl2.4H2O	2.03	
Neodymium Nitrate	Nd(NO3)3.6H2O	0.291	
Nickel Nitrate	Ni(NO3)2.6H2O	2.63	
Potassium Nitrate	KNO3	4.60	
Strontium Nitrate	Sr(NO3)2	0.016	
Zinc Nitrate	Zn(NO3)2.6H2O	0.206	
Zirconyl Nitrate	ZrO(NO3)2	0.191	
EDTA	Na2EDTA	7.26	
HEDTA	HEDTA	2.16	
Sodium Gluconate		3.93	
Glycolic Acid		26.93	
Citric Acid		9.44	
Nitrilotriacetic Acid		0.570	
Iminodiacetic Acid		6.04	
Boric acid	H3BO3	0.200	
Sodium Chloride	NaCl	1.82	
Sodium Fluoride	NaF	0.29	
Sodium Chromate	Na2CrO4	0.55	
Sodium Sulfate	Na2SO4	12.20	
Potassium Molybdate	K2MoO4	0.089	
		98.47	

In separate container mix the following

Add	Formula	Mass Needed	Actual Wt, grams
Sodium Hydroxide	NaOH	25.26	
Aluminum Nitrate	Al(NO3)3.9H2O	5.37	
Sodium Phosphate	Na3PO4.12H2O	4.44	

Sodium formate	NaHCOO	15.71	
Sodium Acetate	NaCH3COO.3H2O	2.37	
Sodium Oxalate	Na2C2O4	1.26	

Add	grams	Actual Wt, grams
Water	200	

Mix thoroughly. Then add this solution to the volumetric flask.

Add	Formula	Mass Needed	Actual Wt, grams
Sodium Carbonate	Na2CO3	148.25	

Mix thoroughly.

Mix	Formula	Mass Needed	Actual Wt, grams
Sodium Nitrate	NaNO3	297.29	
Sodium Nitrite	NaNO2	91.49	
Water		100	

Add and Mix thoroughly.

Mix thoroughly and dilute to the mark.

Record Final Weight		grams

The final addition of water would be 240.24 grams based upon a density of 1.429 g/mL.

Table A.2 Recipe for AN-102 Simulant

SRS AN102-Final at 9.543 Molar Sodium recipe	

Volume of Feed	1000	mL

Tare a 1000 mL Volumetric Flask

Volumetric Flask Tare Weight _____ grams

To the Volumetric Flask add

	grams	Actual Wt, grams
Water	200	

Transition Metals and Complexing agents

Compounds	Formula	Mass Needed	Actual Wt, grams
Aluminum Nitrate	$Al(NO_3)_3 \cdot 9H_2O$	204.12	
Cadmium Nitrate	$Cd(NO_3)_2 \cdot 4H_2O$	0.20	
Calcium Nitrate	$Ca(NO_3)_2 \cdot 4H_2O$	3.46	
Cerium Nitrate	$Ce(NO_3)_3 \cdot 6H_2O$	0.00	
Cesium Nitrate	$CsNO_3$	0.028	
Cobalt Nitrate	$Co(NO_3)_2 \cdot 6H_2O$	0.02	
Copper Nitrate	$Cu(NO_3)_2 \cdot 2.5H_2O$	0.11	
Ferric Nitrate	$Fe(NO_3)_3 \cdot 9H_2O$	0.36	
Lanthanum Nitrate	$La(NO_3)_3 \cdot 6H_2O$	0.06	
Lead nitrate	$Pb(NO_3)_2$	0.35	
Magnesium Nitrate	$Mg(NO_3)_2 \cdot 6H_2O$	0.00	
Manganous Chloride	$MnCl_2 \cdot 4H_2O$	0.13	
Neodymium Nitrate	$Nd(NO_3)_3 \cdot 6H_2O$	0.12	
Nickel Nitrate	$Ni(NO_3)_2 \cdot 6H_2O$	2.47	
Potassium Nitrate	KNO_3	6.03	
Rubidium Nitrate	$RbNO_3$	0.02	
Strontium Nitrate	$Sr(NO_3)_2$	0.007	
Zinc Nitrate	$Zn(NO_3)_2 \cdot 6H_2O$	0.03	
Zirconyl Nitrate	$ZrO(NO_3)_2 \cdot H_2O$	0.04	
Disodium Ethylenediaminetetraacetate	$Na_2C_{10}H_{14}N_2O_8 \cdot 2H_2O$	4.29	
n-(2-Hydroxyethyl)ethylenediaminetriacetic acid	$C_{10}H_{18}N_2O_7$	0.44	
Sodium Gluconate	$HOCH_2(CHOH)_4COONa$	1.97	
Citric Acid	$C_6H_8O_7 \cdot H_2O$	6.20	
Nitrilotriacetic Acid	$C_6H_9NO_6$	0.31	

Iminodiacetic Acid	$C_4H_7NO_4$	5.45	
Succinic Acid	$C_4H_6O_4$	0.04	
Glutaric Acid	$C_5H_8O_4$	0.08	
Adipic Acid	$C_6H_{10}O_4$	0.30	
Azelaic Acid	$C_9H_{16}O_4$	1.25	
Suberic Acid	$C_8H_{14}O_4$	2.19	
Boric acid	NH_4CH_3COO	0.25	
Ammonium Acetate	H_3BO_3	0.75	
Sodium Chloride	NaCl	9.36	
Sodium Fluoride	NaF	4.54	
Sodium Sulfate	Na_2SO_4	22.34	
Potassium Molybdate	K_2MoO_4	0.13	

Mix the solution well. Note that if a stopping point for an extended period of time is desired, Pause Here. Next add the following to the flask with mixing.

Add	Formula	Mass Needed	Actual Wt, grams
Sodium Hydroxide	NaOH	116.44	
Sodium Phosphate	$Na_3PO_4 \cdot 12H_2O$	26.44	
Sodium Tungstate	$Na_2WO_4 \cdot 2H_2O$	0.36	
Sodium Metasilicate	$Na_2SiO_3 \cdot 9H_2O$	0.12	
Sodium Glycolate	NaHCOO	16.36	
Sodium formate	$HOCH_2COONa$	15.22	
Sodium Acetate	$NaCH_3COO \cdot 3H_2O$	0.80	
Sodium Oxalate	$Na_2C_2O_4$	0.84	

Add	grams	Actual Wt, grams
Water	200	

Mix thoroughly.

Add	Formula	Mass Needed	Actual Wt, grams
Sodium Chromate	Na_2CrO_4	0.94	
Sodium Carbonate	Na_2CO_3	115.95	

Mix thoroughly.

Mix	Formula	Mass Needed	Actual Wt, grams
Sodium Nitrate	$NaNO_3$	128.98	
Sodium Nitrite	$NaNO_2$	118.50	
Water	H_2O	100	

Add and Mix thoroughly.

Mix thoroughly and dilute to the mark.

Record Final Gross Weight		grams
Measure the Density		g/mL

For INFO ONLY
The final addition of water would be 116.53 grams based upon a density of 1.434g/mL.

Solution Labeling	AN-102-Final Simulant at 9.543 M Na

APPENDIX B

AN-107 Filtrate Photographs

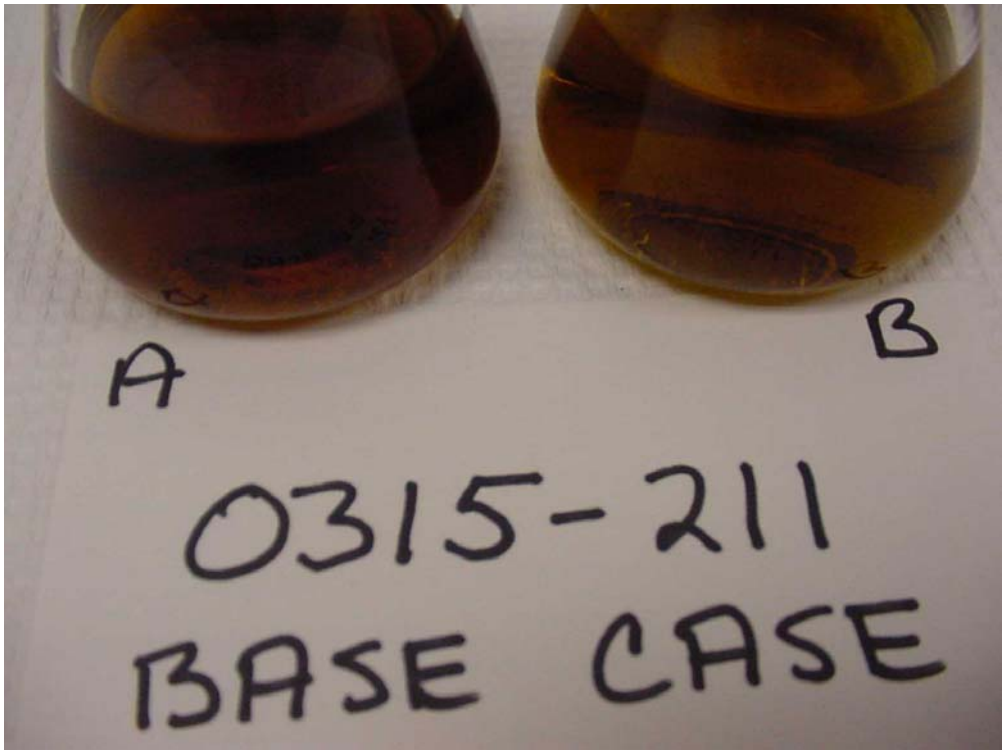

Figure B.1 Simulant AN-107 Sample 0315-211

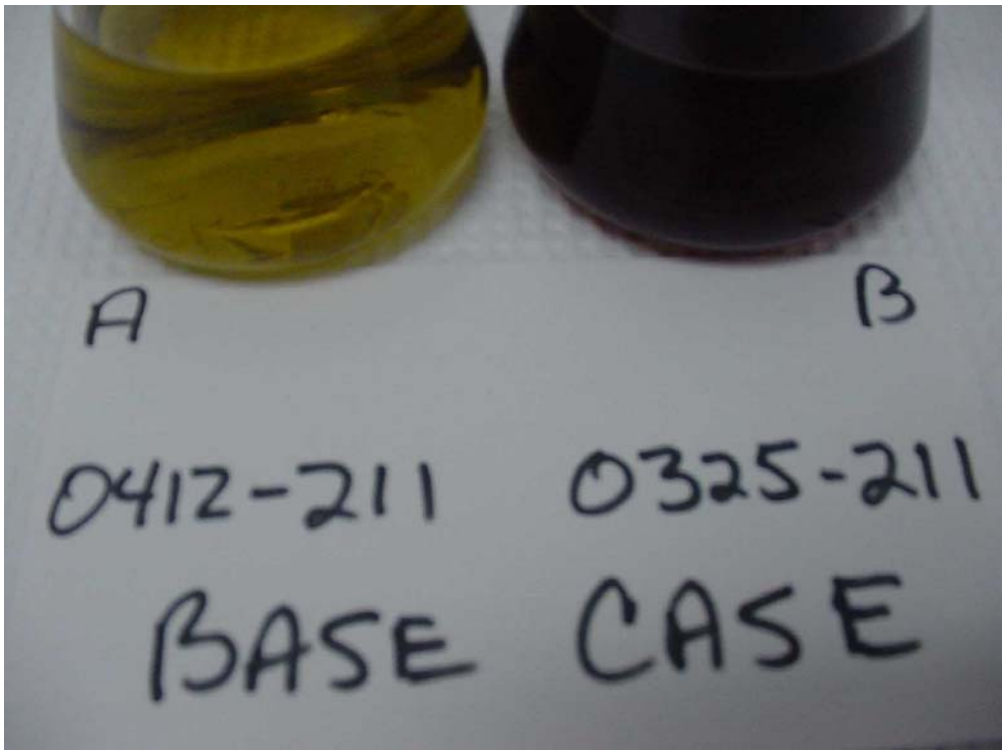

Figure B.2 Simulant AN-107 Samples 0412-211 and 0325-211

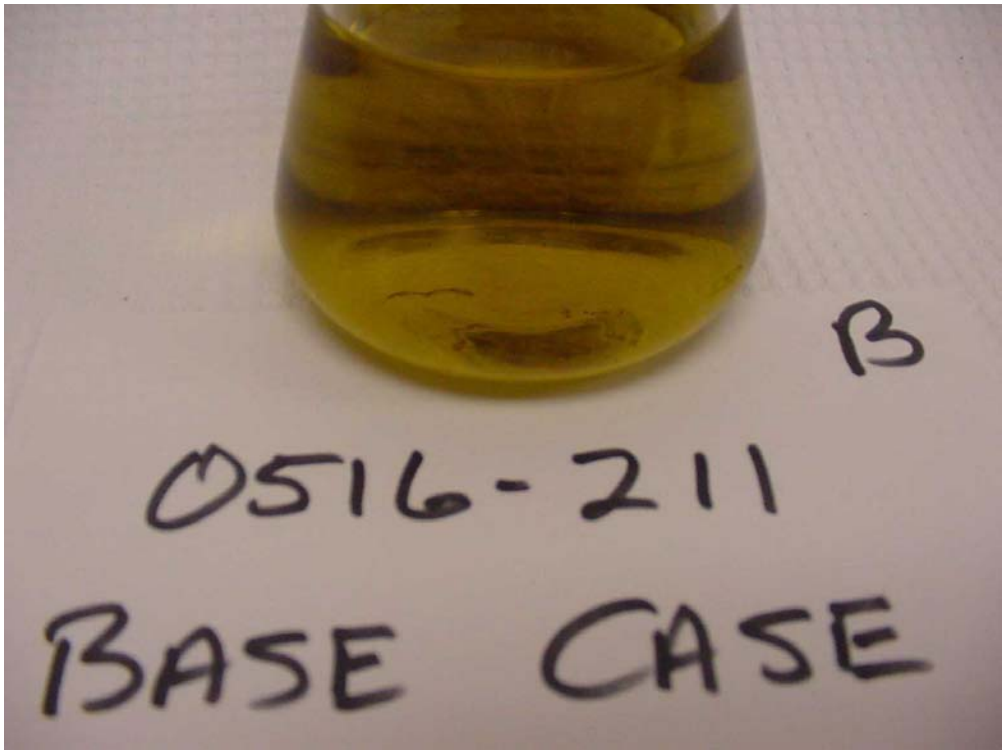

Figure B.3 Simulant AN-107 Sample 0516-211

Figure B.4 Simulant AN-107 Sample 0315-111

Figure B.5 Simulant AN-107 Sample 0315-215

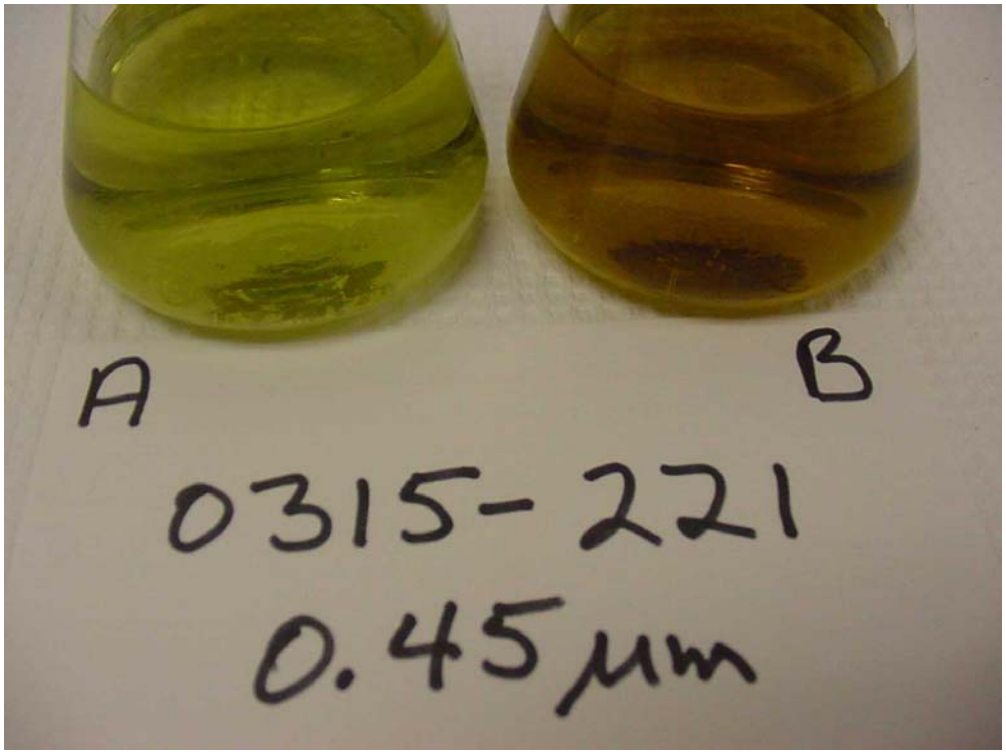

Figure B.6 Simulant AN-107 Sample 0315-221

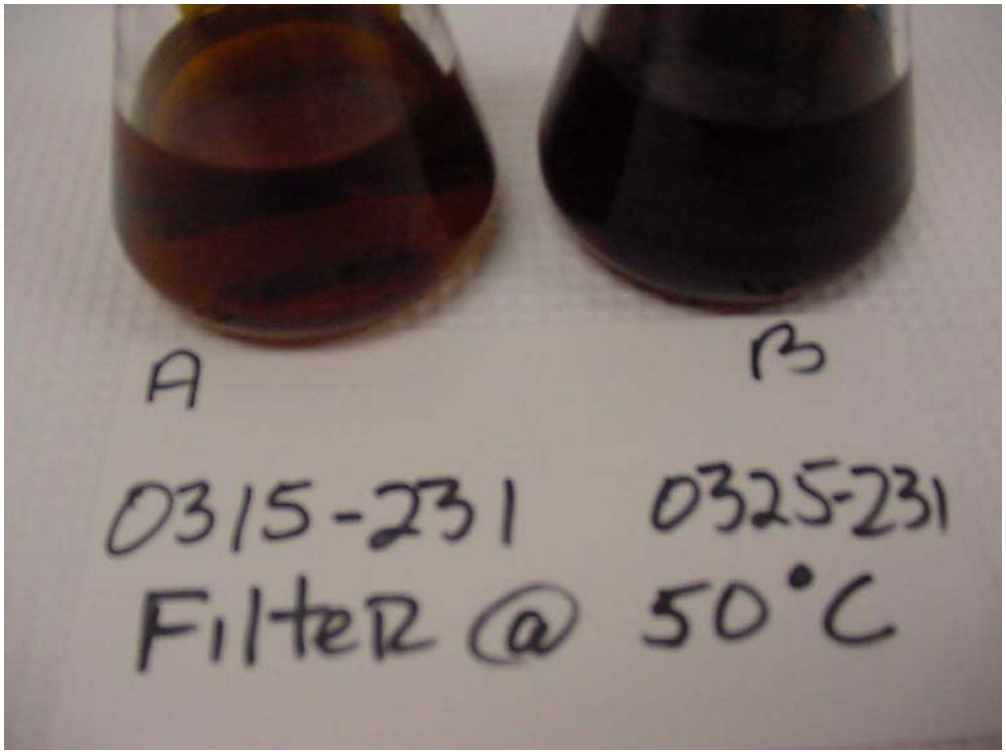

Figure B.7 Simulant AN-107 Samples 0315-231 and 0325-231

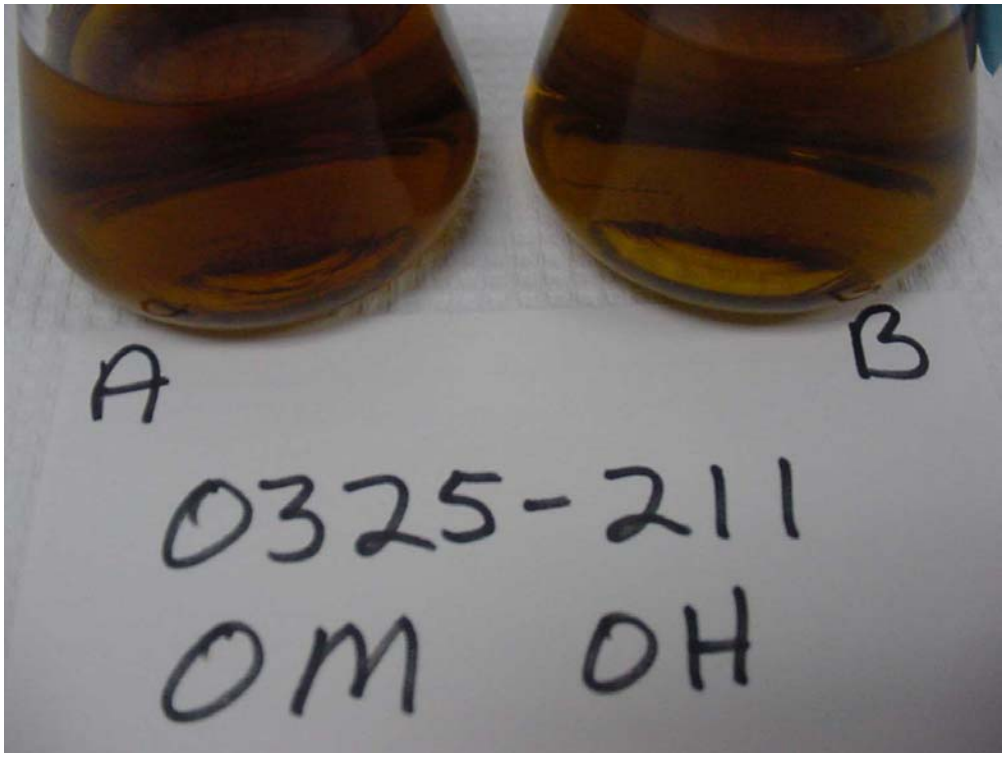

Figure B.8 Simulant AN-107 Sample 0325-211

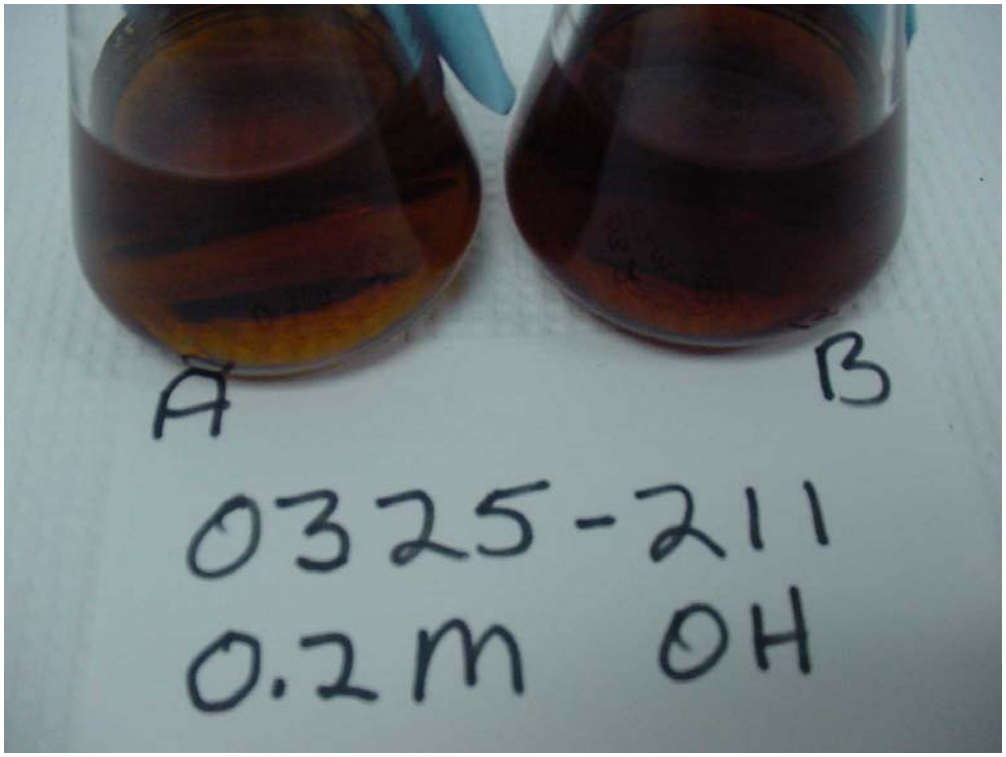

Figure B.9 Simulant AN-107 Sample 0325-211

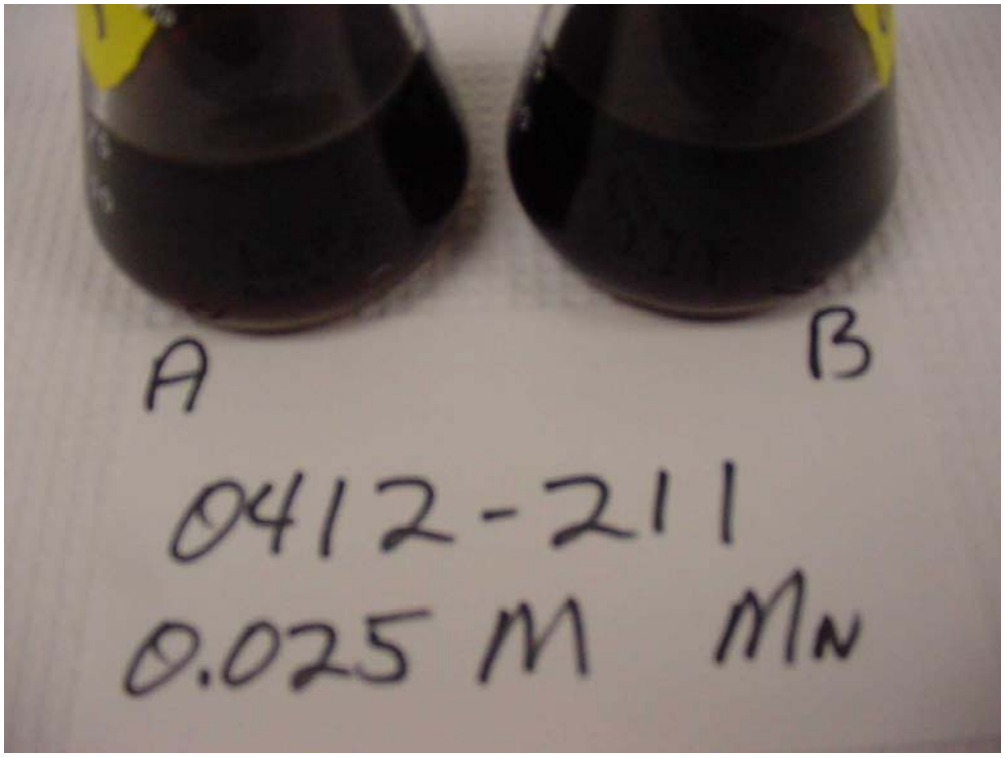

Figure B.10 Simulant AN-107 Sample 0412-211

Figure B.11 Simulant AN-107 Sample 0412-211

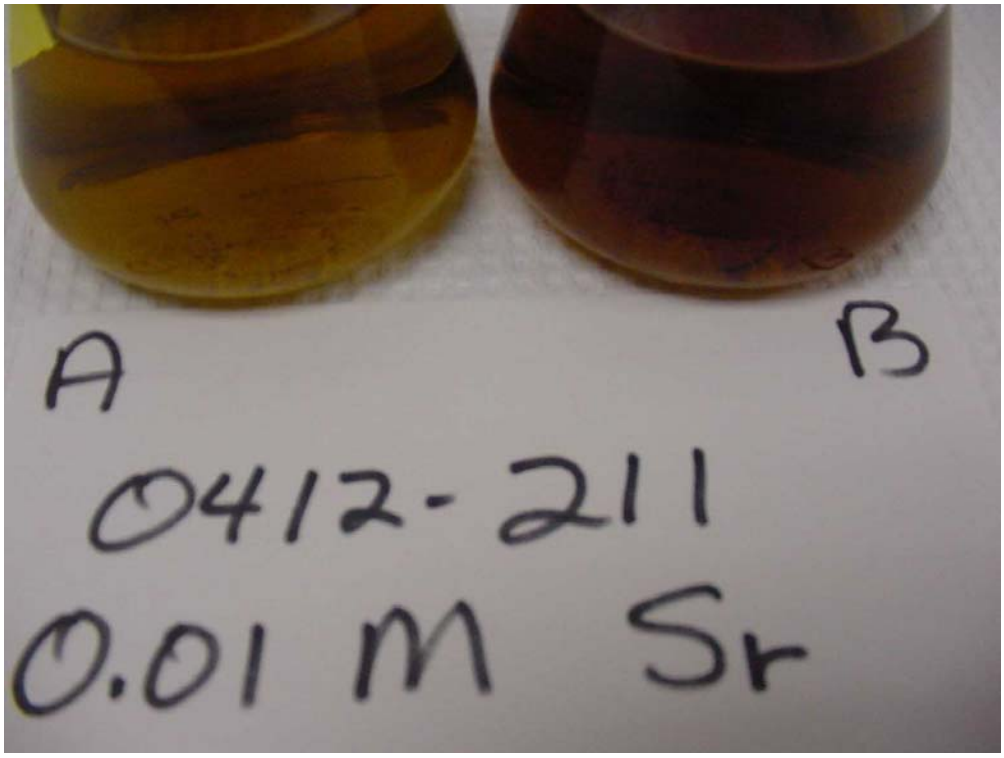

Figure B.12 Simulant AN-107 Sample 0412-211

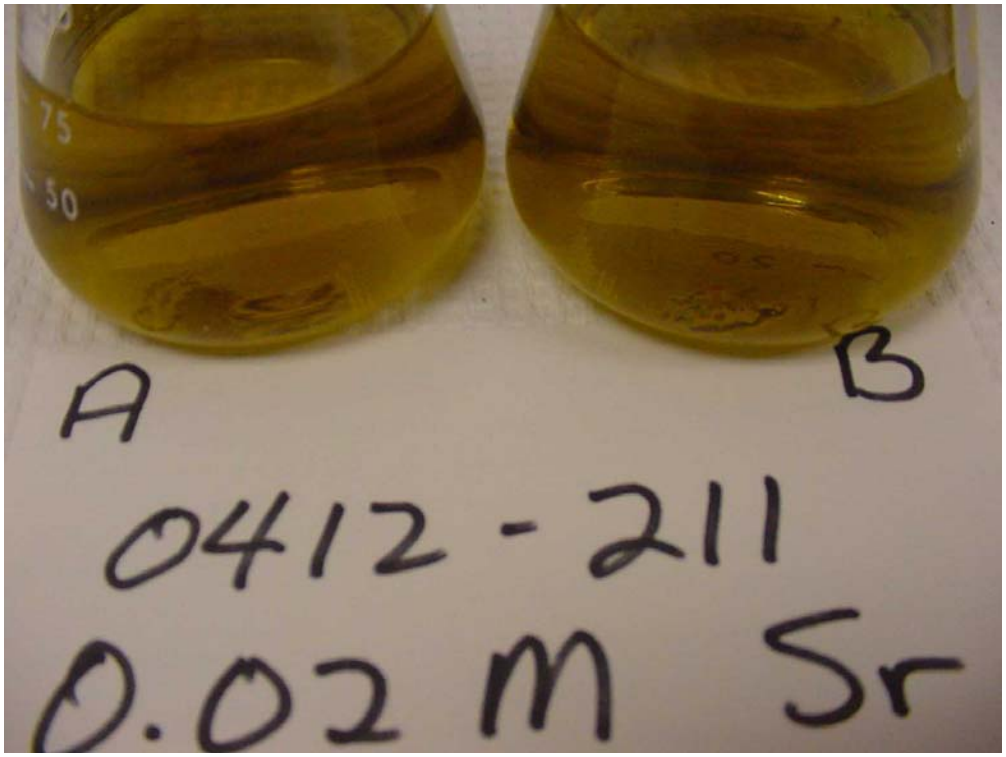

Figure B.13 Simulant AN-107 Sample 0412-211

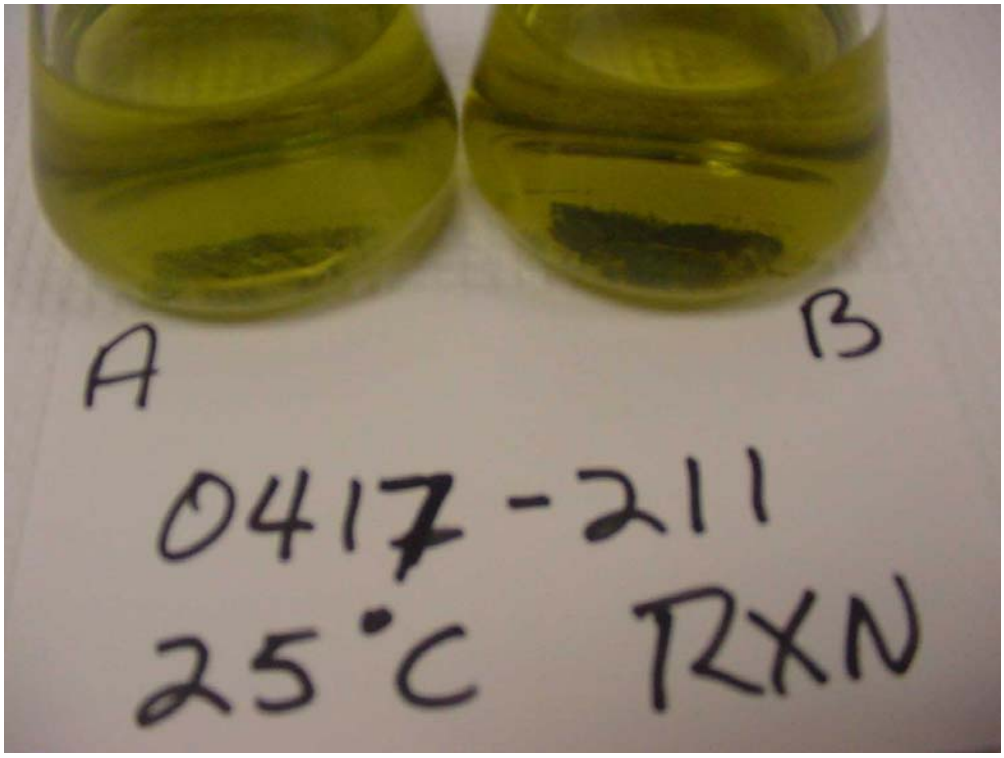

Figure B.14 Simulant AN-107 Sample 0417-211

Figure B.15 Simulant AN-107 Sample 0424-211

Figure B.16 Simulant AN-107 Sample 0516-213

Figure B.17 Simulant AN-107 Sample 0516-212

APPENDIX C

ICP-AES Analysis of AN-107 Primary Effects Samples

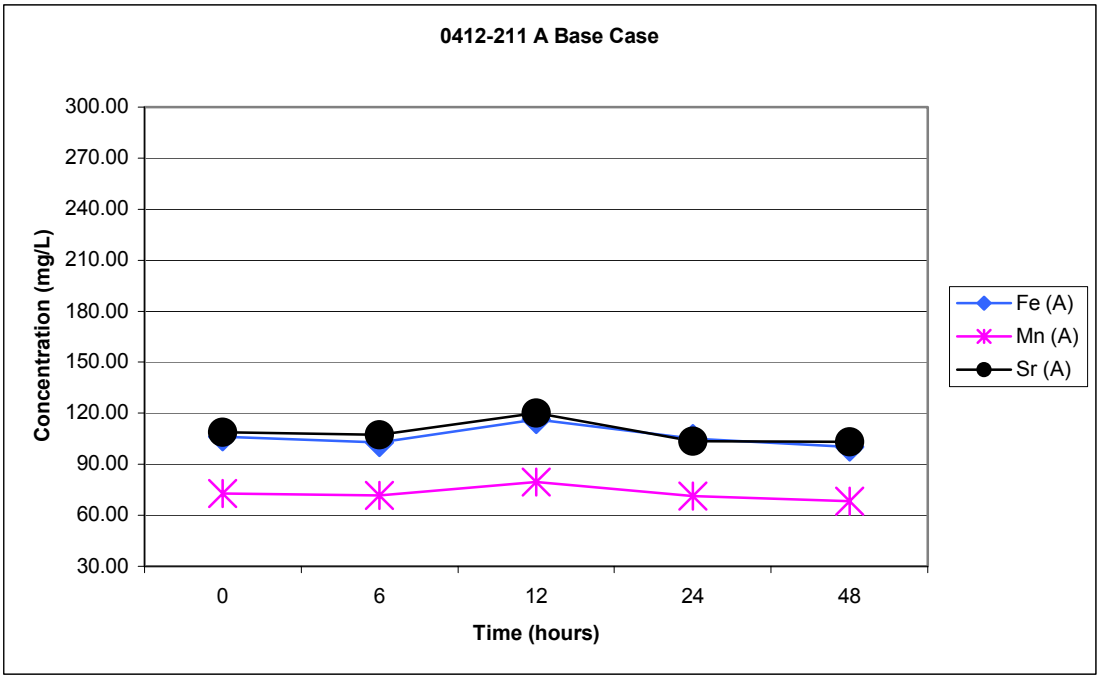

Figure C.1 Iron, Manganese, and Strontium ICP Data for Sample 0412-211A Base Case

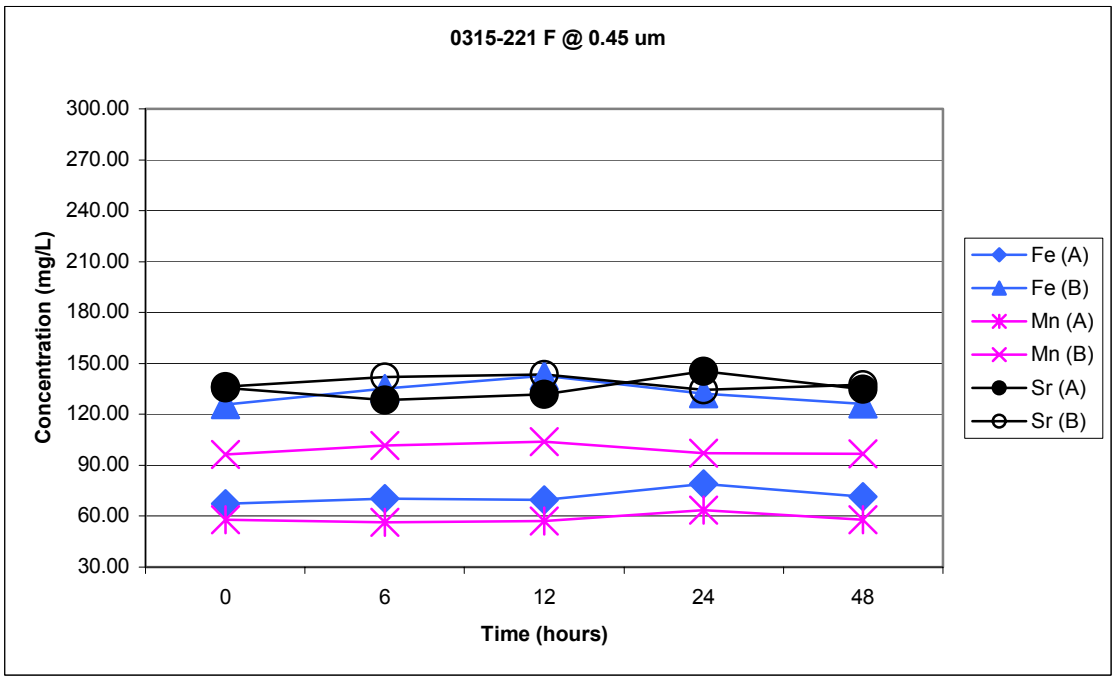

Figure C.2 Iron, Manganese, and Strontium ICP Data for Sample 0315-221 0.45µm Filter

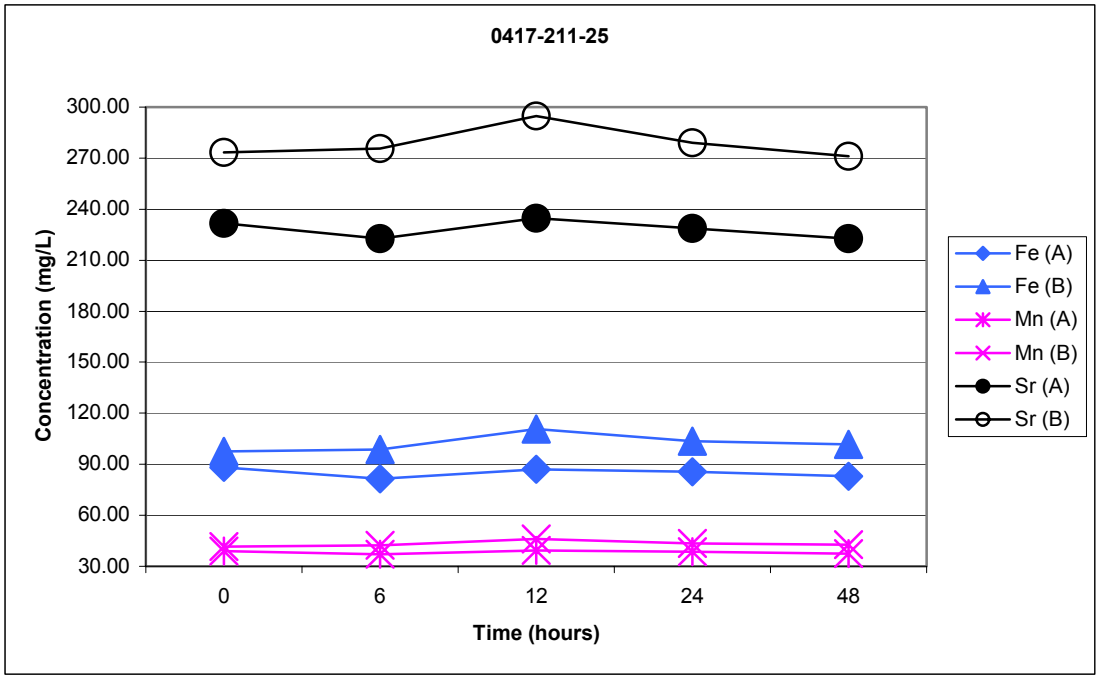

Figure C.3 Iron, Manganese, and Strontium ICP Data for Sample 0417-211-25 °C Rxn

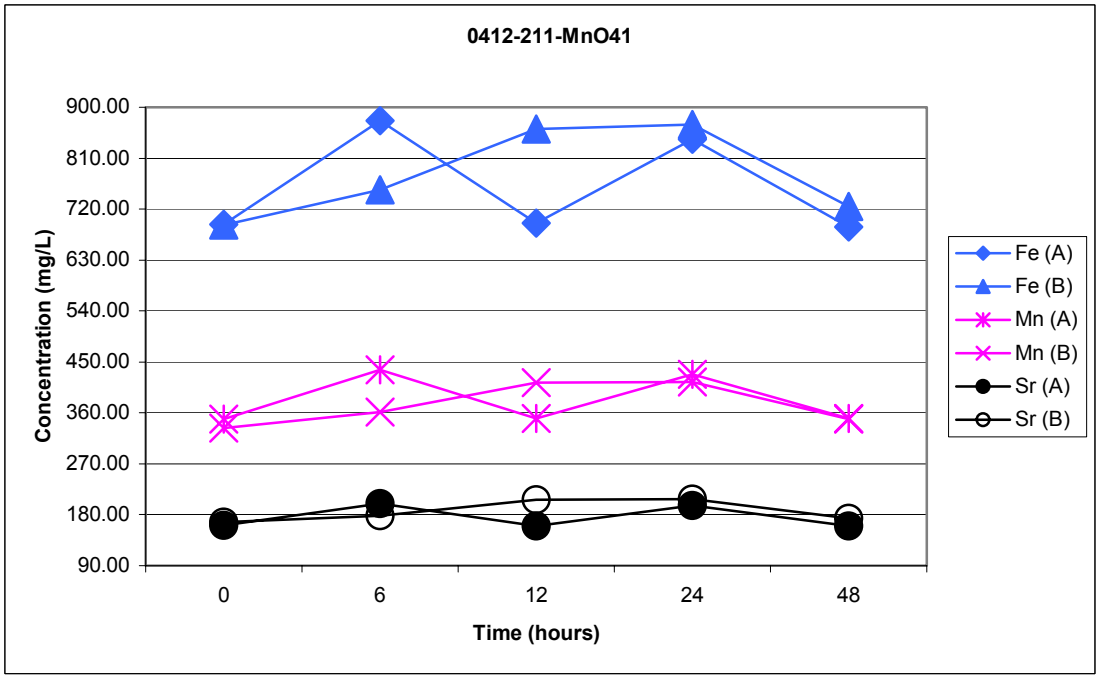

Figure C.4 Iron, Manganese, and Strontium ICP Data for Sample 0417-211-0.01M MnO_4

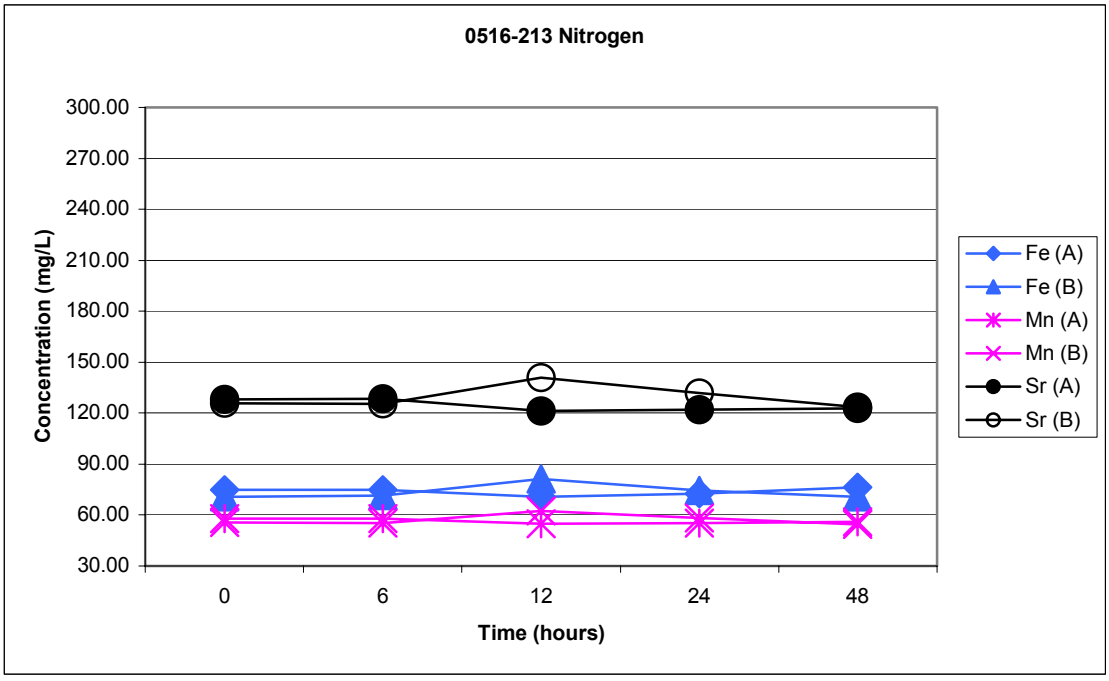

Figure C.5 Iron, Manganese, and Strontium ICP Data for Sample 0516-213 Nitrogen

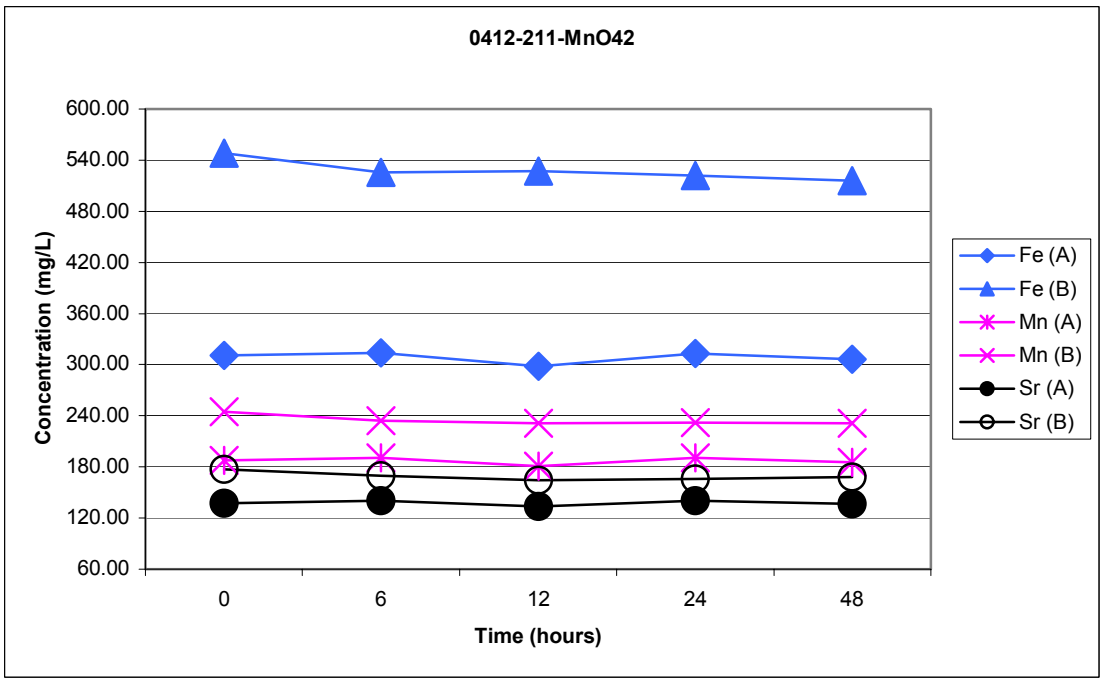

Figure C.6 Iron, Manganese, and Strontium ICP Data for Sample 0412-211-0.025M MnO_4

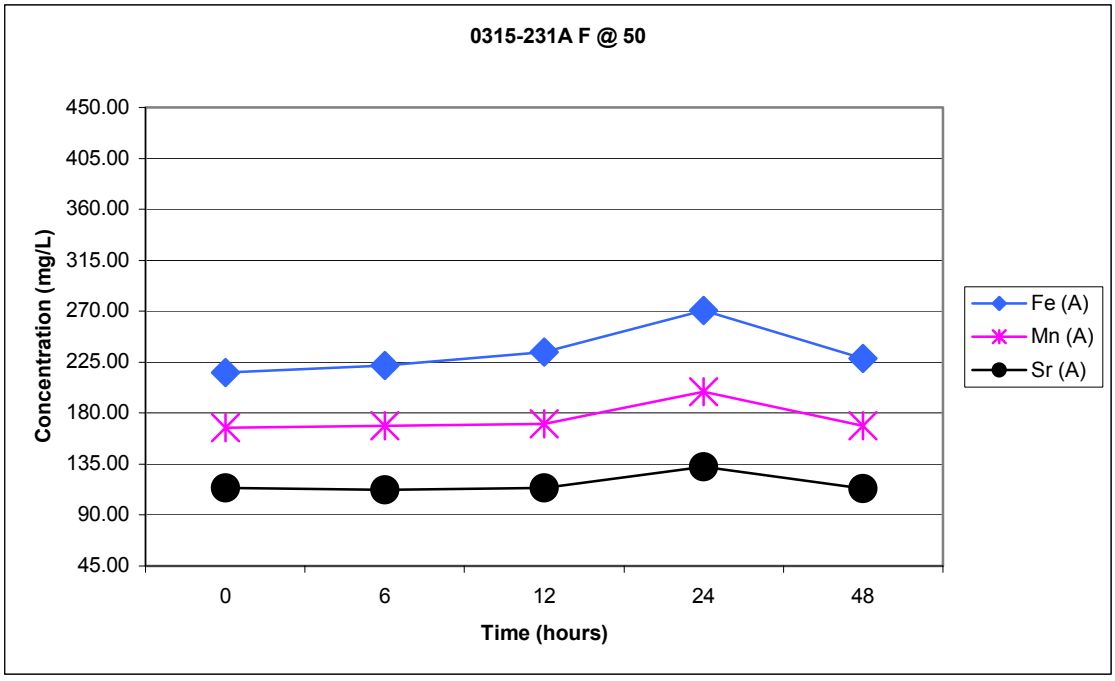

Figure C.7a Iron, Manganese, and Strontium ICP Data for Sample 0315-231A Filter @ 50°C

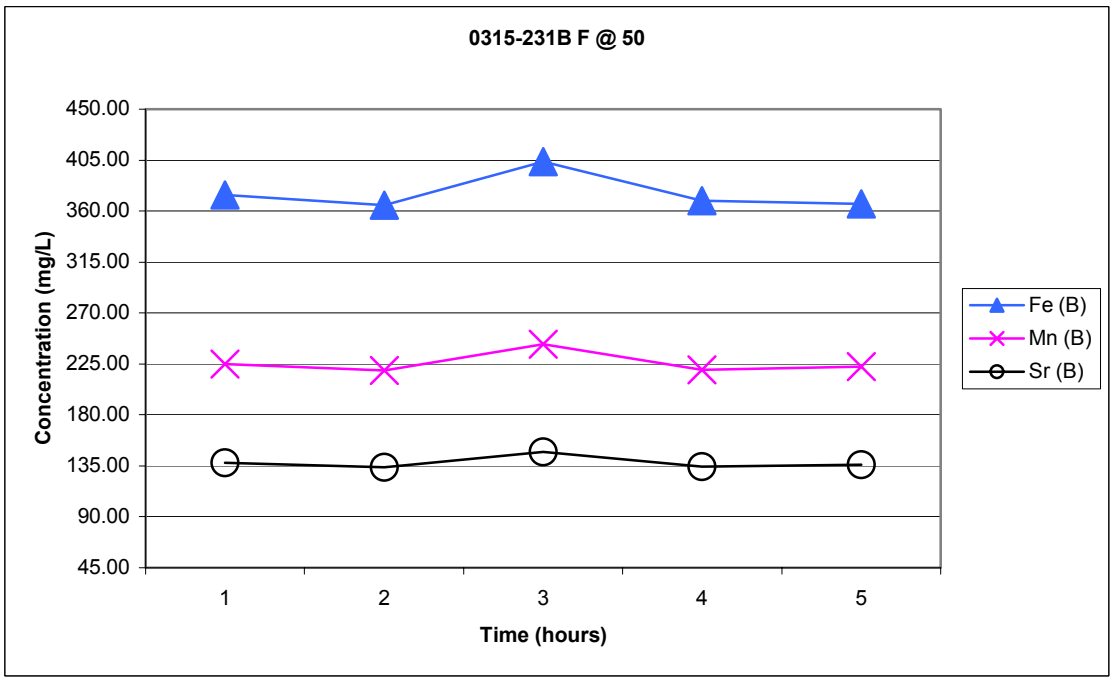

Figure C.7b Iron, Manganese, and Strontium ICP Data for Sample 0325-231B Filter @ 50°C

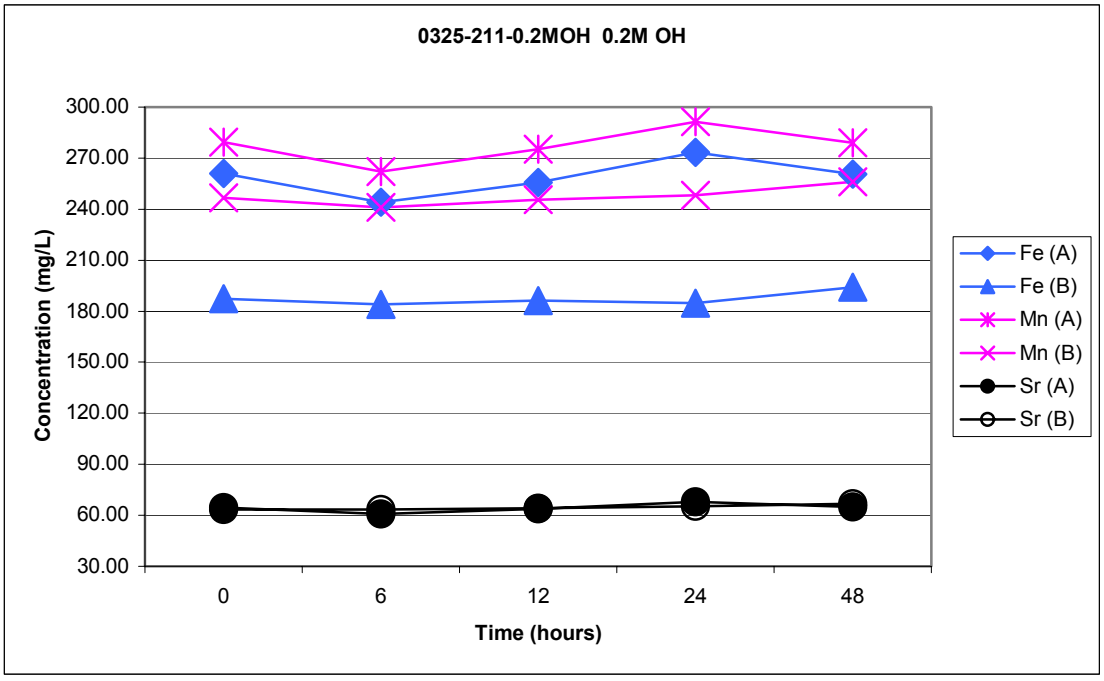

Figure C.8 Iron, Manganese, and Strontium ICP Data for Sample 0325-211-0.2 M OH^-

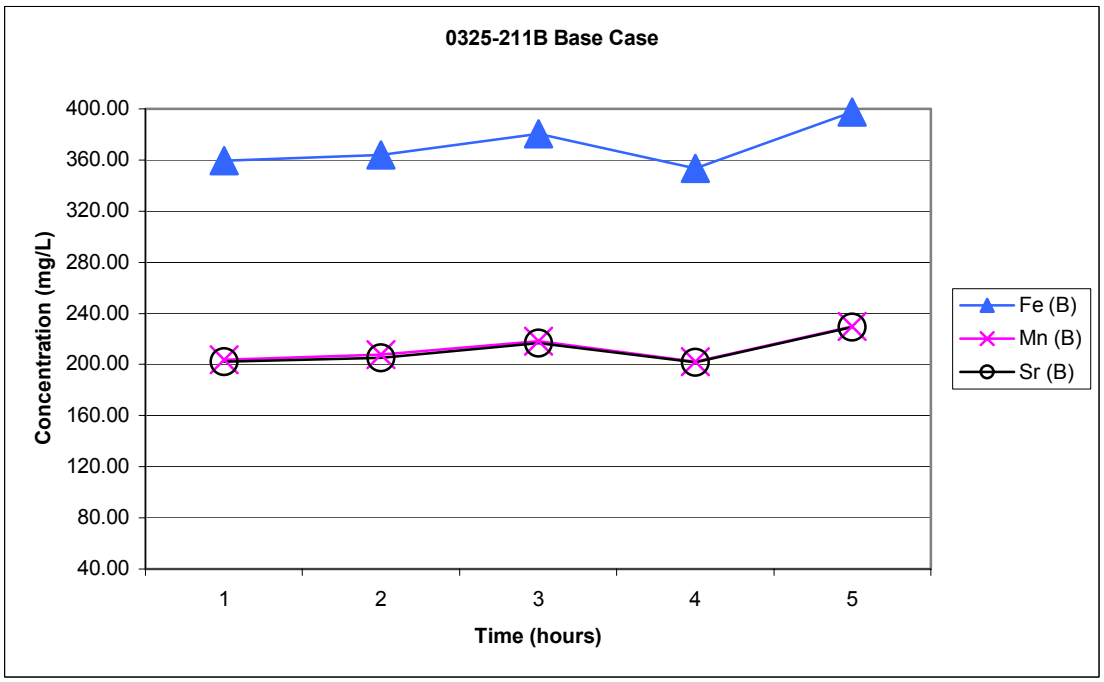

Figure C.9 Iron, Manganese, and Strontium ICP Data for Sample 0325-211B Base Case

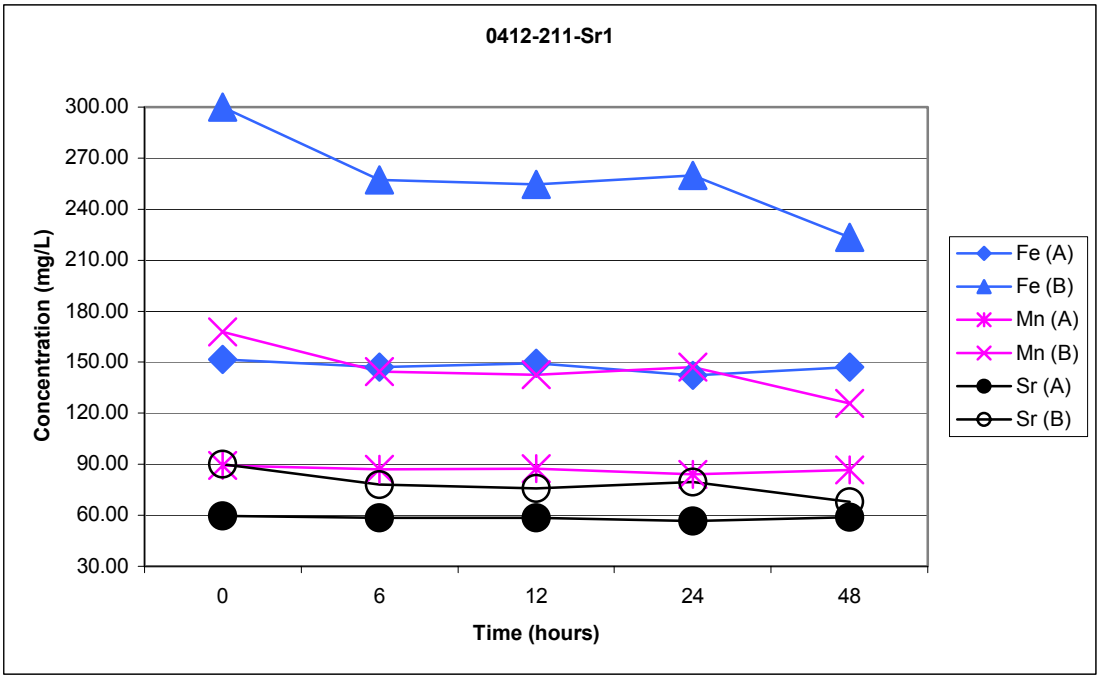

Figure C.10 Iron, Manganese, and Strontium ICP Data for Sample 0412-211-0.01 M Sr

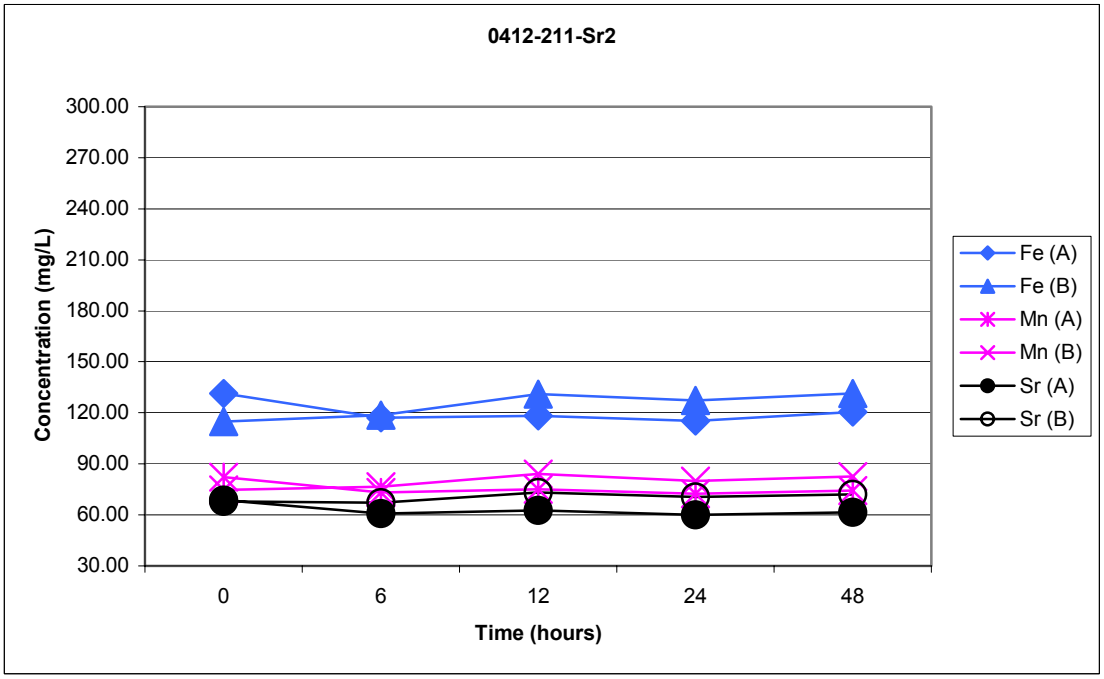

Figure C.11 Iron, Manganese, and Strontium ICP Data for Sample 0412-211-0.02 M Sr

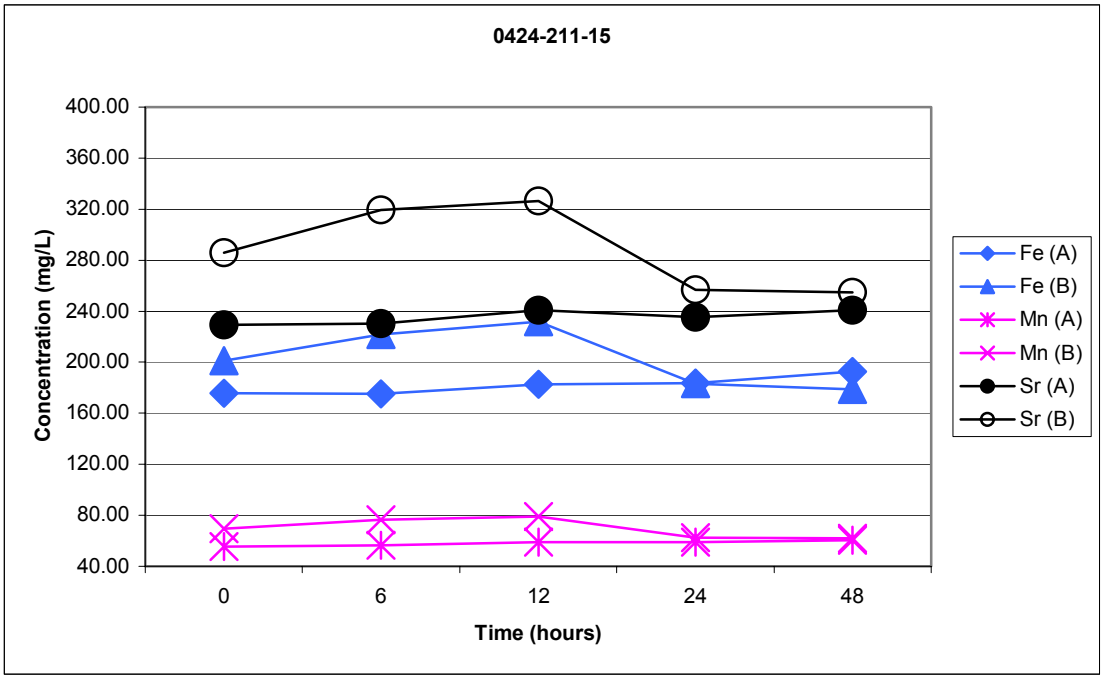

Figure C.12 Iron, Manganese, and Strontium ICP Data for Sample 0412-211-15 ^{o}C Rxn

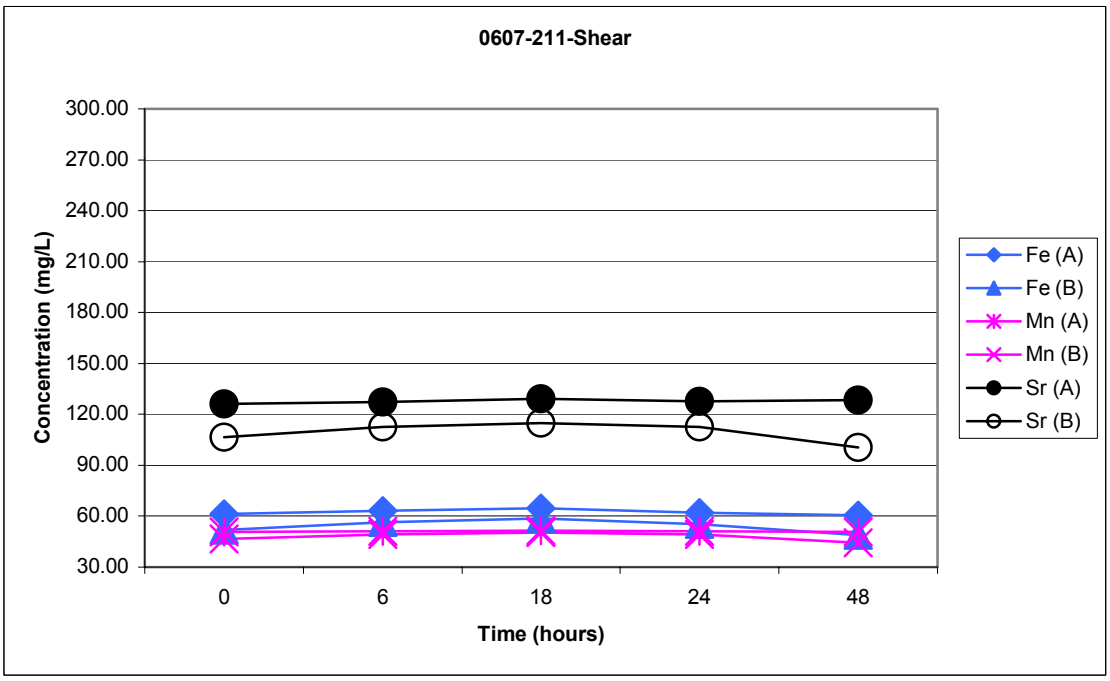

Figure C.13 Iron, Manganese, and Strontium ICP Data for Sample 0607-211 Shear

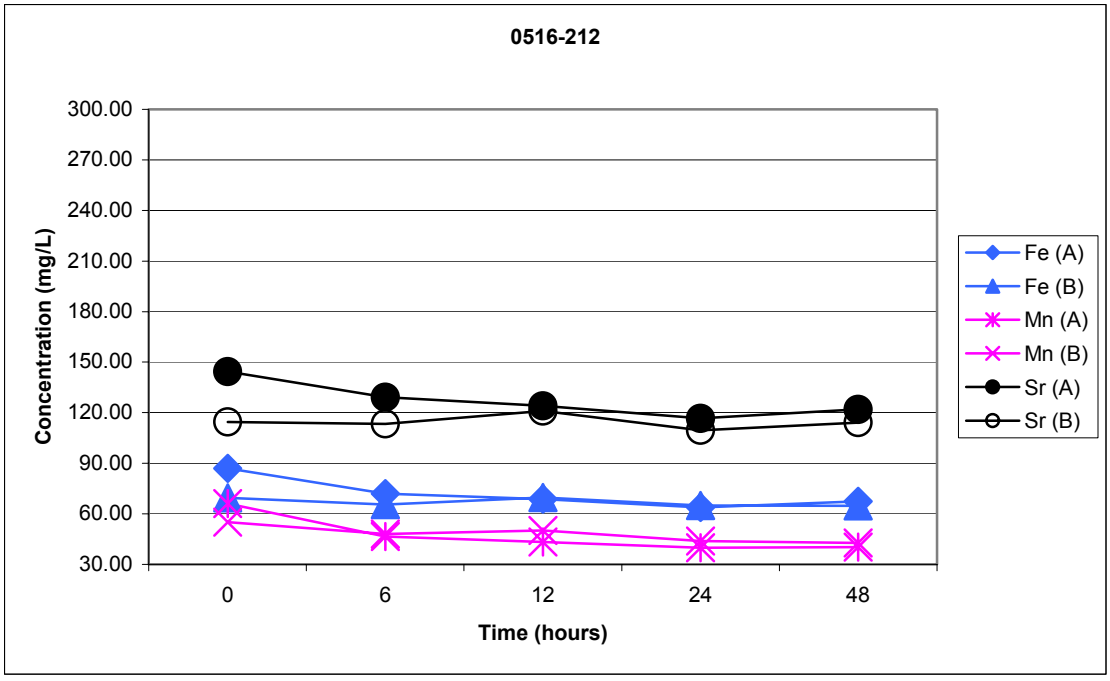

Figure C.13b Iron, Manganese, and Strontium ICP Data for Sample 0516-212 Oxygen Purge

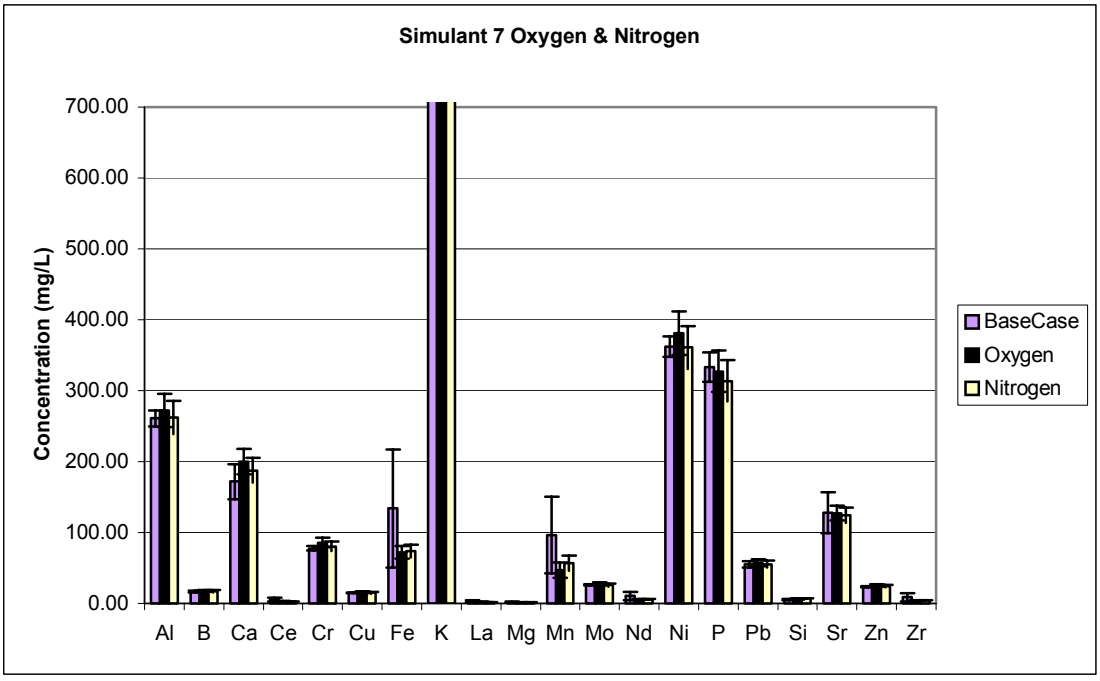

Figure C.14a Cation Concentrations in AN-107 Simulant 7 Base Case, O_2, and N_2 Filtrates

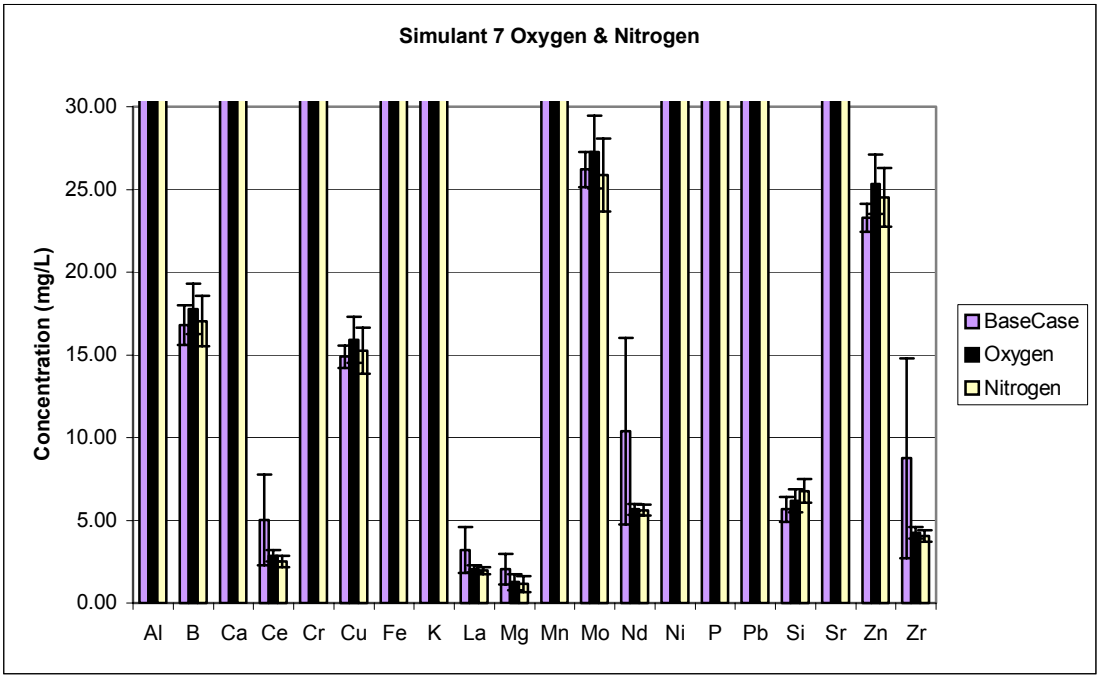

Figure C.14b Cation Concentrations in AN-107 Simulant 7 Base Case, O_2, and N_2 Filtrates

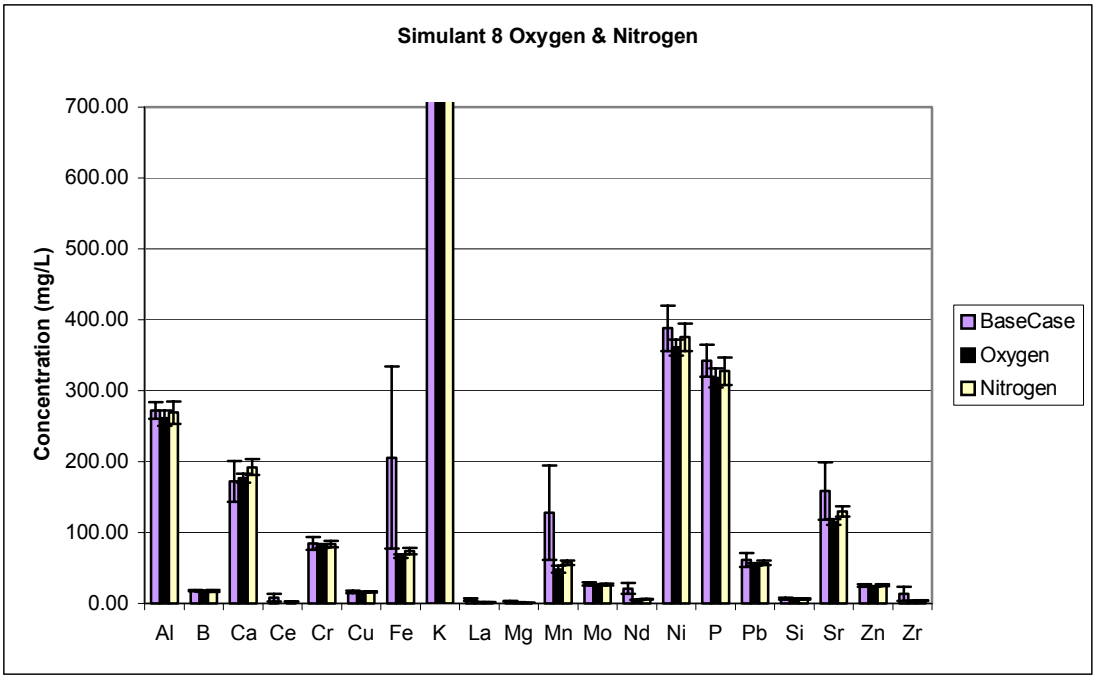

Figure C.15a Cation Concentrations in AN-107 Simulant 8 Base Case, O_2, and N_2 Filtrates

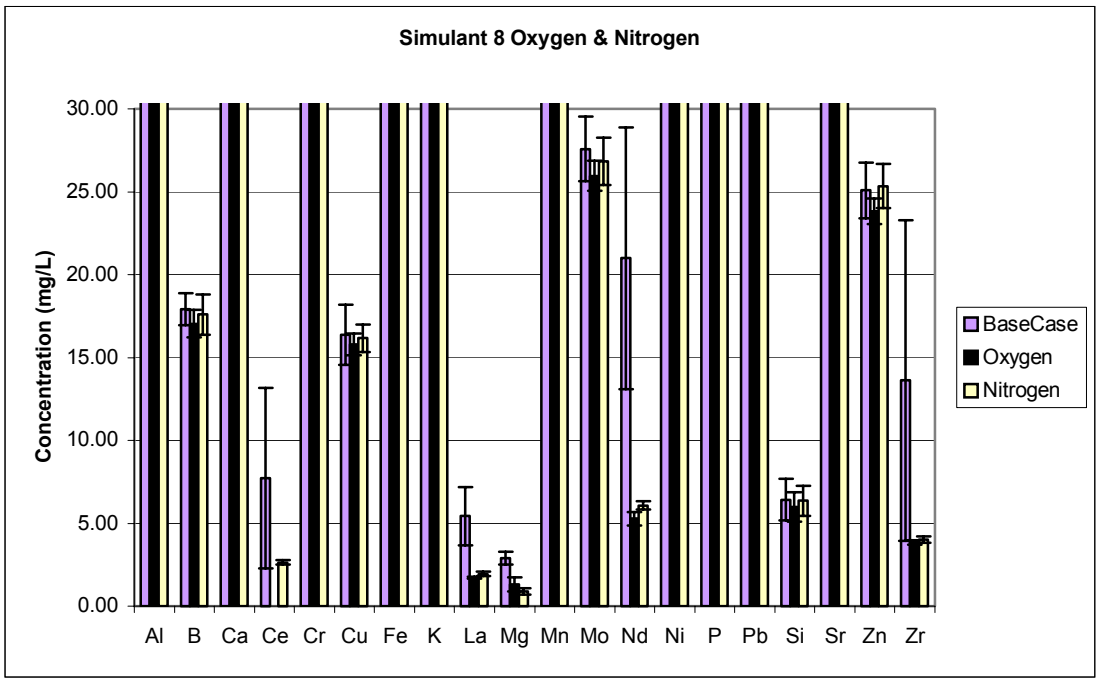

Figure C.15b Cation Concentrations in AN-107 Simulant 8 Base Case, O_2, and N_2 Filtrates

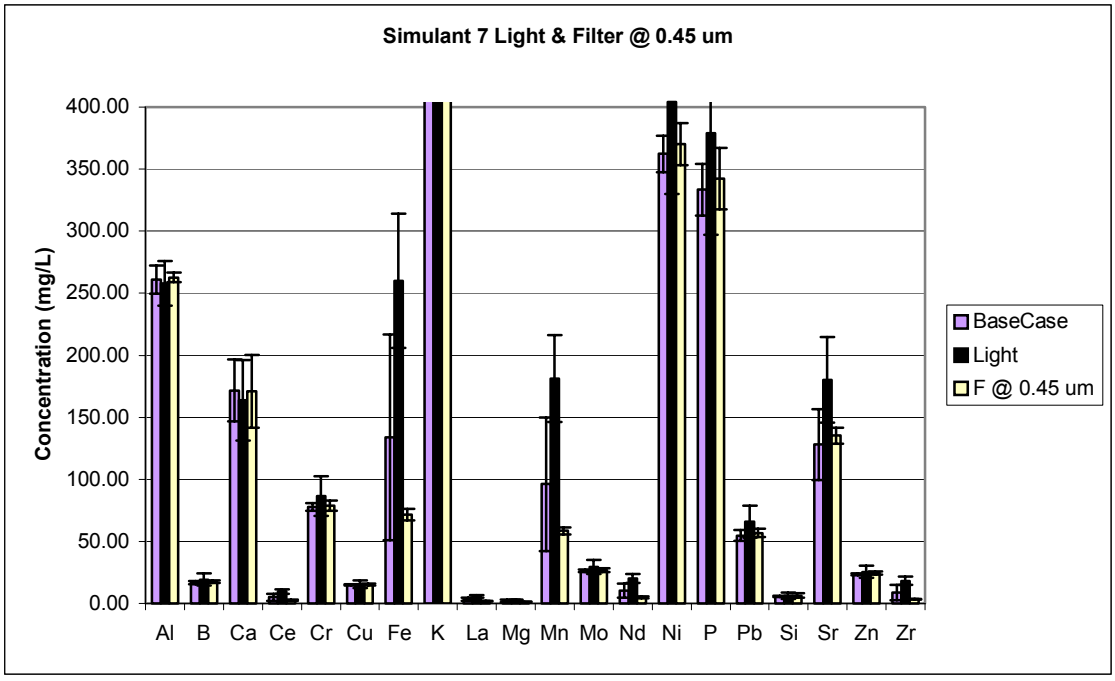

Figure C.16a Cation Concentrations in AN-107 Simulant 7 Base Case, Light, and 0.45µm Filter Filtrates

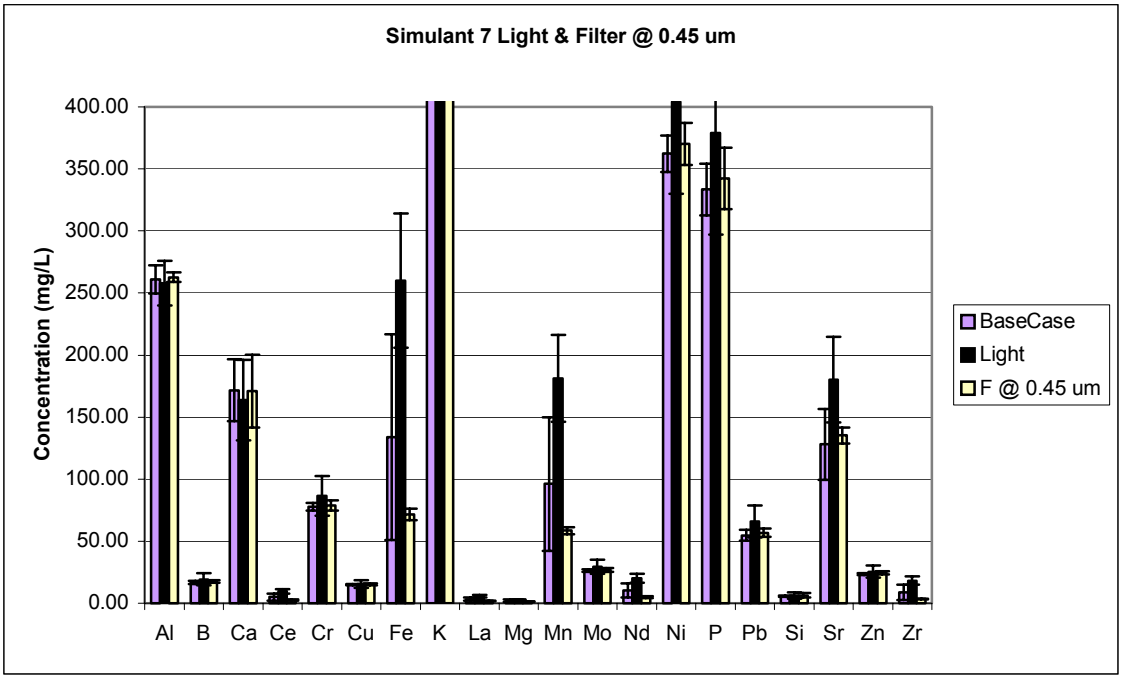

Figure C.16b Cation Concentrations in AN-107 Simulant 7 Base Case, Light, and 0.45µm Filter Filtrates

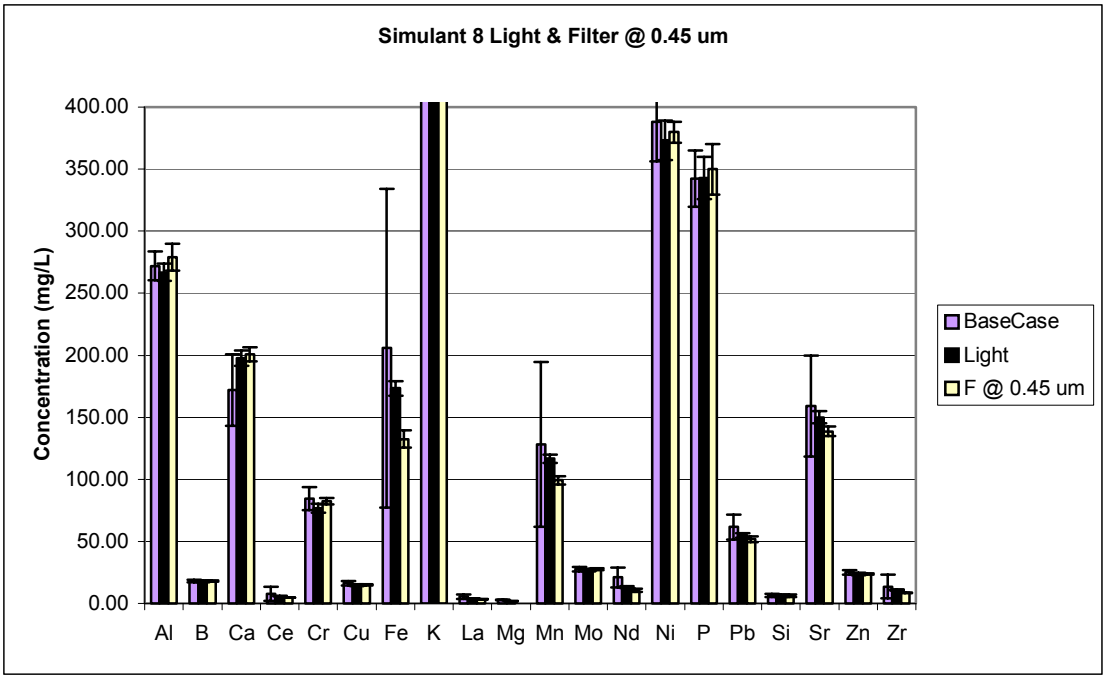

Figure C.17a Cation Concentrations in AN-107 Simulant 8 Base Case, Light, and 0.45µm Filter Filtrates

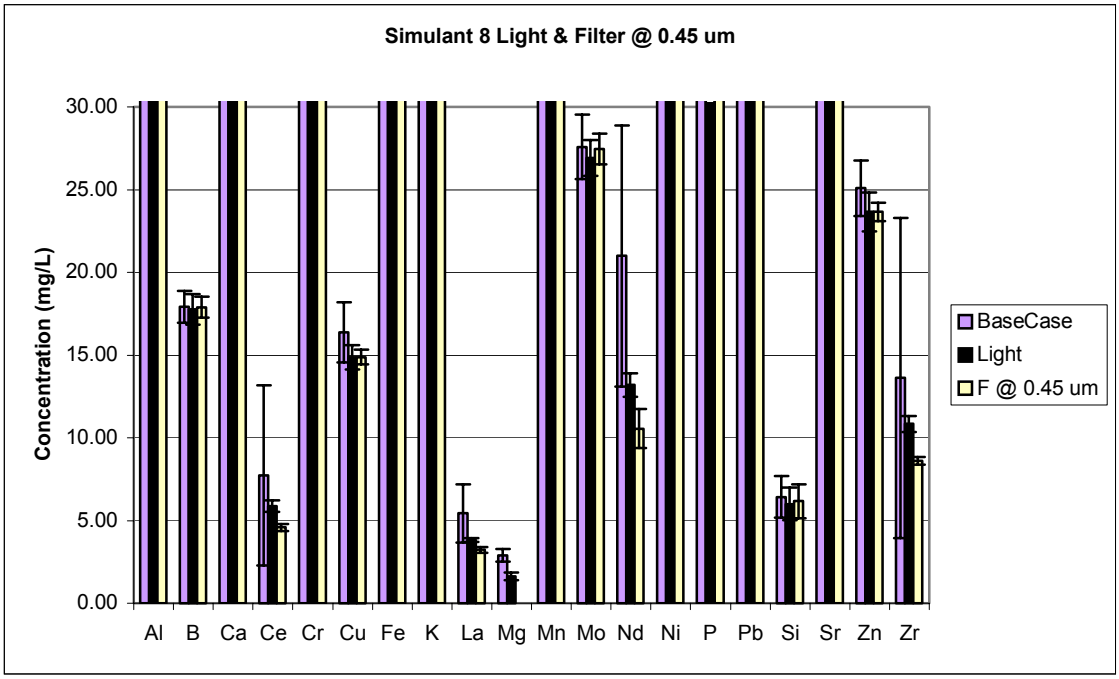

Figure C.17b Cation Concentrations in AN-107 Simulant 8 Base Case, Light, and 0.45µm Filter Filtrates

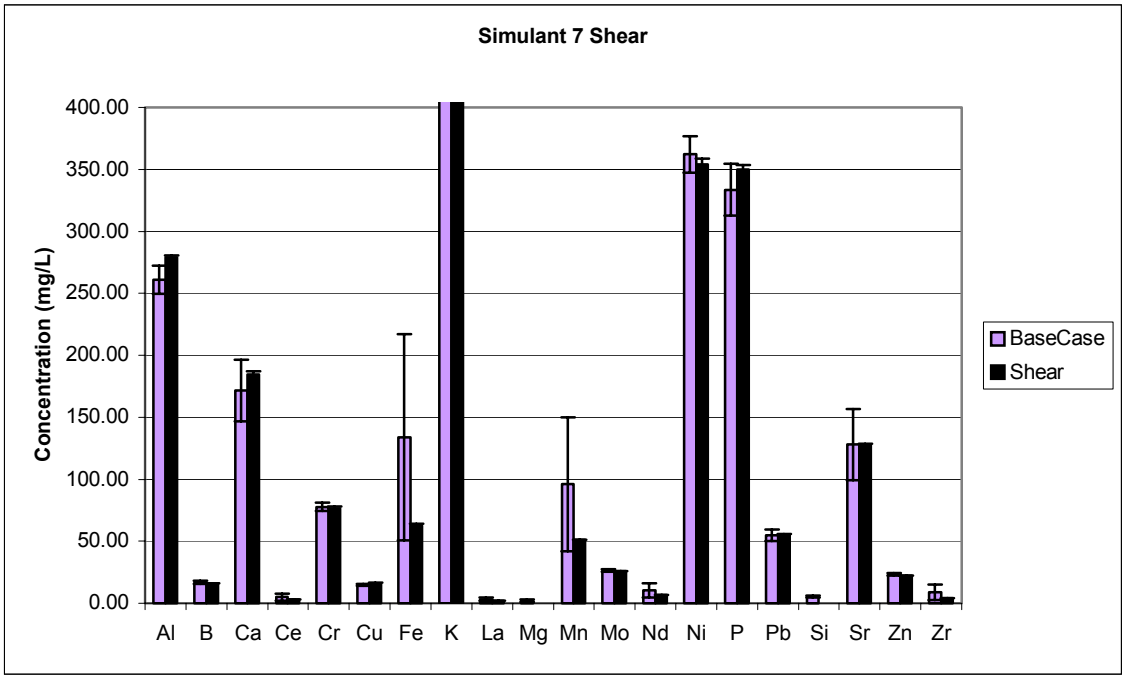

Figure C.18a Cation Concentrations in AN-107 Simulant 7 Base Case and Shear Filtrates

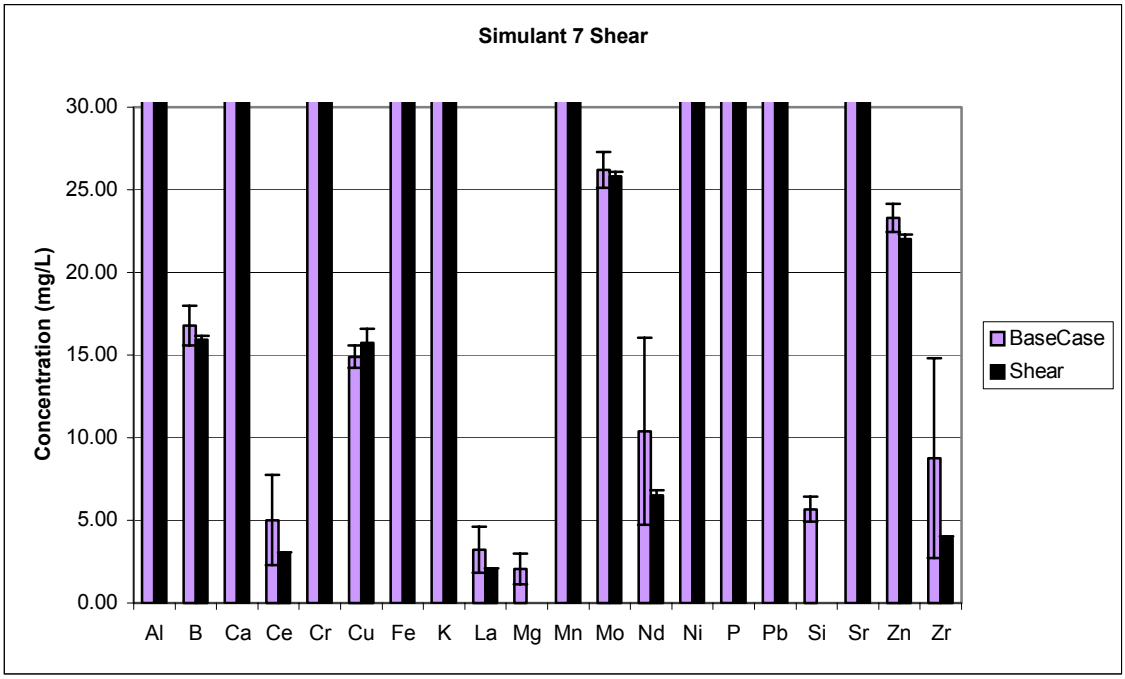

Figure C.18b Cation Concentrations in AN-107 Simulant 7 Base Case and Shear Filtrates

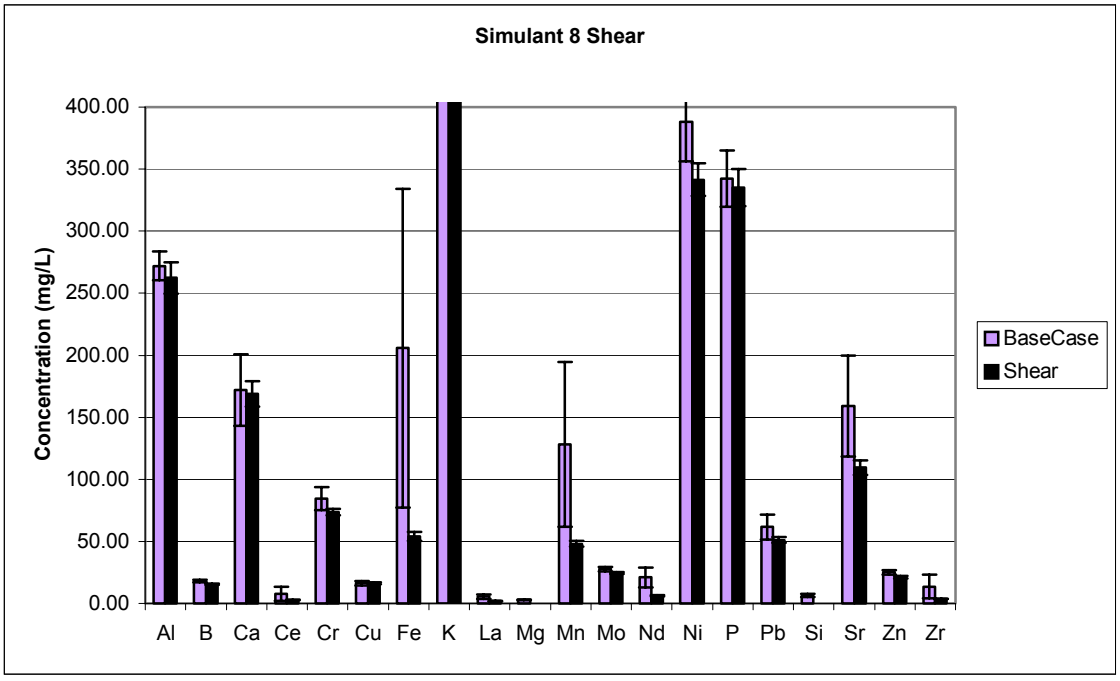

Figure C.19a Cation Concentrations in AN-107 Simulant 8 Base Case and Shear Filtrates

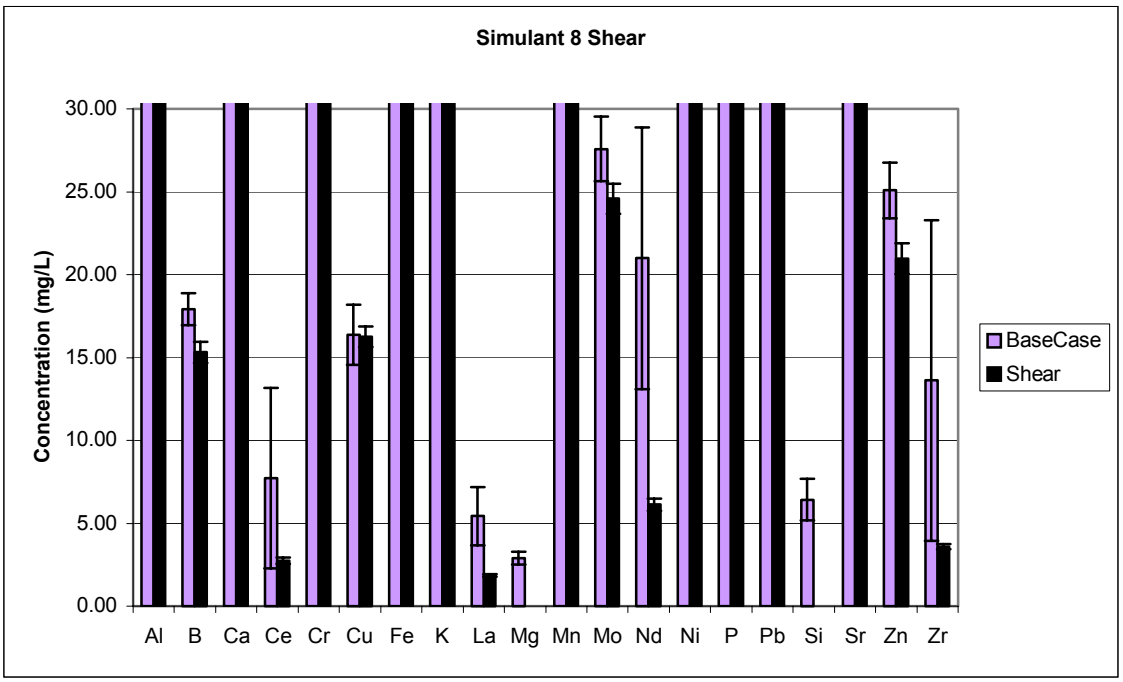

Figure C.19b Cation Concentrations in AN-107 Simulant 8 Base Case and Shear Filtrates

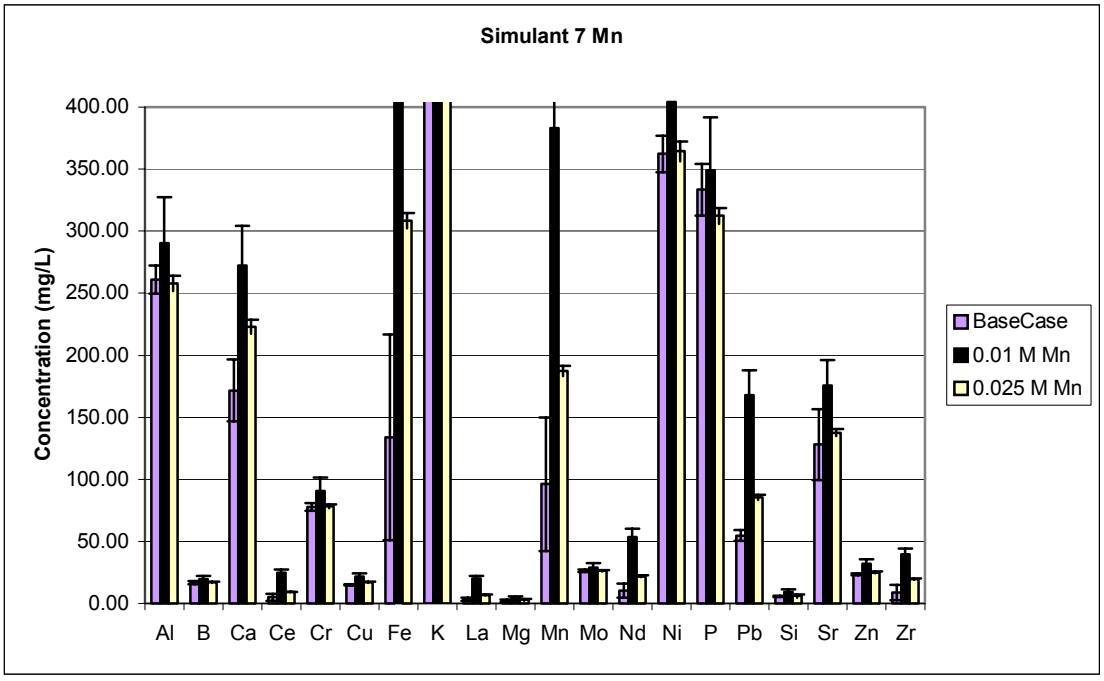

Figure C.20a Cation Concentrations in AN-107 Simulant 7 Base Case, 0.01M Mn, and 0.025M Mn Filtrates

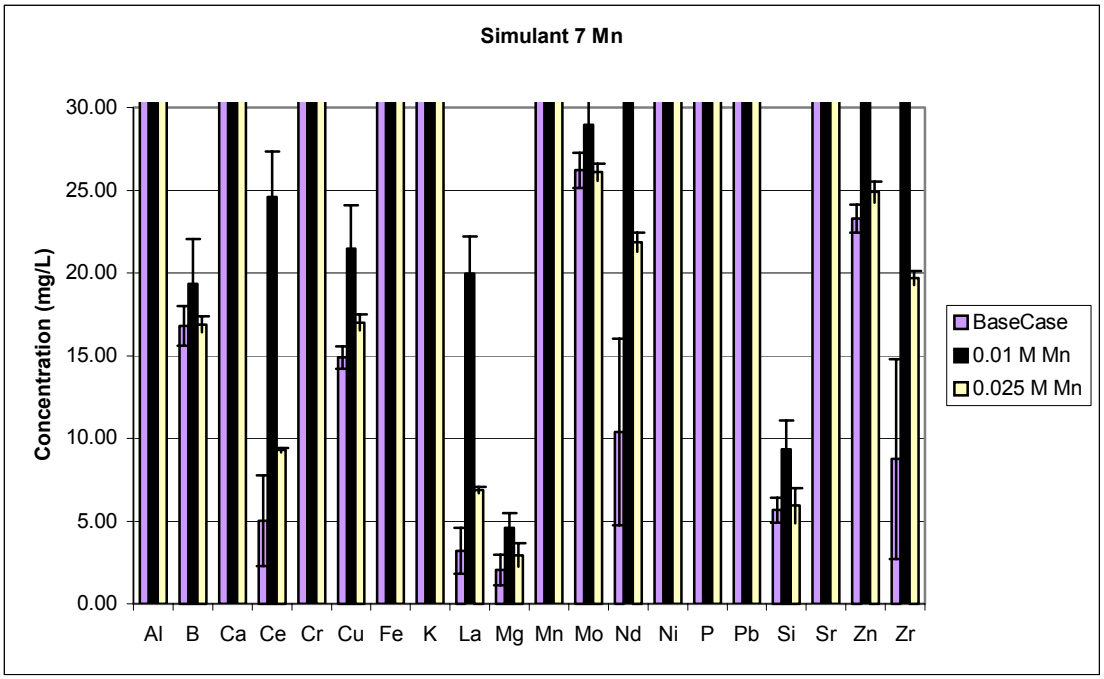

Figure C.20b Cation Concentrations in AN-107 Simulant 7 Base Case, 0.01M Mn, and 0.025M Mn Filtrates

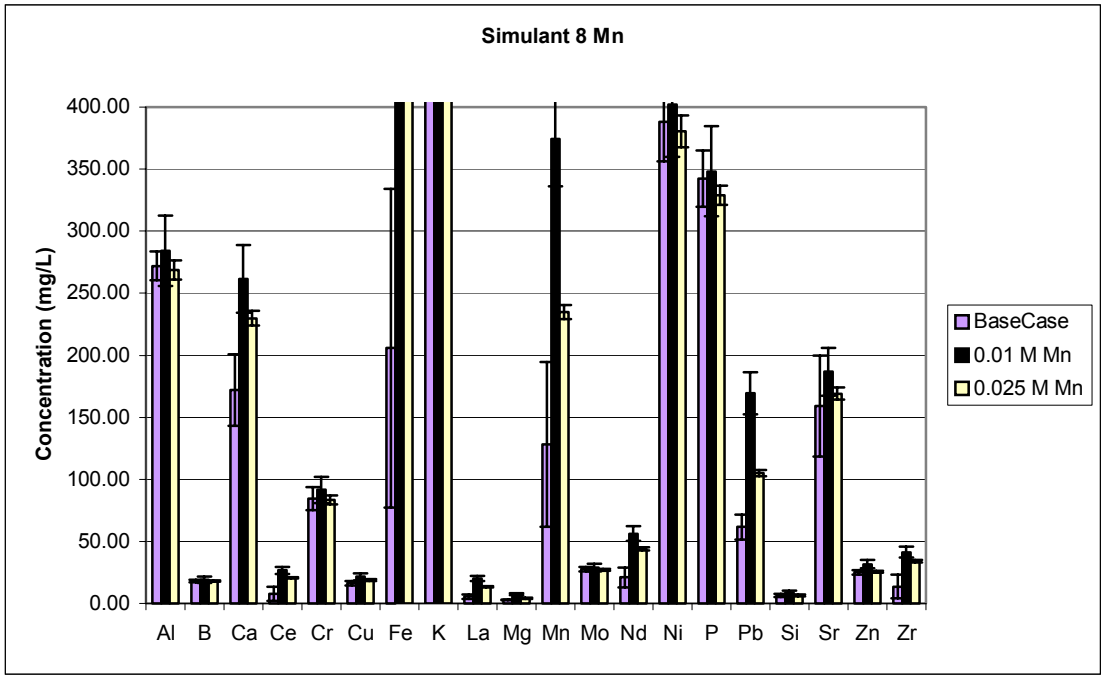

Figure C.21a Cation Concentrations in AN-107 Simulant 8 Base Case, 0.01M Mn, and 0.025M Mn Filtrates

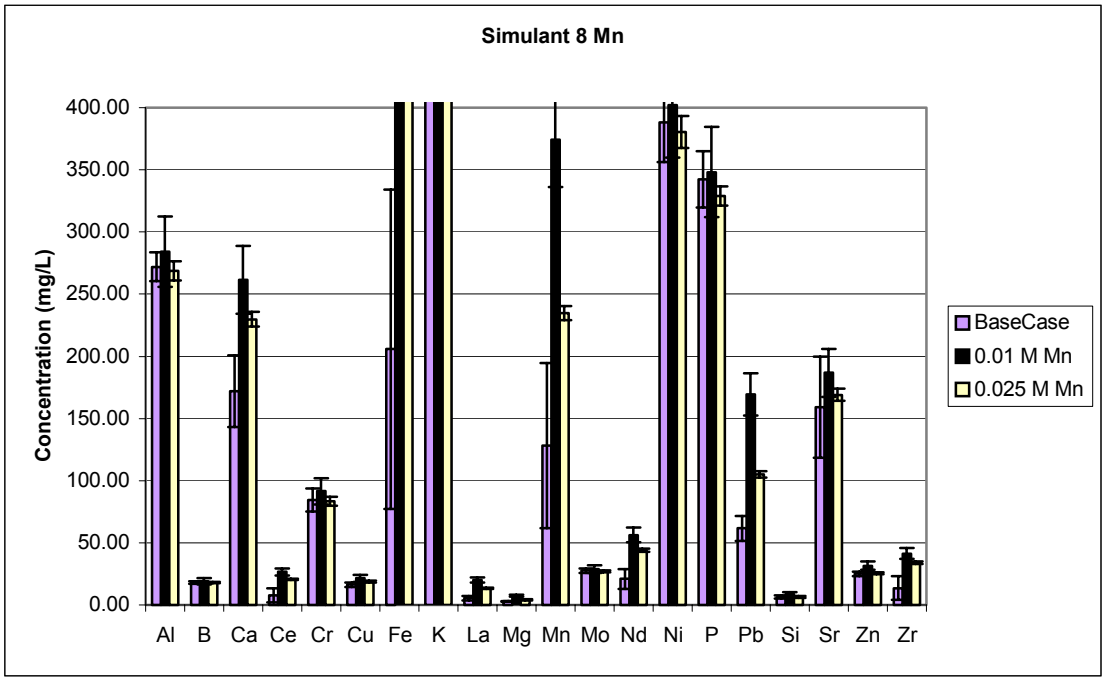

Figure C.21b Cation Concentrations in AN-107 Simulant 8 Base Case, 0.01M Mn, and 0.025M Mn Filtrates

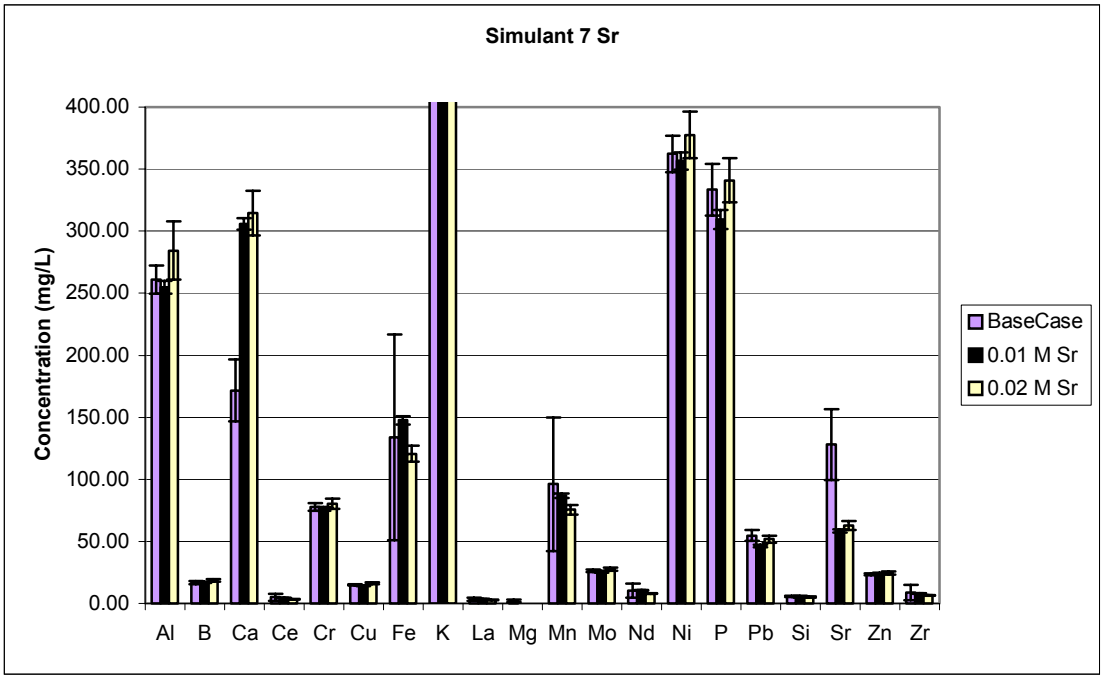

Figure C.22a Cation Concentrations in AN-107 Simulant 7 Base Case, 0.01M Sr, and 0.025M Sr Filtrates

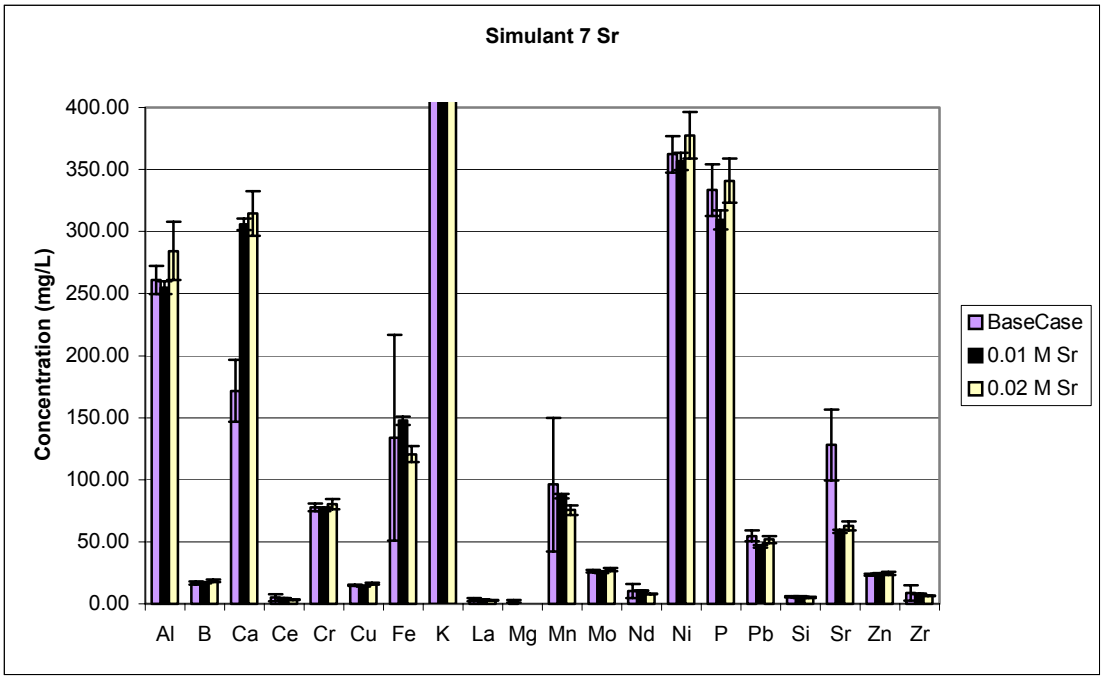

Figure C.22b Cation Concentrations in AN-107 Simulant 7 Base Case, 0.01M Sr, and 0.025M Sr Filtrates

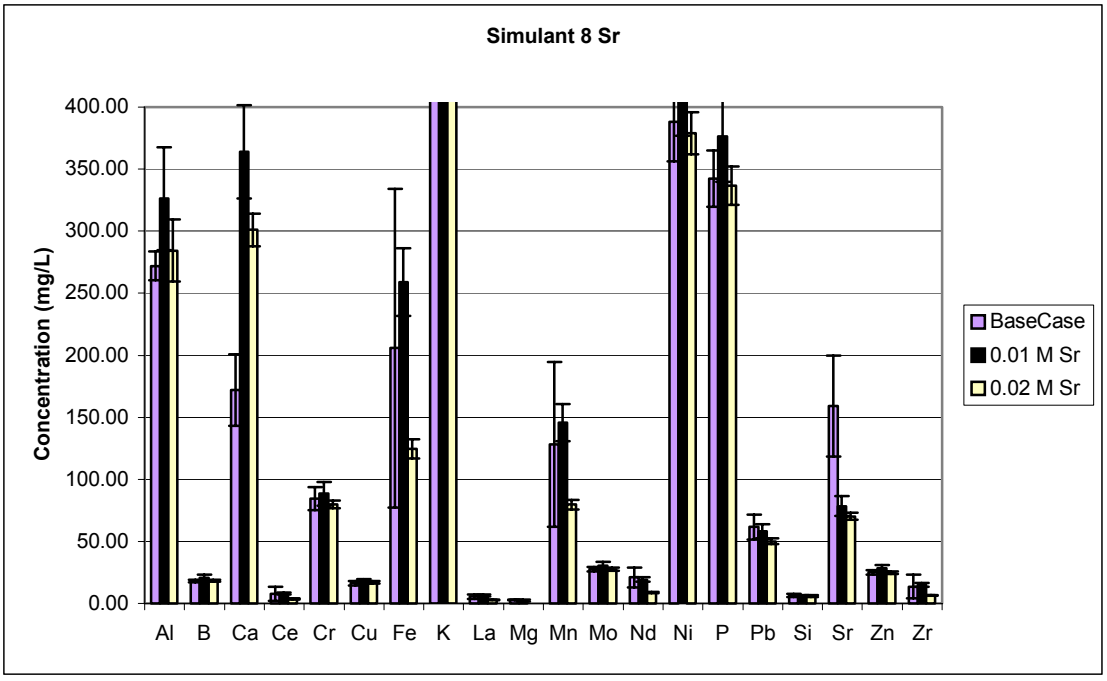

Figure C.23a Cation Concentrations in AN-107 Simulant 8 Base Case, 0.01M Sr, and 0.025M Sr Filtrates

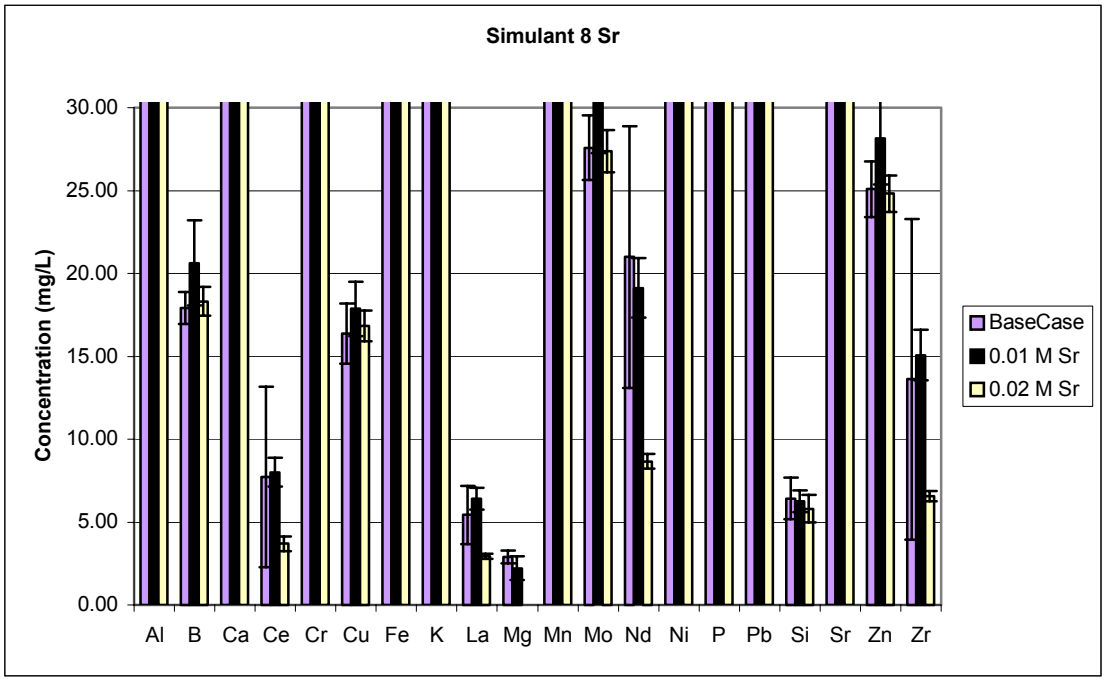

Figure C.23b Cation Concentrations in AN-107 Simulant 8 Base Case, 0.01M Sr, and 0.025M Sr Filtrates

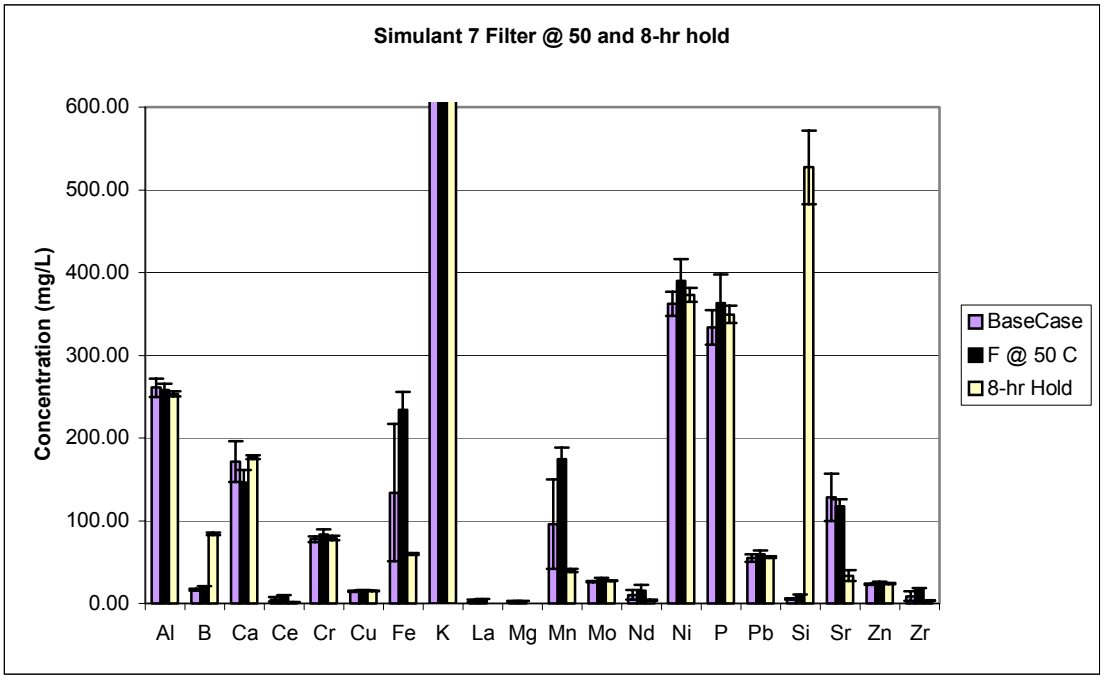

Figure C.24a Cation Concentrations in AN-107 Simulant 7 Base Case, Filter at 50 ^{o}C, and 8-hr Hold Filtrates

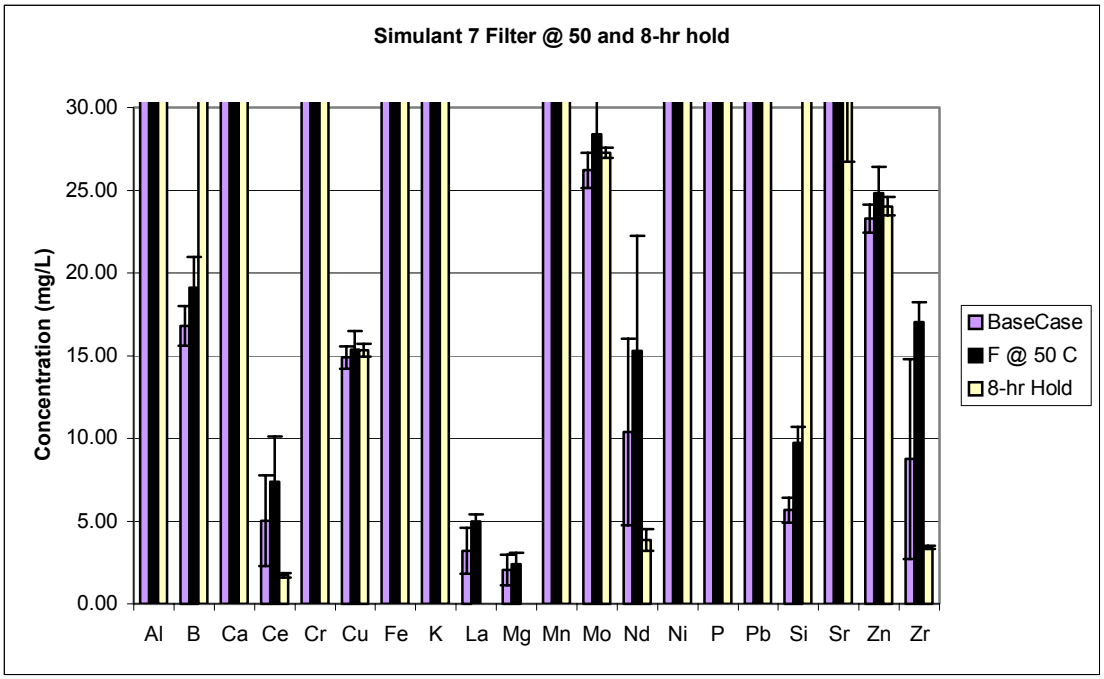

Figure C.24b Cation Concentrations in AN-107 Simulant 7 Base Case, Filter at 50 ^{o}C, and 8-hr Hold Filtrates

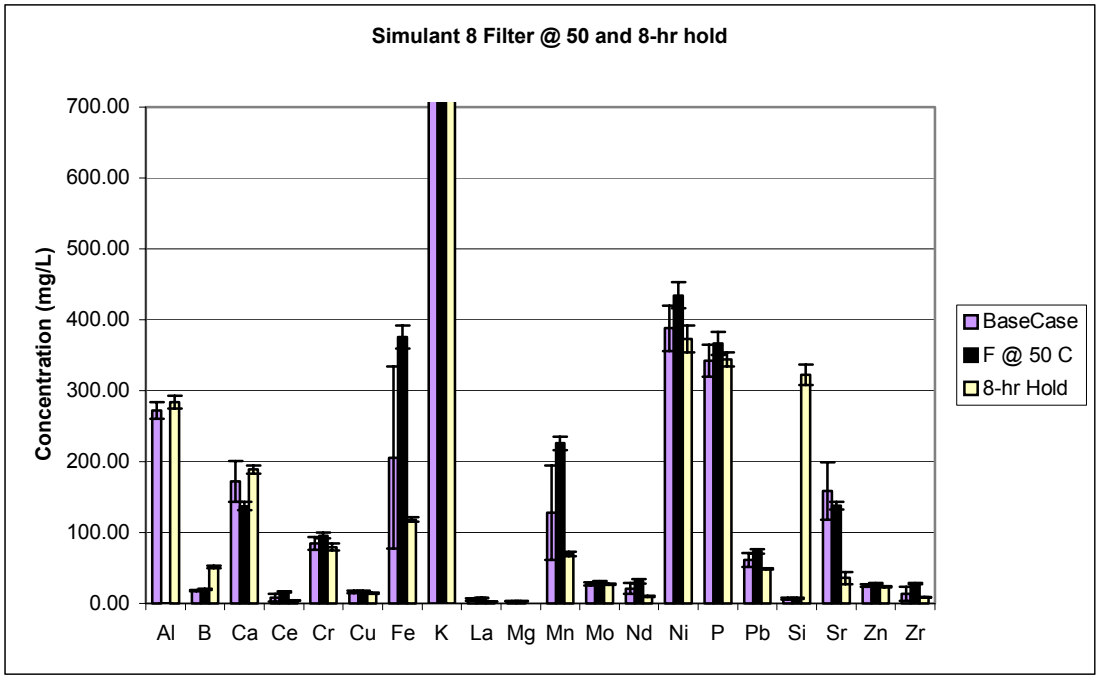

Figure C.25a Cation Concentrations in AN-107 Simulant 8 Base Case, Filter at 50 ^{o}C, and 8-hr Hold Filtrates

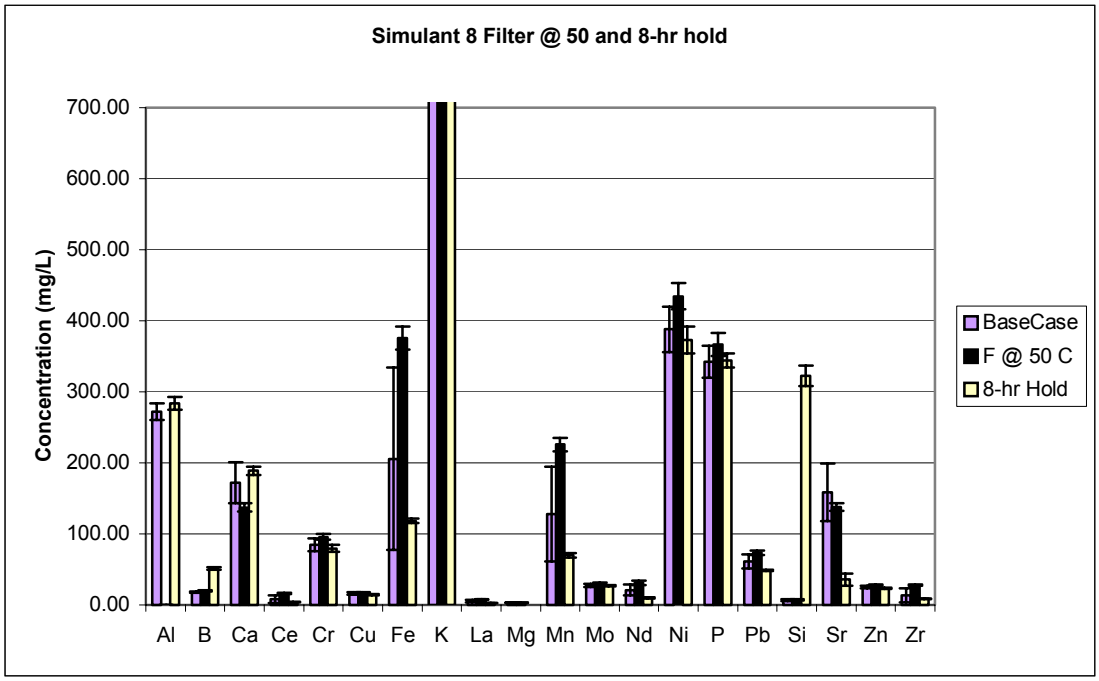

Figure C.25b Cation Concentrations in AN-107 Simulant 8 Base Case, Filter at 50 ^{o}C, and 8-hr Hold Filtrates

Table C.1 ICP-AES Data for AN-107 Primary Effects Samples (Base Case Samples)

	0315-211A-0	0315-211A-6	0315-211A-12	0315-211A-24	0315-211A-48	**average**	**stddev**
	(ppm)	(ppm)	(ppm)	(ppm)	(ppm)		
Al3082	242.31	249.55	250.99	257.72	265.48	253.21	8.78
B_2497	17.27	17.56	17.14	17.94	18.95	17.77	0.73
Ca3179	149.35	152.35	149.06	151.41	154.11	151.26	2.11
Ce4186	8.68	8.91	7.69	9.07	9.20	8.71	0.60
Cr3578	81.82	81.50	79.53	78.70	77.56	79.82	1.82
Cu3247	14.57	14.61	14.00	13.97	14.30	14.29	0.30
Fe2599	242.17	234.99	237.02	246.84	252.60	242.73	7.20
K_7664	1558.79	1632.58	1659.63	1662.86	1726.37	1648.05	60.61
La3949	5.19	5.16	4.49	5.17	5.20	5.04	0.31
Mg2790	2.60	3.01	1.89	2.65	3.64	2.76	0.64
Mn2576	163.85	168.05	166.82	169.40	172.93	168.21	3.34
Mo2020	26.34	27.01	27.11	27.27	27.66	27.08	0.48
Nd4061	18.06	18.51	14.59	19.02	19.54	17.94	1.95
Ni2316	375.14	379.85	371.62	371.62	371.03	373.85	3.73
P_1774	324.87	336.92	345.16	355.74	366.91	345.92	16.29
Pb2203	57.39	59.36	60.33	61.42	62.68	60.23	2.02
Si2516	5.54	6.06	5.29	5.69	7.35	5.99	0.81
Sr3464	164.58	168.08	165.35	167.11	169.26	166.87	1.92
Zn2062	23.98	23.89	23.25	23.43	23.78	23.66	0.31
Zr3391	16.99	17.23	16.77	16.71	16.90	16.92	0.20

	0315-211B-0	0315-211B-6	0315-211B-12	0315-211B-24	0315-211B-48	average	stddev
	(ppm)	(ppm)	(ppm)	(ppm)	(ppm)		
Al3082	263.22	267.54	268.92	268.42	275.15	268.65	4.28
B_2497	16.21	17.00	17.45	17.67	17.74	17.22	0.63
Ca3179	192.83	193.69	192.60	193.48	196.51	193.82	1.57
Ce4186	5.54	5.72	6.04	5.64	5.72	5.73	0.19
Cr3578	78.59	75.59	72.82	72.82	73.74	74.71	2.44
Cu3247	15.17	14.70	14.24	13.94	14.68	14.55	0.47
Fe2599	168.49	169.79	173.61	175.99	178.25	173.22	4.10
K_7664	1580.84	1594.66	1574.96	1549.97	1604.06	1580.90	20.72
La3949	3.74	3.79	3.78	3.75	3.84	3.78	0.04
Mg2790	-	-	-	-	-		
Mn2576	113.51	114.48	114.07	114.66	115.95	114.54	0.91
Mo2020	26.50	26.58	26.28	26.30	26.64	26.46	0.16
Nd4061	12.95	13.39	14.34	13.62	13.58	13.58	0.50
Ni2316	375.14	365.44	358.09	358.68	363.38	364.15	6.89
P_1774	324.87	339.28	345.45	348.68	352.80	342.22	10.88
Pb2203	52.74	53.83	54.33	54.80	54.77	54.10	0.85
Si2516	5.80	5.38	5.74	6.70	7.54	6.23	0.88
Sr3464	148.26	147.00	145.59	146.56	147.91	147.06	1.07
Zn2062	24.62	23.19	22.82	23.24	23.25	23.42	0.69
Zr3391	10.89	10.55	10.38	10.31	10.55	10.54	0.23

Table C.2 ICP-AES Data for AN-107 Primary Effects Samples (Base Case Samples)

	0412-211A-0	0412-211A-6	0412-211A-12	0412-211A-24	0412-211A-48	average	stddev
Element	(ppm)	(ppm)	(ppm)	(ppm)	(ppm)		
Al3082	261.49	257.11	285.20	258.89	244.93	261.52	14.68
B_2497	17.06	16.76	18.77	16.85	15.88	17.06	1.06
Ca3179	206.82	204.43	226.74	177.42	195.82	202.25	17.91
Ce4186	3.67	3.44	4.00	3.23	3.34	3.54	0.31
Cr3578	74.69	73.79	82.11	72.62	71.92	75.03	4.10
Cu3247	14.37	14.70	15.86	15.01	14.13	14.81	0.67
Fe2599	106.08	102.90	116.30	105.03	100.13	106.09	6.15
K_7664	1523.07	1502.63	1685.13	1487.16	1464.67	1532.53	87.94
La3949	2.81	2.69	3.00	2.16	2.61	2.65	0.31
Mg2790	0.56	1.68	1.95	1.24	1.25	1.34	0.53
Mn2576	72.82	71.54	79.69	71.39	68.30	72.75	4.22
Mo2020	25.90	25.68	28.49	25.54	24.67	26.06	1.44
Nd4061	6.88	6.69	7.45	6.41	8.01	7.09	0.64
Ni2316	360.04	357.12	395.66	355.07	344.27	362.43	19.51
P_1774	308.64	306.02	339.01	305.14	294.34	310.63	16.78
Pb2203	52.18	51.95	57.41	51.65	49.76	52.59	2.86
Si2516	4.87	4.57	5.73	5.48	6.03	5.34	0.60
Sr3464	108.89	107.19	120.01	103.69	103.19	108.59	6.81
Zn2062	23.23	23.06	25.48	22.86	22.20	23.36	1.24
Zr3391	5.70	5.59	6.30	5.65	5.44	5.74	0.33

	0325-211B-0	0325-211B-6	0325-211B-12	0325-211B-24	0325-211B-48	average	stddev
	(ppm)	(ppm)	(ppm)	(ppm)	(ppm)		
Al3082	283.33	292.90		282.58		286.27	5.76
B_2497	18.50	18.48	19.38	18.17	19.57	18.82	0.62
Ca3179	128.21	130.67	136.85	127.72	144.86	133.66	7.24
Ce4186	14.28	14.24	15.59	14.02	16.39	14.91	1.04
Cr3578	88.33	89.52	98.14	89.47	103.56	93.80	6.73
Cu3247	17.15	17.66	18.83	17.39	20.32	18.27	1.32
Fe2599	359.31	363.95	380.48	353.22	397.59	370.91	18.02
K_7664	1726.37	1735.36	1895.73	1712.45	1993.75	1812.73	125.66
La3949	6.78	6.80	7.34	6.70	7.73	7.07	0.45
Mg2790	2.64	2.45	3.16	2.79	3.39	2.88	0.38
Mn2576	203.52	207.67	218.34	202.36	229.65	212.31	11.56
Mo2020	28.41	28.73	30.65	28.16	32.36	29.66	1.80
Nd4061	27.52	27.16	29.61	26.97	30.77	28.41	1.69
Ni2316	403.97	409.19	435.87	406.29	463.71	423.81	25.75
P_1774	346.84	350.03	374.68	342.78	393.24	361.51	21.67
Pb2203	71.78	72.50	76.79	71.51	80.74	74.66	4.01
Si2516	5.15	4.84	4.75	5.45	6.73	5.38	0.80
Sr3464	202.25	205.12	216.80	201.70	229.30	211.03	11.90
Zn2062	24.92	25.07	26.71	24.95	28.26	25.98	1.48
Zr3391	24.91	25.29	27.22	25.00	28.74	26.23	1.69

Table C.3 ICP-AES Data for AN-107 Primary Effects Samples (Base Case Samples)

	0412-211A-0	0412-211A-6	0412-211A-12	0412-211A-24	0412-211A-48	average	stddev
Element	(ppm)	(ppm)	(ppm)	(ppm)	(ppm)		
Al3082	261.49	257.11	285.20	258.89	244.93	261.52	14.68
B_2497	17.06	16.76	18.77	16.85	15.88	17.06	1.06
Ca3179	206.82	204.43	226.74	177.42	195.82	202.25	17.91
Ce4186	3.67	3.44	4.00	3.23	3.34	3.54	0.31
Cr3578	74.69	73.79	82.11	72.62	71.92	75.03	4.10
Cu3247	14.37	14.70	15.86	15.01	14.13	14.81	0.67
Fe2599	106.08	102.90	116.30	105.03	100.13	106.09	6.15
K_7664	1523.07	1502.63	1685.13	1487.16	1464.67	1532.53	87.94
La3949	2.81	2.69	3.00	2.16	2.61	2.65	0.31
Mg2790	0.56	1.68	1.95	1.24	1.25	1.34	0.53
Mn2576	72.82	71.54	79.69	71.39	68.30	72.75	4.22
Mo2020	25.90	25.68	28.49	25.54	24.67	26.06	1.44
Nd4061	6.88	6.69	7.45	6.41	8.01	7.09	0.64
Ni2316	360.04	357.12	395.66	355.07	344.27	362.43	19.51
P_1774	308.64	306.02	339.01	305.14	294.34	310.63	16.78
Pb2203	52.18	51.95	57.41	51.65	49.76	52.59	2.86
Si2516	4.87	4.57	5.73	5.48	6.03	5.34	0.60
Sr3464	108.89	107.19	120.01	103.69	103.19	108.59	6.81
Zn2062	23.23	23.06	25.48	22.86	22.20	23.36	1.24
Zr3391	5.70	5.59	6.30	5.65	5.44	5.74	0.33

	0516-211B-0	0516-211B-6	0516-211B-12	0516-211B-24	0516-211B-48	AVG	SD
	(ppm)	(ppm)	(ppm)	(ppm)	(ppm)		
Al3082	264.89	264.00	261.93	289.67	254.18	266.93	13.39
B_2497	17.83	17.74	17.39	18.94	16.52	17.68	0.87
Ca3179	185.50	187.28	184.26	205.45	181.21	188.74	9.60
Ce4186	2.54	2.40	2.46	3.14	2.13	2.53	0.37
Cr3578	84.00	84.18	83.53	92.68	81.43	85.17	4.34
Cu3247	16.14	16.22	15.79	17.83	15.47	16.29	0.91
Fe2599	71.87	72.46	71.99	79.51	69.35	73.04	3.81
K_7664	1611.13	1632.44	1613.50	1748.18	1524.99	1626.05	79.92
La3949	-	-	-	-	-		
Mg2790	-	-	-	-	-		
Mn2576	56.57	56.57	57.31	62.19	54.05	57.34	2.98
Mo2020	26.32	26.14	26.08	29.04	25.49	26.62	1.39
Nd4061	-	-	-	-	-		
Ni2316	370.59	371.78	368.52	410.26	359.94	376.22	19.59
P_1774	320.86	317.90	317.61	351.06	308.14	323.11	16.34
Pb2203	55.38	55.26	55.03	61.09	53.87	56.13	2.84
Si2516	6.52	7.20	7.40	8.85	8.19	7.64	0.91
Sr3464	116.92	117.25	116.98	129.41	113.10	118.73	6.21
Zn2062	25.04	26.61	25.11	27.94	24.51	25.84	1.41
Zr3391	4.01	4.00	4.00	4.42	3.90	4.06	0.20

Table C.4 ICP-AES Data for AN-107 Primary Effects Samples (0.45 μm Filter Samples)

	0315-221A-0	0315-221A-6	0315-221A-12	0315-221A-24	0315-221A-48	average	stddev
	(ppm)	(ppm)	(ppm)	(ppm)	(ppm)		
Al3082	260.01	258.84	262.69	263.16	268.83	262.71	3.87
B_2497	17.05	15.98	17.25	19.40	17.80	17.50	1.25
Ca3179	181.07	119.81	177.28	195.04	181.69	170.98	29.39
Ce4186	2.34	-	2.14	2.99	2.47	2.48	0.36
Cr3578	80.56	76.26	75.35	85.02	76.20	78.68	4.09
Cu3247	15.61	14.67	14.62	16.24	14.90	15.21	0.70
Fe2599	67.27	70.35	69.53	78.97	71.62	71.55	4.44
K_7664	1572.61	1535.86	1530.56	1756.94	1584.95	1596.18	92.83
La3949	1.81	-	1.81	1.98	1.67	1.81	0.13
Mg2790	1.15	1.59	0.64	1.74	1.06	1.24	0.44
Mn2576	57.89	56.48	57.33	63.62	57.80	58.62	2.85
Mo2020	26.52	25.77	26.10	29.46	26.83	26.94	1.47
Nd4061	4.28	-	5.37	5.52	4.42	4.90	0.64
Ni2316	375.14	356.03	357.21	397.49	364.56	370.09	17.10
P_1774	324.28	323.99	332.81	382.79	348.10	342.39	24.61
Pb2203	54.83	54.33	55.24	62.30	57.12	56.77	3.27
Si2516	9.28	5.05	5.20	5.54	7.03	6.42	1.78
Sr3464	135.62	128.33	131.68	145.53	134.74	135.18	6.45
Zn2062	24.88	23.45	23.60	26.20	24.18	24.46	1.12
Zr3391	3.54	3.36	3.37	3.83	3.40	3.50	0.20

	0315-221B-0	0315-221B-6	0315-221B-12	0315-221B-24	0315-221B-48	average	stddev
	(ppm)	(ppm)	(ppm)	(ppm)	(ppm)		
Al3082	269.03	284.37	295.50	273.21	273.44	279.11	10.78
B_2497	17.25	18.10	18.86	17.78	17.43	17.88	0.63
Ca3179	197.46	204.86	208.32	195.18	197.67	200.70	5.60
Ce4186	4.55	4.56	4.90	4.52	4.37	4.58	0.20
Cr3578	81.70	84.15	83.24	78.23	84.18	82.30	2.49
Cu3247	15.09	15.13	15.27	14.21	14.70	14.88	0.43
Fe2599	125.80	135.27	142.79	132.22	126.13	132.44	7.06
K_7664	1581.53	1672.99	1725.98	1598.10	1590.70	1633.86	63.04
La3949	3.24	3.11	3.52	3.21	3.09	3.23	0.17
Mg2790	-	-	-	-	-		
Mn2576	96.50	101.82	103.75	96.94	96.76	99.15	3.39
Mo2020	26.52	28.03	28.77	27.03	26.94	27.46	0.92
Nd4061	10.44	8.68	11.30	11.75	10.56	10.55	1.17
Ni2316	375.92	385.69	387.46	366.74	383.02	379.77	8.50
P_1774	330.63	358.46	377.99	352.54	329.45	349.81	20.36
Pb2203	49.49	53.01	55.09	51.15	50.02	51.75	2.30
Si2516	5.42	5.36	5.96	6.20	7.89	6.17	1.03
Sr3464	136.19	141.81	143.47	134.32	137.58	138.68	3.85
Zn2062	23.39	24.01	24.39	23.54	22.93	23.65	0.56
Zr3391	8.47	8.84	8.80	8.30	8.73	8.63	0.23

Table C.5 ICP-AES Data for AN-107 Primary Effects Samples (Light Samples)

	0315-111A-0	0315-111A-6	0315-111A-12	0315-111A-24	0315-111A-48	average	stddev
	(ppm)	(ppm)	(ppm)	(ppm)	(ppm)		
Al3082	245.05	247.58	249.64	258.13	288.71	257.82	17.95
B_2497	16.58	16.77	17.14	18.14	27.61	19.25	4.71
Ca3179	149.00	147.32	148.91	151.38	222.03	163.73	32.62
Ce4186	8.79	8.40	8.51	9.04	12.98	9.54	1.94
Cr3578	82.08	78.50	77.59	79.73	115.22	86.62	16.07
Cu3247	14.65	14.01	13.74	14.32	20.99	15.54	3.06
Fe2599	228.47	233.55	237.38	243.40	356.03	259.77	54.09
K_7664	1635.23	1591.13	1588.48	1659.34	2436.97	1782.23	367.24
La3949	5.22	4.82	5.10	5.07	7.49	5.54	1.10
Mg2790	3.45	3.00	3.04	2.49	2.64	2.93	0.37
Mn2576	165.46	164.14	166.14	166.61	243.43	181.16	34.83
Mo2020	26.92	26.78	26.65	27.72	39.72	29.56	5.70
Nd4061	18.75	17.69	18.06	19.60	26.23	20.07	3.52
Ni2316	378.38	366.32	365.44	374.56	536.84	404.31	74.29
P_1774	328.69	338.39	343.39	361.03	523.91	379.08	81.81
Pb2203	58.07	59.92	60.12	61.92	88.70	65.74	12.90
Si2516	4.50	4.76	5.03	5.57	10.48	6.07	2.50
Sr3464	165.49	162.96	164.11	166.02	241.67	180.05	34.47
Zn2062	23.40	22.91	23.04	23.41	34.31	25.41	4.98
Zr3391	17.20	16.63	16.52	16.66	24.26	18.25	3.37

	0315-111B-0	0315-111B-6	0315-111B-12	0315-111B-24	0315-111B-48	average	stddev
	(ppm)	(ppm)	(ppm)	(ppm)	(ppm)		
Al3082	269.45	272.39	259.57	259.19	273.39	266.80	6.93
B_2497	17.47	18.24	16.68	19.11	17.29	17.76	0.94
Ca3179	197.33	197.51	189.57	207.45	196.74	197.72	6.37
Ce4186	6.07	5.66	5.64	6.40	5.58	5.87	0.35
Cr3578	76.88	75.91	71.41	80.12	80.29	76.92	3.64
Cu3247	15.09	14.78	13.66	15.44	15.40	14.87	0.73
Fe2599	170.08	174.34	169.87	183.22	168.99	173.30	5.92
K_7664	1596.13	1621.70	1508.81	1707.85	1624.94	1611.88	71.32
La3949	3.88	3.81	3.67	3.97	3.78	3.82	0.11
Mg2790	1.43	1.84	1.69	1.32	1.79	1.61	0.23
Mn2576	115.51	116.07	113.81	122.30	115.60	116.66	3.27
Mo2020	26.53	26.72	25.62	28.57	27.17	26.92	1.08
Nd4061	12.73	13.30	12.30	14.13	13.47	13.19	0.70
Ni2316	373.09	366.91	350.45	391.02	385.43	373.38	16.00
P_1774	333.10	345.16	334.57	371.62	330.46	342.98	16.95
Pb2203	53.63	54.86	53.10	58.27	54.39	54.85	2.03
Si2516	5.00	5.41	5.52	6.66	7.39	6.00	0.99
Sr3464	149.47	149.38	143.06	157.20	151.12	150.05	5.05
Zn2062	23.72	23.40	22.44	25.59	23.11	23.65	1.18
Zr3391	10.80	10.72	10.11	11.35	11.20	10.84	0.48

Table C.6 ICP-AES Data for AN-107 Primary Effects Samples (8-hr Hold Samples)

	0315-215A-0	0315-215A-6	0315-215A-12	0315-215A-24	0315-215A-48	average	stddev
	(ppm)	(ppm)	(ppm)	(ppm)	(ppm)		
Al3082	249.13	256.67	252.26	253.90	255.21	253.43	2.90
B_2497	81.83	85.08	83.65	84.19	85.79	84.11	1.52
Ca3179	175.28	179.75	174.78	174.99	179.22	176.80	2.46
Ce4186	1.77	1.78	1.59	1.60	1.87	1.72	0.12
Cr3578	83.08	80.70	75.63	77.45	78.28	79.03	2.91
Cu3247	15.86	15.31	14.81	15.17	15.44	15.32	0.38
Fe2599	57.34	60.40	59.75	61.09	60.32	59.78	1.45
K_7664	1658.37	1662.24	1596.39	1627.97	1628.27	1634.65	26.80
La3949	-	-	-	-	-		
Mg2790	-	-	-	-	-		
Mn2576	40.80	41.57	40.20	39.04	36.86	39.69	1.83
Mo2020	27.37	27.42	26.85	27.09	27.63	27.27	0.30
Nd4061	3.11	3.78	3.54	4.01	4.85	3.86	0.65
Ni2316	385.61	377.27	365.35	365.35	372.50	373.22	8.58
P_1774	333.46	347.17	349.55	353.43	362.67	349.26	10.62
Pb2203	54.62	56.29	55.82	55.76	57.07	55.91	0.89
Si2516	560.84	567.99	548.32	487.83	470.84	527.16	44.63
Sr3464	28.37	29.39	30.43	34.33	44.91	33.48	6.77
Zn2062	24.47	24.70	23.56	23.40	23.99	24.02	0.56
Zr3391	3.55	3.44	3.32	3.35	3.43	3.42	0.09

	0315-215B-0	0315-215B-6	0315-215B-12	0315-215B-24	0315-215B-48	average	stddev
	(ppm)	(ppm)	(ppm)	(ppm)	(ppm)		
Al3082	283.72	288.33	268.24	289.67	290.20	284.03	9.19
B_2497	49.85	51.56	48.81	53.40	51.86	51.10	1.79
Ca3179	190.51	188.94	178.61	191.39	194.62	188.81	6.07
Ce4186	4.26	4.19	3.37	4.04	3.94	3.96	0.35
Cr3578	83.06	78.59	72.64	77.97	86.08	79.67	5.15
Cu3247	15.29	14.54	13.04	14.35	14.89	14.42	0.85
Fe2599	118.90	120.53	113.93	122.13	116.24	118.35	3.29
K_7664	1638.66	1638.66	1498.94	1609.35	1652.57	1607.64	62.77
La3949	2.42	2.44	2.30	2.52	2.41	2.42	0.08
Mg2790	-	-	-	-	-		
Mn2576	74.62	70.83	66.63	69.97	68.08	70.03	3.05
Mo2020	27.28	27.16	25.36	27.10	27.88	26.96	0.94
Nd4061	9.04	10.91	8.99	9.93	11.13	10.00	1.01
Ni2316	381.84	370.00	345.73	368.52	397.53	372.72	19.05
P_1774	340.70	353.13	330.93	355.50	339.81	344.01	10.18
Pb2203	48.96	49.28	47.00	49.91	49.28	48.89	1.11
Si2516	315.54	330.34	301.33	327.67	337.44	322.46	14.21
Sr3464	30.96	31.44	29.63	36.59	50.02	35.73	8.42
Zn2062	23.50	23.07	22.03	23.90	23.62	23.22	0.73
Zr3391	8.87	8.68	7.95	8.58	9.18	8.65	0.45

Table C.7 ICP-AES Data for AN-107 Primary Effects Samples (0.0 M OH^- Samples)

	0325-211A-0MOH-0	0325-211A-0MOH-6	0325-211A-0MOH-12	0325-211A-0MOH-24	0325-211A-0MOH-48	average	stddev
	(ppm)	(ppm)	(ppm)	(ppm)	(ppm)		
Al3082	37.26	34.25	40.66	40.66	34.72	37.51	3.10
B_2497	20.29	19.42	22.07	21.45	19.18	20.48	1.26
Ca3179	19.17	17.11	20.39	22.68	18.03	19.48	2.17
Ce4186	3.66	3.88	4.73	4.49	3.76	4.10	0.47
Cr3578	92.89	87.24	103.49	97.63	88.20	93.89	6.78
Cu3247	25.59	24.28	28.80	26.99	24.39	26.01	1.90
Fe2599	193.86	181.96	212.98	200.43	180.70	193.99	13.45
K_7664	2093.09	1814.43	2146.52	2008.97	1806.21	1973.84	157.15
La3949	-	-	-	-	-		
Mg2790	-	-	-	-	-		
Mn2576	692.12	649.38	765.01	716.78	655.96	695.85	47.40
Mo2020	31.78	29.98	35.46	33.51	30.28	32.20	2.30
Nd4061	-	-	-	-	-		
Ni2316	460.32	429.36	509.09	482.79	438.13	463.94	32.67
P_1774	212.46	202.98	239.91	227.23	205.55	217.63	15.62
Pb2203	164.62	154.70	180.54	170.92	155.88	165.33	10.79
Si2516	1.19	0.87	1.45	2.36	0.64	1.30	0.67
Sr3464	16.14	14.67	17.19	15.92	14.54	15.69	1.10
Zn2062	36.58	34.03	39.98	38.11	34.72	36.68	2.44
Zr3391	7.11	9.15	11.66	10.88	9.09	9.58	1.77

	0325-211B-0MOH-0	0325-211B-0MOH-6	0325-211B-0MOH-12	0325-211B-0MOH-24	0325-211B-0MOH-48	average	stddev
	(ppm)	(ppm)	(ppm)	(ppm)	(ppm)		
Al3082	49.05	47.70	49.10	50.53	45.29	48.33	1.97
B_2497	19.43	19.76	20.44	20.04	18.00	19.54	0.93
Ca3179	16.13	15.33	16.28	15.97	15.18	15.78	0.49
Ce4186	3.37	3.41	3.94	3.96	3.11	3.56	0.38
Cr3578	91.27	85.57	94.48	94.20	87.65	90.63	3.95
Cu3247	25.40	24.05	26.34	25.82	23.96	25.11	1.07
Fe2599	161.52	158.84	163.96	162.48	148.84	159.13	6.05
K_7664	1853.06	1779.63	1918.82	1915.53	1760.72	1845.55	73.93
La3949	-	-	-	-	-		
Mg2790	-	-	-	-	-		
Mn2576	678.15	664.18	692.40	689.93	634.04	671.74	23.86
Mo2020	31.24	30.00	32.14	31.92	29.35	30.93	1.22
Nd4061	-	-	-	-	-		
Ni2316	452.37	432.10	465.53	463.88	428.81	448.54	17.31
P_1774	206.79	203.83	213.64	212.08	192.62	205.79	8.36
Pb2203	158.21	155.50	161.99	161.19	147.41	156.86	5.87
Si2516	-	-	-	-	-		
Sr3464	11.25	10.77	11.13	11.03	9.99	10.83	0.50
Zn2062	36.17	35.02	37.10	36.83	34.00	35.82	1.30
Zr3391	6.57	6.59	6.38	7.99	6.16	6.74	0.72

Table C.8 ICP-AES Data for AN-107 Primary Effects Samples (0.2 M OH^- Samples)

	0325-211A-0.2MOH-0	0325-211A-0.2MOH-6	0325-211A-0.2MOH-12	0325-211A-0.2MOH-24	0325-211A-0.2MOH-48	average	stddev
	(ppm)	(ppm)	(ppm)	(ppm)	(ppm)		
Al3082	-	-	-	-	-	-	-
B_2497	19.89	18.91	19.88	21.33	20.97	20.20	0.97
Ca3179	184.79	175.00	184.26	194.68	187.04	185.15	7.04
Ce4186	6.59	5.87	6.12	6.75	6.04	6.27	0.38
Cr3578	94.02	90.24	95.99	100.69	96.99	95.59	3.85
Cu3247	23.32	22.25	23.96	25.12	24.56	23.84	1.11
Fe2599	261.07	243.92	255.70	273.39	260.65	258.95	10.63
K_7664	1898.18	1799.22	1916.81	2016.89	1953.23	1916.87	79.87
La3949	2.99	2.77	3.01	3.20	2.96	2.99	0.15
Mg2790	3.29	1.58	2.85	3.41	2.65	2.76	0.73
Mn2576	279.39	262.10	275.33	291.34	279.11	277.46	10.48
Mo2020	31.94	29.94	31.80	33.25	31.89	31.76	1.18
Nd4061	9.11	9.51	9.76	9.70	10.98	9.81	0.70
Ni2316	453.70	432.57	456.20	480.94	457.87	456.25	17.17
P_1774	348.89	323.04	346.67	361.12	344.72	344.89	13.79
Pb2203	194.52	181.01	189.23	199.52	190.01	190.86	6.87
Si2516	1.06	1.24	0.86	0.91	0.88	0.99	0.16
Sr3464	64.50	60.88	63.63	67.92	64.83	64.35	2.53
Zn2062	33.80	32.03	33.42	35.70	33.92	33.77	1.31
Zr3391	21.41	20.20	21.61	22.98	14.92	20.22	3.12

	0325-211B-0.2MOH-0	0325-211B-0.2MOH-6	0325-211B-0.2MOH-12	0325-211B-0.2MOH-24	0325-211B-0.2MOH-48	average	stddev
	(ppm)	(ppm)	(ppm)	(ppm)	(ppm)		
Al3082	267.46	262.57	269.33	271.38	-	267.69	3.77
B_2497	19.38	18.43	18.82	18.72	19.85	19.04	0.57
Ca3179	168.30	164.99	167.66	168.33	175.14	168.89	3.76
Ce4186	5.12	4.96	5.17	5.14	5.33	5.14	0.13
Cr3578	87.93	88.54	88.85	91.66	92.69	89.93	2.10
Cu3247	22.18	21.93	22.32	22.90	23.60	22.58	0.67
Fe2599	187.37	183.81	186.26	184.68	194.18	187.26	4.11
K_7664	1769.75	1771.69	1781.42	1833.97	1851.48	1801.66	38.25
La3949	2.65	2.64	2.60	2.65	2.80	2.67	0.08
Mg2790	2.90	1.99	2.96	2.66	1.47	2.40	0.64
Mn2576	246.75	241.14	245.59	248.31	256.09	247.58	5.46
Mo2020	29.30	29.38	29.61	30.11	30.72	29.82	0.59
Nd4061	8.74	8.97	9.13	8.65	8.73	8.84	0.20
Ni2316	424.51	426.45	428.68	434.24	442.02	431.18	7.07
P_1774	322.76	318.59	326.09	327.48	338.88	326.76	7.59
Pb2203	173.03	171.78	174.03	174.50	179.20	174.51	2.82
Si2516	-	-	-	-	-		
Sr3464	63.50	63.50	64.22	65.30	66.69	64.64	1.36
Zn2062	31.41	31.39	31.55	31.64	32.36	31.67	0.40
Zr3391	16.99	16.96	16.99	16.88	17.81	17.13	0.38

Table C.9 ICP-AES Data for AN-107 Primary Effects Samples (Filter @ 50 °C Samples)

	0315-231A-0	0315-231A-6	0315-231A-12	0315-231A-24	0315-231A-48	average	stddev
	(ppm)	(ppm)	(ppm)	(ppm)	(ppm)		
Al3082	248.55	255.25	261.48	267.39	258.54	258.24	7.02
B_2497	17.51	18.31	19.07	22.24	18.41	19.11	1.84
Ca3179	143.97	126.80	145.62	169.14	144.94	146.09	15.08
Ce4186	8.24	2.62	8.21	9.83	7.96	7.37	2.76
Cr3578	83.94	81.20	79.62	93.43	79.67	83.57	5.78
Cu3247	15.28	14.84	14.64	17.30	14.79	15.37	1.11
Fe2599	215.88	222.21	233.88	270.54	228.11	234.12	21.43
K_7664	1626.41	1622.00	1649.93	1922.76	1639.34	1692.09	129.42
La3949	4.72	-	4.86	5.62	4.79	5.00	0.42
Mg2790	3.34	1.96	2.11	1.80	2.86	2.41	0.66
Mn2576	167.23	168.81	170.43	199.10	168.81	174.88	13.59
Mo2020	27.12	27.29	27.50	32.28	27.64	28.37	2.20
Nd4061	17.04	3.06	17.71	20.48	18.16	15.29	6.96
Ni2316	383.96	380.14	374.56	436.30	375.44	390.08	26.11
P_1774	330.75	344.86	357.80	420.71	360.74	362.97	34.40
Pb2203	55.48	57.18	58.45	67.91	57.92	59.39	4.90
Si2516	9.05	8.78	9.25	10.64	10.87	9.72	0.96
Sr3464	113.95	112.37	114.19	132.74	113.48	117.35	8.63
Zn2062	24.03	24.26	24.12	27.64	24.06	24.82	1.58
Zr3391	16.73	16.60	16.33	19.13	16.37	17.03	1.19

	0325-231B-0	0325-231B-6	0325-231B-12	0325-231B-24	0325-231B-48	average	stddev
	(ppm)	(ppm)	(ppm)	(ppm)	(ppm)		
Al3082	-	-	-	-	-	-	-
B_2497	19.42	18.98	21.42	19.53	19.81	19.83	0.93
Ca3179	135.75	133.27	147.02	134.14	136.63	137.36	5.56
Ce4186	14.70	15.90	17.14	15.61	15.95	15.86	0.88
Cr3578	96.13	91.57	102.99	94.02	94.58	95.86	4.31
Cu3247	16.74	16.22	18.17	16.78	17.01	16.99	0.72
Fe2599	374.34	365.29	403.54	369.09	366.46	375.75	15.93
K_7664	1900.63	1823.25	2023.85	1832.59	1815.36	1879.14	87.69
La3949	7.38	7.92	8.68	7.95	7.98	7.98	0.46
Mg2790	3.66	2.65	2.88	2.84	2.65	2.94	0.42
Mn2576	224.72	219.47	242.33	219.91	222.47	225.78	9.49
Mo2020	30.72	29.81	32.94	29.73	29.93	30.62	1.35
Nd4061	26.12	32.15	34.40	31.83	31.59	31.22	3.06
Ni2316	433.33	420.77	466.03	422.52	429.53	434.44	18.39
P_1774	367.04	357.70	394.78	354.49	358.87	366.58	16.43
Pb2203	74.34	72.33	78.55	71.42	71.60	73.65	2.97
Si2516	6.57	6.38	7.52	7.55	9.01	7.41	1.05
Sr3464	137.56	133.91	147.26	134.29	136.22	137.85	5.46
Zn2062	28.05	27.05	30.11	26.98	27.53	27.94	1.28
Zr3391	28.06	27.06	30.08	27.56	27.84	28.12	1.16

Table C.10 ICP-AES Data for AN-107 Primary Effects Samples (25 °C Rxn Samples)

	0417-211-25A-0	0417-211-25A-6	0417-211-25A-12	0417-211-25A-24	0417-211-25A-48	**average**	**stddev**
Element	(ppm)	(ppm)	(ppm)	(ppm)	(ppm)		
Al3082	242.08	230.03	244.28	240.82	234.73	238.39	5.87
B_2497	14.64	13.87	15.25	14.68	14.36	14.56	0.50
Ca3179	209.62	205.21	218.06	213.74	206.80	210.69	5.24
Ce4186	2.66	2.57	2.65	2.21	2.59	2.54	0.19
Cr3578	74.73	71.21	73.82	72.27	70.74	72.55	1.70
Cu3247	15.00	14.08	14.91	14.57	14.23	14.56	0.41
Fe2599	88.29	81.29	87.14	85.61	83.08	85.08	2.88
K_7664	1474.12	1375.04	1415.02	1412.38	1402.09	1415.73	36.27
La3949	1.43	1.36	1.42	1.38	1.33	1.38	0.04
Mg2790	-	-	-	-	-		
Mn2576	38.87	37.22	39.28	38.66	37.51	38.31	0.89
Mo2020	24.73	23.65	24.60	24.45	23.74	24.23	0.50
Nd4061	4.52	4.20	4.29	4.62	4.42	4.41	0.17
Ni2316	345.74	330.75	347.51	340.45	332.81	339.45	7.51
P_1774	295.18	279.36	292.59	291.03	278.12	287.26	7.92
Pb2203	67.30	64.50	68.18	67.18	64.83	66.40	1.63
Si2516	-	-	-	-	-		
Sr3464	231.70	222.47	234.52	228.82	222.73	228.05	5.37
Zn2062	22.47	21.54	22.76	22.36	21.77	22.18	0.50
Zr3391	6.44	6.09	6.44	6.32	6.13	6.29	0.17

	0417-211-25B-0	0417-211-25B-6	0417-211-25B-12	0417-211-25B-24	0417-211-25B-48	**average**	**stddev**
Element	(ppm)	(ppm)	(ppm)	(ppm)	(ppm)		
Al3082	245.99	252.69	277.71	258.69	256.90	258.40	11.85
B_2497	15.56	15.52	17.82	15.72	16.20	16.17	0.96
Ca3179	212.21	213.65	228.88	219.65	217.74	218.42	6.57
Ce4186	3.24	3.19	3.25	3.68	3.77	3.42	0.28
Cr3578	73.26	75.56	80.44	75.44	73.35	75.61	2.91
Cu3247	15.35	15.84	17.25	15.96	15.66	16.01	0.73
Fe2599	97.58	98.55	110.57	103.52	101.61	102.36	5.17
K_7664	1460.30	1533.21	1641.40	1531.45	1480.58	1529.39	70.22
La3949	1.75	1.65	1.84	1.77	1.71	1.74	0.07
Mg2790	-	-	-	-	-		
Mn2576	41.60	42.34	46.28	43.51	42.92	43.33	1.79
Mo2020	25.00	25.51	27.55	25.92	25.53	25.90	0.98
Nd4061	5.45	5.45	5.24	5.27	4.97	5.28	0.20
Ni2316	354.56	359.27	385.43	362.50	358.68	364.09	12.26
P_1774	299.29	301.06	332.81	314.29	310.46	311.58	13.43
Pb2203	65.53	65.91	72.38	68.00	67.24	67.81	2.74
Si2516	1.84	-	-	-	-	1.84	
Sr3464	273.39	275.45	294.88	279.12	271.04	278.78	9.48
Zn2062	22.62	22.71	24.70	23.20	22.96	23.24	0.85
Zr3391	7.53	7.67	8.24	7.79	7.64	7.78	0.28

Table C.11 ICP-AES Data for AN-107 Primary Effects Samples (15 °C Rxn Samples)

	0424-211-15A-0	0424-211-15A-6	0424-211-15A-12	0424-211-15A-24	0424-211-15A-48	**average**	**stddev**
Element	(ppm)	(ppm)	(ppm)	(ppm)	(ppm)		
Al3082	246.03	250.89	263.16	264.36	271.98	259.28	10.59
B_2497	14.92	15.66	16.43	16.41	16.88	16.06	0.77
Ca3179	253.69	246.86	266.71	247.97	274.82	258.01	12.27
Ce4186	3.43	3.51	3.83	3.25	3.83	3.57	0.26
Cr3578	74.35	74.53	77.24	77.06	76.76	75.99	1.43
Cu3247	15.99	16.73	17.45	17.69	17.81	17.13	0.76
Fe2599	175.67	175.22	182.53	183.66	192.93	182.00	7.22
K_7664	1478.08	1475.10	1554.96	1534.10	1565.39	1521.53	42.55
La3949	2.44	2.15	2.44	2.10	2.49	2.32	0.18
Mg2790	2.61	-	-	-	-	2.61	
Mn2576	55.61	56.71	58.97	58.94	60.35	58.12	1.91
Mo2020	25.09	25.17	26.21	26.14	26.64	25.85	0.69
Nd4061	8.05	7.65	9.44	7.22	8.45	8.16	0.85
Ni2316	350.45	355.81	370.41	367.43	365.05	361.83	8.38
P_1774	299.49	302.47	314.69	315.28	328.40	312.07	11.56
Pb2203	83.50	84.24	87.31	86.90	89.64	86.32	2.48
Si2516	-	-	-	-	2.09	2.09	
Sr3464	229.16	230.32	240.61	235.33	240.66	235.22	5.46
Zn2062	23.48	23.85	24.85	24.59	24.65	24.28	0.59
Zr3391	10.53	10.76	11.17	11.11	11.04	10.92	0.27

	0424-211-15B-0	0424-211-15B-6	0424-211-15B-12	0424-211-15B-24	0424-211-15B-48	**average**	**stddev**
Element	(ppm)	(ppm)	(ppm)	(ppm)	(ppm)		
Al3082	322.14	354.32	354.62	270.02	265.16	313.25	43.76
B_2497	18.12	19.95	21.81	16.49	16.93	18.66	2.21
Ca3179	286.65	316.77	327.50	258.72	256.76	289.28	32.46
Ce4186	3.98	4.51	4.88	3.60	3.59	4.11	0.57
Cr3578	86.21	94.53	97.21	75.90	77.54	86.28	9.64
Cu3247	20.61	22.27	22.98	18.33	18.60	20.56	2.10
Fe2599	201.27	221.86	231.87	183.03	178.53	203.31	23.40
K_7664	1750.45	1934.62	2014.18	1572.25	1543.34	1762.97	210.56
La3949	2.69	2.80	3.02	2.43	2.38	2.67	0.27
Mg2790	-	-	-	-	-		
Mn2576	69.34	76.62	78.91	62.70	61.86	69.89	7.79
Mo2020	29.53	32.84	33.32	26.51	26.09	29.66	3.40
Nd4061	9.04	8.24	10.79	9.15	7.86	9.02	1.13
Ni2316	408.26	452.36	459.52	365.05	368.92	410.82	44.59
P_1774	366.24	409.45	417.80	332.27	322.14	369.58	43.50
Pb2203	98.58	109.90	111.99	88.95	86.99	99.28	11.54
Si2516	-	-	-	-	-		
Sr3464	285.90	319.46	326.31	256.64	254.55	288.57	33.77
Zn2062	27.63	30.78	31.44	24.79	25.05	27.94	3.11
Zr3391	12.40	13.69	14.10	11.07	11.19	12.49	1.39

Table C.12 ICP-AES Data for AN-107 Primary Effects Samples (0.01 M Added Sr Samples)

	0412-211-Sr1A-0	0412-211-Sr1A-6	0412-211-Sr1A-12	0412-211-Sr1A-24	0412-211-Sr1A-48	**average**	**stddev**
Element	(ppm)	(ppm)	(ppm)	(ppm)	(ppm)		
Al3082	261.32	255.75	256.84	247.49	252.87	254.86	5.12
B_2497	17.43	16.91	16.59	16.16	17.30	16.88	0.52
Ca3179	308.56	307.72	307.72	297.64	308.28	305.98	4.68
Ce4186	4.52	4.61	4.37	4.28	4.26	4.41	0.15
Cr3578	77.70	76.83	76.22	73.53	75.99	76.05	1.56
Cu3247	14.66	14.48	14.40	13.63	13.90	14.21	0.43
Fe2599	151.51	147.03	149.58	142.46	147.08	147.53	3.40
K_7664	1517.60	1527.12	1530.48	1442.00	1494.64	1502.37	36.53
La3949	3.86	3.78	3.74	3.68	3.62	3.74	0.09
Mg2790	-	-	-	-	-		
Mn2576	89.24	87.14	87.30	84.08	86.58	86.87	1.85
Mo2020	26.11	25.73	25.62	24.59	25.35	25.48	0.57
Nd4061	10.63	10.70	10.48	10.59	11.09	10.70	0.23
Ni2316	364.00	359.80	357.56	345.52	356.44	356.66	6.87
P_1774	316.96	311.92	313.04	296.80	308.00	309.34	7.70
Pb2203	47.57	46.76	46.82	44.88	46.62	46.53	0.99
Si2516	5.20	4.62	5.10	5.55	6.30	5.35	0.63
Sr3464	59.67	58.60	58.60	56.56	58.77	58.44	1.14
Zn2062	24.53	24.05	24.08	23.18	24.06	23.98	0.49
Zr3391	8.20	8.15	8.11	7.75	8.05	8.05	0.18

	0412-211-Sr1B-0	0412-211-Sr1B-6	0412-211-Sr1B-12	0412-211-Sr1B-24	0412-211-Sr1B-48	**average**	**stddev**
Element	(ppm)	(ppm)	(ppm)	(ppm)	(ppm)		
Al3082	384.16	329.00	326.48	324.24	266.87	326.15	41.51
B_2497	24.70	19.90	19.73	21.02	17.76	20.62	2.56
Ca3179	420.28	362.60	350.84	370.16	316.68	364.11	37.48
Ce4186	9.27	8.28	7.43	8.00	7.04	8.00	0.86
Cr3578	102.93	89.24	84.25	89.18	76.75	88.47	9.56
Cu3247	20.45	17.72	17.70	17.62	15.82	17.86	1.66
Fe2599	300.16	257.10	254.44	259.98	223.47	259.03	27.30
K_7664	2154.60	1821.12	1738.52	1827.84	1580.32	1824.48	209.76
La3949	7.44	6.36	6.15	6.52	5.63	6.42	0.66
Mg2790	3.19	2.28	2.15	2.30	1.15	2.22	0.72
Mn2576	167.64	144.68	142.69	147.06	125.83	145.58	14.90
Mo2020	34.86	30.38	29.43	30.38	26.44	30.30	3.02
Nd4061	22.07	19.32	17.53	18.86	17.84	19.13	1.80
Ni2316	479.92	417.48	409.92	420.28	364.00	418.32	41.29
P_1774	431.48	377.72	365.40	376.32	329.56	376.10	36.57
Pb2203	66.75	58.83	56.84	58.27	50.71	58.28	5.73
Si2516	6.79	5.50	5.99	7.08	5.97	6.26	0.65
Sr3464	90.13	77.98	75.99	79.63	67.93	78.33	7.98
Zn2062	32.28	28.06	27.62	28.39	24.47	28.16	2.78
Zr3391	17.37	14.94	14.67	15.27	13.13	15.08	1.52

Table C.13 ICP-AES Data for AN-107 Primary Effects Samples (0.02 M Added Sr Samples)

	0412-211-Sr2A-0	0412-211-Sr2A-6	0412-211-Sr2A-12	0412-211-Sr2A-24	0412-211-Sr2A-48	**average**	**stddev**
Element	(ppm)	(ppm)	(ppm)	(ppm)	(ppm)		
Al3082	325.36	271.15	279.08	269.11	276.84	284.31	23.31
B_2497	20.44	17.89	18.02	17.95	18.68	18.60	1.08
Ca3179	345.24	305.48	314.16	298.20	310.52	314.72	18.08
Ce4186	3.54	3.10	3.39	2.91	3.28	3.24	0.24
Cr3578	87.14	78.20	81.31	76.78	78.65	80.42	4.10
Cu3247	17.83	16.29	16.28	15.75	15.63	16.36	0.88
Fe2599	131.54	117.26	118.38	115.14	120.62	120.59	6.44
K_7664	1765.12	1585.08	1655.36	1582.56	1603.00	1638.22	76.75
La3949	3.02	2.76	2.87	2.69	2.67	2.80	0.15
Mg2790	-	-	-	-	-		
Mn2576	82.26	73.28	75.24	72.27	74.23	75.45	3.96
Mo2020	29.96	26.68	27.85	26.48	27.17	27.63	1.41
Nd4061	7.96	7.91	7.68	7.89	7.38	7.77	0.24
Ni2316	408.24	367.64	381.92	360.92	368.48	377.44	18.83
P_1774	370.16	326.48	341.60	327.04	339.64	340.98	17.74
Pb2203	56.08	49.62	51.88	49.95	51.16	51.74	2.60
Si2516	5.34	4.62	4.82	4.85	6.33	5.19	0.69
Sr3464	68.60	60.87	62.72	60.09	61.71	62.80	3.39
Zn2062	26.76	23.93	24.74	23.62	24.14	24.64	1.25
Zr3391	7.15	6.49	6.62	6.29	6.42	6.60	0.33

	0412-211-Sr2B-0	0412-211-Sr2B-6	0412-211-Sr2B-12	0412-211-Sr2B-24	0412-211-Sr2B-48	**average**	**stddev**
Element	(ppm)	(ppm)	(ppm)	(ppm)	(ppm)		
Al3082	257.69	265.33	314.43	277.88	305.97	284.26	24.93
B_2497	17.70	17.13	19.12	18.63	18.98	18.31	0.86
Ca3179	284.54	291.02	304.28	307.94	316.97	300.95	13.08
Ce4186	2.94	3.74	4.16	3.70	3.91	3.69	0.46
Cr3578	78.93	77.13	85.14	78.28	79.78	79.85	3.11
Cu3247	15.69	16.52	18.05	16.39	17.49	16.83	0.94
Fe2599	114.89	118.52	130.96	127.10	131.41	124.58	7.49
K_7664	1545.92	1563.13	1736.27	1594.71	1648.85	1617.78	76.96
La3949	2.77	2.80	3.13	2.94	3.04	2.94	0.15
Mg2790	-	-	-	-	-		
Mn2576	74.84	76.53	84.26	80.12	82.57	79.67	3.96
Mo2020	26.35	26.04	29.07	27.25	28.14	27.37	1.26
Nd4061	8.12	8.96	9.10	8.87	8.27	8.66	0.44
Ni2316	369.70	358.70	403.54	376.19	385.78	378.78	16.99
P_1774	321.48	321.20	354.19	336.71	349.96	336.71	15.44
Pb2203	47.88	47.43	52.85	50.34	52.17	50.13	2.44
Si2516	5.90	4.72	5.51	5.83	7.03	5.80	0.83
Sr3464	67.79	67.03	73.29	70.73	71.99	70.17	2.69
Zn2062	24.03	23.41	26.13	24.87	25.61	24.81	1.11
Zr3391	6.31	6.32	7.02	6.51	6.65	6.56	0.29

Table C.14 ICP-AES Data for AN-107 Primary Effects Samples (0.01 M Added MnO_4 Samples)

	0412-211-MnO41A-0	0412-211-MnO41A-6	0412-211-MnO41A-12	0412-211-MnO41A-24	0412-211-MnO41A-48	**average**	**stddev**
Element	(ppm)	(ppm)	(ppm)	(ppm)	(ppm)		
Al3082	262.19	336.82	265.88	324.33	262.39	290.32	37.04
B_2497	17.57	22.40	17.57	22.21	16.95	19.34	2.72
Ca3179	248.95	310.70	249.30	303.88	247.96	272.16	32.16
Ce4186	22.42	27.91	22.65	27.24	22.77	24.60	2.73
Cr3578	82.13	102.92	82.30	102.44	83.13	90.58	11.05
Cu3247	18.79	24.28	19.91	24.31	20.04	21.46	2.63
Fe2599	692.96	876.42	694.95	842.91	688.70	759.19	92.51
K_7664	1730.41	2019.52	1576.48	1958.46	1581.88	1773.35	207.44
La3949	18.34	22.50	18.32	22.36	18.38	19.98	2.24
Mg2790	3.91	6.15	4.29	4.40	4.15	4.58	0.90
Mn2576	349.60	435.66	350.74	428.27	350.46	382.95	44.83
Mo2020	26.42	32.97	26.44	32.43	26.48	28.95	3.43
Nd4061	47.37	61.80	48.76	60.09	49.08	53.42	6.93
Ni2316	368.92	458.09	370.05	452.13	371.19	404.08	46.64
P_1774	320.35	401.01	317.80	390.50	315.24	348.98	42.90
Pb2203	154.50	192.04	153.33	187.01	152.51	167.88	19.86
Si2516	7.76	10.42	7.69	11.76	9.01	9.33	1.76
Sr3464	161.23	199.45	160.06	196.33	160.26	175.47	20.51
Zn2062	29.14	36.52	29.08	35.67	29.17	31.92	3.83
Zr3391	36.07	45.18	36.55	44.73	36.58	39.82	4.69

	0412-211-MnO41B-0	0412-211-MnO41B-6	0412-211-MnO41B-12	0412-211-MnO41B-24	0412-211-MnO41B-48	**average**	**stddev**
Element	(ppm)	(ppm)	(ppm)	(ppm)	(ppm)		
Al3082	251.77	275.34	313.87	313.58	265.81	284.08	28.34
B_2497	16.37	17.60	21.71	21.98	17.34	19.00	2.64
Ca3179	232.14	251.09	289.90	291.02	243.00	261.43	27.34
Ce4186	23.73	25.35	29.47	29.61	25.03	26.64	2.72
Cr3578	79.16	88.38	102.03	102.54	85.31	91.48	10.41
Cu3247	17.97	21.14	24.13	24.03	19.91	21.44	2.67
Fe2599	692.31	754.07	861.51	869.97	724.46	780.46	80.91
K_7664	1465.27	1657.88	1944.39	1944.67	1588.22	1720.09	216.18
La3949	17.77	19.51	22.42	22.37	18.96	20.21	2.10
Mg2790	6.98	6.68	8.30	8.07	7.09	7.42	0.72
Mn2576	332.76	361.24	413.13	414.54	348.55	374.04	37.70
Mo2020	25.40	27.43	31.89	31.92	26.67	28.66	3.05
Nd4061	49.43	54.62	62.10	62.94	52.37	56.29	5.98
Ni2316	357.86	382.96	445.56	448.66	375.06	402.02	42.17
P_1774	309.07	333.61	386.34	387.47	324.58	348.21	36.40
Pb2203	151.49	161.61	187.16	188.38	158.06	169.34	17.22
Si2516	6.85	6.95	9.83	10.45	8.60	8.53	1.63
Sr3464	166.55	178.59	206.59	207.92	174.16	186.76	19.20
Zn2062	28.10	29.92	34.91	35.17	29.38	31.50	3.30
Zr3391	36.29	39.68	45.99	45.97	38.55	41.30	4.45

Table C.15 ICP-AES Data for AN-107 Primary Effects Samples (0.025 M Added MnO_4 Samples)

	0412-211-MnO42A-0	0412-211-MnO42A-6	0412-211-MnO42A-12	0412-211-MnO42A-24	0412-211-MnO42A-48	**average**	**stddev**
Element	(ppm)	(ppm)	(ppm)	(ppm)	(ppm)		
Al3082	260.32	262.61	249.36	263.61	253.34	257.85	6.21
B_2497	16.67	16.86	16.40	17.66	16.84	16.89	0.47
Ca3179	221.88	229.29	215.13	227.28	220.25	222.77	5.67
Ce4186	9.26	9.44	9.41	9.14	9.23	9.29	0.13
Cr3578	77.88	79.82	76.62	79.51	76.85	78.14	1.48
Cu3247	17.59	17.10	16.71	17.26	16.37	17.01	0.48
Fe2599	310.60	313.74	298.01	312.88	306.59	308.37	6.42
K_7664	1537.82	1582.72	1520.09	1597.60	1523.52	1552.35	35.54
La3949	6.90	6.88	6.63	7.18	6.77	6.87	0.20
Mg2790	2.45	3.57	2.29	3.87	2.56	2.94	0.72
Mn2576	187.93	190.91	181.10	190.96	185.16	187.21	4.18
Mo2020	25.98	26.59	25.33	26.56	25.95	26.08	0.52
Nd4061	22.51	21.65	22.39	21.56	21.14	21.85	0.58
Ni2316	361.79	370.66	354.64	374.37	360.65	364.42	7.98
P_1774	311.74	318.03	302.87	318.32	310.60	312.31	6.35
Pb2203	85.11	87.52	82.51	87.12	85.11	85.47	1.99
Si2516	4.80	5.17	5.63	6.86	7.22	5.94	1.06
Sr3464	137.19	140.31	133.36	140.60	136.62	137.62	2.98
Zn2062	24.58	25.22	23.91	25.47	25.24	24.89	0.64
Zr3391	19.65	20.03	19.19	20.23	19.35	19.69	0.44

	0412-211-MnO42B-0	0412-211-MnO42B-6	0412-211-MnO42B-12	0412-211-MnO42B-24	0412-211-MnO42B-48	**average**	**stddev**
Element	(ppm)	(ppm)	(ppm)	(ppm)	(ppm)		
Al3082	281.62	269.18	265.21	266.35	261.03	268.68	7.81
B_2497	18.82	18.09	17.62	17.91	17.35	17.96	0.56
Ca3179	240.41	229.46	225.94	227.31	226.05	229.84	6.08
Ce4186	21.55	20.72	20.09	20.14	20.48	20.60	0.59
Cr3578	88.89	83.51	79.39	81.51	83.28	83.32	3.53
Cu3247	19.70	18.35	18.47	19.08	18.26	18.77	0.61
Fe2599	548.26	525.38	527.10	522.24	516.23	527.84	12.14
K_7664	1739.45	1619.62	1592.73	1574.72	1597.60	1624.82	66.05
La3949	14.34	13.50	13.16	13.24	13.42	13.53	0.47
Mg2790	4.82	3.74	3.73	4.14	4.63	4.21	0.50
Mn2576	244.47	234.06	230.89	232.00	231.37	234.56	5.67
Mo2020	28.46	27.19	26.23	26.66	26.75	27.06	0.86
Nd4061	45.82	44.39	42.81	42.99	43.30	43.86	1.25
Ni2316	400.40	382.10	365.51	374.66	378.38	380.21	12.86
P_1774	341.48	330.90	323.18	323.75	324.90	328.84	7.71
Pb2203	109.57	105.68	102.65	103.02	104.28	105.04	2.80
Si2516	6.38	6.22	6.10	6.46	7.81	6.59	0.70
Sr3464	177.01	169.88	164.19	166.08	167.80	168.99	4.95
Zn2062	26.92	25.77	24.85	25.31	25.58	25.69	0.77
Zr3391	35.84	33.92	32.89	33.61	33.98	34.05	1.09

Table C.16 ICP-AES Data for AN-107 Primary Effects Samples (Nitrogen Purge Samples)

	0516-213A-0	0516-213A-6	0516-213A-12	0516-213A-24	0516-213A-48	**AVG**	**SD**
	(ppm)	(ppm)	(ppm)	(ppm)	(ppm)		
Al3082	267.82	268.83	255.60	256.22	260.89	261.87	6.25
B_2497	16.82	18.00	16.52	16.55	17.32	17.04	0.62
Ca3179	190.30	190.33	188.55	183.49	186.33	187.80	2.91
Ce4186	2.42	2.50	2.71	2.36	2.62	2.52	0.15
Cr3578	83.50	84.21	78.82	77.58	76.87	80.20	3.42
Cu3247	15.92	15.71	14.74	14.88	14.96	15.24	0.54
Fe2599	74.80	74.89	70.74	72.67	76.28	73.88	2.17
K_7664	1631.26	1633.03	1546.90	1517.89	1535.35	1572.88	55.08
La3949	2.02	2.06	1.94	1.89	1.91	1.97	0.07
Mg2790	1.16	0.30	1.84	1.28	1.20	1.16	0.55
Mn2576	58.08	57.96	54.97	55.32	56.09	56.48	1.46
Mo2020	26.70	26.85	25.49	25.15	25.13	25.86	0.85
Nd4061	5.29	6.12	6.29	4.99	5.31	5.60	0.57
Ni2316	372.37	374.44	354.02	353.42	350.17	360.88	11.55
P_1774	323.53	324.12	308.14	305.18	308.73	313.94	9.13
Pb2203	56.77	56.92	54.46	53.93	54.17	55.25	1.47
Si2516	5.16	5.95	9.63	6.01	7.12	6.77	1.74
Sr3464	128.08	128.43	121.24	122.01	122.93	124.54	3.45
Zn2062	25.06	25.25	24.00	24.00	24.28	24.52	0.59
Zr3391	4.19	4.23	4.00	3.93	3.95	4.06	0.14

	0516-213B-0	0325-211A-0MOH-6	0516-213B-12	0516-213B-24	0516-213B-48	**AVG**	**SD**
	(ppm)	(ppm)	(ppm)	(ppm)	(ppm)		
Al3082	260.01	259.95	294.16	274.90	255.74	268.95	15.86
B_2497	16.50	16.69	19.43	18.13	17.21	17.59	1.21
Ca3179	186.30	185.06	210.01	196.81	182.78	192.19	11.33
Ce4186	2.62	2.42	2.72	2.80	2.63	2.64	0.14
Cr3578	82.14	81.81	91.11	84.66	79.77	83.90	4.39
Cu3247	15.75	15.73	17.41	16.61	15.37	16.17	0.83
Fe2599	70.86	71.48	81.43	74.65	70.89	73.86	4.51
K_7664	1641.91	1593.37	1796.72	1658.49	1561.10	1650.32	90.52
La3949	1.87	1.87	2.19	1.89	1.86	1.94	0.14
Mg2790	0.84	1.18	0.66	0.78	0.96	0.88	0.20
Mn2576	55.65	55.35	62.54	58.40	54.61	57.31	3.26
Mo2020	26.10	26.06	29.15	27.19	25.59	26.82	1.43
Nd4061	6.13	6.30	6.28	5.92	5.73	6.07	0.24
Ni2316	366.15	364.97	406.41	380.66	358.46	375.33	19.17
P_1774	316.42	319.38	358.75	331.82	311.10	327.49	19.06
Pb2203	55.14	55.38	62.25	57.93	54.43	57.03	3.20
Si2516	5.29	5.61	6.59	6.83	7.47	6.36	0.90
Sr3464	125.95	125.27	140.87	131.99	123.70	129.55	7.06
Zn2062	24.60	24.62	27.45	25.86	24.16	25.34	1.34
Zr3391	3.94	3.97	4.34	4.03	3.83	4.02	0.19

Table C.17 ICP-AES Data for AN-107 Primary Effects Samples (Oxygen Purge Samples)

	0516-212A-0	0516-212A-6	0516-212A-12	0516-212A-24	0516-212A-48	**AVG**	**SD**
	(ppm)	(ppm)	(ppm)	(ppm)	(ppm)		
Al3082	309.32	276.38	264.03	247.72	260.92	271.67	23.38
B_2497	20.39	17.60	17.22	16.38	17.26	17.77	1.53
Ca3179	229.22	202.85	192.99	182.25	192.10	199.88	17.95
Ce4186	3.37	2.97	2.83	2.54	2.52	2.85	0.35
Cr3578	97.09	86.96	84.42	79.56	82.11	86.03	6.76
Cu3247	18.04	16.37	15.42	14.31	15.44	15.91	1.39
Fe2599	86.99	71.99	68.67	63.79	67.49	71.79	8.99
K_7664	1856.81	1676.25	1608.76	1501.90	1593.37	1647.42	132.54
La3949	2.39	2.12	2.00	1.87	1.89	2.05	0.21
Mg2790	0.93	0.69	1.23	1.89	1.58	1.27	0.48
Mn2576	66.07	46.44	43.33	39.81	40.26	47.18	10.89
Mo2020	30.81	27.68	26.68	24.98	26.18	27.27	2.21
Nd4061	5.64	5.97	5.20	5.51	5.97	5.66	0.33
Ni2316	430.09	386.87	371.78	349.87	366.45	381.01	30.45
P_1774	375.03	332.41	319.38	297.18	313.17	327.44	29.47
Pb2203	65.12	57.78	55.71	52.13	54.70	57.09	4.93
Si2516	6.95	5.67	5.28	6.22	6.78	6.18	0.71
Sr3464	144.45	129.17	124.14	116.71	121.95	127.29	10.59
Zn2062	28.42	25.13	24.38	24.62	23.99	25.31	1.79
Zr3391	4.79	4.31	4.14	3.91	4.07	4.24	0.34

	0516-212B-0	0516-212B-6	0516-212B-12	0516-212B-24	0516-212B-48	**AVG**	**SD**
	(ppm)	(ppm)	(ppm)	(ppm)	(ppm)		
Al3082	264.06	256.63	277.88	250.03	257.43	261.21	10.56
B_2497	17.10	17.17	18.13	15.78	16.99	17.03	0.84
Ca3179	177.07	174.37	186.75	168.93	176.77	176.78	6.46
Ce4186	-	-	-	-	-		
Cr3578	81.02	79.59	85.48	78.65	82.08	81.36	2.65
Cu3247	15.98	15.21	16.81	15.26	15.73	15.80	0.65
Fe2599	69.50	65.48	69.68	64.97	64.74	66.87	2.50
K_7664	1556.07	1538.90	1674.18	1517.59	1569.98	1571.35	60.73
La3949	1.77	1.69	1.75	1.65	1.78	1.73	0.05
Mg2790	1.69	1.35	1.65	1.22	0.65	1.31	0.42
Mn2576	55.12	48.10	50.08	43.84	42.80	47.99	4.98
Mo2020	26.00	25.43	27.36	24.96	26.04	25.96	0.90
Nd4061	5.48	5.07	5.85	5.23	4.78	5.28	0.41
Ni2316	359.94	354.31	377.40	347.21	365.56	360.88	11.46
P_1774	321.46	313.17	338.33	302.22	314.35	317.90	13.33
Pb2203	55.47	54.17	57.87	52.01	54.64	54.83	2.13
Si2516	5.08	5.54	5.82	6.10	7.42	5.99	0.88
Sr3464	114.46	113.37	120.95	109.61	114.14	114.50	4.09
Zn2062	23.67	23.49	24.85	22.85	24.23	23.82	0.76
Zr3391	3.87	3.77	4.04	3.69	3.86	3.85	0.13

Table C.18 ICP-AES Data for AN-107 Primary Effects Samples (Shear Samples)

	0607-211A-SHEAR-48	0607-211A-SHEAR-24	0607-211A-SHEAR-18	0607-211A-SHEAR-6	0607-211A-SHEAR-0	AVG	SD
	(ppm)	(ppm)	(ppm)	(ppm)	(ppm)		
Al3082	276.96	279.47	279.10	280.94	279.01	279.10	1.42
B_2497	15.71	15.99	16.28	15.85	15.73	15.91	0.23
Ca3179	184.03	183.94	188.50	185.22	181.86	184.71	2.44
Ce4186	2.90	3.00	2.95	3.09	2.97	2.98	0.07
Cr3578	78.12	77.63	75.15	75.00	77.05	76.59	1.43
Cu3247	17.24	15.72	15.35	15.21	15.20	15.74	0.86
Fe2599	60.37	61.90	64.72	63.31	61.35	62.33	1.71
K_7664	1405.76	1402.70	1376.08	1384.96	1412.80	1396.46	15.33
La3949	2.05	2.10	2.04	2.07	2.05	2.06	0.02
Mg2790	-	-	-	-	-		
Mn2576	50.77	51.04	51.53	51.10	50.67	51.02	0.34
Mo2020	26.14	25.84	25.47	25.66	25.98	25.82	0.26
Nd4061	6.94	6.56	6.16	6.58	6.42	6.53	0.28
Ni2316	360.77	355.27	350.06	349.15	354.65	353.98	4.66
P_1774	347.92	346.70	346.39	351.90	355.57	349.70	3.95
Pb2203	55.75	54.96	54.62	55.57	55.45	55.27	0.47
Si2516	-	-	-	-	-		
Sr3464	128.40	127.63	129.35	127.27	126.35	127.80	1.14
Zn2062	22.40	22.07	22.03	21.67	22.00	22.03	0.26
Zr3391	4.02	4.01	3.93	3.85	3.87	3.94	0.08

	0607-211B-SHEAR-48	0607-211B-SHEAR-24	0607-211B-SHEAR-18	0607-211B-SHEAR-6	0607-211B-SHEAR-0	AVG	SD
	(ppm)	(ppm)	(ppm)	(ppm)	(ppm)		
Al3082	243.31	268.82	274.18	269.52	255.63	262.29	12.66
B_2497	14.40	15.59	16.15	15.17	15.32	15.33	0.64
Ca3179	153.39	173.96	178.95	174.88	164.17	169.07	10.31
Ce4186	2.57	2.71	3.06	2.72	2.63	2.74	0.19
Cr3578	71.16	77.39	73.07	75.03	71.94	73.72	2.52
Cu3247	15.56	17.19	16.34	16.32	15.82	16.25	0.63
Fe2599	48.99	55.11	58.51	56.21	51.71	54.11	3.76
K_7664	1268.62	1380.37	1359.25	1362.92	1291.93	1332.62	49.14
La3949	1.76	1.88	1.94	1.85	1.79	1.84	0.07
Mg2790	-	-	-	-	-		
Mn2576	44.42	49.33	50.18	49.36	46.57	47.97	2.41
Mo2020	23.22	25.43	25.08	25.02	24.14	24.58	0.89
Nd4061	5.63	6.49	6.42	6.11	5.95	6.12	0.35
Ni2316	322.77	356.49	345.78	348.23	333.85	341.42	13.21
P_1774	314.00	346.09	347.62	343.33	324.97	335.20	14.94
Pb2203	47.62	52.14	53.55	52.72	49.94	51.20	2.40
Si2516	-	-	-	-	-		
Sr3464	100.56	112.76	114.93	112.61	106.70	109.51	5.87
Zn2062	19.55	21.89	21.51	21.38	20.55	20.98	0.93
Zr3391	3.37	3.74	3.67	3.72	3.52	3.60	0.16

APPENDIX D

AN-107 Final Filter Photographs

Figure D.1

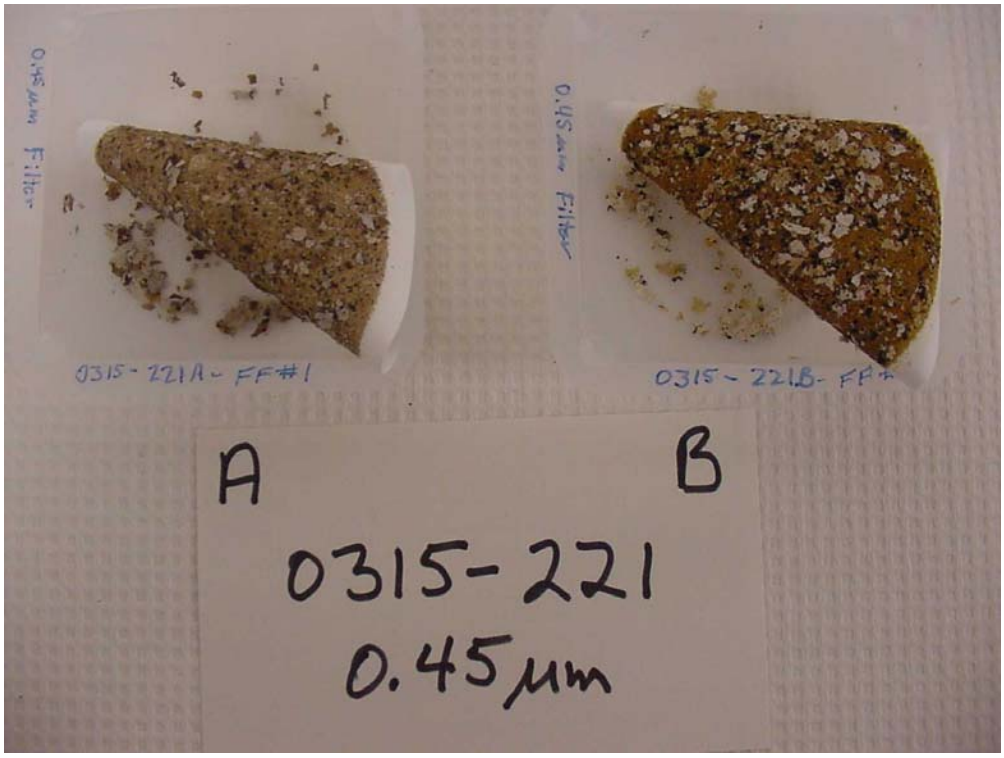

Figure D.2

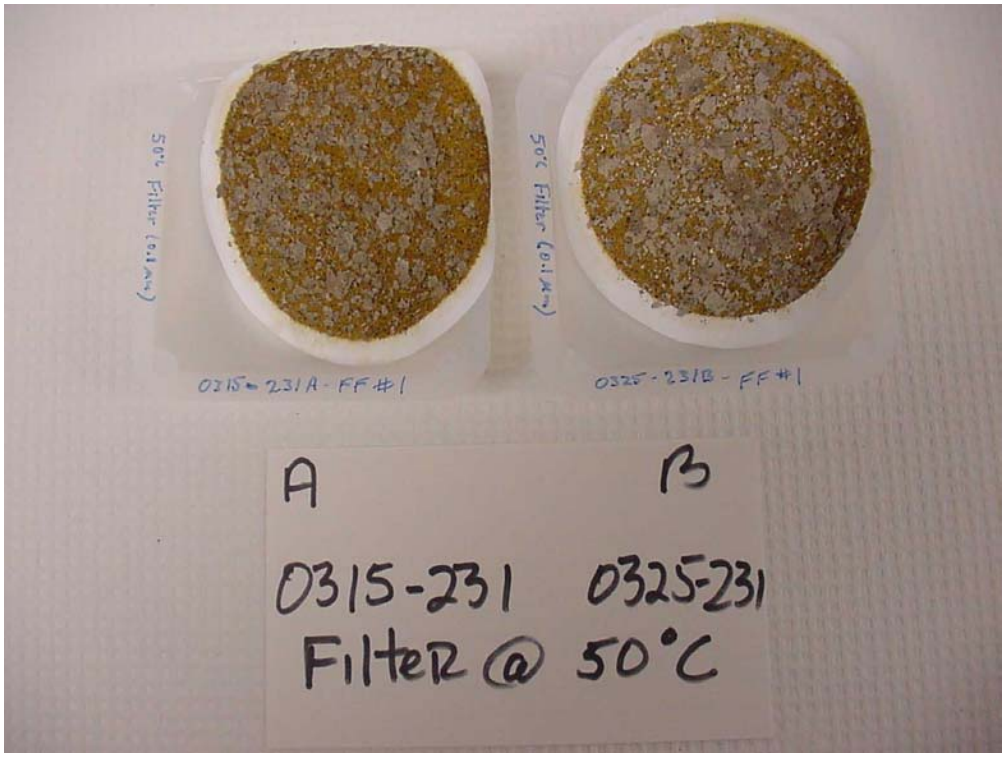

Figure D.3

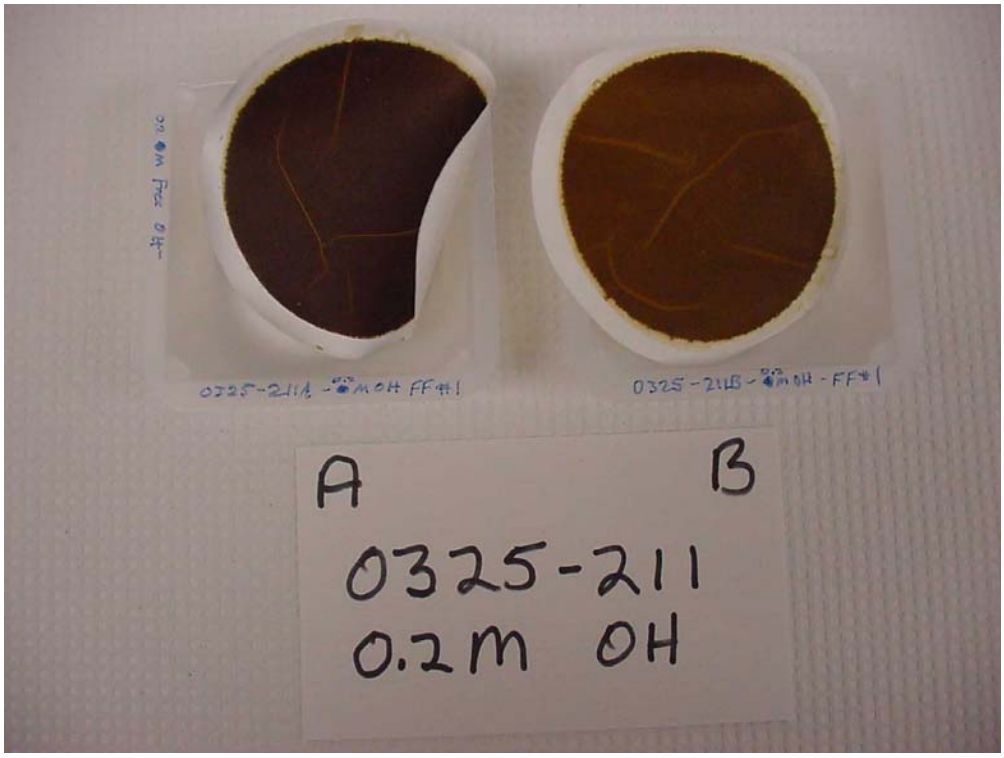

Figure D.4

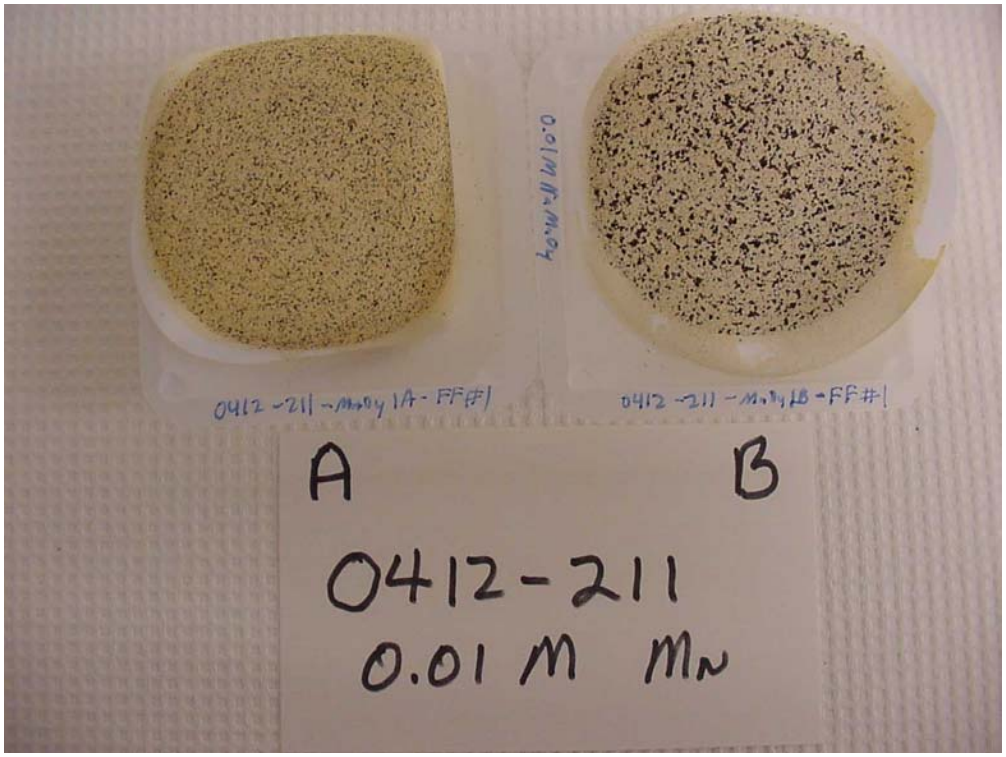

Figure D.5

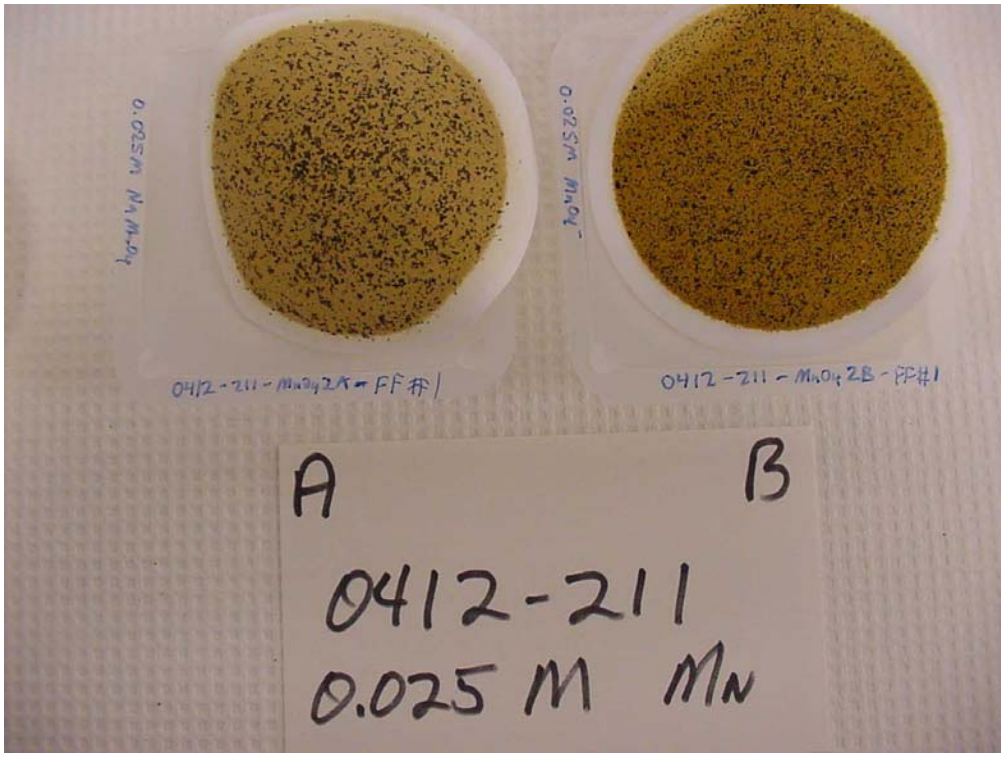

Figure D.6

Figure D.7

Figure D.8

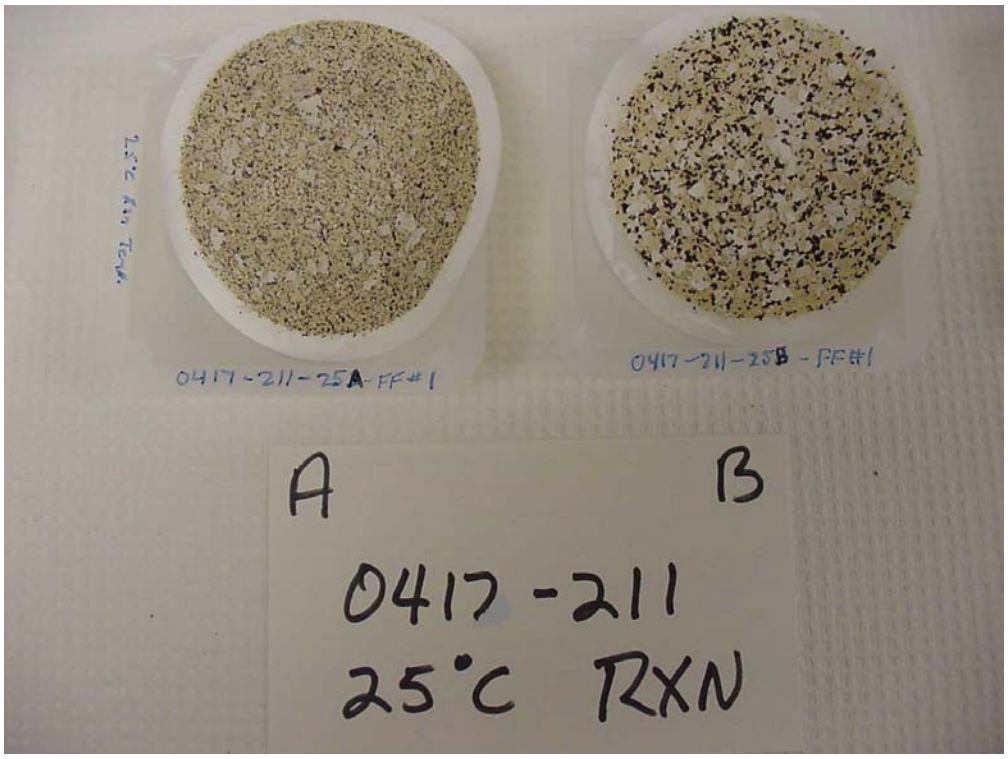

Figure D.9

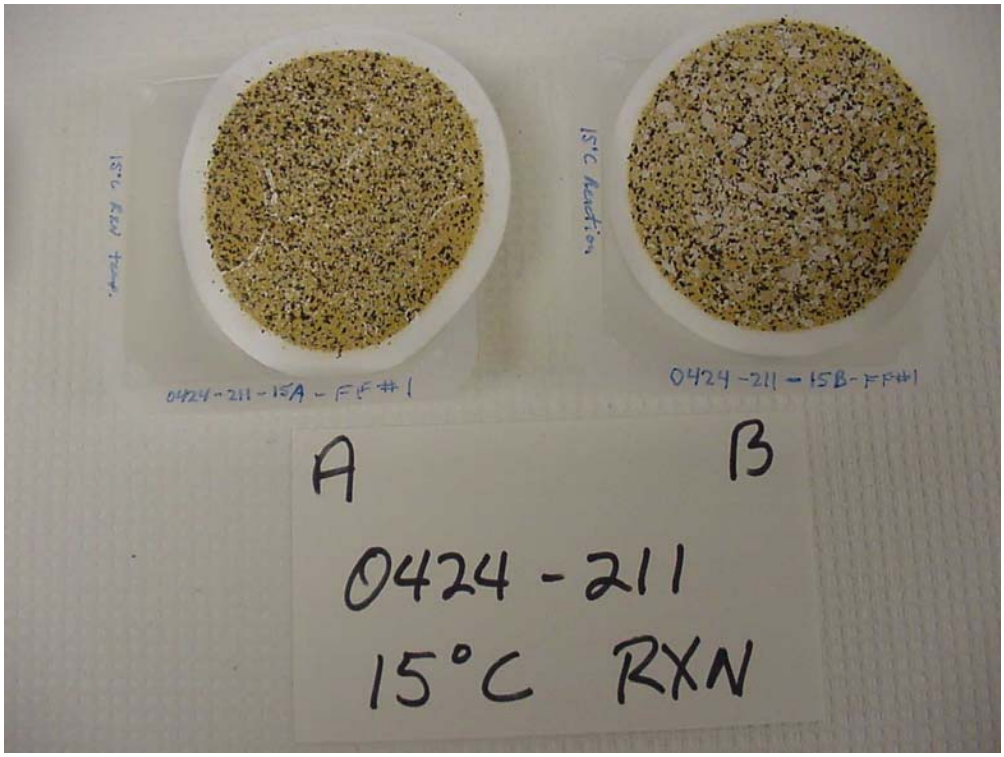

Figure D.10

Figure D.11

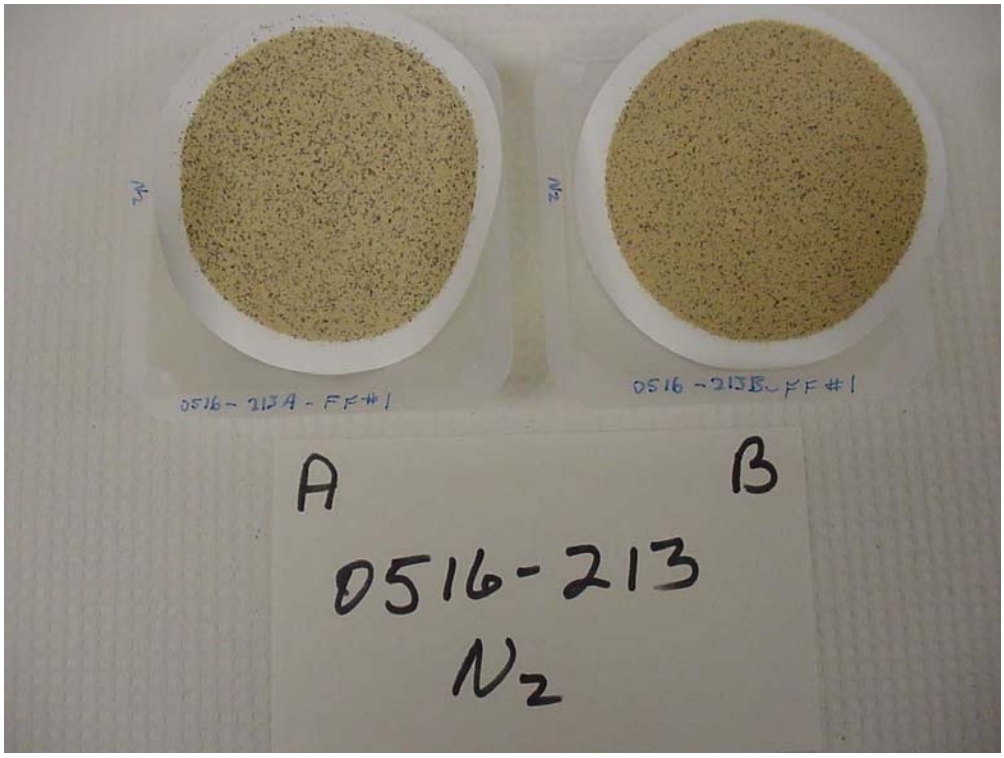

Figure D.12

Figure D.13

Figure D.14

APPENDIX E

ICP-AES Analysis of AN-107 Secondary Effects Samples

Table E.1 ICP-AES Data for AN-107 Secondary Effects Samples (0.03 M $NaMnO_4$/Dark/N_2)

	0701-SIM7-DkN2-384	0701-SIM7-DkN2-192	0701-SIM7-DkN2-120	0701-SIM7-DkN2-0	**AVG**	**SD**
	(ppm)	(ppm)	(ppm)	(ppm)		
Al3082	263.42	266.64	261.28	267.96	264.83	3.04
B_2497	17.84	17.46	16.73	16.85	17.22	0.52
Ca3179	307.03	307.30	300.70	308.35	305.84	3.48
Ce4186	8.21	8.57	8.39	8.35	8.38	0.15
Cr3578	83.71	87.30	85.03	85.98	85.51	1.52
Cu3247	18.50	18.91	18.64	19.04	18.77	0.25
Fe2599	294.36	297.00	290.40	295.42	294.29	2.81
K_7664	1339.01	1386.79	1354.06	1368.58	1362.11	20.41
La3949	6.52	6.77	6.56	6.70	6.64	0.12
Mg2790	-	-	-	-		
Mn2576	73.58	74.37	73.02	74.16	73.78	0.61
Mo2020	27.14	27.22	26.45	26.64	26.86	0.37
Nd4061	18.23	18.77	18.60	18.69	18.57	0.24
Ni2316	371.98	381.74	373.03	375.67	375.61	4.38
P_1774	314.69	315.48	308.88	313.37	313.10	2.95
Pb2203	110.83	112.62	109.06	110.46	110.74	1.47
Si2516	-	-	-	-		
Sr3464	104.20	110.56	109.56	112.99	109.33	3.71
Zn2062	21.68	22.35	21.38	21.72	21.78	0.41
Zr3391	21.17	21.67	21.48	21.64	21.49	0.23
	0701-SIM8-DkN2-384	0701-SIM8-DkN2-192	0701-SIM8-DkN2-120	0701-SIM8-DkN2-0	**AVG**	**SD**
	(ppm)	(ppm)	(ppm)	(ppm)		
Al3082	264.53	264.26	270.86	267.43	266.77	3.08
B_2497	16.92	16.93	17.01	16.56	16.85	0.20
Ca3179	290.40	294.89	301.75	292.51	294.89	4.93
Ce4186	8.19	8.37	8.42	8.33	8.33	0.10
Cr3578	87.04	86.91	85.64	85.91	86.37	0.70
Cu3247	19.07	19.37	19.86	19.24	19.38	0.34
Fe2599	293.30	293.57	305.45	298.06	297.59	5.67
K_7664	1377.82	1387.85	1376.23	1384.94	1381.71	5.58
La3949	6.43	6.63	6.62	6.65	6.58	0.10
Mg2790	-	-	-	-		
Mn2576	81.31	81.55	83.32	81.58	81.94	0.93
Mo2020	26.72	26.74	26.77	26.58	26.70	0.08
Nd4061	18.62	18.56	18.37	18.89	18.61	0.21
Ni2316	377.78	381.48	380.95	375.41	378.91	2.85
P_1774	314.42	314.16	321.29	321.29	317.79	4.04
Pb2203	114.55	114.81	115.68	115.21	115.06	0.49
Si2516	-	-	-	-		
Sr3464	99.95	116.32	125.72	132.11	118.52	13.98
Zn2062	22.26	22.50	22.82	22.18	22.44	0.29
Zr3391	22.27	22.47	22.50	22.13	22.34	0.17

Table E.2 ICP-AES Data for AN-107 Secondary Effects Samples (0.01 M $NaMnO_4$/Dark/N_2)

	0724-SIM7-DkN2-384	0724-SIM7-Dk2-192	0725-SIM8-LtAtm-120	0724-SIM7-Dk2N2-0	AVG	SD
	(ppm)	(ppm)	(ppm)	(ppm)		
Al3082	278.12	266.51	260.84	265.74	267.80	7.32
B_2497	16.06	15.30	15.15	15.47	15.50	0.40
Ca3179	306.50	295.67	274.51	288.96	291.41	13.39
Ce4186	27.92	25.70	26.29	26.86	26.69	0.94
Cr3578	85.37	79.08	83.46	85.09	83.25	2.91
Cu3247	20.80	19.51	20.28	20.58	20.29	0.57
Fe2599	869.72	841.34	799.54	818.12	832.18	30.31
K_7664	1370.50	1259.56	1283.03	1308.83	1305.48	47.79
La3949	13.33	12.52	12.57	13.63	13.01	0.55
Mg2790	-	-	-	-		
Mn2576	425.18	407.12	388.03	399.38	404.93	15.61
Mo2020	26.34	24.55	24.93	25.31	25.28	0.77
Nd4061	43.11	39.84	41.05	41.43	41.36	1.35
Ni2316	358.62	340.56	343.66	352.17	348.75	8.21
P_1774	343.40	325.08	335.40	336.69	335.14	7.57
Pb2203	198.84	189.22	184.21	185.89	189.54	6.54
Si2516	-	-	-	-		
Sr3464	128.05	152.53	157.38	221.62	164.89	39.94
Zn2062	26.11	25.27	24.83	25.05	25.32	0.56
Zr3391	39.14	25.62	37.13	37.93	34.95	6.27
	0724-SIM8-DkN2-384	0724-SIM8-Dk2N2-192	0724-SIM8-Dk2N2-120	0724-SIM8-Dk2N2-0	AVG	SD
	(ppm)	(ppm)	(ppm)	(ppm)		
Al3082	276.06	277.61	278.90	293.35	281.48	8.00
B_2497	16.54	16.39	16.85	16.86	16.66	0.23
Ca3179	307.02	284.06	294.38	300.05	296.38	9.70
Ce4186	28.23	27.74	27.12	29.33	28.10	0.94
Cr3578	89.27	91.18	82.90	89.68	88.26	3.67
Cu3247	21.58	22.03	20.97	22.26	21.71	0.57
Fe2599	867.40	832.57	869.72	891.91	865.40	24.52
K_7664	1379.53	1375.40	1324.06	1413.32	1373.08	36.83
La3949	13.56	13.73	13.10	14.57	13.74	0.61
Mg2790	-	-	-	-		
Mn2576	441.44	421.06	423.89	433.96	430.09	9.38
Mo2020	26.70	26.52	25.19	26.99	26.35	0.80
Nd4061	43.42	43.76	42.83	45.64	43.91	1.21
Ni2316	379.00	372.04	351.91	372.04	368.75	11.69
P_1774	332.05	348.30	343.91	370.49	348.69	16.07
Pb2203	201.34	194.17	192.44	202.25	197.55	4.96
Si2516	-	-	-	-		
Sr3464	126.32	151.11	168.24	245.49	172.79	51.43
Zn2062	27.81	26.39	25.74	26.63	26.64	0.86
Zr3391	41.05	38.06	32.25	40.48	37.96	4.02

Table E.3 ICP-AES Data for AN-107 Secondary Effects Samples (0.03 M $NaMnO_4$/Light/N_2)

	0701-SIM7-LtN2-384	0701-SIM7-LtN2-192	0701-SIM7-LtN2-120	0701-SIM7-LtN2-0	**AVG**	**SD**
	(ppm)	(ppm)	(ppm)	(ppm)		
Al3082	265.85	269.02	267.70	261.28	265.96	3.38
B_2497	16.06	16.87	16.80	15.78	16.38	0.54
Ca3179	298.06	305.71	303.60	294.62	300.50	5.08
Ce4186	7.86	7.86	7.96	8.01	7.92	0.08
Cr3578	85.43	85.83	84.16	85.09	85.13	0.71
Cu3247	19.06	19.40	19.10	18.80	19.09	0.24
Fe2599	280.90	291.72	290.14	281.69	286.11	5.61
K_7664	1425.07	1442.50	1435.10	1344.55	1411.81	45.40
La3949	5.65	5.90	5.90	5.99	5.86	0.15
Mg2790	-	-	-	-		
Mn2576	64.84	73.95	73.89	72.12	71.20	4.33
Mo2020	26.72	26.90	26.53	26.34	26.62	0.24
Nd4061	17.18	17.21	17.38	17.33	17.27	0.09
Ni2316	378.31	379.90	373.82	375.41	376.86	2.75
P_1774	315.48	321.02	317.33	311.26	316.27	4.06
Pb2203	110.80	113.23	112.75	110.25	111.76	1.46
Si2516	-	-	-	-		
Sr3464	93.17	112.09	118.59	128.57	113.10	14.92
Zn2062	21.91	22.27	21.78	21.55	21.88	0.30
Zr3391	21.09	21.39	21.05	20.92	21.11	0.20
	0702-SIM7-DkAtm-384	0702-SIM7-DkAtm-192	0702-SIM7-DkAtm-120	0702-SIM7-DkAtm-0	**AVG**	**SD**
	(ppm)	(ppm)	(ppm)	(ppm)		
Al3082	272.71	273.24	268.75	285.65	275.09	7.32
B_2497	16.82	16.54	16.79	16.96	16.78	0.18
Ca3179	325.51	316.01	312.84	324.46	319.70	6.25
Ce4186	8.69	8.62	8.35	8.97	8.66	0.26
Cr3578	88.04	87.83	90.18	92.51	89.64	2.18
Cu3247	20.03	19.72	19.81	20.73	20.07	0.46
Fe2599	304.13	306.24	299.11	315.74	306.31	6.97
K_7664	1390.49	1406.33	1409.50	1467.84	1418.54	33.90
La3949	7.01	6.98	6.98	7.31	7.07	0.16
Mg2790	-	-	-	-		
Mn2576	67.98	67.95	67.37	70.09	68.35	1.19
Mo2020	27.46	27.03	27.35	28.09	27.48	0.44
Nd4061	19.41	19.49	19.02	19.96	19.47	0.39
Ni2316	376.99	377.26	384.65	391.78	382.67	7.03
P_1774	319.97	322.08	322.08	335.81	324.98	7.28
Pb2203	110.56	111.65	111.99	116.08	112.57	2.42
Si2516	-	-	-	-		
Sr3464	95.81	100.43	101.03	104.44	100.43	3.55
Zn2062	28.12	21.48	21.59	22.20	23.35	3.20
Zr3391	22.46	22.29	22.56	23.24	22.63	0.42

Table E.4 ICP-AES Data for AN-107 Secondary Effects Samples (0.01 M $NaMnO_4$/Light/N_2)

	0724-SIM7-LtN2-384	0724-SIM7-LtN2-192	0724-SIM7-LtN2-120	0724-SIM7-LtN2-0	**AVG**	**SD**
	(ppm)	(ppm)	(ppm)	(ppm)		
Al3082	277.87	277.35	276.58	275.03	276.71	1.24
B_2497	15.64	16.74	16.23	15.50	16.03	0.57
Ca3179	279.93	284.06	276.83	275.54	279.09	3.79
Ce4186	27.66	27.40	26.94	27.63	27.41	0.33
Cr3578	85.04	86.56	88.86	88.06	87.13	1.69
Cu3247	20.46	21.27	21.42	21.08	21.06	0.42
Fe2599	866.36	862.24	852.17	835.15	853.98	13.90
K_7664	1360.18	1335.15	1356.05	1334.63	1346.50	13.51
La3949	11.86	12.12	12.28	12.69	12.23	0.35
Mg2790	-	-	-	-		
Mn2576	419.77	428.28	422.35	413.06	420.86	6.31
Mo2020	26.34	25.63	25.88	25.66	25.88	0.33
Nd4061	40.89	40.74	41.25	41.31	41.05	0.28
Ni2316	355.78	361.72	361.20	357.85	359.14	2.82
P_1774	347.01	323.79	324.56	328.43	330.95	10.90
Pb2203	200.62	194.71	194.97	191.64	195.49	3.74
Si2516	-	-	-	-		
Sr3464	115.02	153.38	169.35	248.04	171.45	55.92
Zn2062	25.95	26.88	26.37	26.08	26.32	0.41
Zr3391	38.39	37.98	31.81	38.52	36.67	3.25
	0724-SIM8-LtN2-384	0724-SIM8-LtN2-192	0724-SIM8-LtN2-120	0724-SIM8-LtN2-0	**AVG**	**SD**
	(ppm)	(ppm)	(ppm)	(ppm)		
Al3082	269.35	257.25	260.58	259.03	261.55	5.37
B_2497	16.09	15.09	15.16	14.90	15.31	0.53
Ca3179	286.90	259.81	260.32	263.42	267.61	12.96
Ce4186	26.94	25.49	25.77	26.34	26.13	0.64
Cr3578	88.65	83.54	83.51	86.84	85.64	2.54
Cu3247	21.07	20.34	20.34	20.68	20.61	0.35
Fe2599	832.82	787.67	797.99	786.90	801.35	21.58
K_7664	1356.05	1263.94	1266.01	1291.81	1294.45	42.98
La3949	12.47	11.78	11.99	12.96	12.30	0.53
Mg2790	-	-	-	-		
Mn2576	408.16	392.16	394.22	393.71	397.06	7.45
Mo2020	26.21	24.41	24.60	24.97	25.05	0.81
Nd4061	41.18	39.29	39.47	40.22	40.04	0.86
Ni2316	373.84	348.04	348.30	357.59	356.94	12.11
P_1774	320.95	310.63	319.15	320.18	317.73	4.79
Pb2203	194.53	181.76	182.64	182.90	185.46	6.07
Si2516	-	-	-	-		
Sr3464	113.60	132.43	150.08	251.37	161.87	61.50
Zn2062	27.32	25.22	25.13	25.73	25.85	1.01
Zr3391	40.43	35.94	37.00	38.39	37.94	1.94

Table E.5 ICP-AES Data for AN-107 Secondary Effects Samples (0.03 M $NaMnO_4$/Dark/Atm)

	0702-SIM7-DkAtm-384	0702-SIM7-DkAtm-192	0702-SIM7-DkAtm-120	0702-SIM7-DkAtm-0	AVG	SD
	(ppm)	(ppm)	(ppm)	(ppm)		
Al3082	272.71	273.24	268.75	285.65	275.09	7.32
B_2497	16.82	16.54	16.79	16.96	16.78	0.18
Ca3179	325.51	316.01	312.84	324.46	319.70	6.25
Ce4186	8.69	8.62	8.35	8.97	8.66	0.26
Cr3578	88.04	87.83	90.18	92.51	89.64	2.18
Cu3247	20.03	19.72	19.81	20.73	20.07	0.46
Fe2599	304.13	306.24	299.11	315.74	306.31	6.97
K_7664	1390.49	1406.33	1409.50	1467.84	1418.54	33.90
La3949	7.01	6.98	6.98	7.31	7.07	0.16
Mg2790	-	-	-	-		
Mn2576	67.98	67.95	67.37	70.09	68.35	1.19
Mo2020	27.46	27.03	27.35	28.09	27.48	0.44
Nd4061	19.41	19.49	19.02	19.96	19.47	0.39
Ni2316	376.99	377.26	384.65	391.78	382.67	7.03
P_1774	319.97	322.08	322.08	335.81	324.98	7.28
Pb2203	110.56	111.65	111.99	116.08	112.57	2.42
Si2516	-	-	-	-		
Sr3464	95.81	100.43	101.03	104.44	100.43	3.55
Zn2062	28.12	21.48	21.59	22.20	23.35	3.20
Zr3391	22.46	22.29	22.56	23.24	22.63	0.42

	0702-SIM8-DkAtm-384	0702-SIM8-DkAtm-192	0702-SIM8-DkAtm-120	0702-SIM8-DkAtm-0	AVG	SD
	(ppm)	(ppm)	(ppm)	(ppm)		
Al3082	274.30	275.62	270.86	277.08	274.46	2.66
B_2497	16.46	15.92	15.77	12.18	15.08	1.95
Ca3179	286.70	291.98	295.68	331.33	301.42	20.27
Ce4186	8.18	8.40	8.25	8.79	8.41	0.27
Cr3578	87.75	91.24	87.62	89.42	89.01	1.70
Cu3247	20.55	20.97	20.63	21.11	20.81	0.27
Fe2599	297.53	297.79	298.32	315.39	302.26	8.76
K_7664	1420.85	1450.94	1421.64	1417.65	1427.77	15.55
La3949	5.66	6.04	6.05	6.32	6.02	0.27
Mg2790	-	-	-	-		
Mn2576	77.85	78.72	78.09	84.82	79.87	3.32
Mo2020	27.24	27.59	26.98	28.27	27.52	0.56
Nd4061	17.62	17.98	17.54	19.80	18.23	1.06
Ni2316	384.65	393.89	384.12	410.76	393.36	12.44
P_1774	324.98	318.38	317.06	319.38	319.95	3.49
Pb2203	118.06	117.08	117.11	124.04	119.07	3.34
Si2516	-	-	-	-		
Sr3464	98.58	128.54	138.57	177.67	135.84	32.65
Zn2062	22.49	23.01	22.73	24.50	23.18	0.90
Zr3391	22.28	22.93	22.39	23.94	22.89	0.76

Table E.6 ICP-AES Data for AN-107 Secondary Effects Samples (0.01 M $NaMnO_4$/Dark/Atm)

	0725-SIM7-DkAtm-384	0725-SIM7-DkAtm-192	0725-SIM7-DkAtm-120	0725-SIM7-DkAtm-0	**AVG**	**SD**
	(ppm)	(ppm)	(ppm)	(ppm)		
Al3082	273.22	258.00	271.67	261.61	266.13	7.47
B_2497	16.11	15.60	16.43	15.43	15.89	0.46
Ca3179	290.77	263.68	276.83	271.93	275.80	11.36
Ce4186	27.06	25.44	26.60	26.21	26.33	0.69
Cr3578	91.49	85.97	91.05	89.76	89.56	2.51
Cu3247	21.64	20.43	21.74	21.40	21.30	0.60
Fe2599	827.66	775.81	812.96	787.93	801.09	23.52
K_7664	1383.14	1276.33	1360.18	1318.38	1334.51	47.15
La3949	12.32	11.83	12.60	12.96	12.43	0.48
Mg2790	-	-	-	-		
Mn2576	424.41	391.90	407.64	397.32	405.32	14.30
Mo2020	26.45	24.67	26.21	25.69	25.75	0.79
Nd4061	39.99	38.85	40.74	40.53	40.03	0.84
Ni2316	378.74	351.40	371.26	366.62	367.01	11.54
P_1774	328.18	310.12	335.92	326.89	325.27	10.86
Pb2203	197.11	179.93	190.77	185.61	188.35	7.33
Si2516	-	-	-	-		
Sr3464	139.50	159.42	184.52	227.69	177.78	38.03
Zn2062	27.35	24.78	26.24	25.83	26.05	1.06
Zr3391	40.51	35.76	39.60	39.04	38.73	2.07
	0725-SIM8-DkAtm-384	0725-SIM8-DkAtm-192	0725-SIM8-DkAtm-120	0725-SIM8-DkAtm-0	**AVG**	**SD**
	(ppm)	(ppm)	(ppm)	(ppm)		
Al3082	272.45	271.93	259.03	265.48	267.22	6.31
B_2497	15.99	16.06	14.91	15.84	15.70	0.53
Ca3179	293.60	264.19	259.55	267.80	271.29	15.26
Ce4186	27.24	26.60	25.53	26.26	26.41	0.71
Cr3578	87.23	92.00	86.28	90.12	88.91	2.63
Cu3247	20.91	22.10	20.95	21.68	21.41	0.58
Fe2599	852.95	801.61	778.13	793.09	806.44	32.49
K_7664	1375.66	1361.98	1286.90	1329.22	1338.44	39.50
La3949	11.62	11.99	11.65	12.35	11.90	0.34
Mg2790	-	-	-	-		
Mn2576	432.41	404.80	392.93	397.06	406.80	17.77
Mo2020	26.14	25.83	24.71	25.60	25.57	0.61
Nd4061	39.11	40.51	39.50	40.17	39.82	0.63
Ni2316	373.58	367.91	353.20	366.62	365.33	8.63
P_1774	329.72	332.30	319.15	330.50	327.92	5.95
Pb2203	201.81	187.39	181.12	185.48	188.95	8.97
Si2516	-	-	-	-		
Sr3464	142.49	165.92	179.36	237.77	181.39	40.56
Zn2062	28.04	25.93	25.38	25.98	26.33	1.17
Zr3391	40.40	39.89	38.31	39.45	39.51	0.89

Table E.7 ICP-AES Data for AN-107 Secondary Effects Samples (0.03 M $NaMnO_4$/Light/Atm)

	0702-SIM-DkAtm-384	0702-SIM8-LtAtm-192	0702-SIM8-LtAtm-120	0702-SIM8-LtAtm-0	**AVG**	**SD**
	(ppm)	(ppm)	(ppm)	(ppm)		
Al3082	267.96	264.79	277.20	294.10	276.01	13.16
B_2497	16.32	15.91	16.24	17.33	16.45	0.61
Ca3179	254.76	252.38	272.18	285.91	266.31	15.77
Ce4186	7.64	7.86	8.00	8.82	8.08	0.52
Cr3578	83.69	87.86	90.79	91.00	88.33	3.41
Cu3247	19.82	20.24	21.55	21.73	20.84	0.95
Fe2599	275.88	273.50	287.76	312.31	287.36	17.76
K_7664	1373.06	1390.22	1445.66	1465.99	1418.74	44.19
La3949	4.62	4.90	5.20	6.01	5.18	0.60
Mg2790	-	-	-	-		
Mn2576	62.41	73.84	80.15	85.17	75.39	9.82
Mo2020	26.38	26.66	27.54	28.43	27.25	0.93
Nd4061	15.96	16.50	17.00	18.30	16.94	1.00
Ni2316	370.39	378.05	388.87	397.85	383.79	12.05
P_1774	316.54	313.10	327.62	346.90	326.04	15.22
Pb2203	113.49	113.28	116.13	123.34	116.56	4.70
Si2516	-	-	-	-		
Sr3464	83.08	105.68	122.05	220.36	132.79	60.53
Zn2062	21.92	22.27	22.90	23.59	22.67	0.73
Zr3391	20.65	21.23	21.92	22.54	21.58	0.82
	0702-SIM7-LtAtm-384	0702-SIM7-LtAtm-192	0702-SIM7-LtAtm-120	0708-SIM7-LtAtm-0	**AVG**	**SD**
	(ppm)	(ppm)	(ppm)	(ppm)		
Al3082	275.09	268.49	266.11	263.52	268.30	4.96
B_2497	16.23	15.03	15.49	20.35	16.78	2.44
Ca3179	285.38	279.84	282.48	271.13	279.71	6.15
Ce4186	8.16	8.36	8.24	8.51	8.32	0.16
Cr3578	85.91	83.48	84.24	78.91	83.13	2.99
Cu3247	20.10	19.46	19.29	18.46	19.33	0.68
Fe2599	300.43	297.79	297.00	296.47	297.92	1.76
K_7664	1390.49	1347.46	1372.01	1316.30	1356.56	32.11
La3949	5.15	5.39	5.30	5.52	5.34	0.16
Mg2790	-	-	-	-		
Mn2576	65.68	74.95	73.84	74.18	72.16	4.35
Mo2020	26.98	26.10	26.51	25.37	26.24	0.68
Nd4061	17.17	17.01	17.09	16.65	16.98	0.23
Ni2316	378.05	363.26	372.50	359.04	368.21	8.64
P_1774	319.70	312.58	312.58	313.90	314.69	3.40
Pb2203	114.07	112.91	114.15	112.33	113.37	0.89
Si2516	-	-	-	-		
Sr3464	85.14	115.71	107.37	151.17	114.85	27.44
Zn2062	21.84	21.27	21.94	21.06	21.53	0.43
Zr3391	21.84	21.06	21.39	20.35	21.16	0.63

Table E.8 ICP-AES Data for AN-107 Secondary Effects Samples (0.01 M $NaMnO_4$/Light/Atm)

	0725-SIM7-LtAtm-384	0725-SIM7-LtAtm-192	0725-SIM7-LtAtm-120	0725-SIM7-LtAtm-0	**AVG**	**SD**
	(ppm)	(ppm)	(ppm)	(ppm)		
Al3082	586.63	261.87	263.16	256.14	341.95	163.15
B_2497	34.35	15.66	15.49	14.93	20.11	9.50
Ca3179	665.58	274.77	276.06	277.09	373.37	194.80
Ce4186	56.74	25.98	26.16	25.88	33.69	15.37
Cr3578	179.94	88.70	88.55	86.53	110.93	46.02
Cu3247	43.76	21.41	21.24	20.78	26.80	11.31
Fe2599	1859.12	795.41	800.57	784.32	1059.86	532.88
K_7664	2922.17	1327.67	1329.22	1296.19	1718.81	802.38
La3949	23.67	11.44	11.48	11.85	14.61	6.04
Mg2790	-	-	-	-		
Mn2576	936.96	406.61	406.87	398.09	537.13	266.58
Mo2020	55.15	25.38	25.38	24.82	32.69	14.98
Nd4061	80.37	38.96	38.75	38.16	49.06	20.88
Ni2316	783.45	362.23	361.72	356.56	465.99	211.66
P_1774	693.54	321.21	326.63	316.05	414.36	186.17
Pb2203	425.11	184.93	186.51	181.25	244.45	120.46
Si2516	-	-	-	-		
Sr3464	276.70	153.90	168.86	227.32	206.70	56.41
Zn2062	58.94	25.59	25.65	25.39	33.89	16.70
Zr3391	84.32	37.07	39.29	38.47	49.79	23.04
	0725-SIM8-LtAtm-384	0725-SIM8-LtAtm-192	0725-SIM8-LtAtm-120	0725-SIM8-LtAtm-0	**AVG**	**SD**
	(ppm)	(ppm)	(ppm)	(ppm)		
Al3082	285.09	263.93	266.77	268.58	271.09	9.52
B_2497	16.08	15.13	15.00	15.43	15.41	0.48
Ca3179	294.64	274.51	280.19	290.77	285.03	9.30
Ce4186	27.89	25.76	26.29	26.42	26.59	0.91
Cr3578	95.87	80.13	81.58	79.44	84.26	7.80
Cu3247	24.40	19.91	20.37	20.20	21.22	2.13
Fe2599	843.92	821.99	826.37	847.01	834.82	12.48
K_7664	1464.92	1290.52	1299.03	1274.52	1332.25	89.03
La3949	12.90	12.07	12.18	12.72	12.47	0.41
Mg2790	-	-	-	-		
Mn2576	430.60	406.35	409.70	415.90	415.64	10.73
Mo2020	27.32	24.45	24.44	24.33	25.14	1.46
Nd4061	42.36	40.20	40.20	40.07	40.71	1.11
Ni2316	390.61	341.59	344.43	343.91	355.14	23.68
P_1774	341.33	329.98	331.79	333.34	334.11	5.01
Pb2203	201.11	186.59	185.81	188.34	190.46	7.18
Si2516	-	-	-	-		
Sr3464	120.87	146.60	164.32	238.03	167.45	50.32
Zn2062	28.61	24.96	25.17	25.54	26.07	1.71
Zr3391	41.98	35.86	37.93	37.59	38.34	2.59

Table E.9 Percent of Cation Mass Present in the Solids Relative to Time Zero Cation Mass in the AN-107 Secondary Effects Study

Element	0.03 M Mn SIM7-DkN2	0.03 M Mn SIM7-LtN2	0.03 M Mn SIM7-DkAtm	0.03 M Mn SIM7-LtAtm	0.01 M Mn SIM7-LtN2	0.01 M Mn SIM7-DkAtm	0.01 M Mn SIM7-LtAtm	0.01 M Mn SIM7-Dk2N2
Al	0.05	0.05	0.03	0.07	0.03	0.09	0.11	0.55
B	0.17	0.13	0.00	0.04	ND	ND	ND	ND
Ca	0.15	0.60	0.11	1.06	2.22	1.57	2.14	0.91
Ce	0.06	2.50	ND	3.78	2.53	1.81	4.52	0.65
Cr	0.08	0.14	0.05	0.15	0.10	0.26	0.71	0.06
Cu	ND	0.09	0.02	0.04	0.26	0.31	0.46	ND
Fe	0.02	0.52	0.02	0.75	0.22	0.79	2.67	0.04
K	0.10	0.11	0.08	0.10	0.10	0.13	0.15	0.10
La	0.36	3.86	ND	7.12	6.34	5.43	8.49	2.79
Mg	ND	ND	ND	ND	ND	ND	ND	ND
Mn	0.04	7.58	0.01	10.01	1.61	1.84	5.57	0.13
Mo	0.06	0.06	0.04	0.06	ND	ND	ND	0.06
Nd	0.03	0.94	ND	1.71	1.06	1.61	2.85	0.50
Ni	0.11	0.11	0.09	0.10	0.11	0.13	0.15	0.10
P	0.05	0.08	0.06	0.07	0.10	0.10	0.11	0.06
Pb	0.09	0.36	0.06	0.45	0.30	0.68	1.83	0.09
Si	ND	ND	ND	ND	ND	ND	ND	ND
Sr	2.46	19.28	0.67	32.51	50.87	33.71	43.63	22.89
Zn	0.01	0.29	0.03	0.16	0.11	0.30	0.99	0.04
Zr	0.11	0.19	0.08	0.21	0.15	0.46	1.12	0.11

APPENDIX F

AN-102 Filtrate and Filter Photographs

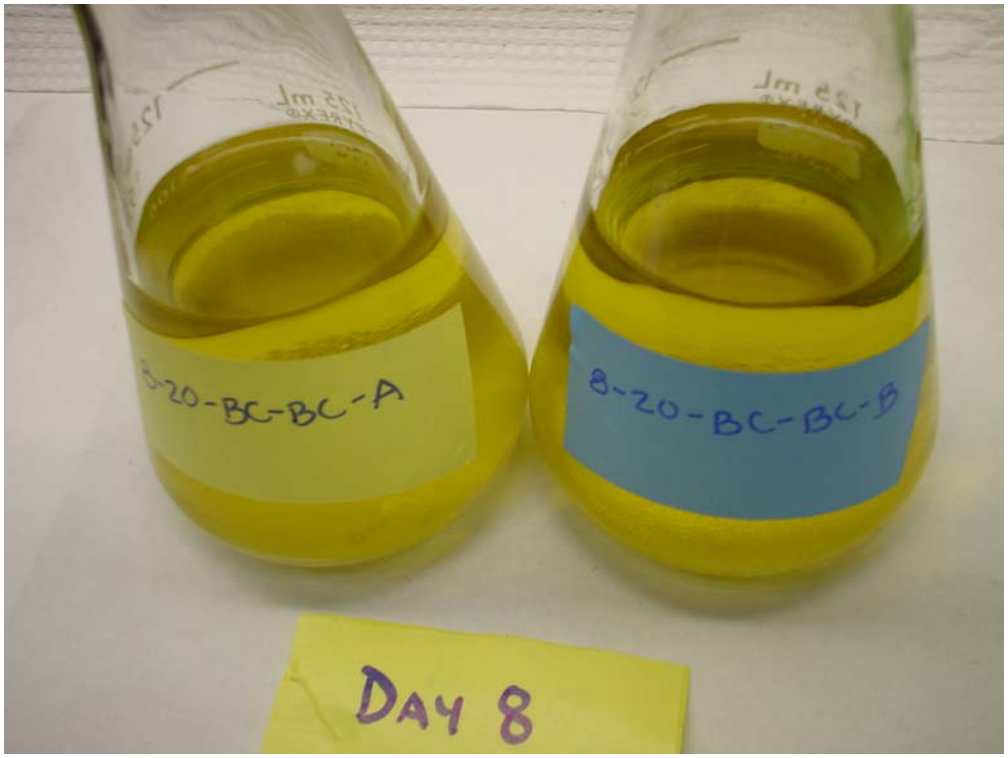

Figure F.1 Simulant AN-102 Sample 8-20-BC-BC Filtrates

Figure F.2 Simulant AN-102 Sample 8-20-BC-BC Filter

Figure F.3 Simulant AN-102 Sample 9-10-BC-BC Filtrates

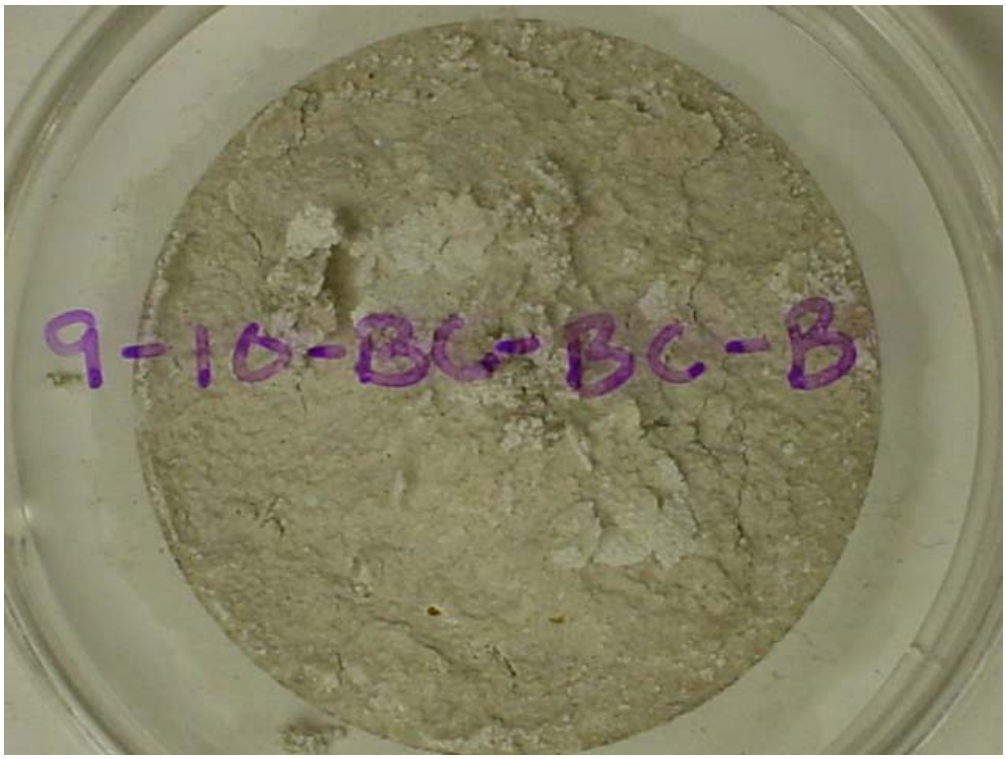

Figure F.4 Simulant AN-102 Sample 9-10-BC-BC Filter

Figure F.5 Simulant AN-102 Sample 8-20-BC-Light Filtrates

Figure F.6 Simulant AN-102 Sample 8-20-BC-Light Filter

Figure F.7 Simulant AN-102 Sample 8-20-BC-O_2 Filtrates

Figure F.8 Simulant AN-102 Sample 8-20-BC-O_2 Filter

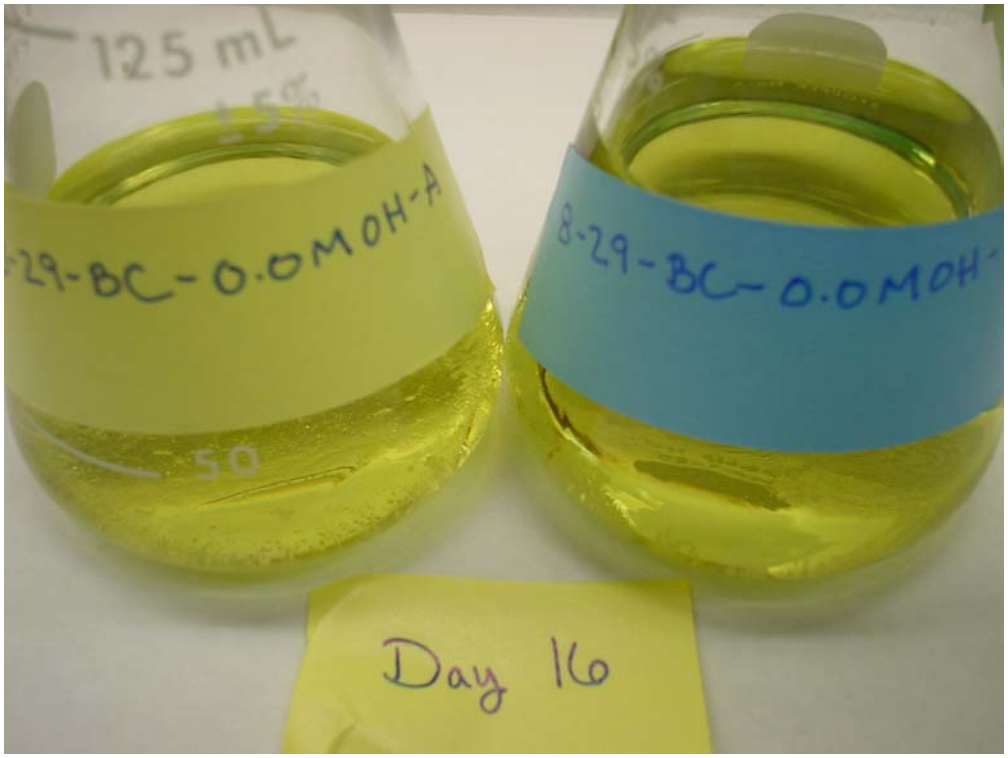

Figure F.9 Simulant AN-102 Sample 8-29-BC-0.0M OH Filtrates

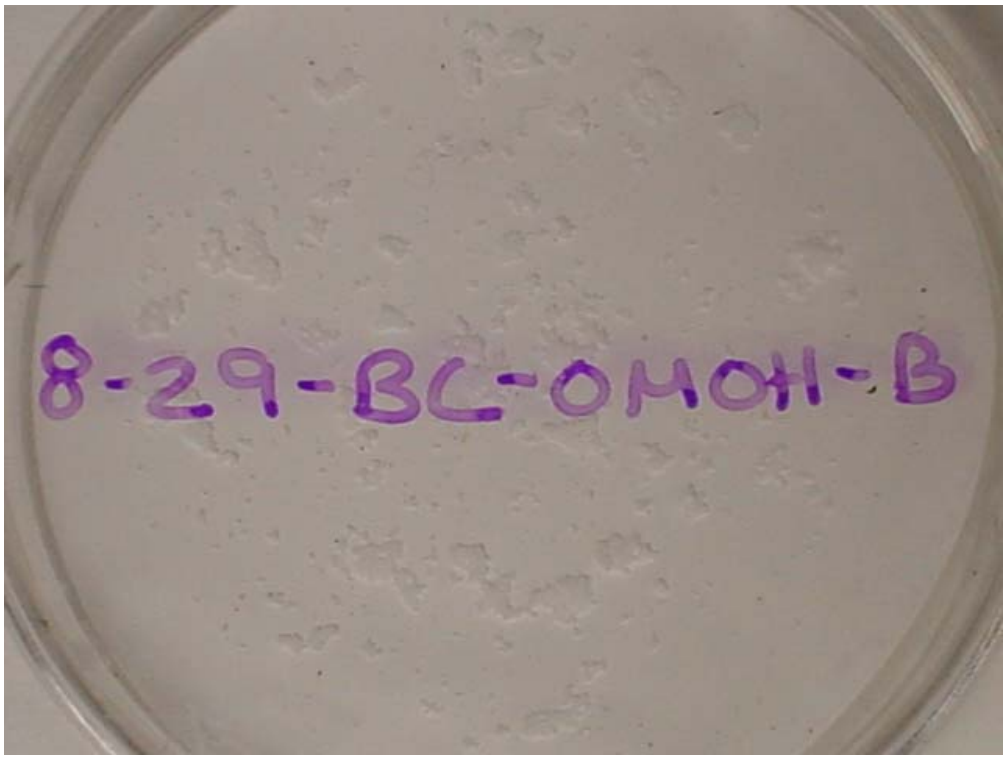

Figure F.10 Simulant AN-102 Sample 8-29-BC-0.0M OH Filter

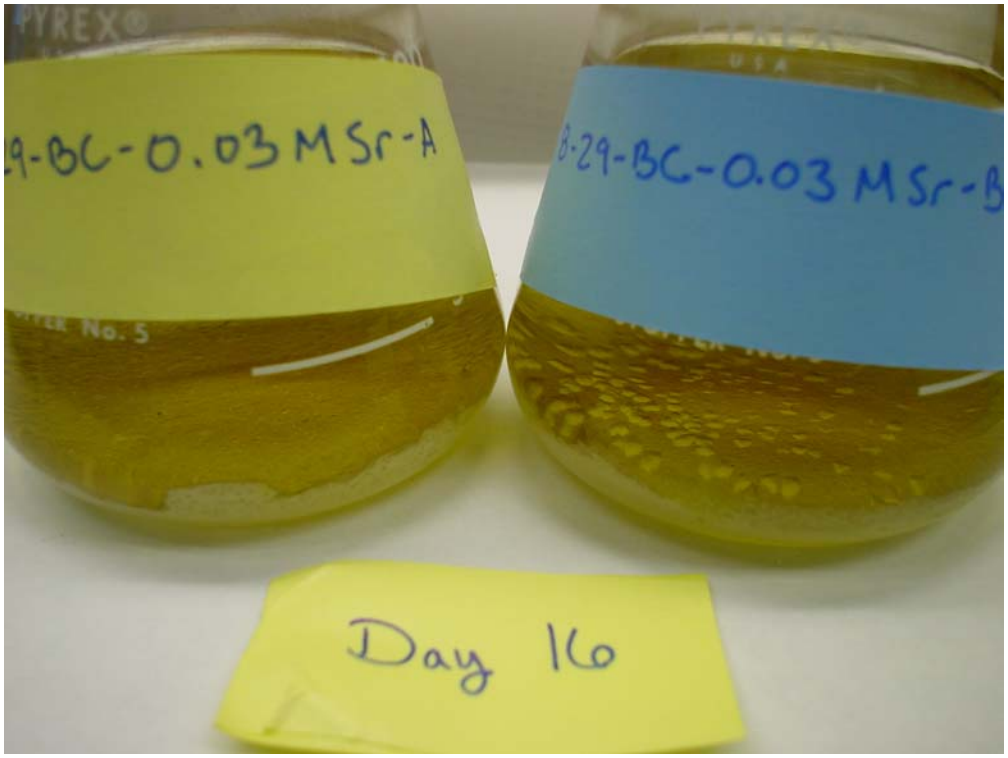

Figure F.11 Simulant AN-102 Sample 8-29-BC-0.03M Sr Filtrates

Figure F.12 Simulant AN-102 Sample 8-29-BC-0.03M Sr Filter

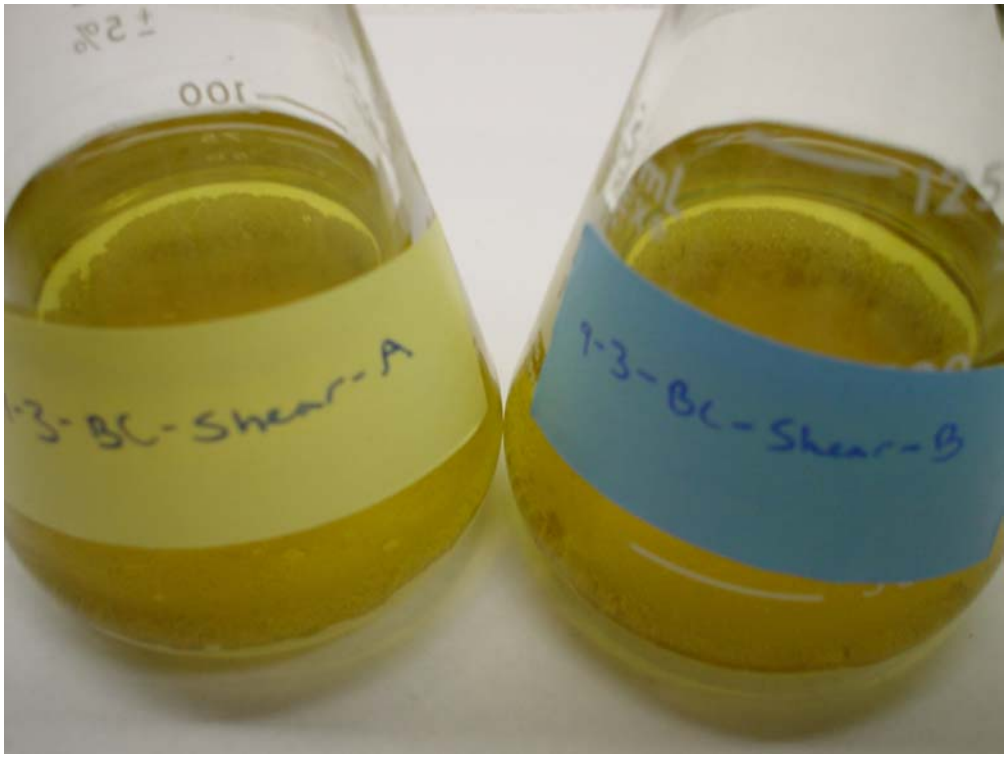

Figure F.13 Simulant AN-102 Sample 9-3-BC-Shear Filtrates

Figure F.14 Simulant AN-102 Sample 9-3-BC-Shear Filter

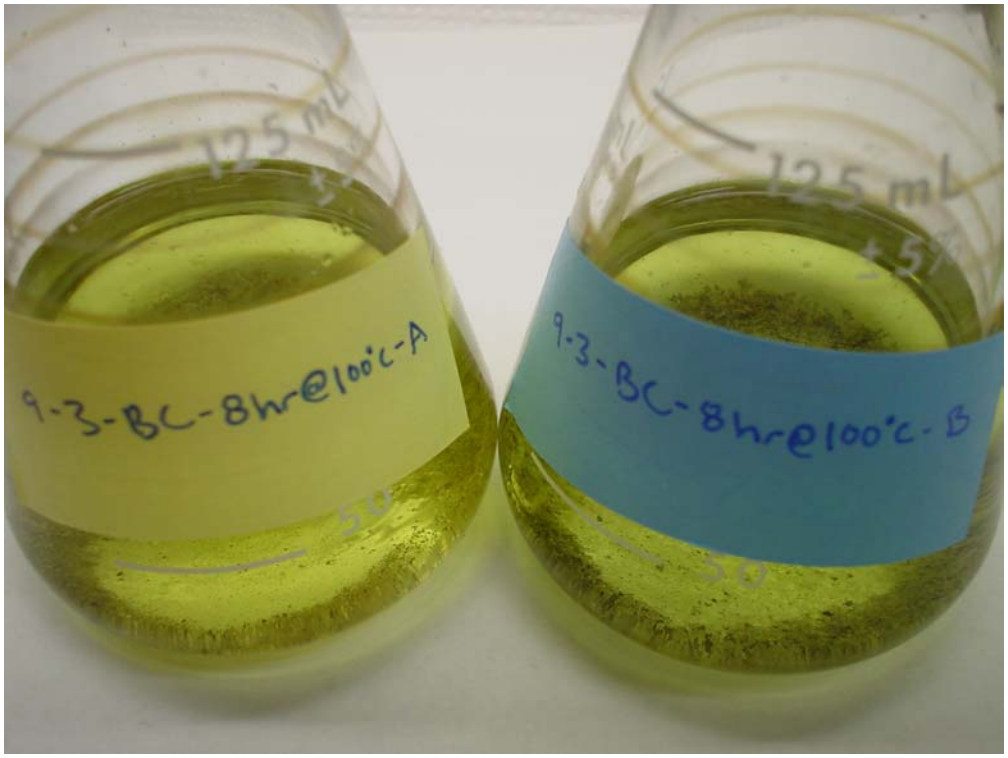

Figure F.15 Simulant AN-102 Sample 9-3-BC-8hr@100°C Filtrates

Figure F.16 Simulant AN-102 Sample 9-3-BC-8hr@100°C Filter

Figure F.17 Simulant AN-102 Sample 9-10-BC-0.01M Mn Filtrates

Figure F.18 Simulant AN-102 Sample 9-10-BC-0.01M Mn Filter

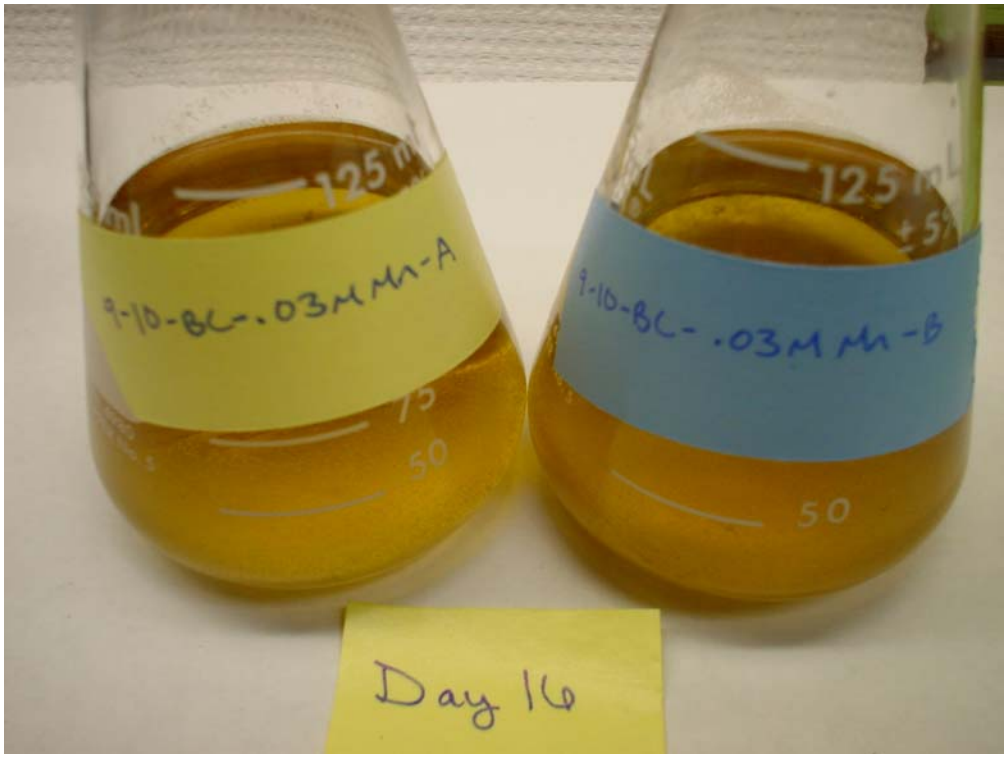

Figure F.19 Simulant AN-102 Sample 9-10-BC-0.03M Mn Filtrates

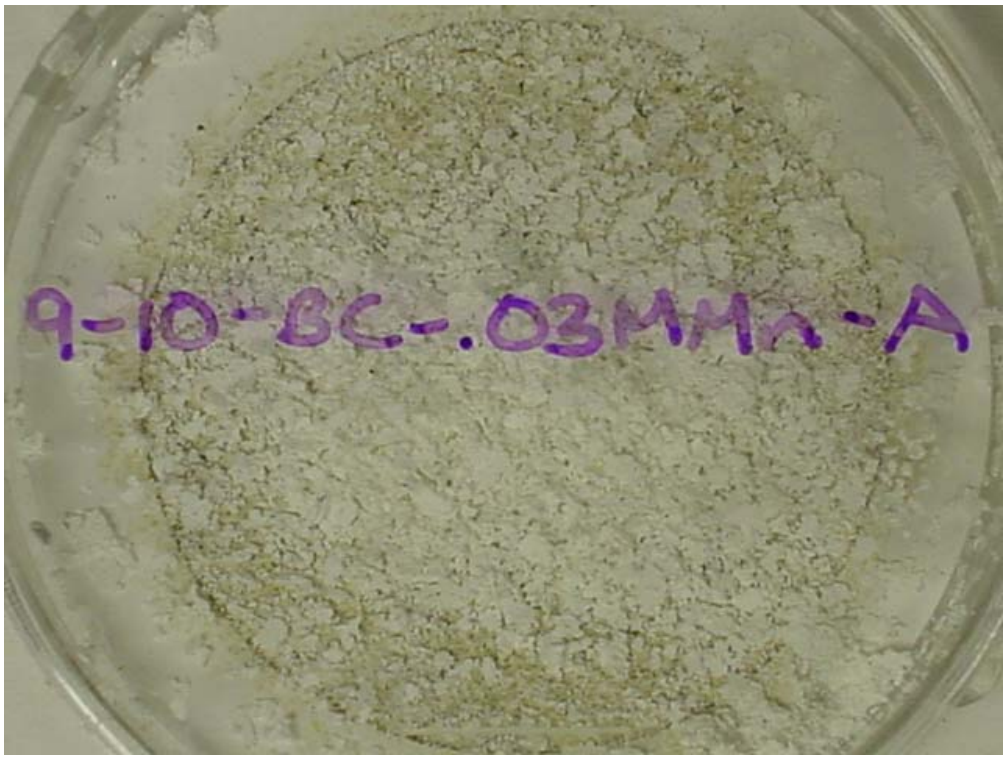

Figure F.20 Simulant AN-102 Sample 9-10-BC-0.03M Mn Filter

Figure F.21 Simulant AN-102 Sample 9-24-BC-25°C Rxn Filtrates

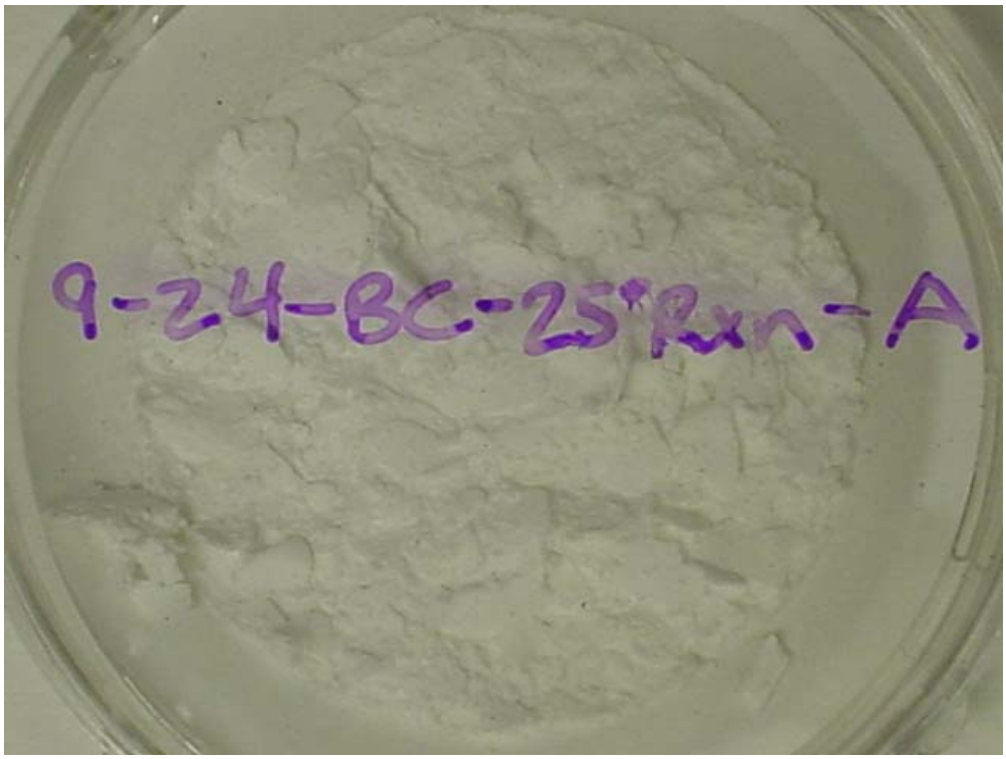

Figure F.22 Simulant AN-102 Sample 9-24-BC-25°C Rxn Filters

Figure F.23 Simulant AN-102 Sample 9-24-NOC-BC Filtrates

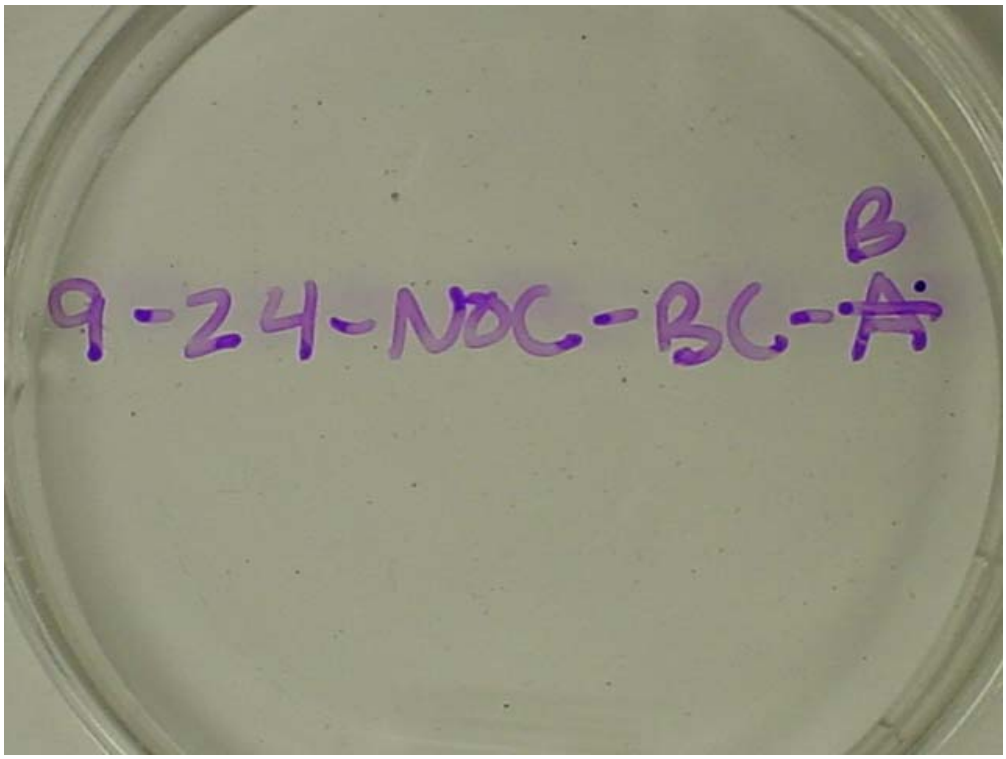

Figure F.24 Simulant AN-102 Sample 9-24-NOC-BC Filter

Figure F.25 Simulant AN-102 Sample 9-24-NOC-0.01M Mn Filtrates

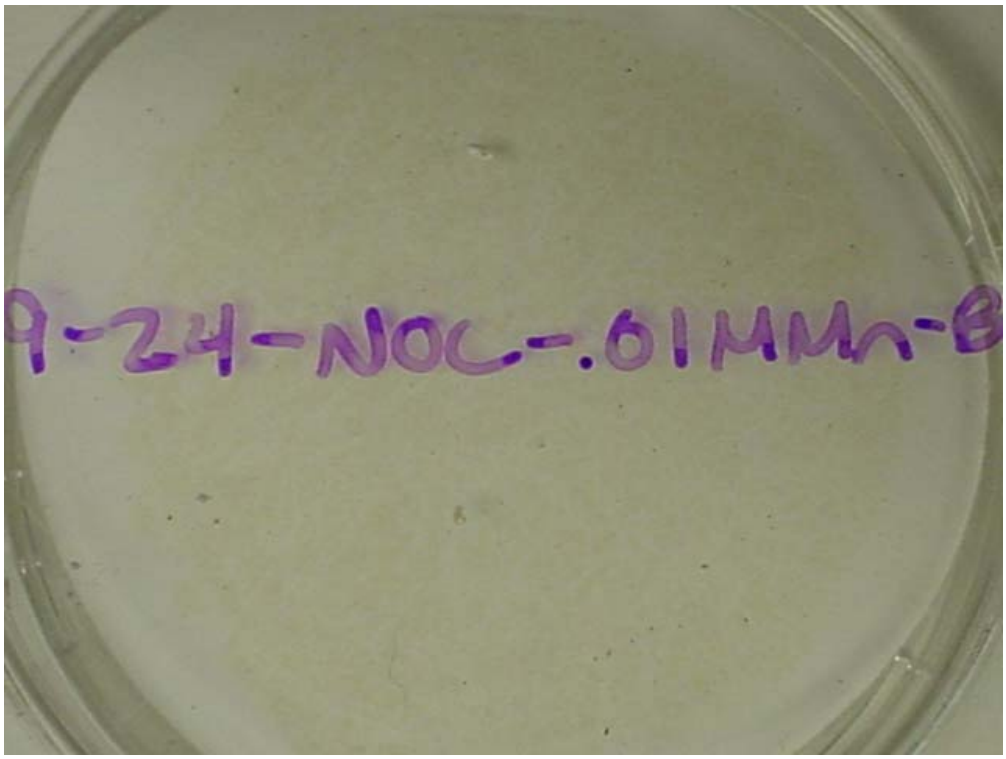

Figure F.26 Simulant AN-102 Sample 9-24-NOC-0.01M Mn Filter

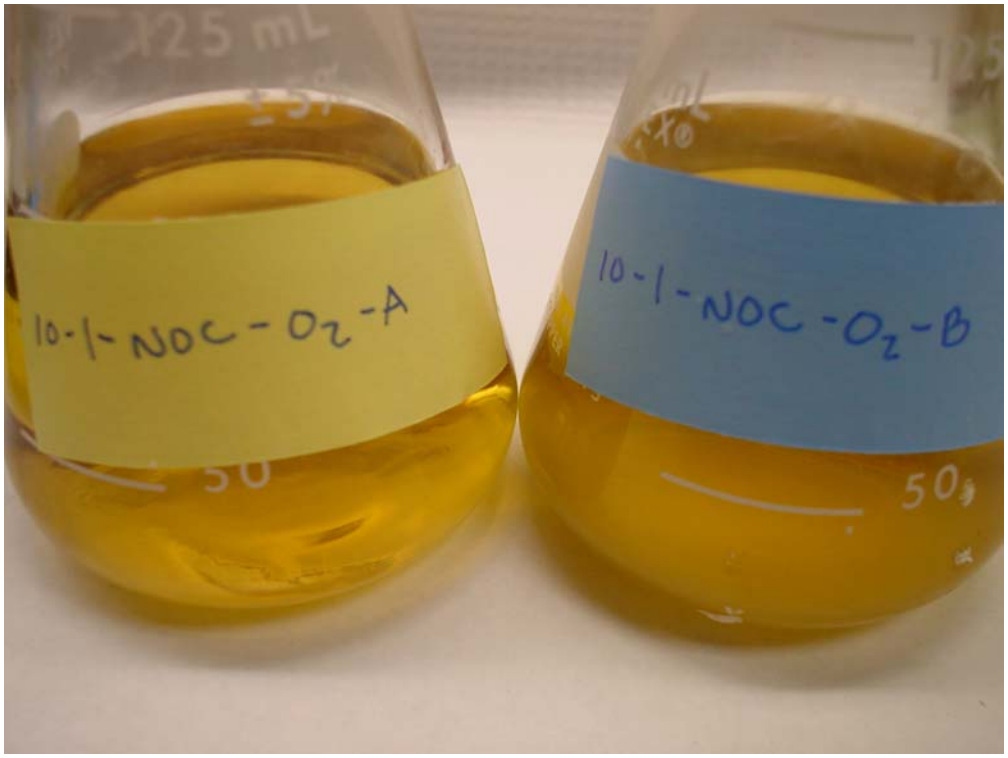

Figure F.27 Simulant AN-102 Sample 10-1-NOC-O_2 Filtrates

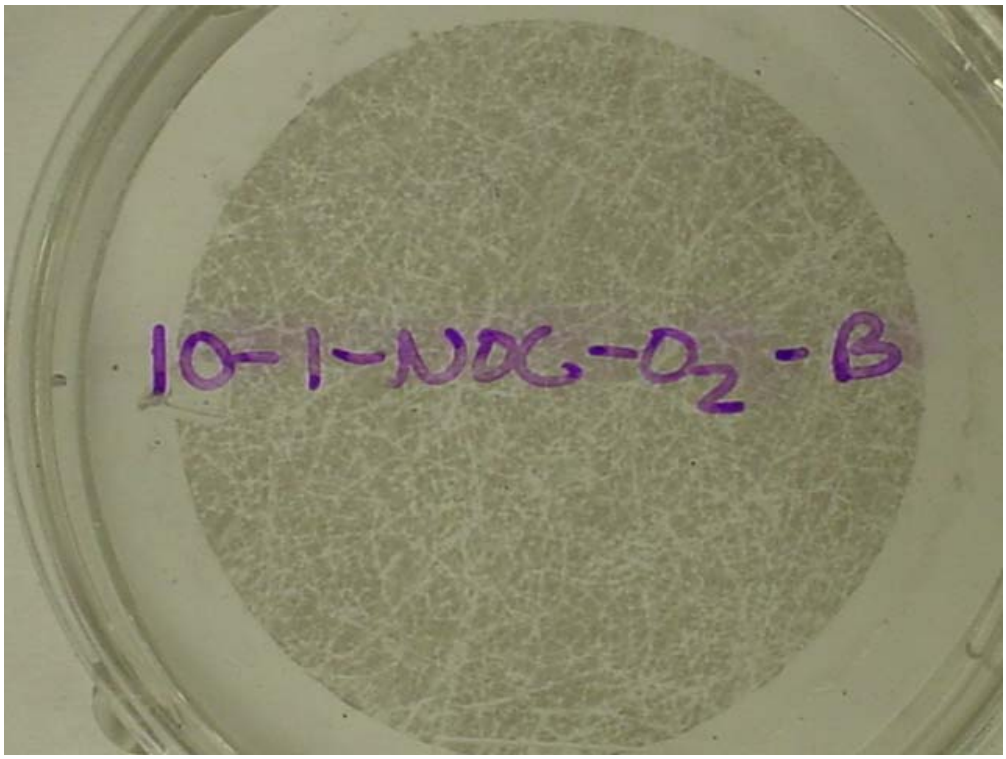

Figure F.28 Simulant AN-102 Sample 10-1-NOC-O_2 Filter

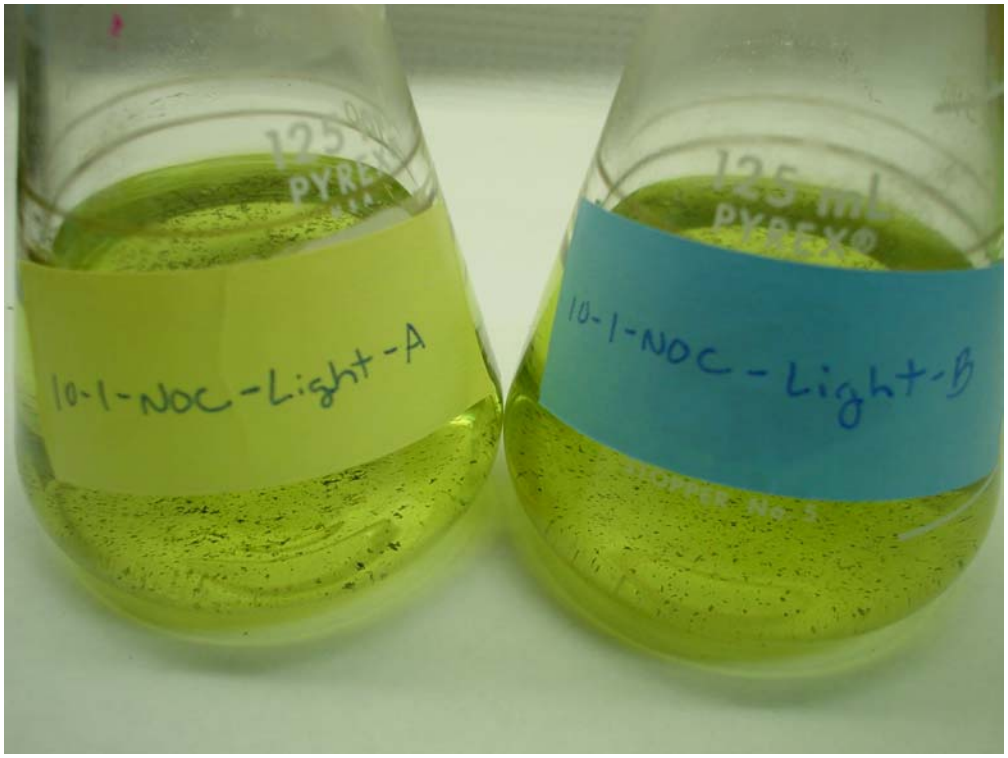

Figure F.29 Simulant AN-102 Sample 10-1-NOC-Light Filtrates

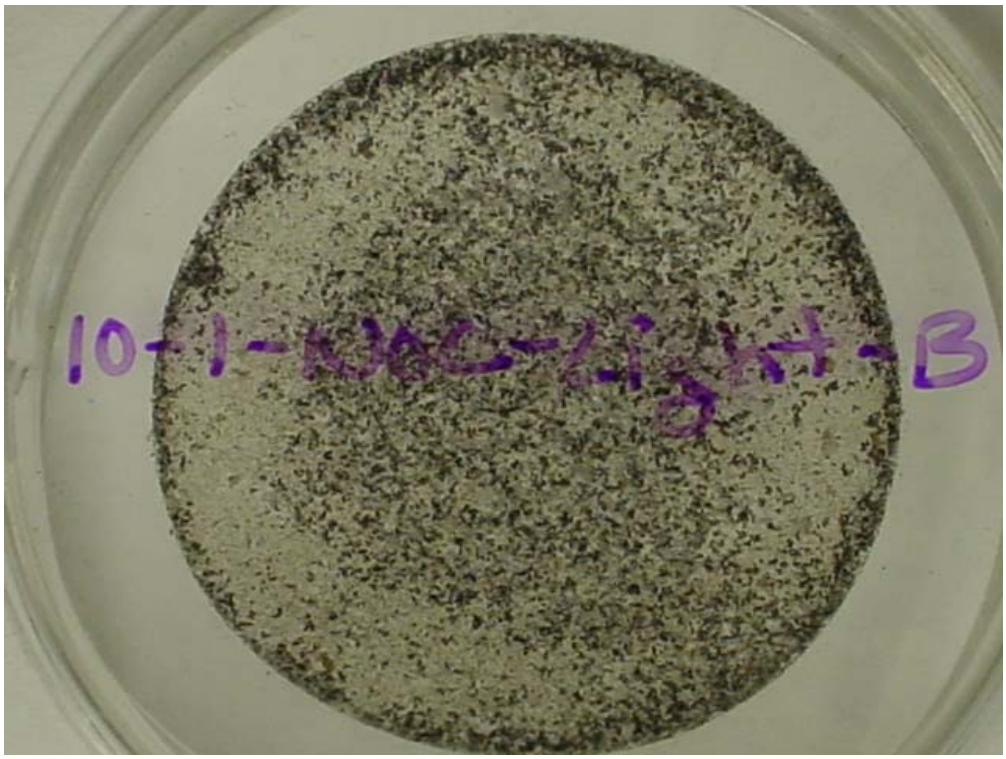

Figure F.30 Simulant AN-102 Sample 10-1-NOC-Light Filter

Figure F.31 Simulant AN-102 Sample 11-19-BC-0.0M OH, 0.03M Sr Filtrates

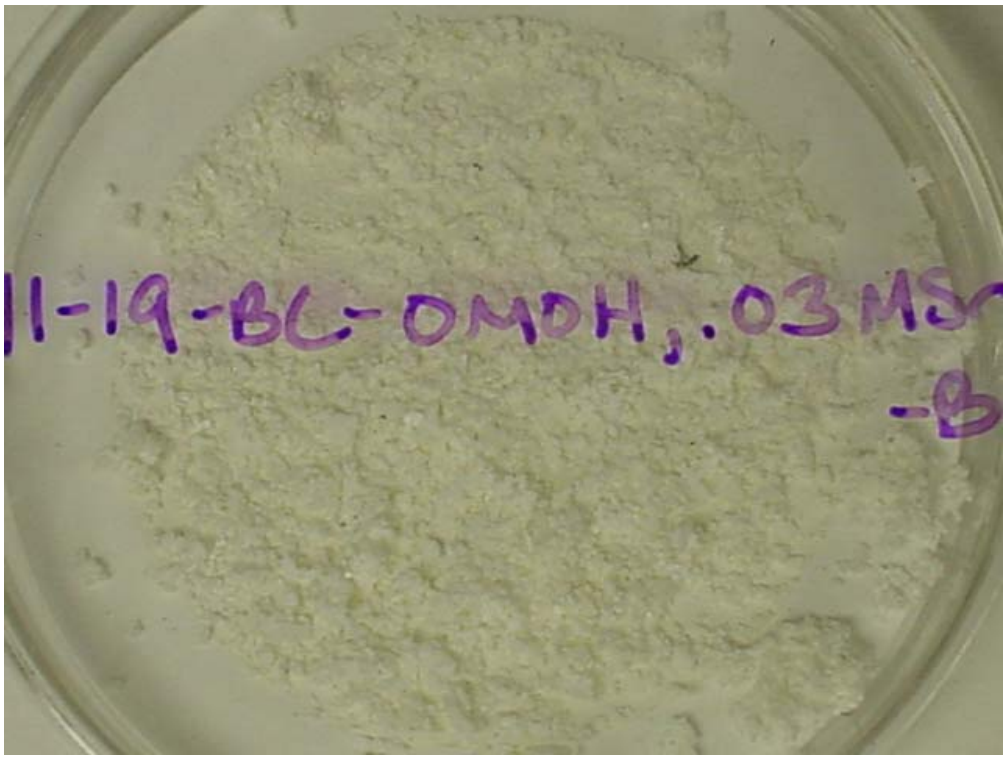

Figure F.32 Simulant AN-102 Sample 11-19-BC-0.0M OH, 0.03M Sr Filter

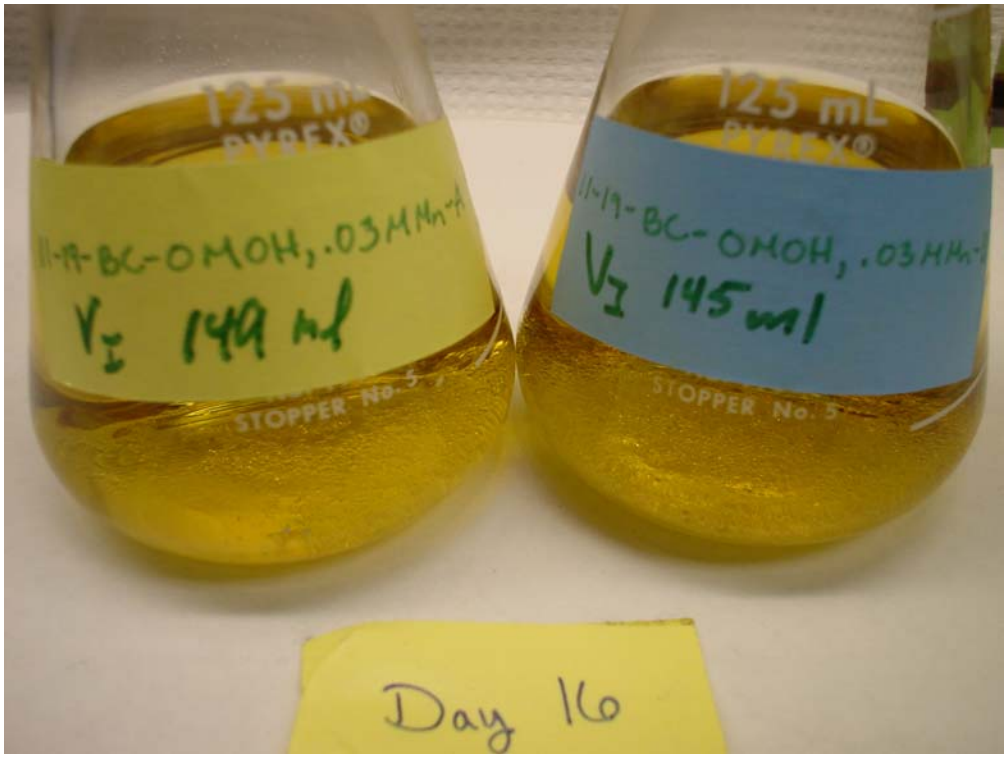

Figure F.33 Simulant AN-102 Sample 11-19-BC-0.0M OH, 0.03M Mn Filtrates

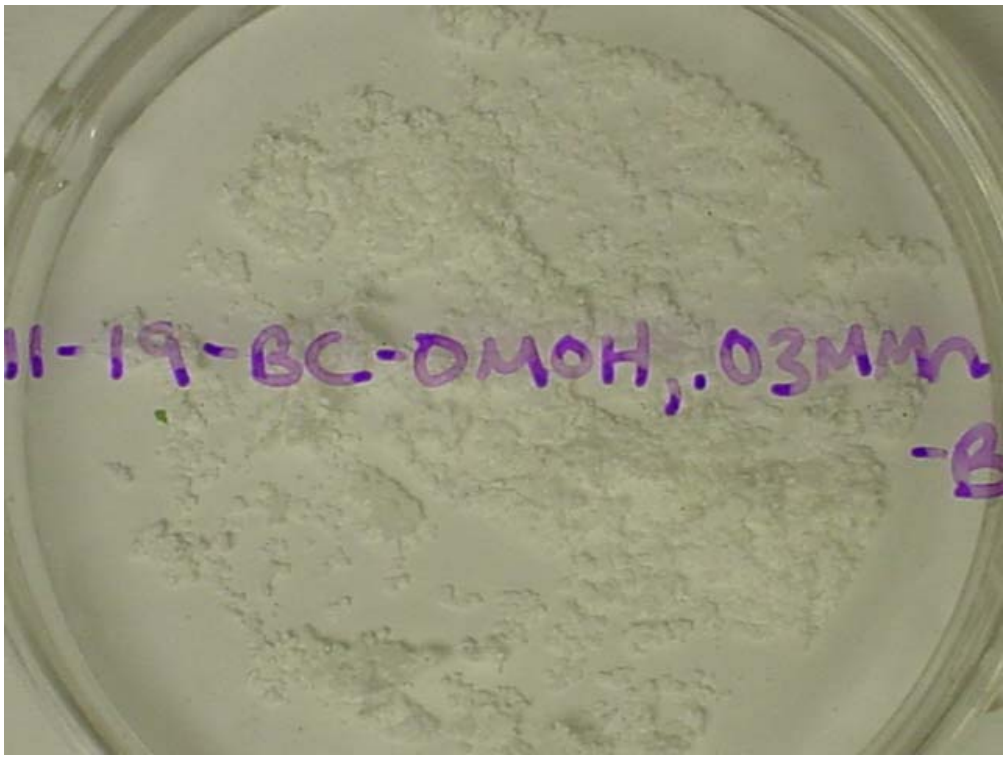

Figure F.34 Simulant AN-102 Sample 11-19-BC-0.0M OH, 0.03M Mn Filter

Figure F.35 Simulant AN-102 Sample 11-19-BC-0.0M OH, Light Filtrates

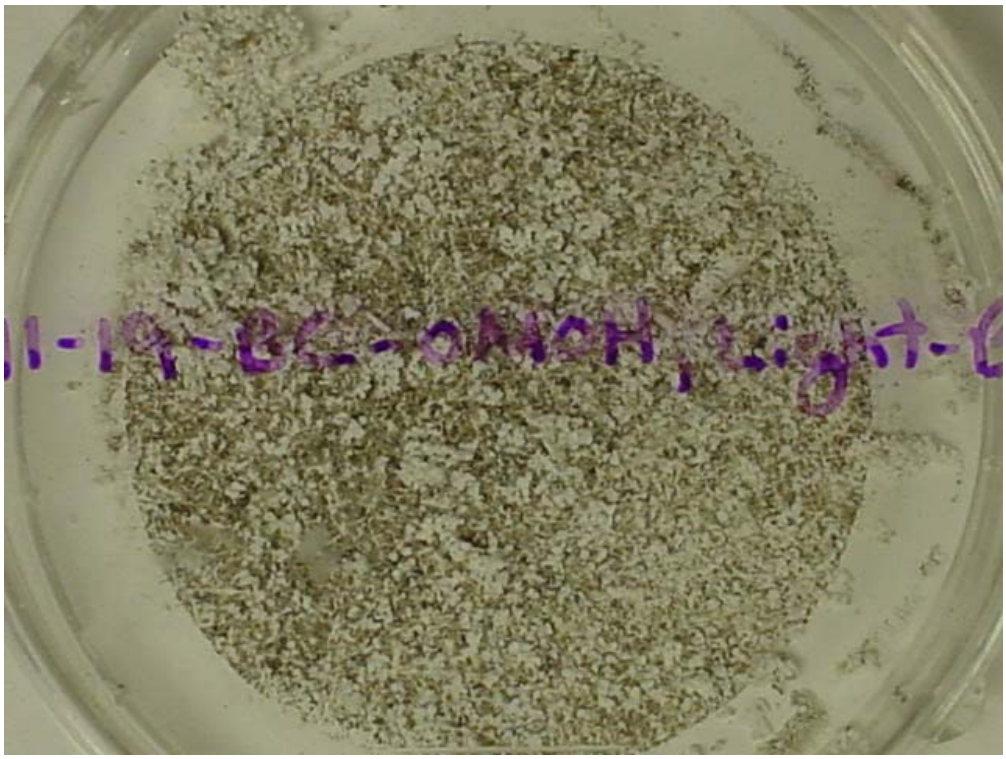

Figure F.36 Simulant AN-102 Sample 11-19-BC-0.0M OH, Light Filter

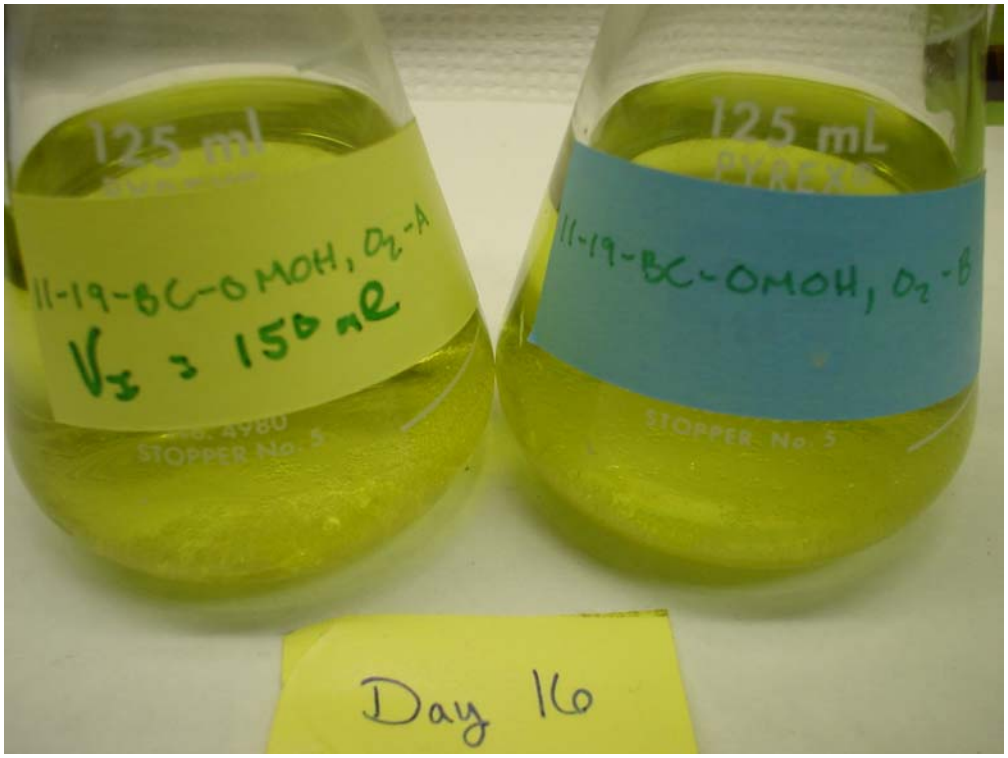

Figure F.37 Simulant AN-102 Sample 11-19-BC-0.0M OH, O_2 Filtrates

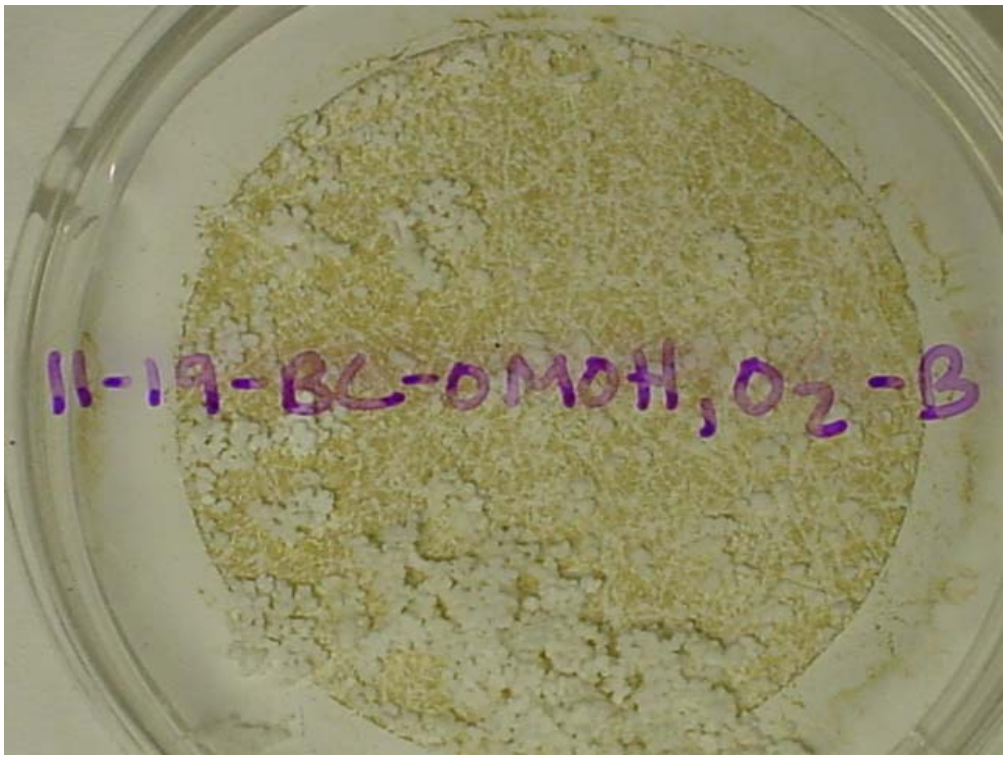

Figure F.38 Simulant AN-102 Sample 11-19-BC-0.0M OH, O_2 Filter

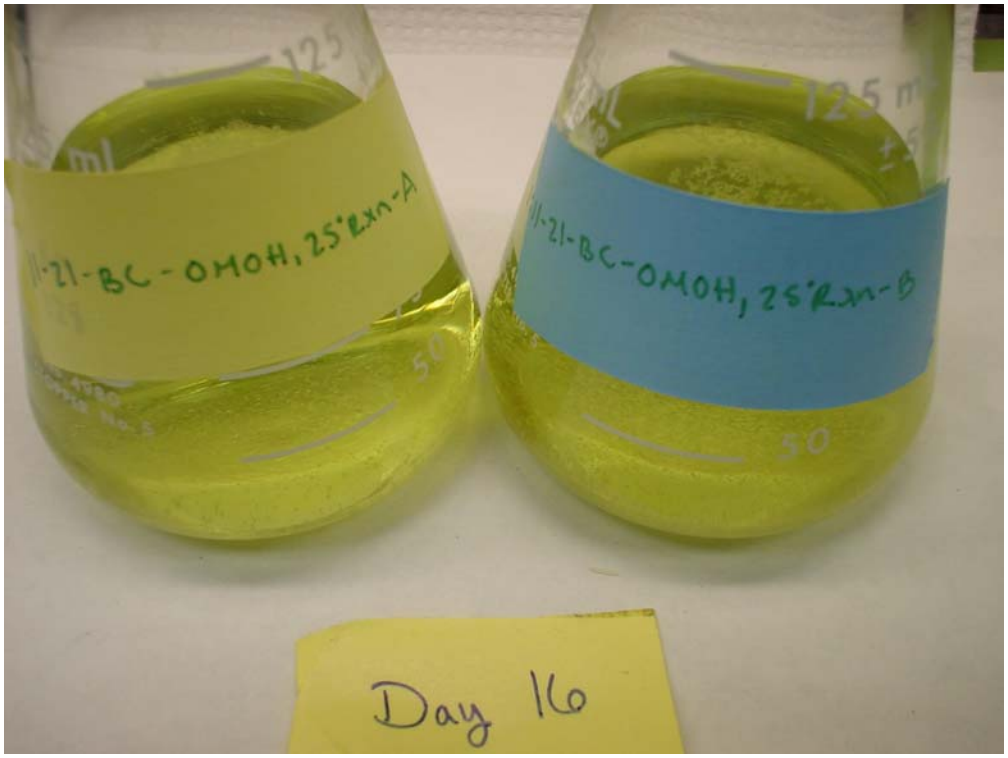

Figure F.39 Simulant AN-102 Sample 11-19-BC-0.0M OH, 25°C Rxn Filtrates

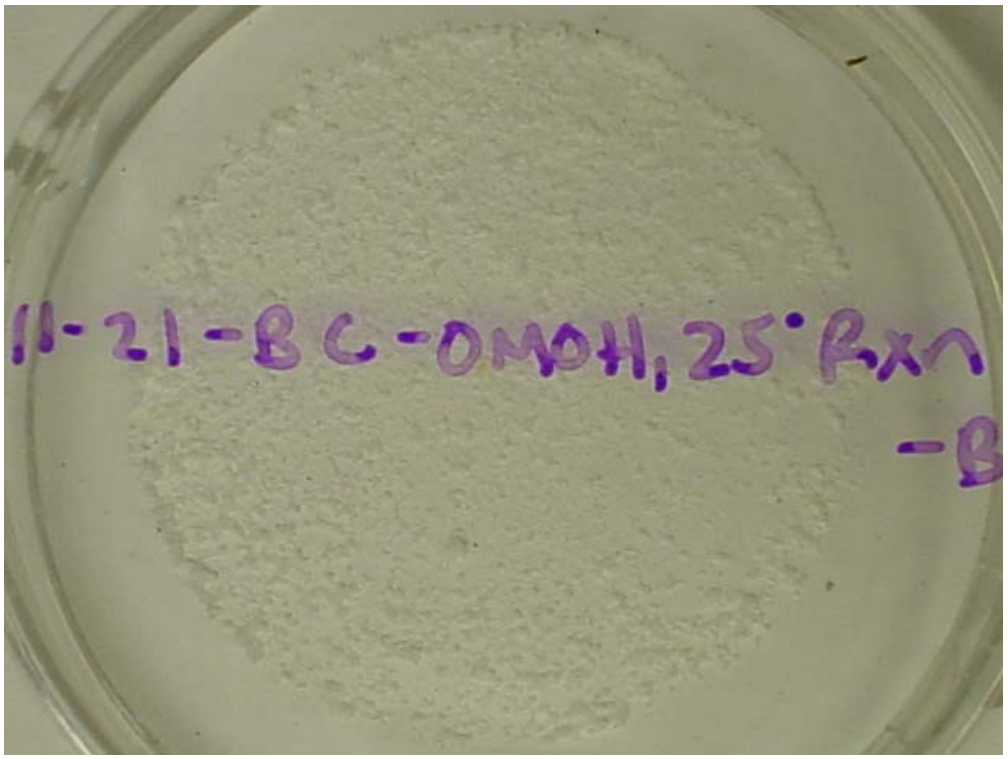

Figure F.40 Simulant AN-102 Sample 11-19-BC-0.0M OH, 25°C Rxn Filter

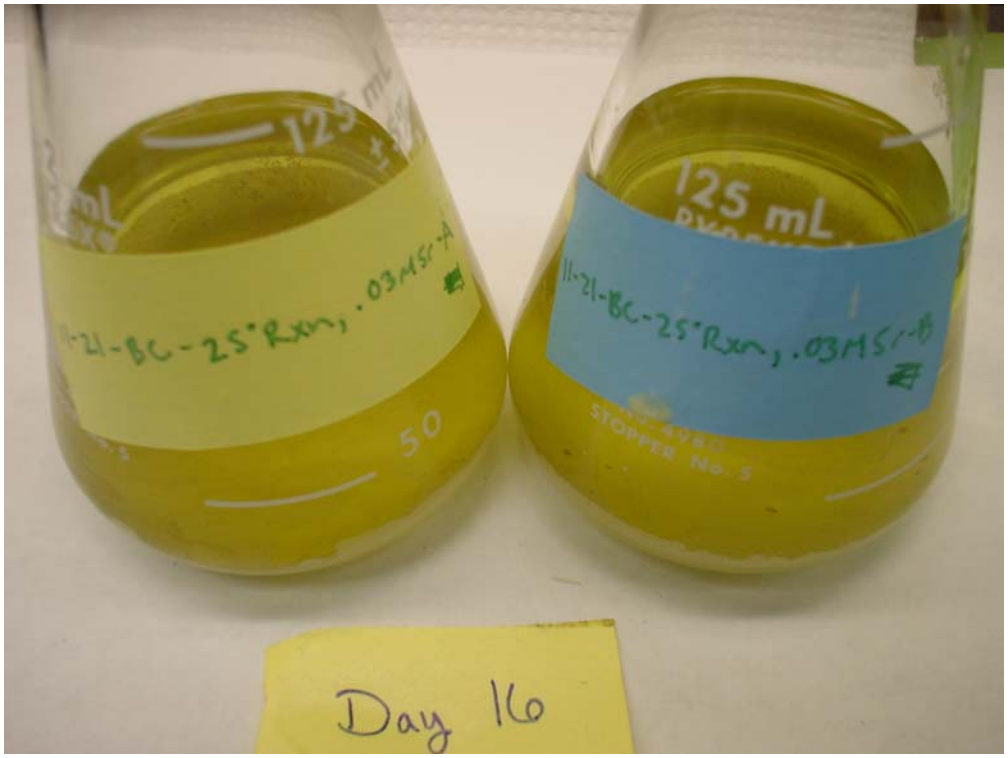

Figure F.41 Simulant AN-102 Sample 11-19-BC-25°C Rxn, 0.03M Sr Filtrates

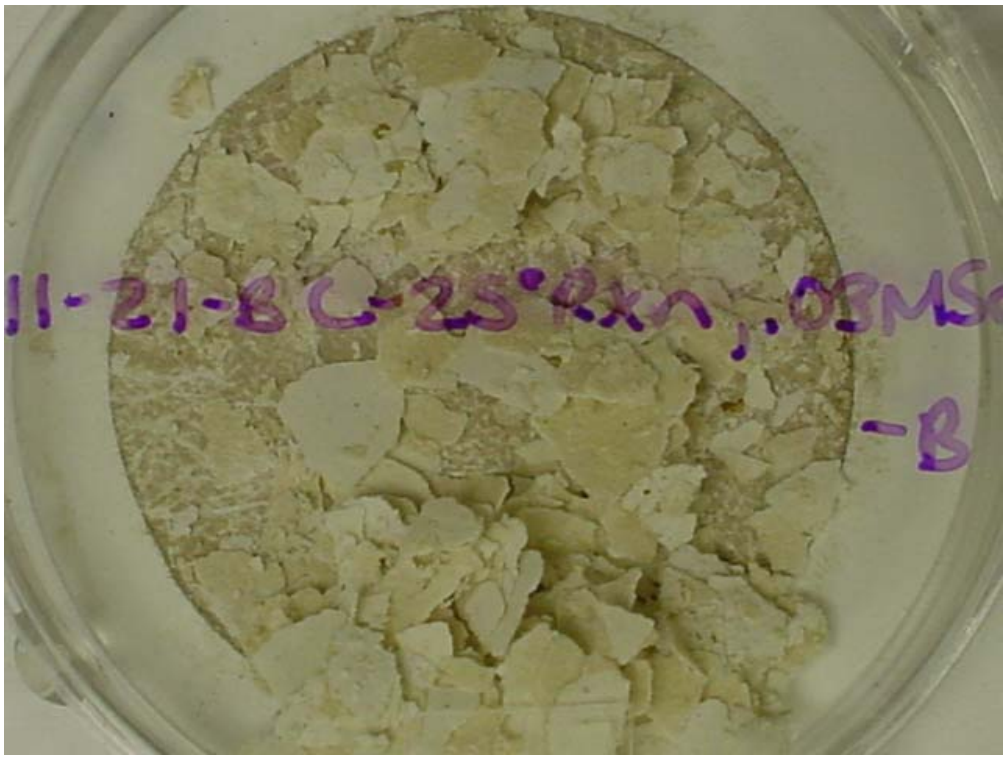

Figure F.42 Simulant AN-102 Sample 11-19-BC-25°C Rxn, 0.03M Sr Filter

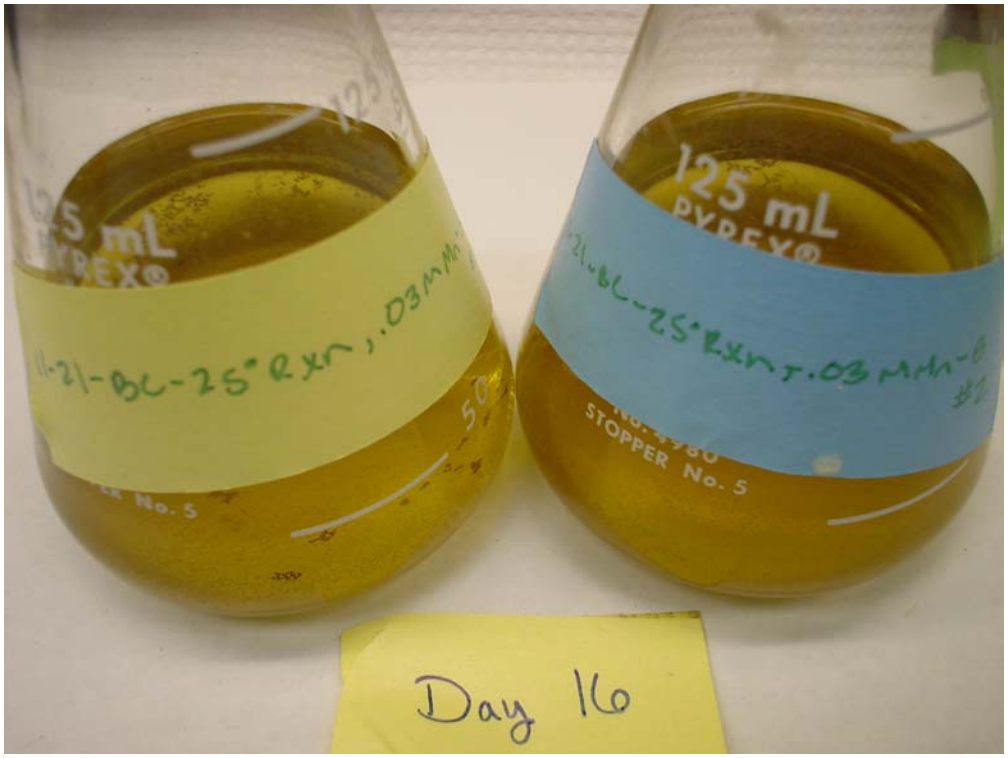

Figure F.43 Simulant AN-102 Sample 11-19-BC-25°C Rxn, 0.03M Mn Filtrates

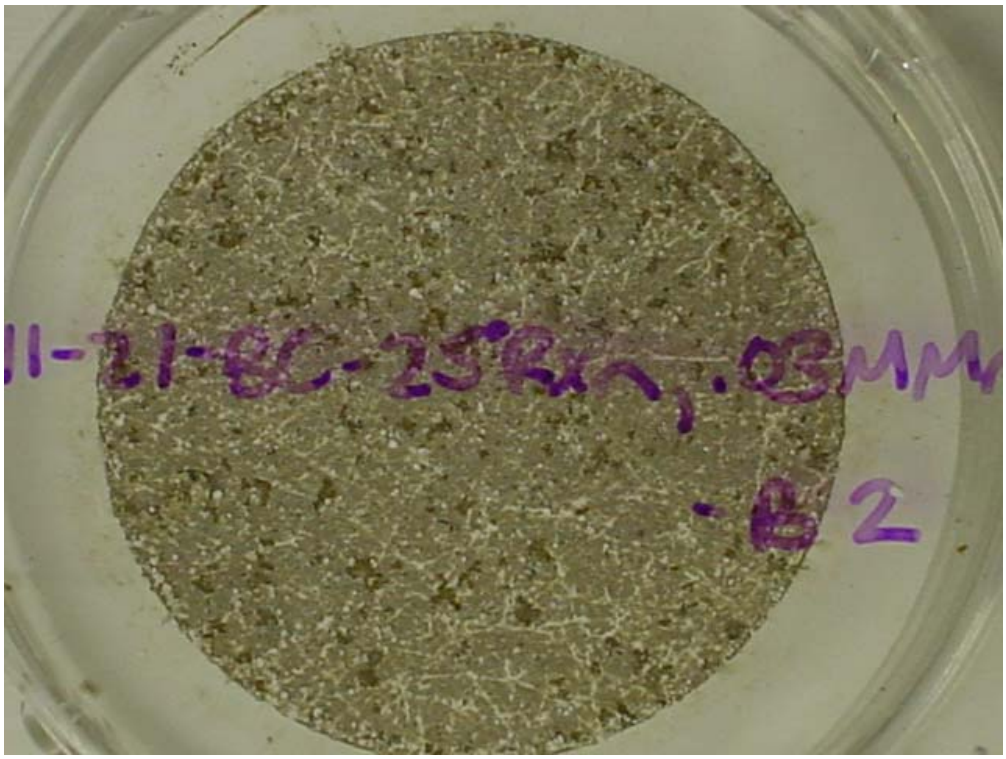

Figure F.44 Simulant AN-102 Sample 11-19-BC-25°C Rxn, 0.03M Mn Filter

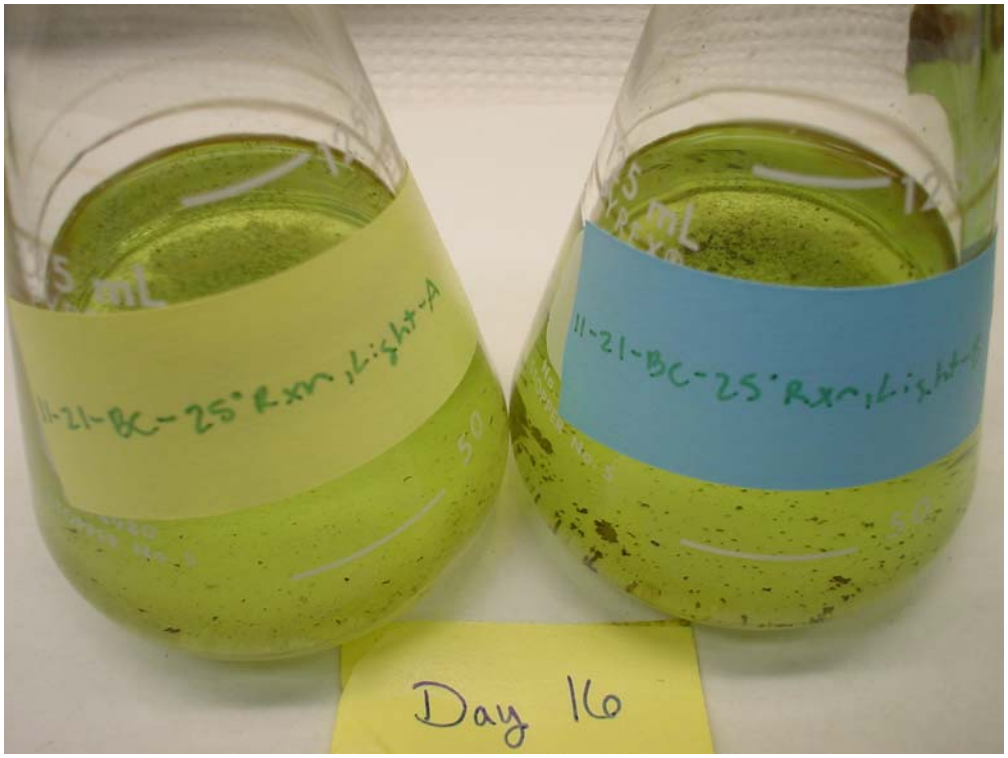

Figure F.45 Simulant AN-102 Sample 11-19-BC-25°C Rxn, Light Filtrates

Figure F.46 Simulant AN-102 Sample 11-19-BC-25°C Rxn, Light Filter

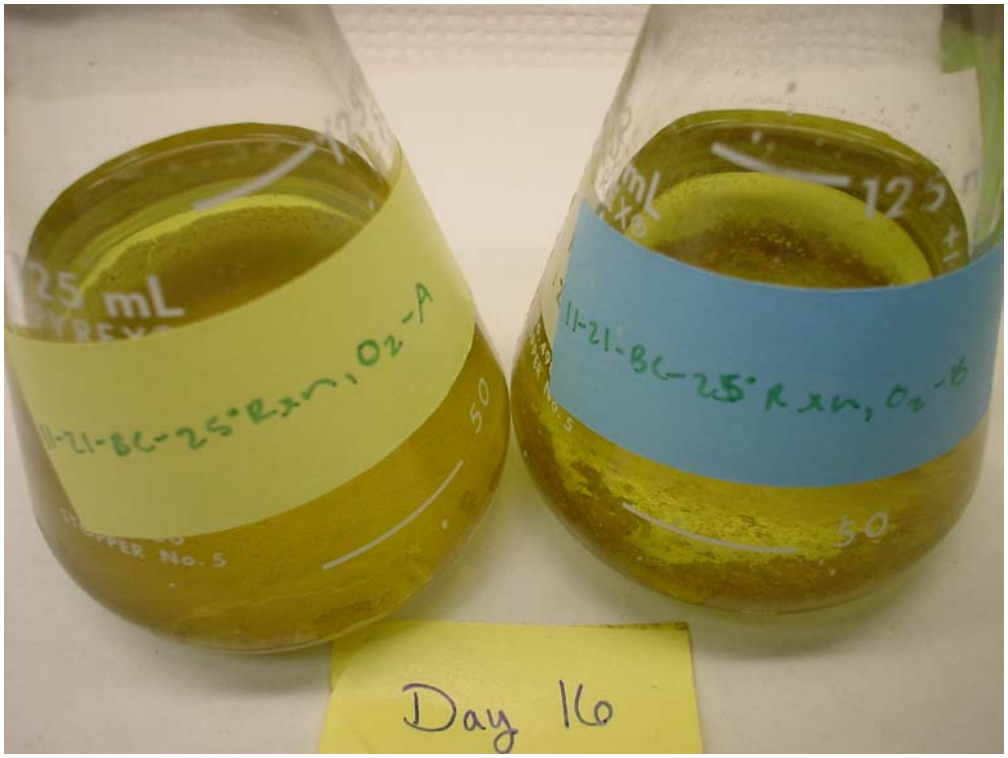

Figure F.47 Simulant AN-102 Sample 11-19-BC-25°C Rxn, O_2 Filtrates

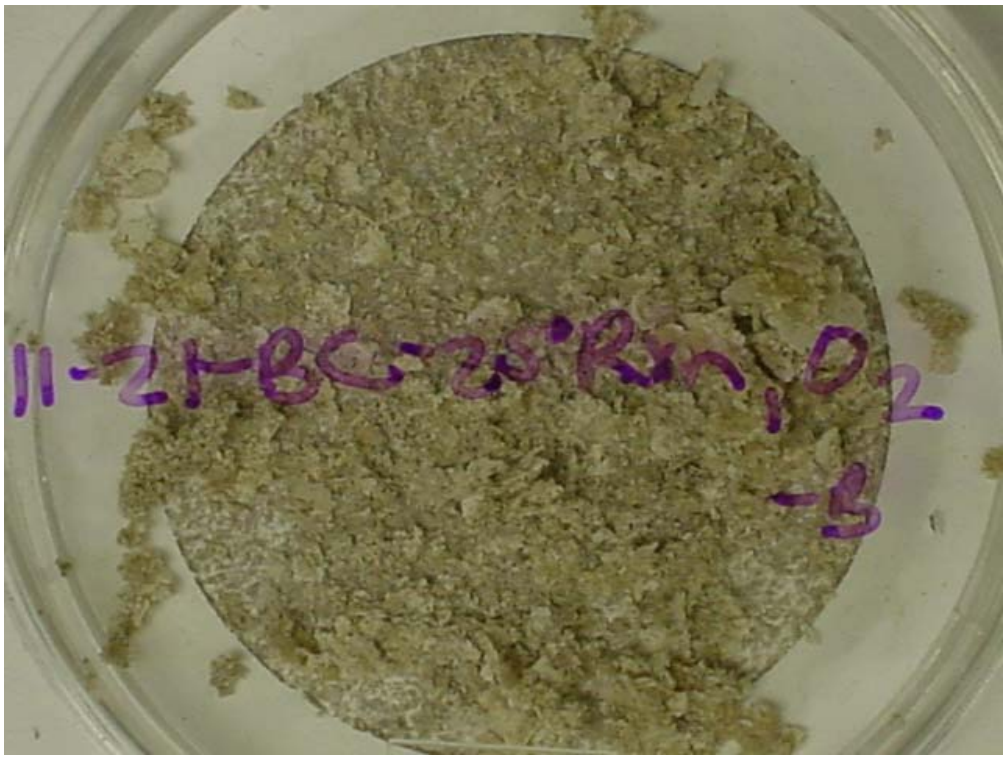

Figure F.48 Simulant AN-102 Sample 11-19-BC-25°C Rxn, O_2 Filter

APPENDIX G

ICP-AES Analysis of AN-102 Primary and Secondary Effects Samples

Table G.1 ICP-AES Data for AN-102 Primary Effects Samples

	8-20-BC-BC-A-			8-20-BC-BC-B-			8-20-BC-Light-A-			8-20-BC-Light-B-			8-20-BC-O2-A-			8-20-BC-O2-I	
	0	8	16	0	8	16	0	8	16	0	8	16	0	8	16	0	8
Al	9939.046	9711.868	9535.174	10500.68	10216.71	10494.37	9800.215	9390.032	9749.731	10103.12	10506.99	10513.3	9743.421	9440.516	9686.626	10260.88	10229.33
B	11.92054	12.84188	12.05307	13.79477	13.29624	14.35009	13.18265	11.4157	13.13216	13.29624	14.40688	14.46368	12.4317	11.56085	12.50742	13.29624	13.84525
Ca	58.23335	57.65278	57.79161	57.45084	55.34944	57.45715	85.38114	57.91151	102.7981	55.94263	59.77311	64.99821	61.89975	60.30319	68.5952	77.80853	56.8829
Ce	0.113589	0.100968	-0.25873	-0.11359	-0.04417	-0.25873	0.075726	-0.25873	-0.24611	-0.00631	-0.05048	0.056795	-0.27135	-0.13883	-0.39125	0.227178	0.107279
Cr	204.6497	200.9896	199.7906	214.4941	210.6447	215.7562	201.9362	187.8638	193.6694	205.5963	212.7902	214.431	203.1352	197.7712	200.2954	215.9455	205.6594
Cu	2.978559	2.61886	2.404303	3.142632	3.079527	3.174184	3.010111	2.49896	2.587307	3.098458	2.890212	2.776622	2.549444	2.467408	2.555755	2.74507	2.574686
Fe	5.294514	5.793044	6.026533	6.272643	5.654213	6.152743	6.998351	5.925565	6.24109	6.159053	5.837218	6.272643	6.089638	6.045464	6.228469	6.039154	5.944496
K	1664.711	1635.683	1637.576	1764.417	1730.972	1776.407	1648.935	1556.802	1619.907	1724.661	1760	1765.679	1636.945	1597.82	1626.848	1772.621	1701.943
La	0.063105	-0.01262	-0.00631	0.201936	0.107279	0.189315	-0.01262	0.012621	-0.04417	0.189315	0.347078	0.25242	0.012621	-0.07573	0.100968	0.157763	0.138831
Mg	3.420294	4.202797	2.795554	4.903263	4.953747	3.634851	3.571746	3.811545	5.250341	3.773682	4.549875	2.290714	2.303335	1.678594	3.344568	4.562496	2.044604
Mn	16.02868	15.76995	11.06863	19.7014	18.60337	15.97189	16.23062	9.680316	2.953317	19.87809	10.91086	4.032413	15.73209	9.421585	7.048835	18.88103	12.70305
Mo	37.73051	37.14364	36.60093	39.8256	38.99892	39.86977	37.44023	35.35776	36.68928	38.94844	40.04647	40.29889	37.16257	36.25385	36.99849	40.4882	38.72126
Nd	2.013051	1.924704	2.530513	2.726138	2.75138	3.098458	1.99412	2.00043	1.918394	2.240229	2.74507	3.294084	1.779563	1.817426	2.233919	3.186805	2.555755
Ni	289.2736	286.8125	283.7203	308.0158	299.6228	309.0255	288.7056	271.7935	281.0068	300.5694	308.7099	311.4866	289.6522	281.133	287.6328	311.2972	295.7103
P	1328.361	1149.774	1051.33	1632.528	912.4991	912.4991	1260.208	1193.948	1237.49	1405.981	1033.661	977.4973	1210.986	1090.455	1070.262	1647.673	936.479
Pb	40.99935	40.79742	39.74987	45.82058	45.15167	44.97497	41.49788	38.96106	40.55131	45.75748	47.65063	45.20846	40.43141	39.03048	40.545	45.2337	43.98422
Si	3.912513	6.058085	6.821657	7.74299	8.329867	11.23901	14.26174	6.821657	21.73338	5.830907	8.632772	10.93611	5.401793	6.651273	10.32399	16.09179	8.449767
Sr	26.64295	26.78179	26.07501	28.78222	27.12886	28.66863	25.75317	24.55418	25.45658	28.10699	29.79821	29.95597	26.13811	24.90125	25.80366	27.82933	27.67157
Zn	1.602868	1.937325	1.583937	1.893152	1.886841	1.899462	1.905773	1.716458	2.031983	1.842668	5.199857	2.467408	1.602868	1.571316	2.240229	2.050914	1.817426
Zr	0.694156	0.713087	0.713087	0.927644	0.908713	0.908713	0.75095	0.694156	0.675224	0.927644	0.952886	0.959197	0.719398	0.681535	0.719398	0.915023	0.864539

	8-29-BC-0MOH-A-			8-29-BC-0MOH-B-			8-29-BC-.03MSr-A-			8-29-BC-.03MSr-B-			9-3-BC-Shear-A-			9-3-BC-Shear	
	0	8	16	0	8	16	0	8	16	0	8	16	0	8	16	0	8
Al	9667.179	9812.55	9447.057	9751.979	9739.865	9194.677	9708	8976	9539.773	9768	9852	9542.614	9888.55	9326.915	9552.396	9781.271	9774.961
B	13.15609	13.18031	17.43719	12.88957	12.22329	17.55765	13.326	12.3	18.19886	12.72	13.02	18.21023	11.51035	11.9647	17.70943	12.67779	12.75352
Ca	48.82652	77.10726	46.89113	52.72126	53.33908	46.03074	82.98	69.54	69.0625	80.46	102.84	63.94886	60.41039	56.30226	59.87802	60.24632	58.51093
Ce	-0.03029	0.0424	#VALUE!	-0.19383	-0.01817	#VALUE!	0.198	-0.108	#VALUE!	-0.342	0.252	#VALUE!	-0.22718	0.283972	#VALUE!	#VALUE!	-0.0631
Cr	200.6121	204.7916	209.0169	204.0041	199.7036	201.0153	201.66	189.78	208.2102	198.84	198.3	203.2386	207.6785	189.0625	208.0791	203.4504	209.7609
Cu	4.336905	4.439876	4.34209	4.427762	4.45199	4.433865	3.66	3.192	3.383523	3.906	3.75	3.204545	2.858655	2.833413	3.155249	2.555752	2.883897
Fe	5.675531	5.984444	3.103132	6.093473	5.778502	2.753241	5.82	5.73	2.59375	6.012	5.292	2.991477	6.260014	5.673137	3.301657	5.988662	5.45227
K	1637.848	1670.556	1631.869	1660.865	1636.636	1581.393	1627.2	1586.4	1630.114	1624.2	1630.2	1618.182	1680.486	1537.868	1626.925	1635.681	1672.282
La	-0.11509	-0.01817	#VALUE!	0.030286	-0.02423	#VALUE!	0.192	0.072	#VALUE!	0.252	0.24	#VALUE!	0.145141	0.201936	#VALUE!	0.183004	0.13252
Mg	3.010393	3.585821	#VALUE!	3.216336	3.785706	#VALUE!	1.002	4.11	#VALUE!	4.698	5.136	#VALUE!	3.956682	5.307128	#VALUE!	2.454784	5.010535
Mn	4.83359	5.009246	4.712057	4.518619	4.53679	4.445337	18.33	17.178	12.1108	18.324	17.802	11.5	15.70683	14.51414	10.72067	16.25584	15.82042
Mo	37.43306	37.96609	35.99289	37.82072	37.24529	35.01778	36.948	35.4	35.96591	36.678	36.696	35.22727	37.56639	34.9286	35.49655	37.22563	37.62319
Nd	1.193255	0.860112	#VALUE!	1.502168	1.798968	#VALUE!	3.456	2.862	1.911932	3.63	2.484	1.815341	3.641157	3.275148	1.691166	4.007166	4.347933
Ni	311.9422	316.3033	304.8641	316.3033	311.6999	299.9885	286.38	277.62	284.9432	286.14	284.52	282.3011	291.2926	271.3514	281.3729	293.5643	297.6662
P	1513.071	1528.82	1393.828	1420.397	1397.986	1348.228	1556.4	885	872.1591	1530.6	1089.6	916.4773	1520.83	1352.971	1193.975	1515.15	1157.976
Pb	41.04311	40.94014	36.45176	38.35375	37.53603	32.89549	36.936	34.752	32.92614	38.64	38.046	34.17614	38.33627	35.73635	33.88307	39.6173	39.61099
Si	3.918963	10.50306	8.061833	3.985591	4.869932	7.797981	9.93	8.04	19.11932	11.628	25.812	19.21591	7.894432	8.683245	19.02113	8.708487	10.43125
Sr	31.1397	31.81205	28.56201	30.68542	30.91559	27.91958	40.578	38.628	38.89205	44.472	44.436	42.64205	27.16038	25.47548	25.40035	27.91133	26.49778
Zn	0.296799	1.586968	#VALUE!	0.466399	0.284685	#VALUE!	1.596	1.266	#VALUE!	1.878	4.314	0.295455	1.211616	1.198995	#VALUE!	1.217926	1.173753
Zr	0.56937	0.617827	#VALUE!	0.581484	0.629941	#VALUE!	0.822	0.726	#VALUE!	0.87	0.882	0.198864	0.706776	0.662602	#VALUE!	0.807744	0.795123

Table G.2 ICP-AES Data for AN-102 Primary Effects Samples

	9-3-BC-8hr100C-A-				9-3-BC-8hr100C-B-				9-10-BC-BC-A-			9-10-BC-BC-B-		
	0	0+8hr	8	16	0	0+8hr	8	16	0	8	16	0	8	16
Al	9257.50	9869.62	9636.13	9355.19	9850.69	9497.30	10122.04	9056.40	8974.30	9151.43	9372.06	9226.01	9288.16	9272.62
B	11.68	47.61	47.06	53.48	12.26	35.50	37.38	41.20	17.13	17.30	17.99	16.85	17.70	16.92
Ca	55.82	63.55	57.03	54.41	62.68	59.36	58.49	53.19	55.31	55.78	57.77	55.10	55.59	53.70
Ce	0.23	-0.31	-0.01	#VALUE!	0.13	-0.29	0.00	#VALUE!	#VALUE!	#VALUE!	#VALUE!	#VALUE!	#VALUE!	#VALUE!
Cr	197.52	208.56	206.92	214.62	200.42	200.86	207.62	204.55	191.82	201.24	202.48	199.00	202.39	205.34
Cu	2.56	2.95	2.63	2.58	2.90	2.31	2.60	2.42	2.14	2.38	2.54	2.58	2.74	2.64
Fe	6.02	6.17	5.58	2.64	5.34	6.28	6.47		4.45	3.44	2.70	3.49	3.30	2.92
K	1581.41	1688.06	1659.03	1653.22	1641.36	1628.74	1672.91	1591.97	1512.08	1562.42	1597.54	1577.34	1605.00	1600.33
La	0.07	-0.04	-0.04	#VALUE!	0.22	0.08	0.12	#VALUE!	0.32	0.30	0.35	0.38	0.43	0.31
Mg	4.11	5.41	4.32	#VALUE!	4.30	5.32	3.05	#VALUE!	2.80	3.56	3.63	2.73	3.32	2.39
Mn	15.64	10.36	5.38	3.83	16.78	11.04	5.40	3.34	20.19	15.38	12.71	16.79	16.55	12.10
Mo	35.68	37.88	37.41	36.75	36.84	36.85	38.29	35.47	35.64	35.77	36.08	35.52	35.67	35.58
Nd	3.16	2.51	2.56	1.60	3.35	2.17	2.48	1.63	3.00	2.42	3.19	3.43	2.93	3.51
Ni	279.81	293.63	293.25	286.24	287.13	287.70	295.58	280.57	269.26	276.53	280.70	275.79	282.34	280.63
P	1480.44	1583.30	1119.48	992.89	1566.27	1555.54	1655.24	1405.82	1394.62	1074.87	1030.43	1451.18	1050.32	973.56
Pb	36.89	38.40	37.45	34.09	38.93	38.63	39.64	34.81	39.46	39.06	39.81	39.53	39.78	38.84
Si	6.46	94.15	99.52	117.04	10.27	37.05	36.30	41.65	14.91	17.05	20.27	15.34	17.61	20.15
Sr	27.99	18.77	19.34	17.90	26.89	22.48	23.56	20.59	28.75	26.69	26.85	25.14	25.32	24.73
Zn	1.06	1.50	1.03	#VALUE!	1.15	1.27	1.27	#VALUE!	1.46	1.36	1.38	1.49	1.54	1.49
Zr	0.74	0.85	0.80	#VALUE!	0.78	0.90	0.90	#VALUE!	0.66	0.65	0.68	0.74	0.78	0.81

	9-10-BC-.01MMn-A-			9-10-BC-.01MMn-B-			9-10-BC-.03MMn-A-			9-10-BC-.03MMn-B-			9-24-BC-25Rxn-A-			9-24-BC-25Rxr	
	0	8	16	0	8	16	0	8	16	0	8	16	0	8	16	0	8
Al	9327.02	9318.12	9341.85	9009.70	9564.28	9160.94	9019.73	9526.56	8570.56	9095.60	9347.50	9289.83	8898.05	9220.75	9119.16	8790.49	9376.12
B	17.14	17.26	17.27	15.82	18.04	17.17	16.89	17.84	11.31	16.29	16.87	17.64	15.64	17.28	18.11	15.96	17.23
Ca	61.89	64.15	63.55	60.56	63.94	61.00	58.30	59.15	49.89	54.81	56.27	58.36	38.69	40.73	40.04	40.04	40.61
Ce	0.40	0.29	0.35	#VALUE!	0.41	#VALUE!	#VALUE!	#VALUE!	#VALUE!	#VALUE!	#VALUE!	0.45	#VALUE!	#VALUE!	#VALUE!	#VALUE!	#VALUE!
Cr	198.31	201.19	201.72	196.59	199.80	201.67	199.24	209.29	182.58	200.94	202.85	201.37	201.42	203.69	206.59	200.49	208.77
Cu	12.70	13.24	13.29	12.53	13.64	13.16	4.53	4.89	4.69	4.76	5.33	5.10	#VALUE!	#VALUE!	#VALUE!	#VALUE!	#VALUE!
Fe	9.48	8.91	8.88	8.64	9.72	9.48	3.28	3.91	10.08	3.69	6.05	3.94	2.84	3.05	3.28	3.10	2.95
K	1549.86	1557.86	1578.62	1519.31	1570.32	1552.23	1539.61	1623.98	1391.20	1556.90	1573.90	1576.02	1569.26	1600.33	1601.23	1584.80	1631.71
La	1.70	1.61	1.63	1.82	1.81	1.76	0.76	0.79	#VALUE!	0.84	0.87	0.84	1.09	1.17	1.08	1.23	1.22
Mg	2.95	4.77	4.34	3.22	3.54	3.42	2.32	3.49	3.56	3.74	3.44	3.78	#VALUE!	2.80	3.28	3.50	3.56
Mn	71.06	69.93	65.87	68.86	71.77	64.65	30.56	31.81	26.99	31.20	31.68	28.25	11.73	12.35	12.14	13.47	12.48
Mo	35.44	35.88	35.56	34.94	35.94	35.50	34.99	36.63	33.17	35.05	36.21	35.78	34.90	36.03	35.94	35.17	36.18
Nd	9.76	9.99	9.65	9.77	10.41	10.13	4.85	5.46	3.72	5.39	5.50	5.52	4.83	4.99	4.56	5.52	5.28
Ni	297.16	303.98	301.90	297.16	305.46	301.90	285.28	297.39	266.01	287.86	292.44	290.53	278.95	286.39	289.68	285.80	291.26
P	1544.82	906.01	853.82	1490.84	909.57	847.88	1527.77	972.38	840.67	1530.20	972.69	914.72	1005.74	1085.81	1073.26	981.24	1059.52
Pb	83.25	82.92	82.30	81.70	83.90	81.53	54.63	56.60	50.17	54.81	55.30	54.84	20.13	20.71	20.58	19.92	20.12
Si	14.70	17.23	19.07	14.73	17.67	19.97	14.60	17.47	11.63	15.33	17.95	20.84	9.51	13.59	16.35	9.56	13.57
Sr	52.31	53.50	52.61	35.23	36.30	34.61	32.63	33.69	29.90	29.01	28.79	28.77	117.49	105.98	84.41	125.28	106.88
Zn	1.73	1.81	1.81	1.86	1.90	1.81	1.47	1.49	1.50	1.57	1.57	1.61	0.82	0.86	0.81	0.99	0.96
Zr	5.05	5.18	5.11	5.18	5.38	5.30	1.84	1.93	1.73	1.98	2.04	2.03	0.86	0.92	0.91	0.89	0.96

Table G.3 ICP-AES Data for AN-102 NOC Samples

	9-24-NOC-BC-A-			9-24-NOC-BC-B-			9-24-NOC-.01MMn-A-			9-24-NOC-.01MMn-B-		
	0	8	16	0	8	16	0	8	16	0	8	16
Al	9072.258	9288.074	9194.82	9034.957	9242.779	9423.958	9248.1478	9365.543	9490.765	9245.539	9475.112	9375.978
B	17.07343	19.15432	18.38431	17.38516	17.93669	19.59928	18.381509	18.38934	19.1511	18.26933	18.1102	18.06845
Ca	61.33433	63.1994	62.55995	48.17223	48.59853	50.51689	59.375978	58.48899	59.21945	56.42805	56.14108	55.14974
Ce	#VALUE!	#VALUE!	#VALUE!	#VALUE!	#VALUE!	#VALUE!	#VALUE!	#VALUE!	#VALUE!	#VALUE!	#VALUE!	#VALUE!
Cr	202.4406	203.08	205.2382	196.872	207.8759	204.3856	198.31994	200.9026	203.7462	200.6678	202.6505	205.6767
Cu	3.7115	4.007247	4.023234	3.762123	4.183097	4.316317	11.058646	11.16039	11.50214	11.35083	11.66649	11.48127
Fe	2.637749	3.255888	3.258553	2.800277	2.882873	3.245231	9.2716268	9.245539	9.469895	8.882918	9.096838	9.089012
K	1576.521	1588.245	1592.241	1556.805	1604.764	1600.767	1560.576	1577.794	1605.186	1572.837	1582.49	1605.447
La	1.598636	1.673239	1.574656	1.521368	1.53469	1.372162	1.9878952	2.013983	2.021809	1.993113	2.066159	2.110508
Mg	3.652883	2.192795	2.219439	2.352659	2.653735	3.66354	#VALUE!	#VALUE!	#VALUE!	#VALUE!	#VALUE!	#VALUE!
Mn	15.78919	16.39135	16.16487	16.50591	16.38602	16.82564	55.984556	55.95847	56.55849	54.00188	54.26276	54.02797
Mo	35.27656	36.12917	35.99595	35.14334	36.07588	36.50218	34.775123	35.37514	35.74037	35.19253	35.32297	35.40123
Nd	6.450496	6.338591	6.421187	6.242673	5.936268	5.930939	9.9316498	9.107273	9.65251	9.514244	9.321194	9.362934
Ni	294.6819	300.2771	301.6093	293.8826	302.9415	305.8723	300.53219	302.3583	306.0106	305.228	306.0106	308.8803
P	1031.12	1090.27	1075.615	1045.774	1103.858	1132.367	980.6428	1003.6	1009.861	990.8171	987.9474	988.9909
Pb	40.1524	40.55206	39.91261	42.04412	42.52371	43.02995	83.142022	83.89857	84.42033	82.15068	81.81154	82.35939
Si	8.672599	10.59363	11.08388	8.355537	10.65224	11.8006	9.1985808	8.997704	9.629031	9.441198	9.879474	10.29427
Sr	80.03837	58.27028	42.73686	101.4867	77.61377	61.06789	102.08181	91.95972	73.15037	103.0992	94.90765	77.95054
Zn	0.57018	0.583502	0.583502	0.623468	0.663434	0.631461	#VALUE!	#VALUE!	#VALUE!	#VALUE!	#VALUE!	#VALUE!
Zr	2.669722	2.709688	2.749654	2.581797	2.731003	2.72301	6.2193468	6.216738	6.295002	6.446311	6.435876	6.493269

Contaminated

	10-1-NOC-BC-A-			10-1-NOC-BC-B-			10-1-NOC-O2-A-			10-1-NOC-O2-B-			1(
	0	8	16	0	8	16	0	8	16	0	8	16	0
Al	9423.958222	9282.745391	9415.965043	9533.198337	9535.86273	9767.664926	9589.150591	9458.595332	9439.944581	9594.479378	9431.951401	9365.341575	9397.314292
B	18.36033252	17.60897368	18.06192049	18.13918789	18.60012789	18.41628477	19.01310881	17.88340616	17.9073857	18.41362038	18.35233934	18.29372269	18.11787275
Ca	72.57806672	70.10018118	71.13929447	64.8779708	65.01119045	64.10529681	87.92497069	84.67441117	85.07407013	49.7708622	48.38537781	48.03900671	85.60694874
Ce	#VALUE!	#VALUE!	#VALUE!	#VALUE!	#VALUE!	#VALUE!	#VALUE!	#VALUE!	#VALUE!	#VALUE!	#VALUE!	#VALUE!	#VALUE!
Cr	211.9791112	211.7126719	210.487051	210.0341042	203.2931898	208.7285516	204.7319621	205.2914846	209.9808164	203.985932	199.4831077	202.3073644	205.9575829
Cu	3.730150272	3.7194927	3.929979751	4.316316743	4.276350847	4.366940211	3.652882873	3.375785996	3.511670042	4.321645529	4.318981136	4.137802409	3.524992007
Fe	3.269210274	2.896195247	3.373121603	3.540978365	3.682191197	3.189278482	2.850900565	3.098689119	3.223915592	3.461046574	3.314504956	3.183949696	3.298518597
K	1640.466802	1637.535969	1641.26612	1641.26612	2632.953213	2691.036982	1617.286582	1622.615368	1640.466802	1623.148247	1648.992859	1664.1799	1615.155068
La	1.052435255	1.044442076	0.967174678	0.988489822	1.025791325	0.929873175	1.10039433	1.007140573	1.028455718	0.849941383	0.72471491	0.556858148	1.052435255
Mg	#VALUE!	#VALUE!	#VALUE!	#VALUE!	#VALUE!	#VALUE!	#VALUE!	#VALUE!	#VALUE!	#VALUE!	#VALUE!	#VALUE!	#VALUE!
Mn	16.84962166	16.39401044	16.67110732	17.4064798	17.47575402	17.47575402	16.62314825	16.28743472	16.25013322	16.63114143	16.48193542	16.28743472	16.36470212
Mo	36.12916978	35.91601833	35.94266226	35.8893744	36.31567729	36.44889694	36.12916978	35.96930619	36.26238943	36.07588191	35.5430033	35.67622296	36.02259405
Nd	6.002877544	6.072151764	5.866993499	5.499307258	5.366087605	5.888308643	6.117446446	6.128104018	6.07748055	5.355430033	4.918469573	4.81988703	6.415858467
Ni	308.5367153	306.6716402	307.2045188	307.2045188	305.0730044	305.8723223	301.8757327	299.2113397	304.2736865	303.7408078	299.7442183	300.8099755	301.3428541
P	1016.732388	995.9501226	998.6145156	1018.863903	1026.324203	1038.846851	1048.705105	1030.320793	1023.126932	1111.318342	1101.193648	1106.788873	1026.057764
Pb	39.45966109	38.74027497	39.06000213	41.00500906	41.48459981	41.48459981	37.14163913	36.28903336	36.2357455	42.44378131	42.07076628	42.71022061	36.98177555
Si	9.07225834	9.322711286	10.08739209	9.647767239	10.0847277	9.767664926	9.018970479	9.114888628	9.890227006	9.181498455	9.866247469	9.916870937	9.050943195
Sr	66.66311414	47.98571885	36.74198018	73.59053608	54.64670148	39.35308537	41.48459981	37.64787381	29.8678461	99.56836833	54.24704252	40.76521368	37.96760098
Zn	#VALUE!	#VALUE!	#VALUE!	#VALUE!	#VALUE!	#VALUE!	#VALUE!	#VALUE!	#VALUE!	#VALUE!	#VALUE!	#VALUE!	#VALUE!
Zr	2.326015134	2.27006288	2.310028775	2.477885538	2.453906	2.528509006	2.286049238	2.256740914	2.280720452	2.222103805	2.120856869	2.150165192	2.342001492

Table G.4 ICP-AES Data for AN-102 Secondary Effect Samples

	11-19-BC-0MOH,.03MSr-A-			11-19-BC-0MOH,.03MSr-B-			11-19-BC-0MOH,.03MMn-A-			11-19-BC-0MOH,.03MMn-B-			11-19-BC-0MOH,Light-A-			11-19-BC-0MOH,L	
	0	8	16	0	8	16	0	8	16	0	8	16	0	8	16	0	8
Al	9694.544	9931.395	9844.277	9808.886	9724.491	9425.025	9604.795	9895.85	9747.524	9621.587	9842.676	9694.35	9639.211	9759.665	9708.042	9209.017	9817.024
B	20.57606	20.69857	20.77752	20.14592	21.18861	23.43189	19.09765	19.73853	20.34022	19.41949	20.28705	19.69095	19.56235	20.61489	19.74016	17.91614	19.44763
Ca	52.02548	52.76054	52.48829	50.3648	50.88206	49.22139	49.25536	47.32433	50.31883	47.63217	50.90653	47.46426	47.86624	49.3289	48.78399	43.67902	45.80131
Ce	#VALUE!	#VALUE!	#VALUE!	#VALUE!	#VALUE!	#VALUE!	#VALUE!	#VALUE!	#VALUE!	#VALUE!	#VALUE!	#VALUE!	#VALUE!	#VALUE!	#VALUE!	#VALUE!	#VALUE!
Cr	216.4053	223.0752	222.9664	216.8954	215.1258	211.505	218.0109	223.2443	222.4607	218.7106	225.791	219.858	230.0677	233.2224	230.2111	215.9	232.4194
Cu	4.554612	4.704345	4.63084	4.786018	4.685288	4.546445	6.198899	6.543127	6.324836	6.447974	6.461967	6.520738	4.448205	4.614546	4.531375	4.488356	4.843983
Fe	2.461069	2.458347	2.395731	2.589023	2.575411	2.599913	<0.15	2.49915	0	2.49915	2.524337	2.739829	2.592635	2.52954	2.741769	2.541012	2.477917
K	1711.042	1761.951	1756.779	1714.854	1709.409	1700.152	1690.354	1743.528	1728.975	1693.153	1737.091	1702.388	1752.61	1800.218	1760.067	1654.812	1775.554
La	#VALUE!	#VALUE!	#VALUE!	#VALUE!	#VALUE!	#VALUE!	0.414193	0.456172	0.475762	0.489755	0.475762	0.57931	#VALUE!	#VALUE!	#VALUE!	#VALUE!	#VALUE!
Mg	#VALUE!	#VALUE!	#VALUE!	2.16977	#VALUE!	2.150713	#VALUE!	2.33963	#VALUE!	#VALUE!	#VALUE!	#VALUE!	#VALUE!	2.586899	2.208329	#VALUE!	2.37467
Mn	6.258848	6.365022	6.060111	6.403136	6.370467	6.332353	14.70944	15.35312	14.89695	15.28595	15.08445	15.24118	4.476884	4.451073	0	4.499828	4.422393
Mo	37.35163	37.65109	37.89611	36.94326	36.61657	36.23544	36.74562	37.3893	37.10944	36.5777	37.72513	36.82958	37.97178	38.37329	38.00046	35.64873	37.71366
Nd	1.320375	1.260481	1.557225	1.353044	1.290428	1.211478	2.773413	3.081259	3.011294	3.064467	3.140029	3.344327	0.937823	0.920615	0.937823	1.086957	0.980842
Ni	303.55	308.9949	311.9895	306.0002	304.3668	302.1888	308.1259	314.5626	312.8835	310.6446	316.8015	311.4842	316.0491	322.0718	318.9171	302.5697	320.351
P	1691.441	1231.896	1126.538	1683.273	1179.353	1061.2	1713.583	1319.82	1184.927	1603.038	1283.718	1205.357	1719.342	1506.252	1376.62	1622.691	1494.494
Pb	35.22814	36.15376	36.26266	35.60928	35.71817	34.98312	54.74062	57.20338	55.55221	56.50373	55.5802	56.3638	38.40197	38.54537	38.11518	36.96799	38.86085
Si	8.888707	10.25264	9.572035	9.672765	11.66558	12.2754	8.865965	10.01619	11.08525	9.817489	10.07496	10.09175	9.596191	10.0694	10.36194	8.55799	10.26443
Sr	27.04454	27.16977	27.1126	26.14886	26.28226	25.39475	28.71364	29.60919	29.27336	29.69315	29.80509	29.5812	30.68716	31.03132	30.88792	29.25318	30.31433
Zn	#VALUE!	#VALUE!	#VALUE!	#VALUE!	#VALUE!	#VALUE!	#VALUE!	#VALUE!	#VALUE!	#VALUE!	#VALUE!	#VALUE!	#VALUE!	#VALUE!	#VALUE!	#VALUE!	#VALUE!
Zr	0.579876	0.588043	0.577153	0.585321	0.612545	0.61799	1.458071	1.603598	1.486057	1.575612	1.511244	1.625987	0.539176	0.493289	0.513365	0.539176	0.587932

Table G.5 ICP-AES Data for AN-102 Secondary Effect Samples

	11-19-BC-0MOH,O2-A-			11-19-BC-0MOH,O2-B-			11-21-BC-OMOH,25Rxn-A-			11-21-BC-OMOH,25Rxn-B-			11-21-25Rxn,.03MSr-A-			11-21-25Rxn,.03M	
	0	8	16	0	8	16	0	8	16	0	8	16	0	8	16	0	8
Al	9498.681	9848.572	9862.912	9708.042	9725.25	9679.362	9740.593	9952.914	9813.306	9679.514	9449.742	9560.266	9653.33	8638.256	8713.446	9601.275	9381.487
B	18.62739	20.51738	20.46002	18.70483	19.71722	18.70196	18.78024	19.07109	18.35559	18.41376	17.54994	17.54121	17.99372	15.3765	16.02719	18.1065	18.01974
Ca	47.20661	47.86624	49.95985	46.0881	47.60812	45.85867	41.88251	43.16226	41.73709	44.50017	42.84232	43.59853	47.45691	46.5604	48.06421	45.11443	45.89525
Ce	#VALUE!	#VALUE!	#VALUE!	#VALUE!	#VALUE!	#VALUE!	#VALUE!	#VALUE!	#VALUE!	#VALUE!	#VALUE!	#VALUE!	0.332574	#VALUE!	#VALUE!	0.497415	#VALUE!
Cr	230.039	241.9984	225.4503	220.5174	219.5136	222.2382	220.145	224.3914	224.3041	214.328	211.0123	213.31	200.4411	198.0118	199.3711	201.0773	215.19
Cu	4.471148	4.657566	4.726397	4.720661	4.752208	4.643226	#VALUE!	#VALUE!	#VALUE!	1.931249	1.902164	1.945792	#VALUE!	#VALUE!	#VALUE!	#VALUE!	#VALUE!
Fe	2.604107	2.526672	2.466445	2.770449	2.601239	2.701618	3.100469	2.978312	3.161548	2.928868	3.222627	3.02194	3.169578	3.15801	2.741569	3.166686	3.048116
K	1745.44	1821.154	1783.297	1737.696	1738.27	1747.734	1676.755	1704.967	1678.791	1650.869	1621.784	1636.036	1608.792	1517.406	1535.047	1600.695	1678.488
La	#VALUE!	#VALUE!	#VALUE!	0.203625	#VALUE!	#VALUE!	0.25304	0.285034	0.244315	0.285034	0.258857	0.247223	1.012183	1.284026	1.130753	1.116293	1.243539
Mg	2.563955	#VALUE!	2.552484	2.618447	3.177699	#VALUE!	#VALUE!	#VALUE!	#VALUE!	#VALUE!	#VALUE!	#VALUE!	#VALUE!	#VALUE!	2.452374	#VALUE!	2.391643
Mn	4.316279	4.405185	3.797178	4.138465	4.307675	3.748423	3.065567	3.123738	3.100469	3.74325	3.624001	3.66472	10.18834	9.589707	7.484368	10.22883	10.42837
Mo	37.02535	38.51669	39.17632	37.16875	37.22611	37.02535	36.47269	36.76354	36.70537	35.57105	34.78576	34.98935	34.64557	33.57554	34.00934	34.52989	34.29853
Nd	1.218883	1.098428	0.825972	0.788689	0.949294	0.874728	1.902164	2.2221	2.033047	2.00687	1.89053	1.739288	5.488922	4.757258	4.901856	5.717386	5.344324
Ni	313.7547	324.0794	315.1887	305.1509	309.166	306.298	302.194	305.975	302.7757	301.0306	294.341	297.2495	270.2238	271.5541	277.4248	275.6607	281.0397
P	1768.957	1387.519	1306.355	1683.779	1497.075	1322.99	689.0255	699.2053	699.2053	781.2252	763.1925	764.065	722.12	648.6645	650.978	1100.098	1043.126
Pb	37.45555	38.43065	39.14764	36.91063	37.28347	37.05403	28.86985	29.20142	28.6488	32.08084	30.85927	31.44097	19.26907	17.74212	18.2511	17.83177	17.40376
Si	9.794081	9.894459	10.91258	10.01778	10.80073	10.68888	8.411405	8.452124	9.04546	8.684805	8.335784	8.431765	9.80082	10.59321	13.14391	10.63949	12.91545
Sr	30.22829	30.57244	31.60491	29.68338	30.83056	29.74074	87.95328	87.10981	74.77774	76.4065	72.30551	64.04535	94.36434	90.08425	79.75999	105.5562	96.24411
Zn	#VALUE!	#VALUE!	#VALUE!	#VALUE!	#VALUE!	#VALUE!	#VALUE!	#VALUE!	#VALUE!	#VALUE!	#VALUE!	#VALUE!	#VALUE!	#VALUE!	#VALUE!	#VALUE!	0.399089
Zr	0.539176	0.54778	0.567856	0.542044	0.579328	0.613743	0.459544	0.479904	0.474087	0.465361	0.450819	0.439185	0.749015	0.806854	0.882045	0.760583	0.899397

	11-21-25Rxn,.03MMn-A2-			11-21-25Rxn,.03MMn-B2-			11-21-25Rxn,Light-A-			11-21-25Rxn,Light-B-			11-21-25Rxn,O2-A-			11-21-25Rxn,O	
	0	8	16	0	8	16	0	8	16	0	8	16	0	8	16	0	8
Al	9262.239	9386.763	9487.569	9618.023	9864.106	9668.425	9690.068	9978.463	10099.89	9702.211	9978.463	9869.177	9799.355	9759.89	9759.89	9838.819	9981.499
B	17.10134	17.77733	17.87517	18.18352	18.93956	18.08864	17.74691	19.12513	19.1646	18.74263	18.65763	18.76692	18.29941	18.16888	18.35102	18.31459	18.88531
Ca	50.31376	49.89868	50.10622	46.87452	53.72336	47.37855	44.62531	43.07709	43.50209	47.78248	48.63248	47.66105	49.60392	49.90749	51.09143	56.70754	58.86291
Ce	0.373573	#VALUE!	0.257943	0.358749	0.287592	0.32317	0.27018	0.47661	0.415896	#VALUE!	0.279288	0.267145	0.443217	#VALUE!	#VALUE!	#VALUE!	0.288395
Cr	209.8532	215.8718	217.5915	221.0307	224.9443	220.7046	224.7052	207.2497	207.8872	224.4926	230.5034	230.9284	211.6818	232.3248	230.5338	228.4391	230.8373
Cu	2.155457	2.235508	2.202895	2.75436	2.819587	2.730641	#VALUE!	#VALUE!	#VALUE!	#VALUE!	#VALUE!	#VALUE!	#VALUE!	#VALUE!	#VALUE!	#VALUE!	#VALUE!
Fe	3.513365	3.471857	3.720906	4.044076	3.655679	3.765379	3.178415	2.595554	3.072164	3.527525	3.160201	3.327166	3.19663	3.163237	2.856627	3.154129	3.01145
K	1639.867	1670.702	1687.008	1713.692	1746.009	1715.471	1726.423	1659.94	1673.297	1734.923	1781.37	1780.155	1655.083	1769.227	1766.798	1767.102	1793.513
La	1.470573	1.470573	1.434995	1.467608	1.518011	1.423135	1.050365	0.919828	0.898578	1.211259	1.223401	1.214294	0.998757	1.126258	1.226437	1.308402	1.396438
Mg	3.196125	3.329544	3.222808	3.252457	4.304984	2.917427	3.396988	2.495375	2.376981	#VALUE!	3.642883	3.65199	3.230023	2.86877	2.971985	3.299845	2.61984
Mn	22.23352	22.47368	18.75574	24.57577	25.21914	21.86292	9.753819	7.868627	1.961085	9.78114	7.583268	2.89002	9.872212	7.422374	5.515932	10.98329	9.507924
Mo	35.13365	35.45979	35.63768	36.201	36.46784	36.23065	35.85204	35.8824	35.97347	36.00382	36.24668	36.27704	35.97347	36.15561	36.06454	37.18776	37.36991
Nd	5.597665	5.689576	5.375301	5.737014	5.535403	5.701436	4.659854	4.951285	4.690212	4.280387	5.109143	4.945213	4.84807	4.574854	4.438245	4.987714	5.421824
Ni	280.5948	284.1527	286.9693	292.6025	296.4865	294.1146	289.4574	282.2323	281.8377	291.5824	295.0431	293.8289	284.6913	290.5806	291.6128	294.436	300.5378
P	1093.442	1109.749	1111.528	1106.191	1118.94	1099.965	1073.133	1138.097	1145.687	1075.258	1090.74	1088.918	1012.418	968.0961	958.9889	816.9165	834.2202
Pb	37.97992	38.18746	37.71309	42.10109	42.04179	41.98249	17.37351	18.65763	18.48459	16.76333	17.13976	16.83315	18.21441	17.59816	17.54655	17.57084	17.88959
Si	9.67139	16.1259	19.15006	10.45115	16.624	14.76503	11.1199	12.7167	15.7069	11.38704	13.78528	15.23332	10.77383	12.74705	15.10582	10.16971	14.28314
Sr	104.2447	103.2663	93.68974	114.088	114.8292	96.06163	112.1097	105.674	92.8328	105.4007	99.96677	81.96486	97.53819	83.69523	65.48082	87.55062	88.37026
Zn	0.67006	0.512922	0.581114	0.693778	0.678954	0.678954	0.34911	#VALUE!	#VALUE!	0.473575	0.418932	0.467503	#VALUE!	0.379467	0.397681	0.461432	0.467503
Zr	1.660325	1.663289	1.675149	1.983495	2.057616	2.022038	0.792327	0.695183	0.66179	0.819649	0.843935	0.86822	0.670898	0.78322	0.801434	0.910721	0.928935

APPENDIX H

XRD Analysis of AN-107 Post-filtration Solids

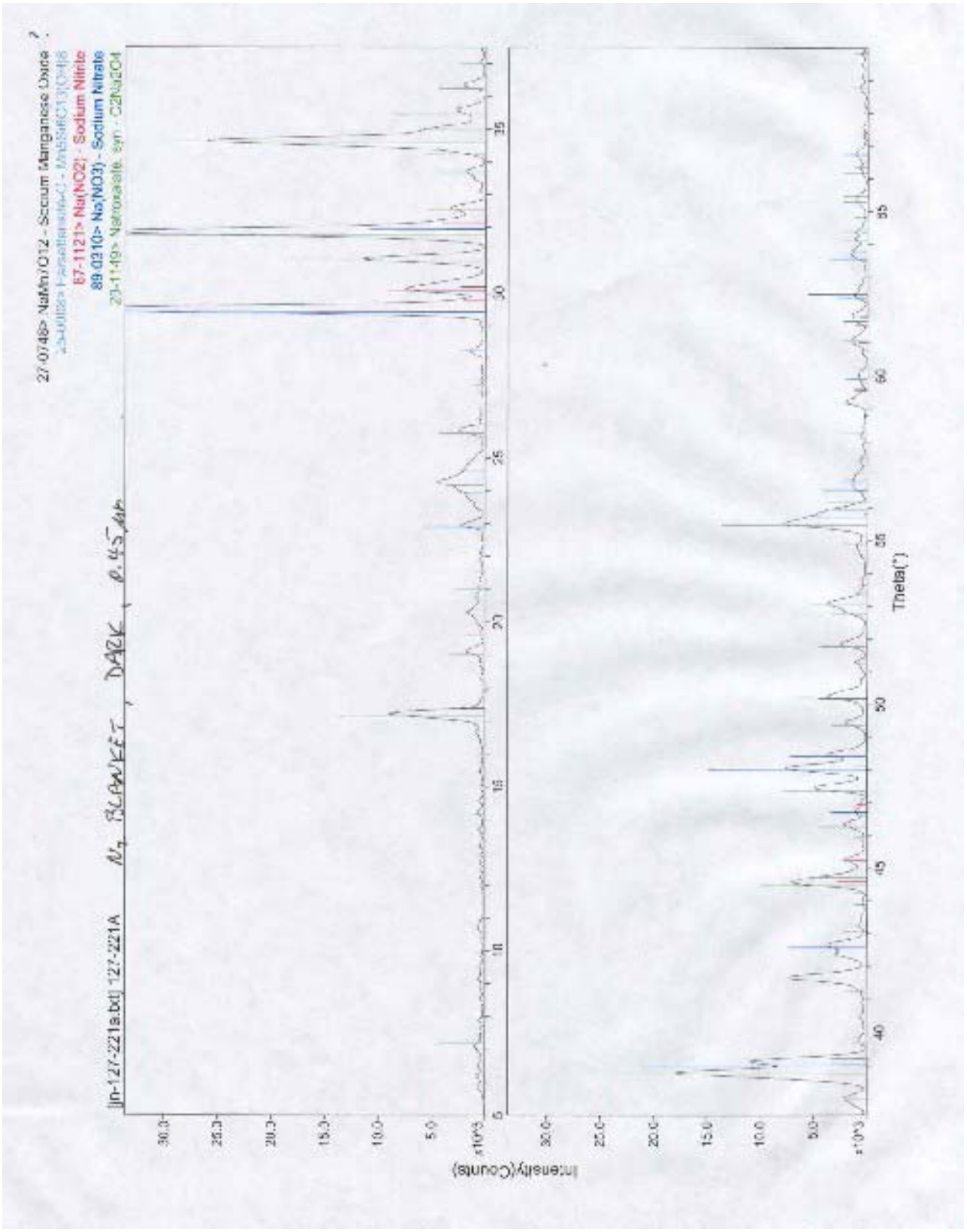
27-0748> Nafm7O12 - Sodium Manganese Oxide
57-1121> Na(NO2) - Sodium Nitrite
89-0310> Na(NO3) - Sodium Nitrate
23-1149> Nahonaaite, syn - C2Na2O4
In-127-221a.txt] 127-221A
Intensity(Counts)
Theta(°)

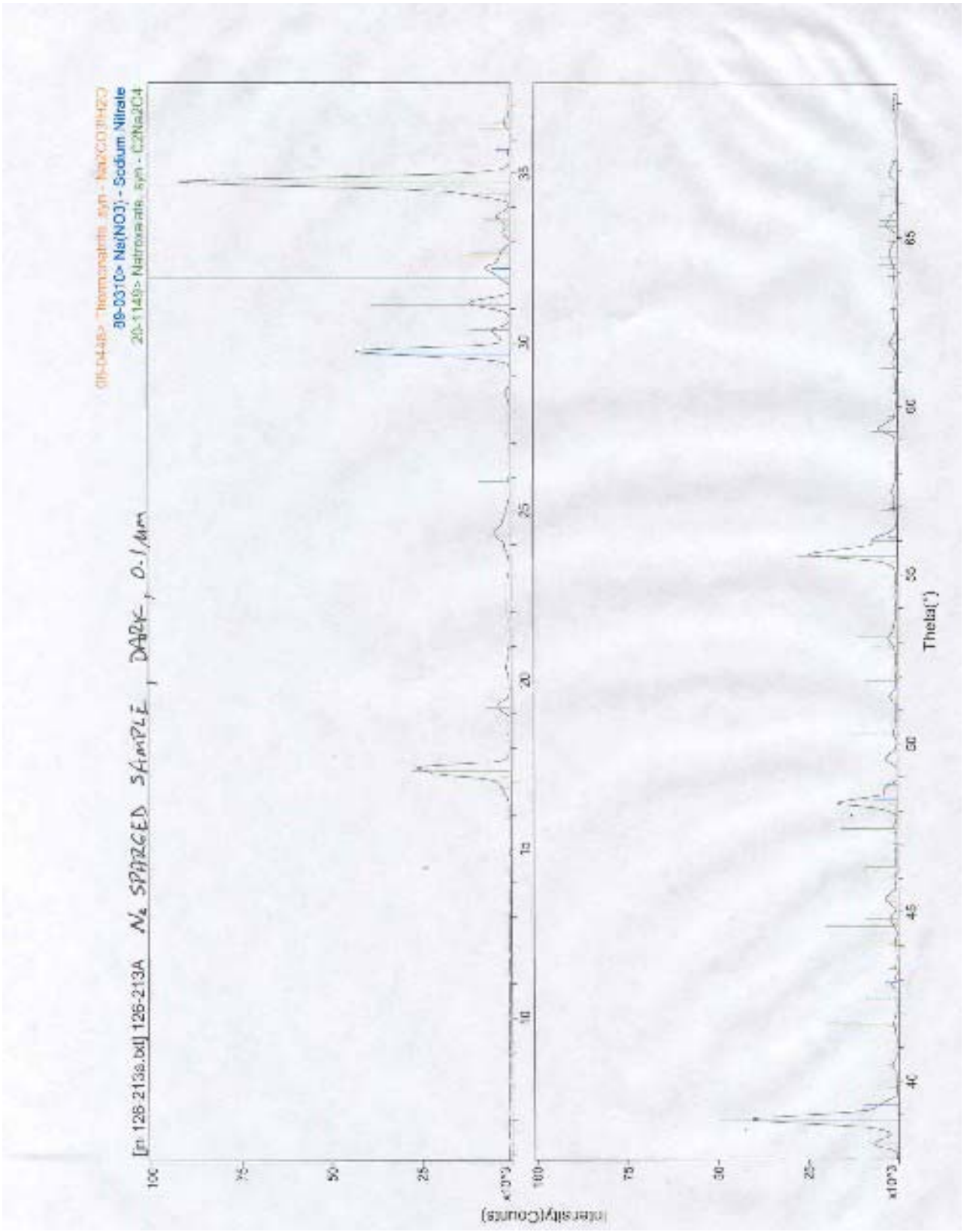
[n 126-213a.txt] 126-213A N4 SPIKED SAMPLE DARK, 0.1/mm
00-0448> Thermonatrite, syn - Na2CO3·H2O
99-0310> Na(NO3) - Sodium Nitrate
20-1149> Natroxalate, syn - C2Na2O4
Theta(°)
Intensity(Counts)

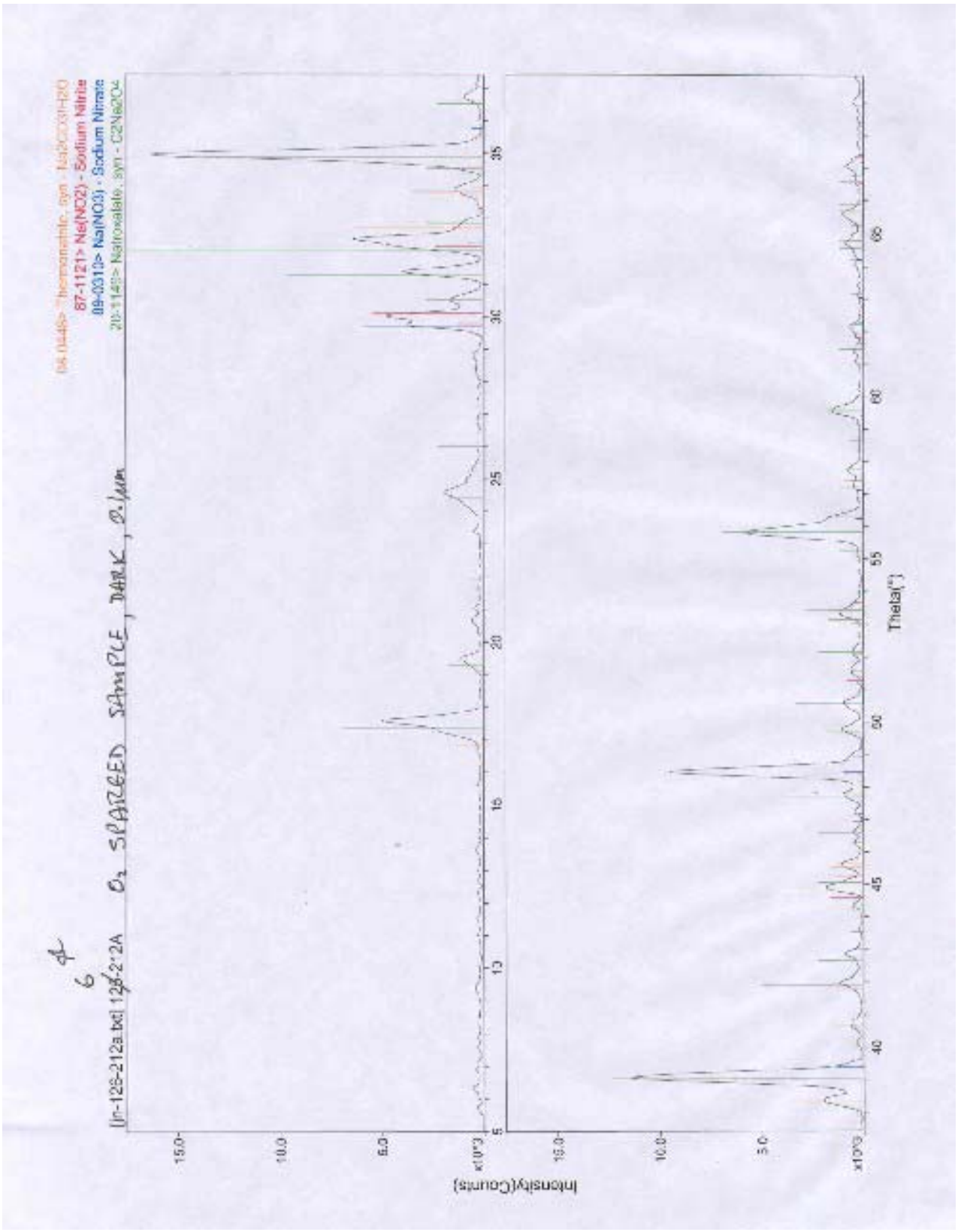
04-0446> Thermonatrite, syn - Na2CO3(H2O
87-1121> Na(NO2) - Sodium Nitrite
09-0310> Na(NO3) - Sodium Nitrate
20-1145> Natroxalate, syn - C2Na2O4
In-126-212a.txt 126-212A O2 SPARGED SAMPLE, DARK, 2.1µm
Intensity(Counts)
Theta(°)

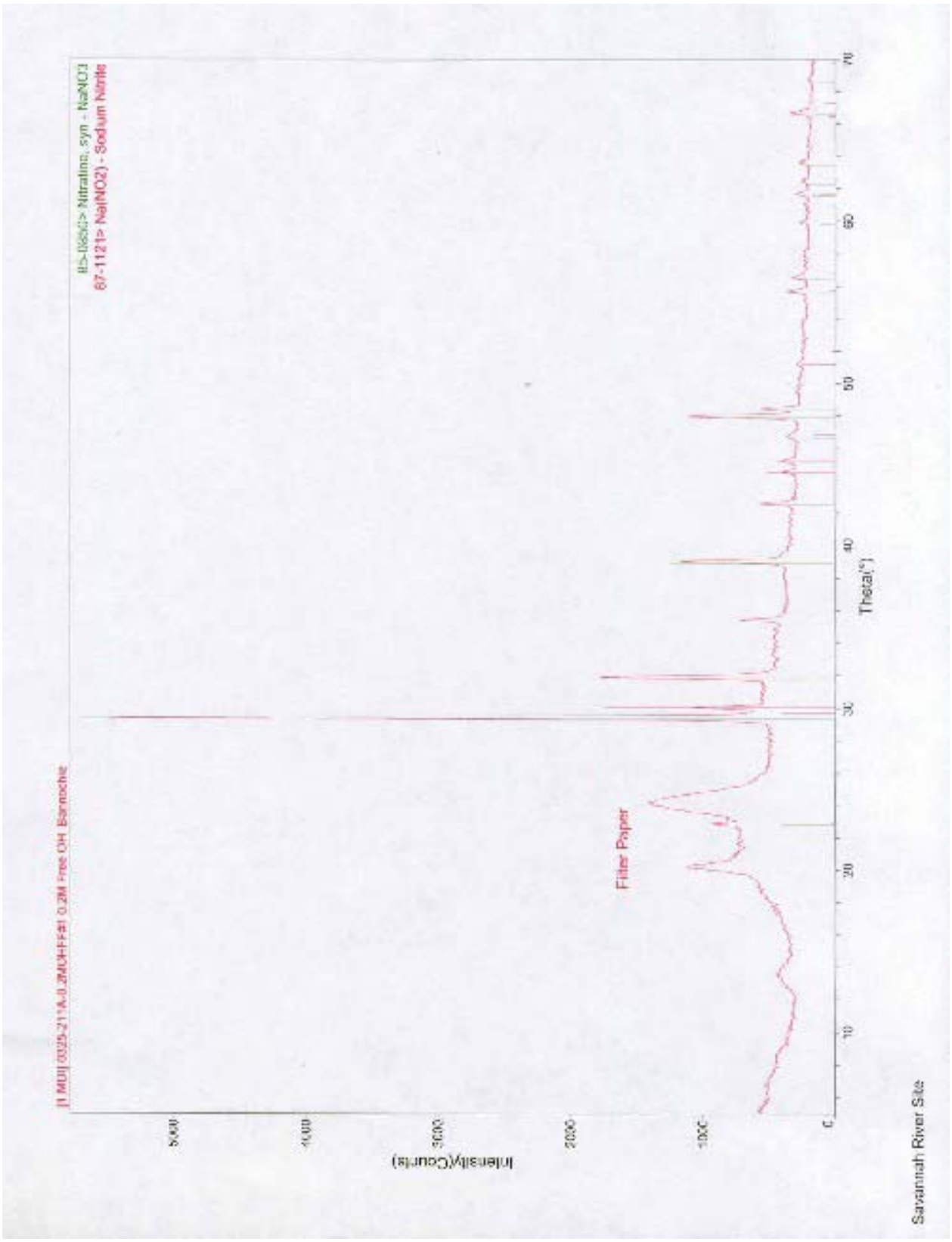
[1 MUI] 0325-211A-0.2MUH-FS1 0.2M Free OH Baroche
85-0656 > Nitratine, syn - NaNO3
87-1121 > NaNO2) - Sodium Nitrite
Filter Paper
Intensity(Counts)
Theta(°)
Savannah River Site

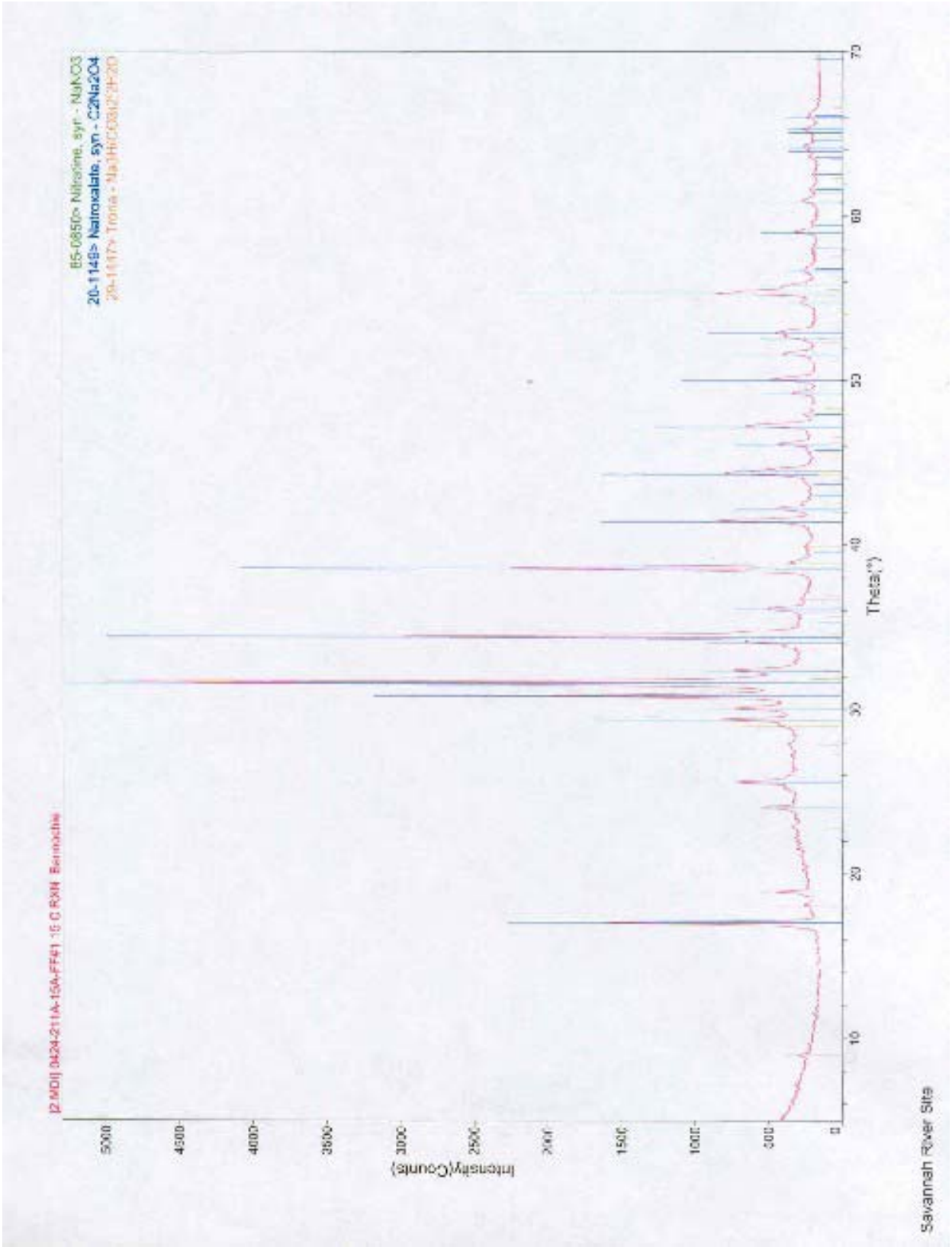
[2 MDI] 0424-211A-15A-FF61 15 C RXN Bernoulli
Savannah River Site
Intensity(Counts)
Theta(°)
0
500
1000
1500
2000
2500
3000
3500
4000
4500
5000
10
20
30
40
50
60
70

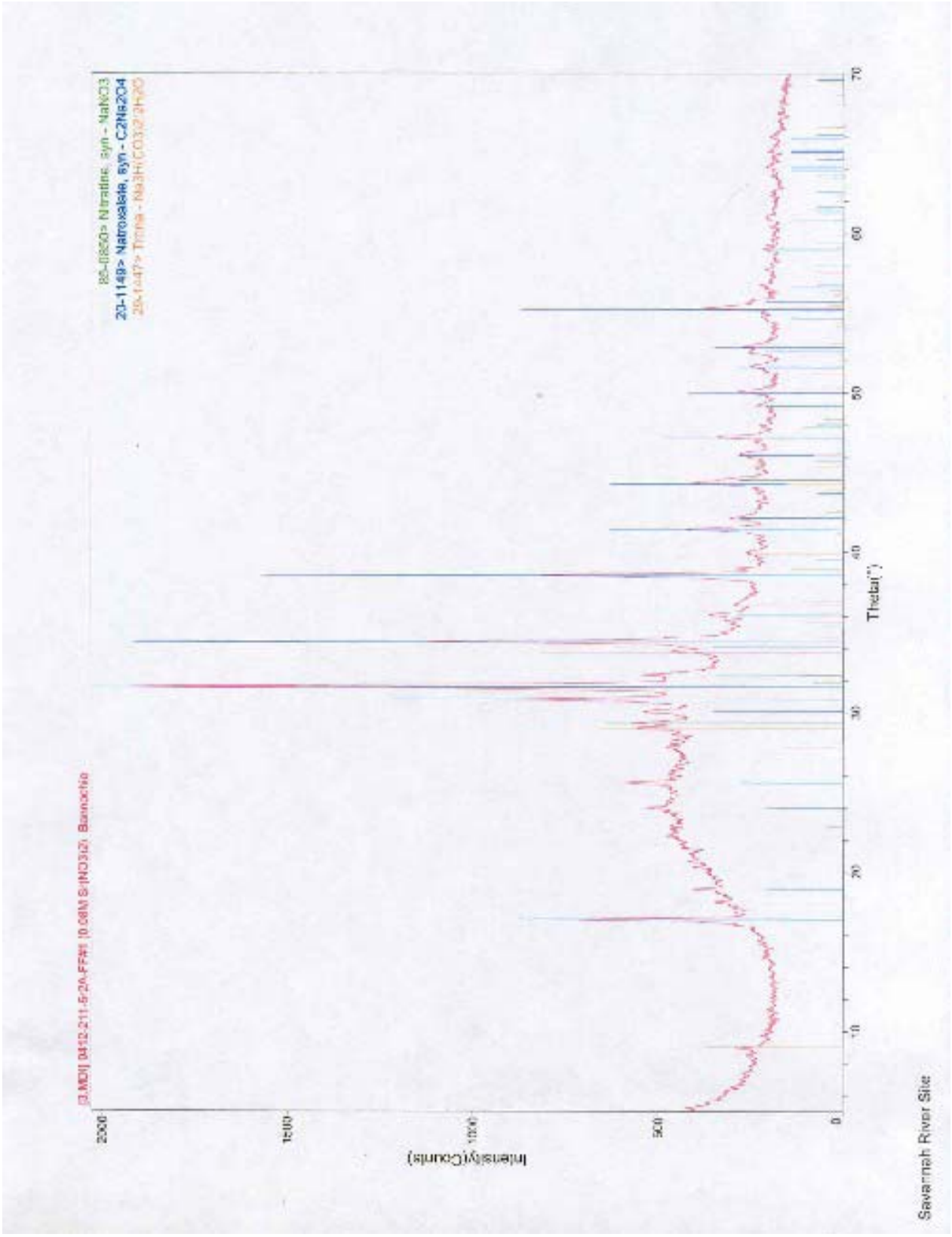
85-0850> Nitratine, syn - NaNO3
20-1149> Natroxalate, syn - C2Na2O4
25-1447> Trona - Na3H(CO3)2·2H2O
Intensity(Counts)
Theta(°)
Savannah River Site

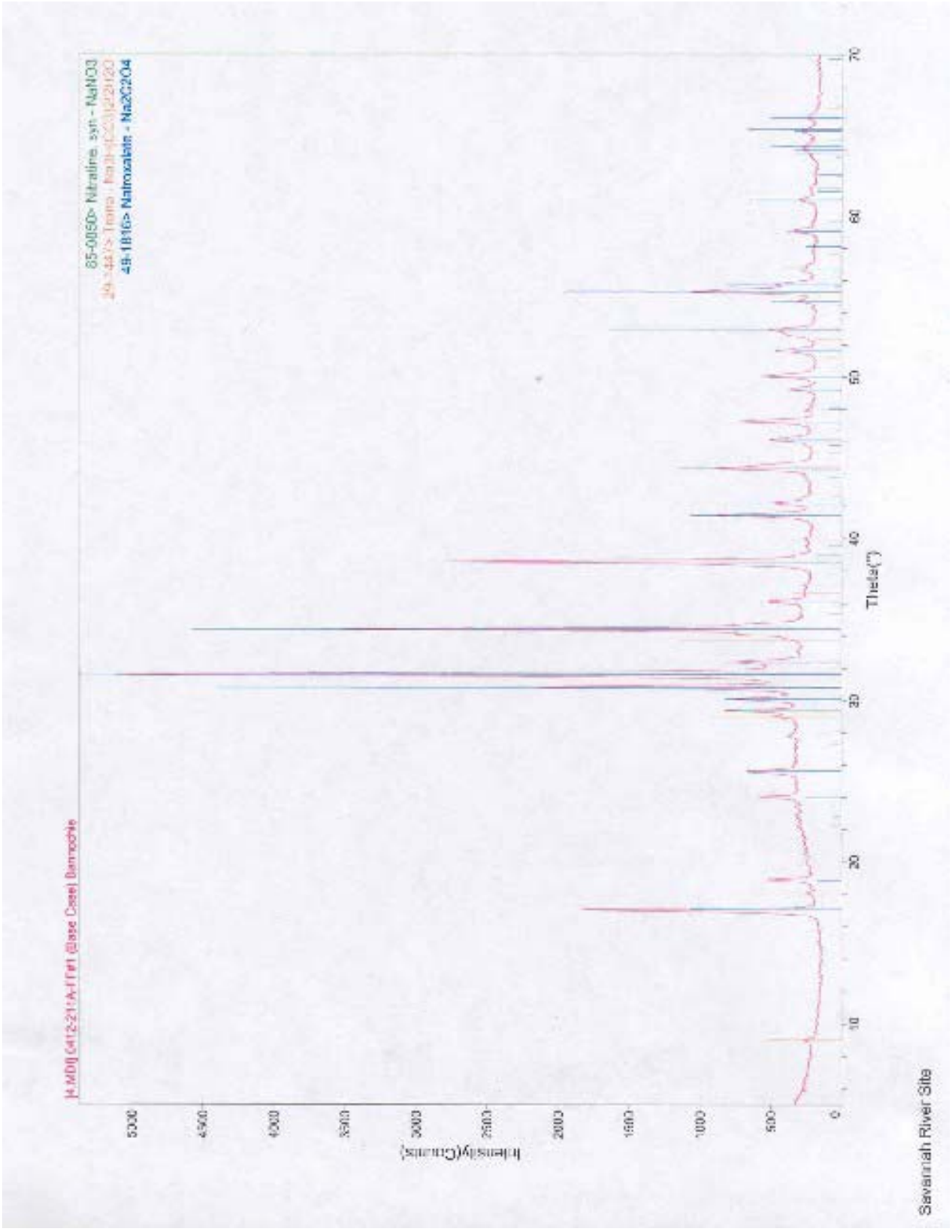
85-0050> Nitratine, syn - NaNO3
49-1816> Natrozeolite - Na2O2O4
Intensity(Counts)
Theta(°)
Savannah River Site

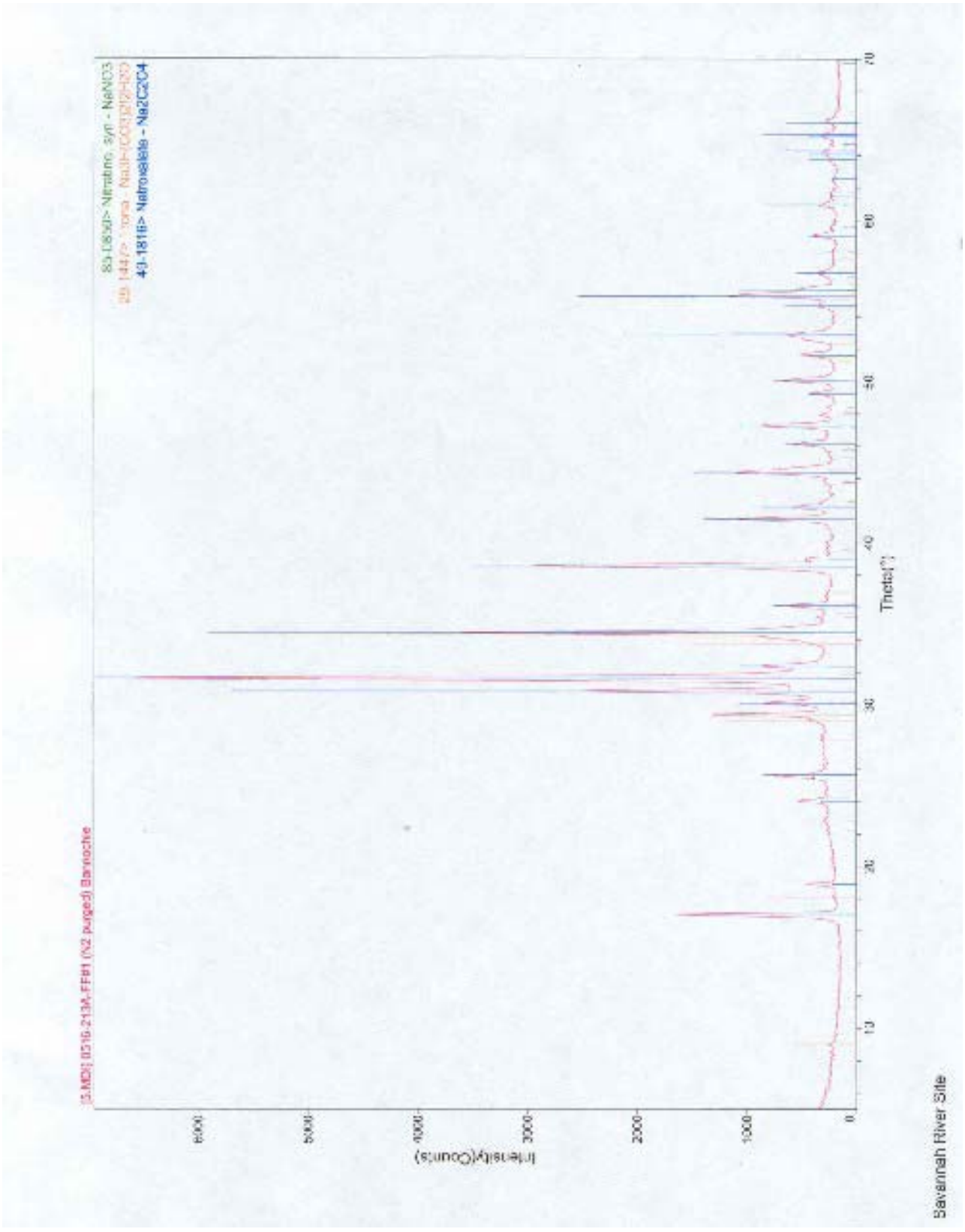
83-1808> Nitratine, syn - NaNO3
49-1816> Natroxalate - Na2C2O4
Intensity(Counts)
Theta(°)
Savannah River Site

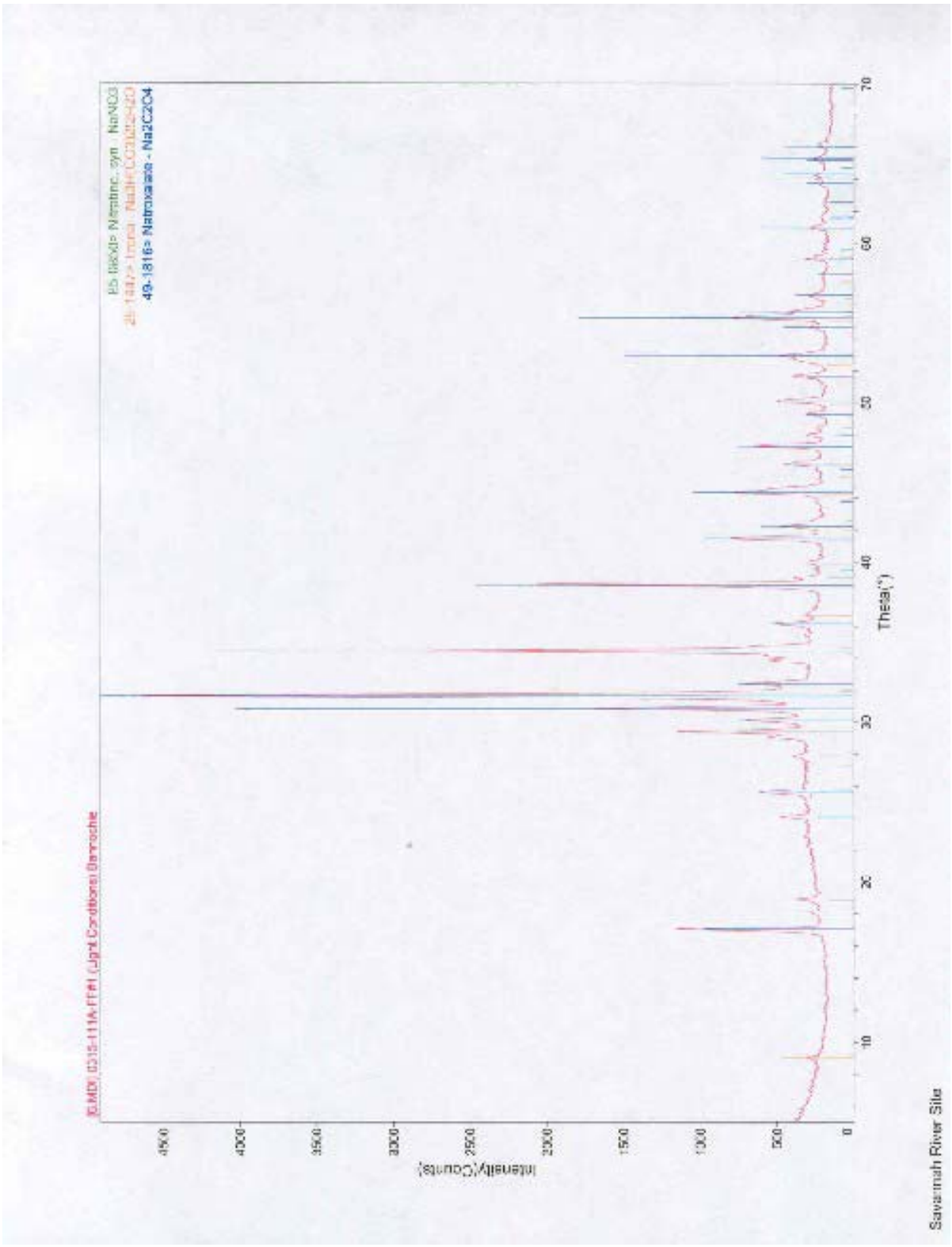
49-1816> Natroxalate - Na2C2O4
Theta(°)
Intensity(Counts)
Savannah River Site

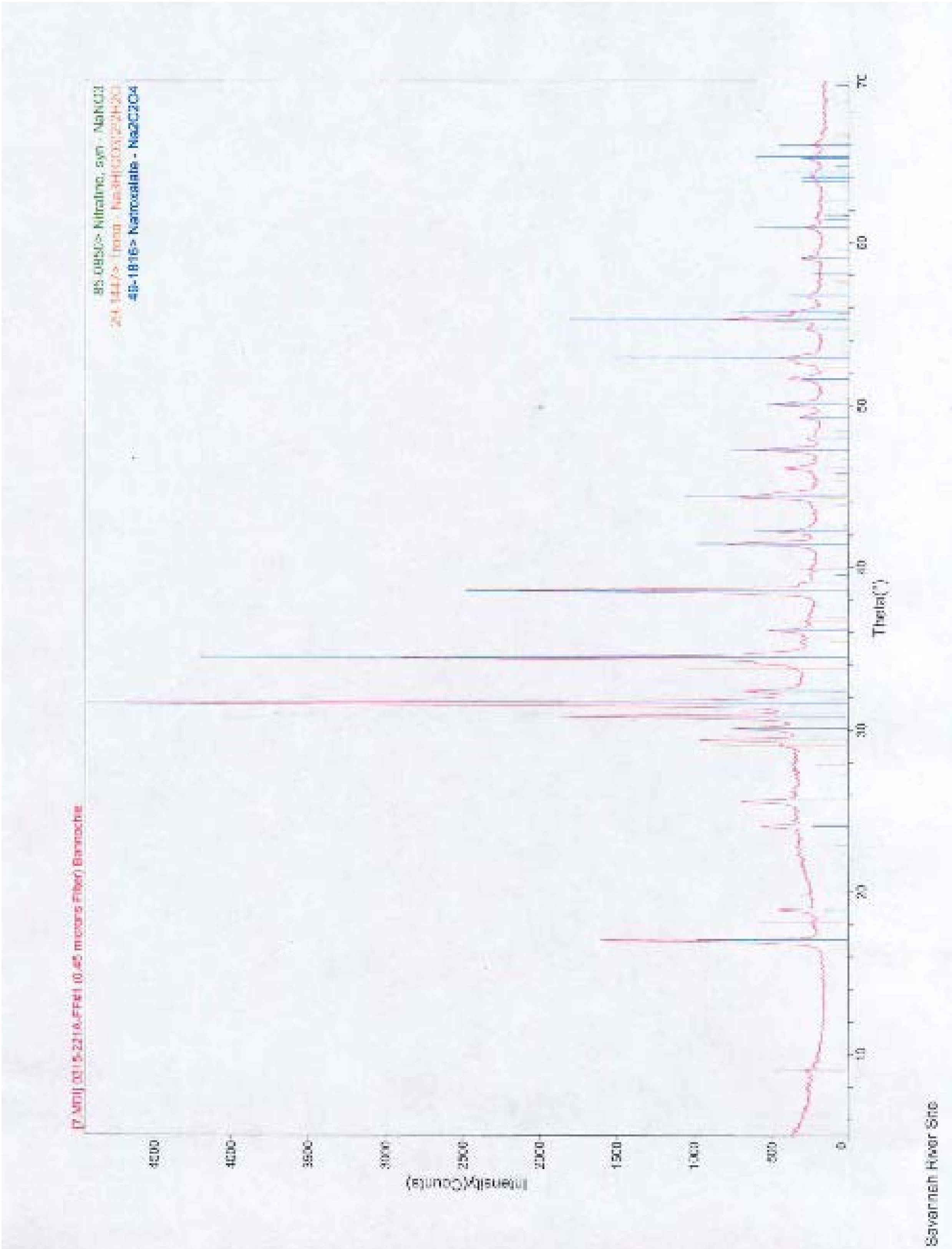
49-1816> Natroxalate - Na2C2O4
Theta(°)
Intensity(Counts)
Savannah River Site

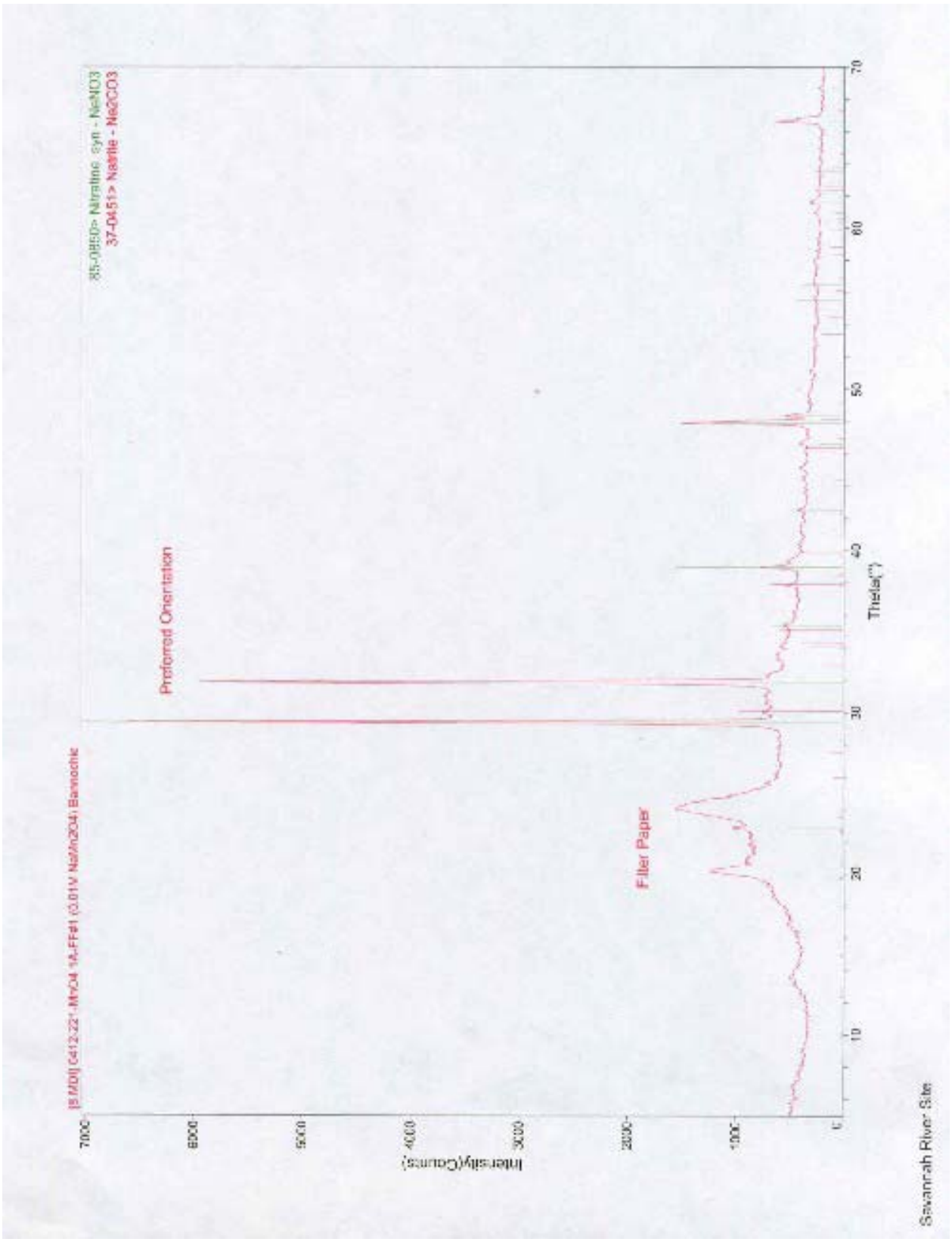
Preferred Orientation
Filter Paper
Intensity(Counts)
Theta(°)
Savannah River Site

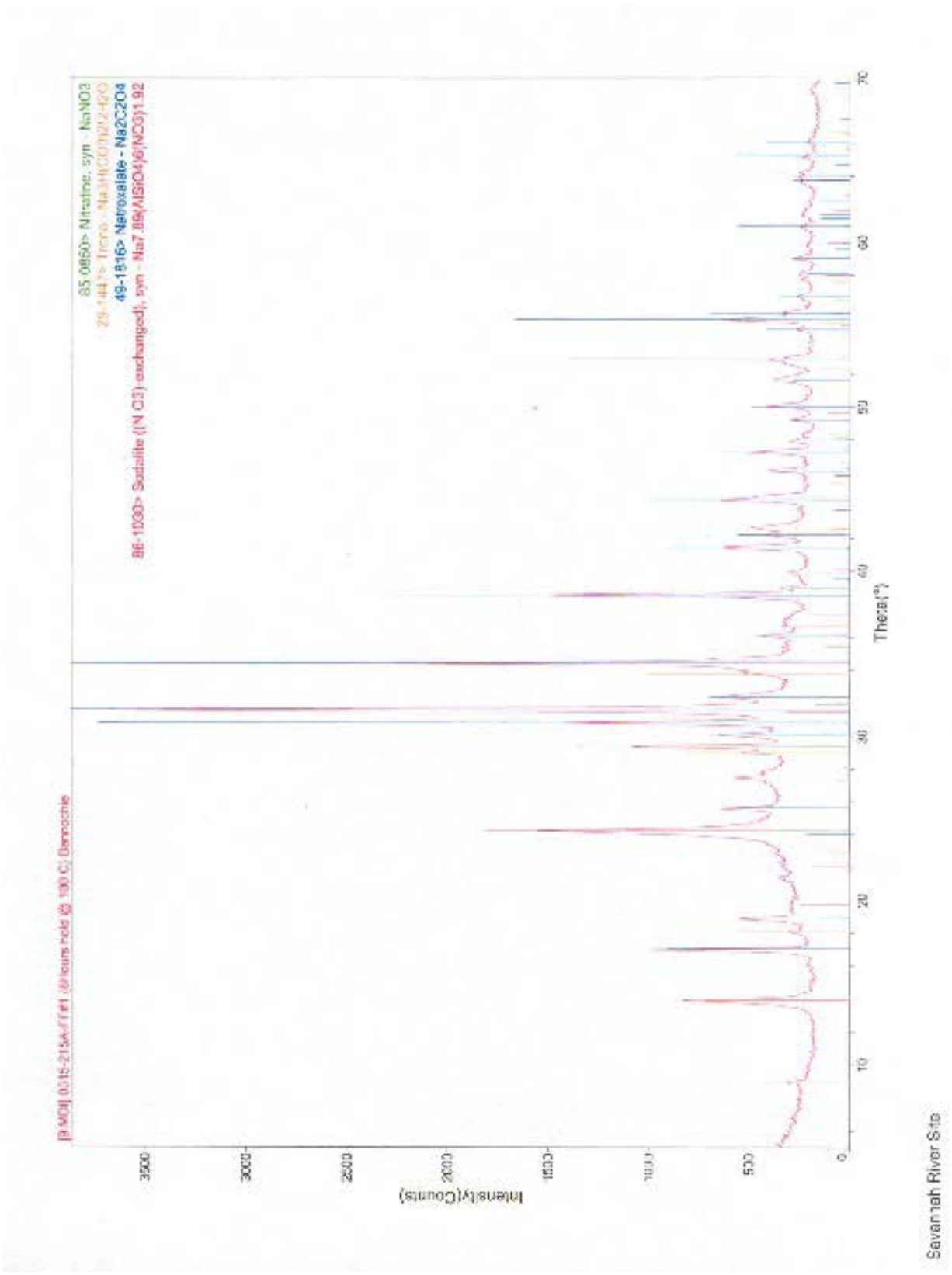
85-0850> Nitratine, syn - NaNO3
29-1447> Trona - Na3H(CO3)2(H2O)2
49-1816> Natroxalate - Na2C2O4
86-1000> Sodalite ((N O3) exchanged), syn - Na7.89(AlSiO4)6(NO3)1.92
Intensity(Counts)
Theta(°)
Savannah River Site

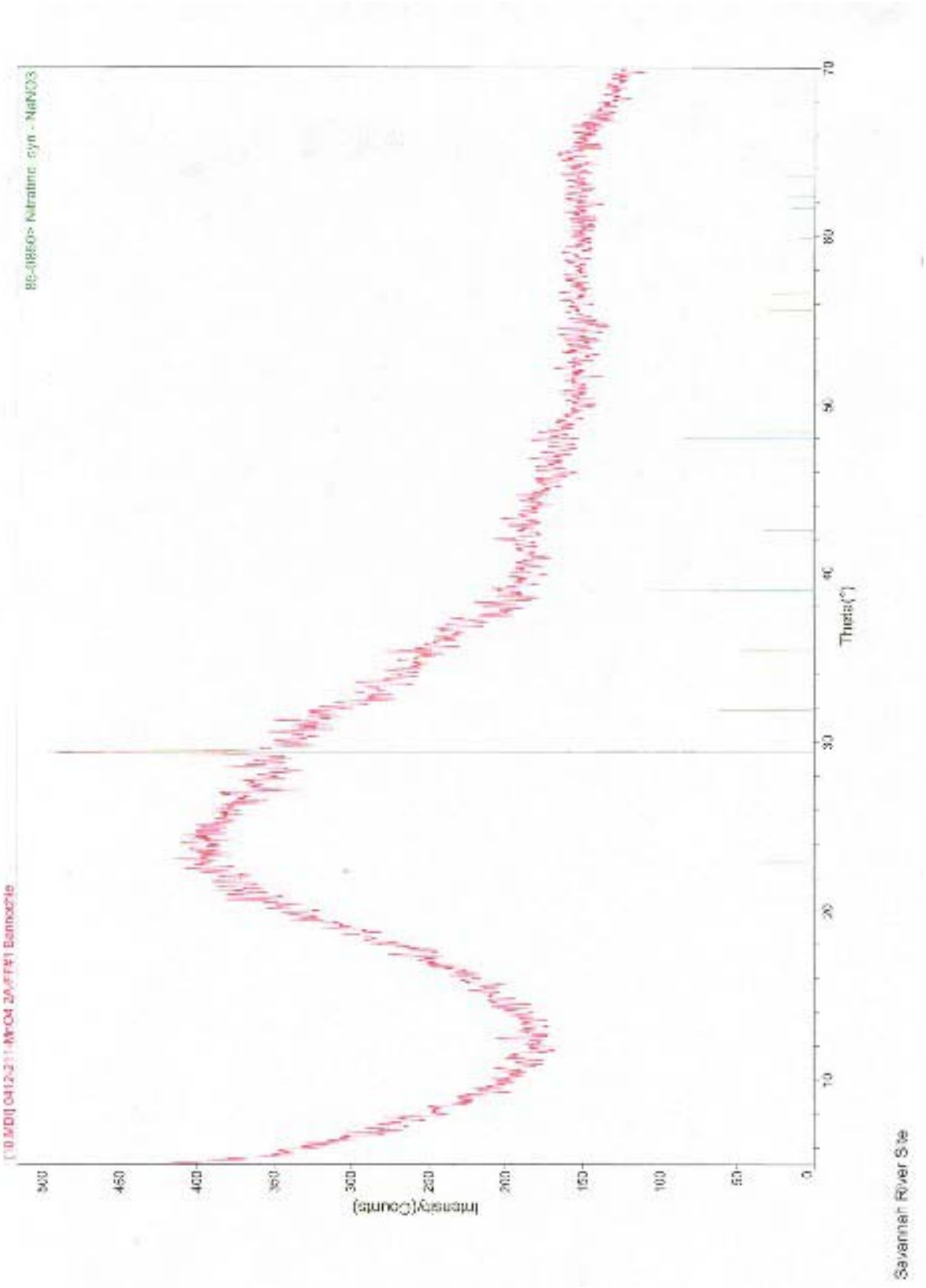
Intensity(Counts)
Theta(°)
Savannah River Site

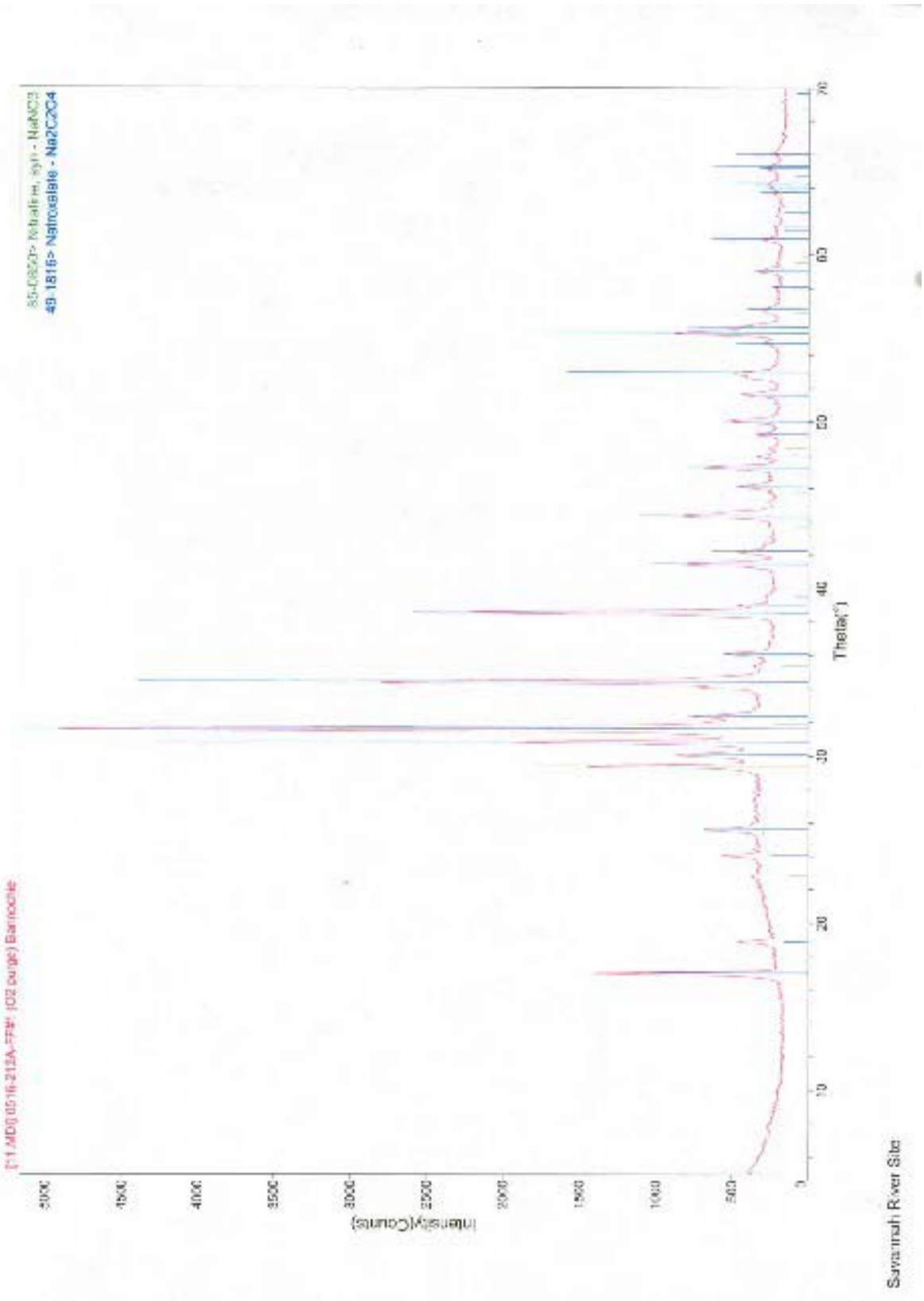
49-1816> Natrosilite - Na2Si2O4
Theta(°)
Intensity(Counts)
Savannah River Site

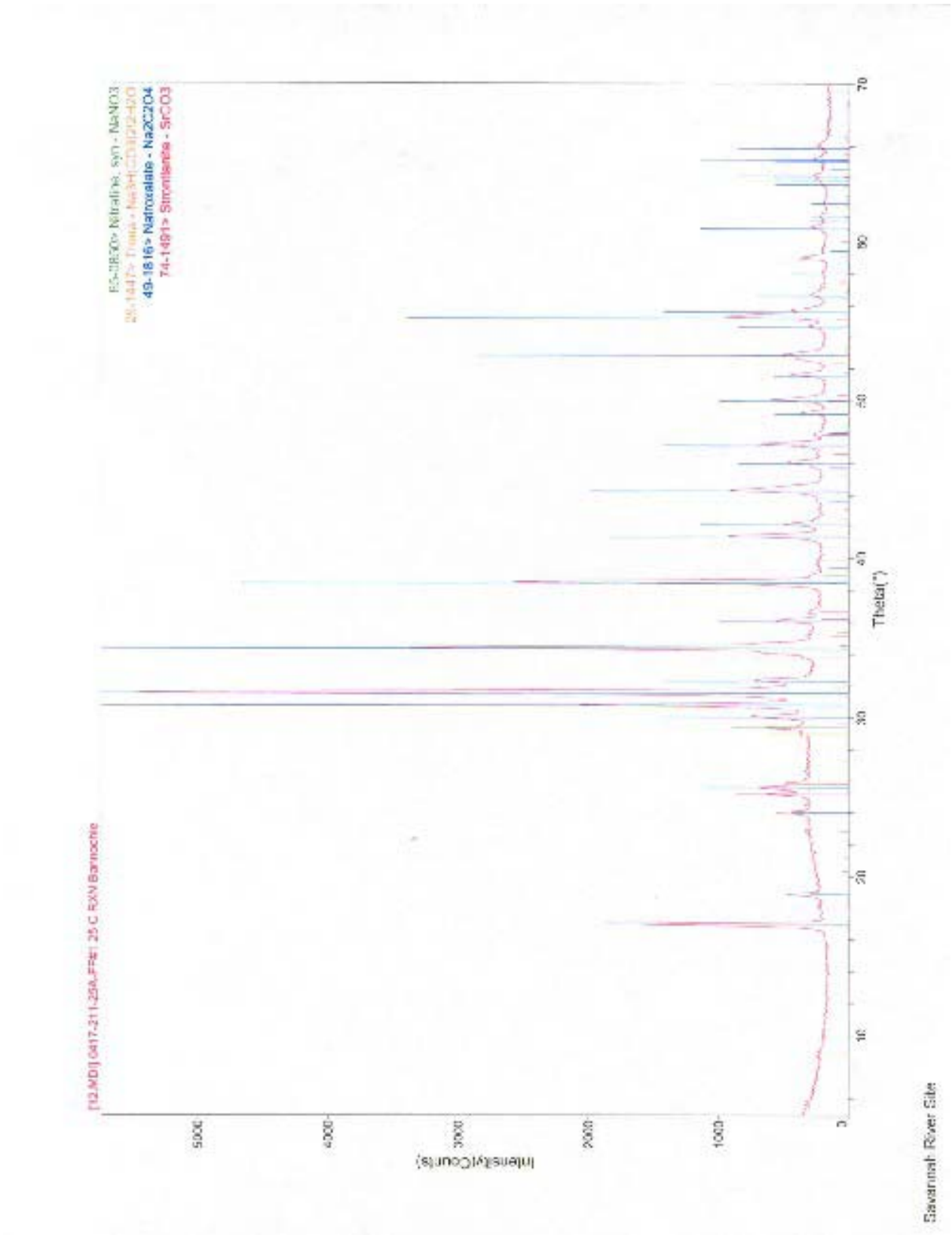
[12-MD] 0417-211-25A_FR: 25 C R2N Barnoche
Intensity(Counts)
Theta(°)
Savannah River Site
49-1816> Natrozalate - Na2C2O4
74-1491> Strontianite - SrCO3

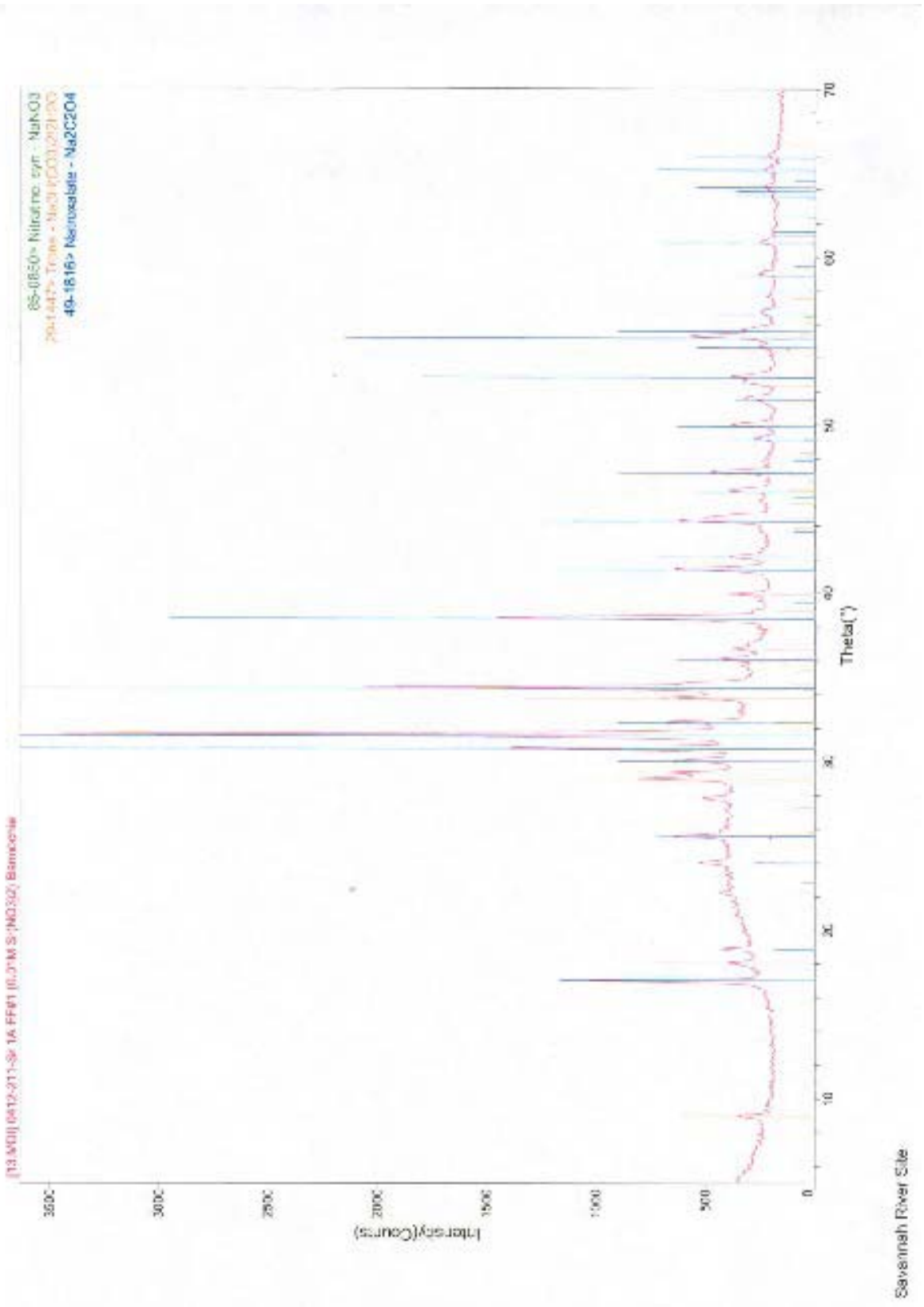
Intensity(Counts)
Theta(°)
Savannah River Site

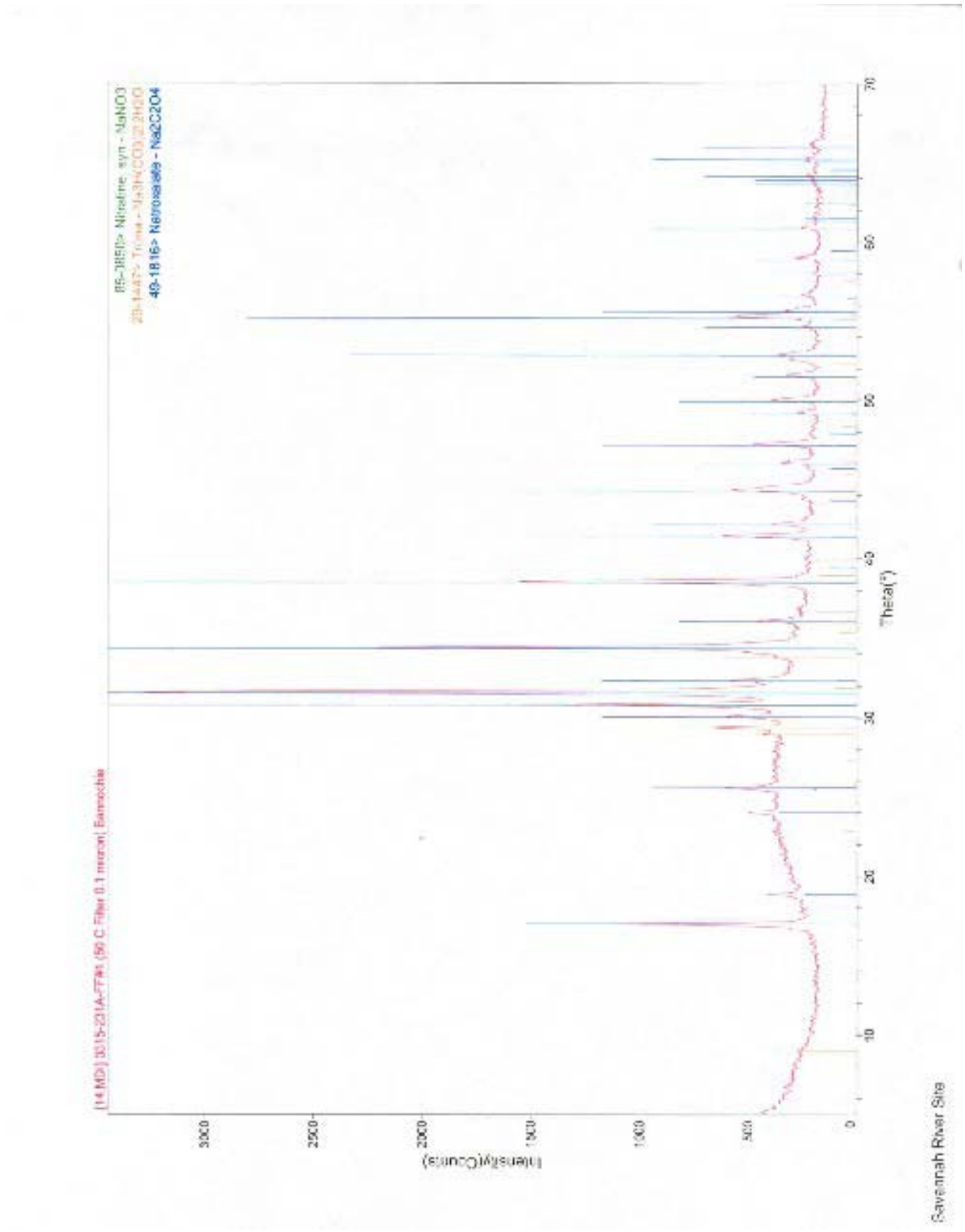
(14 MD) 3315-231A-FT#1 (50 C Filter 0.1 micron) Eamsoche
05-3858> Nitratine, syn - NaNO3
29-1447> Trona - Na3H(CO3)2.2H2O
40-1816> Nitroxalite - Na2C2O4
Intensity(Counts)
3000
2500
2000
1500
1000
500
0
10
20
30
40
50
60
70
Theta(°)
Savannah River Site